INTERFERENCE IN THE EARTH SYSTEM THROUGH TERRESTRIAL CARBON DIOXIDE REMOVAL:

Numerical simulations of trade-offs, risks and opportunities

Dissertation
zur Erlangung des akademischen Grades
doctor rerum naturalium
(Dr. rer. nat.)
im Fach Geographie
eingereicht an der
Mathematisch-Naturwissenschaftlichen Fakultät
der Humboldt-Universität zu Berlin

von

M.Sc. Vera Sophia Heck

Präsident der Humboldt-Universität zu Berlin:
Prof. Dr.-Ing. Dr. Sabine Kunst

Dekan der Mathematisch-Naturwissenschaftlichen Fakultät:
Prof. Dr. Elmar Kulke

Gutachter/innen:
1. Prof. Wolfgang Lucht
2. Prof. William Steffen
3. Prof. Tobias Krüger

Tag der mündlichen Prüfung: 16. März 2017

Acknowledgements

I wish to thank my supervisors Dieter Gerten and Wolfgang Lucht for providing me with great guidance, advice, encouragement, and careful manuscript editing throughout the development of this thesis. Thank you for granting me the freedom to explore my own research ideas and visit conferences, summer schools and workshops and for giving me the opportunity to work at the Potsdam Institute of Climate Impact Research (PIK), which provided an outstanding research environment surrounded by the nature of the Telegraph Hill. I would also like to thank the other members of my PhD committee.

Furthermore, I would like to thank the organisers and members of the German Research Foundation (DFG) Priority Programme (SPP) 1689 on the risks, challenges and opportunities of climate engineering. The many organised workshops and conferences gave opportunities for various enlightening and challenging interdisciplinary discussions and provided a great research environment. Furthermore, thanks to the CE-Land project for the always fun and productive project meetings.

Special thanks go to Lena, who always provided moral support and smiling penguins, taught me about weather forecasts and made times in the office much more fun. Furthermore, I would like to thank the members of the OPEN and COPAN group for providing a constructive and motivating atmosphere with plenty of fruitful and interesting discussions. I would like to acknowledge the work of all those who were involved in the development of LPJmL, with special thanks to Sibyll for going bug-hunting with me. Without their work this thesis would not have been possible.

And, last but not least thank you Markus for standing by my side and supporting me at all times!

Abstract

Terrestrial carbon dioxide removal (tCDR) strategies are being discussed as options to counteract anthropogenic global warming. In particular policy makers now increasingly consider targeted land use change such as afforestation and biomass plantations as options to extract carbon from the atmosphere. In light of this, it is important to understand sustainability limits and implications of tCDR in the context of Earth system dynamics.

This thesis provides a model based assessment of biogeochemical and hydrological side-effects of large-scale biomass plantations and afforestation in the context of planetary boundaries, delimiting a safe operating space for humanity. Simulations with a dynamic global vegetation model (LPJmL) indicate considerable biogeochemical and hydrological consequences of biomass plantations which are even larger than those of historical agricultural land use. In particular, biomass plantations on current agricultural land use areas show a 22% increase in net primary productivity compared to natural vegetation on the same area, which drives other alterations in regional and global carbon and water cycles.

Additionally, land use scenarios of biomass plantations are developed with a multi-objective optimisation model under consideration of regional environmental constraints and evaluated against the global planetary boundaries for biogeochemical flows, biosphere integrity, land system change and freshwater use. This shows clear trade-offs between planetary boundaries and tCDR. Respecting environmental constraints according to the planetary boundary framework yields almost zero tCDR potential. The transgression of regional environmental constraints into a zone of increasing risk of triggering feedbacks at the planetary scale can provide considerable annual net carbon extraction rates of 1.4 GtC - 6.9 GtC, depending on the biomass conversion pathway and the timely operationalisation of large-scale carbon capture and storage plants.

The importance of co-evolutionary dynamics of the Earth's carbon cycle and societal interventions through tCDR is demonstrated with a conceptual modelling approach in the context of carbon-related planetary boundaries. It becomes apparent that focussing on climate change without an integrated trade-offs assessments may lead to navigating the Earth system out of the safe operating space due to collateral transgression of other boundaries. The success of tCDR depends on the degree of anticipation of climate change, the potential tCDR rate and the underlying emission pathway.

Integrating population growth and changing food demands while minimising carbon and

biodiversity loss demonstrates opportunities and limitations for terrestrial carbon sequestration. Without substantial improvements of crop and livestock productivities, feeding 9 billion people diminishes opportunities for tCDR. Higher productivities, however, combined with the displacement of agricultural production into concentrated regions of high productivity yield sustainable terrestrial carbon sequestration potentials of up to 98 GtC.

Zusammenfassung

Gezielte Landnutzungsänderungen zur terrestrischen Kohlenstoffdioxid-Entfernung werden derzeit als Möglichkeit diskutiert um dem anthropogenen Treibhauseffekt entgegenzuwirken. Auch auf politischer Ebene werden insbesondere Biomasseplantagen und Aufforstung zunehmend als Optionen wahrgenommen um die atmosphärische Kohlenstoffdioxidkonzentration zu reduzieren. Für die notwendige Bewertung solcher Maßnahmen ist ein umfassendes Verständnis möglicher Konsequenzen und den Grenzen ihrer Nachhaltigkeit im Kontext des Erdsystems erforderlich.

In dieser Dissertation werden biogeochemische und hydrologische Auswirkungen von großflächigen Biomasseplantagen und Aufforstung quantitativ und im Kontext der *Planetarischen Grenzen* des sicheren Handlungsraums für die Menschheit analysiert. Simulationen mit einem etablierten dynamischen globalen Vegetationsmodell (LPJmL) zeigen, dass die biogeochemischen und hydrologischen Auswirkungen von Biomasseplantagen auf die Biosphäre nicht zu vernachlässigen sind und die der historischen landwirtschaftlichen Bodennutzung noch überschreiten können. Insbesondere ein starker Anstieg der Netto-Primärproduktion auf Biomasseplantagen um bis zu 22% verglichen mit natürlicher Vegetation verändert die globalen Kohlenstoff- und Wasserkreisläufe signifikant.

Des Weiteren werden Landnutzungsszenarien zur räumlichen Verteilung von Biomasseplantagen unter Berücksichtigung von regionalen Umweltschutzanforderungen entwickelt und gegen die globalen *Planetarischen Grenzen* für biogeochemische Flüsse, Intaktheit der Biosphäre, Landnutzungswandel und Süßwassernutzung evaluiert. Die Ergebnisse zeigen eindeutige Konflikte zwischen der Einhaltung der *Planetarischen Grenzen* und terrestrischer Kohlenstoffdioxid-Entfernung. Bei Einhaltung von regionalen Umweltgrenzwerten aus dem Konzept der *Planetarischen Grenzen* können nur marginale Potentiale erzielt werden. Unter kompletter Ausnutzung des Risikobereichs könnten in der zweiten Hälfte des 21. Jahrhunderts etwa 1.4 GtC - 6.9 GtC pro Jahr entzogen werden, abhängig von Biomasseverwertungspfaden und der rechtzeitigen großskaligen Inbetriebnahme von Kohlenstoffbindungs- und speicherungsanlagen.

Die Relevanz von koevolutionärer Dynamik zwischen dem Kohlenstoffkreislauf der Erde und gesellschaftlichem Eingreifen durch tCDR wird mit einem konzeptionellen Modellierungsansatz im Kontext der *Planetarischen Grenzen* aufgezeigt. Es wird deutlich, dass eine Fokussierung auf das Klimaproblem ohne die ganzheitliche Berücksichtigung von erdsystemischen

Interaktionen die ungewollte Überschreitung anderer Systemgrenzen zur Folge haben kann. Als erfolgskritisch erweisen sich die Antizipation des Klimawandels, die eingesetzten Extraktionsraten und die zugrunde gelegten Emissionspfade.
Die Kombination von Bevölkerungswachstum und steigendem Nahrungsmittelbedarf mit der Minimierung von Kohlenstoff- und Biodiversitätsverlusten zeigt Möglichkeiten und Grenzen für terrestrische Kohlenstoffsequestrierung auf. Ohne substanzielle Produktivitätssteigerungen in Ackerbau und Viehwirtschaft kann terrestrische Kohlenstoffspeicherung nicht mit der Nahrungsmittelproduktion für 9 Milliarden Menschen vereinbart werden. Produktivitätssteigerungen hingegen ermöglichen zusammen mit räumlicher Umverteilung der Nahrungsmittelproduktion in hochproduktive konzentrierte Regionen ein Kohlenstoffspeicherungspotential von bis zu 98 GtC.

Contents

List of Figures

List of Tables

Abbreviations

B2H2	Biomass to Hydrogen
B2L	Biomass to Liquid
BECCS	BioEnergy with Carbon Capture and Storage
BFT	Biomass Functional Type
BII	Biodiversity Intactness Index
CCS	Carbon Capture and Storage
CDR	Carbon Dioxide Removal
CE	Climate Engineering
CFT	Crop Functional Type
CMIP5	Coupled Model Intercomparison Project phase 5
CO_2	Carbon dioxide
DGVM	Dynamic Global Vegetation Model
EFR	Environmental Flow Requirement
ET	EvapoTranspiration
GAEZ	Global Agro-Ecological Zones
GCM	General Circulation Model
GHG	GreenHouse Gas
IAM	Integrated Assessment Model
IFL	Intact Forest Landscapes
ILP	Improved Livestock Productivity
INDC	Intended Nationally Determined Contributions
IPCC	Intergovernmental Panel on Climate Change
LCC	Land Cover Change
LPJ	Lund-Potsdam-Jena dynamic vegetation model
LPJmL	Lund-Potsdam-Jena managed Land dynamic vegetation model

LUC	Land Use Change
LULCC	Land Use and Land Cover Change
MAR	Mean Annual Runoff
MCSOS	Manageable Core of the Safe Operating Space
MD	Manageable Domain
MENA	Middle East and North Africa
N_2O	Nitrous oxide
NE	Negative Emissions
NEP	Net Ecosystem Productivity
NPP	Net Primary Production
PB	Planetary Boundary
PES	Payments for Ecosystem Services
PFT	Plant Functional Type
PNV	Potential Natural Vegetation
RCP	Representative Concentration Pathway
RMS	Ruminant Meat Substitution
SDG	Sustainable Development Goal
SOS	Safe Operating Space
SRM	Solar Radiation Management
SRWC	Short Rotation Woody Coppice
tCDR	terrestrial Carbon Dioxide Removal
TCRE	Transient Climate Response to Cumulative CO_2 Emissions
UN-REDD	United Nations Collaborative Programme on Reducing Emissions from Deforestation and Forest Degradation in Developing Countries
UNFCCC	United Nations Framework Convention on Climate Change
WSI	Water Stress Indicator

1. Introduction

Emissions from the burning of fossil fuels are increasing atmospheric carbon dioxide (CO_2) concentrations. With CO_2 being the predominant anthropogenic greenhouse gas (GHG), continued emissions are expected to increase the Earth's surface temperature in the next decades and centuries, which is likely to impact the whole Earth system (Schellnhuber et al., 2016). Terrestrial carbon dioxide removal (tCDR) strategies which aim at increasing the carbon sink of the terrestrial biosphere by large-scale biomass cultivation are proposed to impede critical atmospheric CO_2 concentrations (e.g. Dyson, 1977; Obersteiner et al., 2001; Shepherd et al., 2009). Such strategies are the focal point of this thesis, which assesses associated potentials and side effects.

1.1. Humans in the Earth system

The Earth system is a complex system of interacting oceans, atmosphere, land, water and life, which are connected via physical, chemical and biological processes. With the evolution of the *Homo sapiens* the human species spread over the Earth's surface to inhabit a very thin biological layer. Under the relative stability of the Holocene epoch (Fig. 1.1) – the current interglacial period – the human species prospered through the invention of agriculture and cultural development. At the latest with the industrial revolution a few hundred years ago, humans have become a dominant component of the Earth system (Vitousek et al., 1997). This ushered in a new geological epoch, the Anthropocene (Crutzen, 2002). This epoch is characterised by the widespread use of fossil fuels and the exploitation of natural resources on land and in the oceans, which modified the Earth's natural cycles – the carbon, water, nitrogen, phosphorus and other cycles – far beyond their natural variability (e.g. Boucher et al., 2004; Vitousek et al., 1997).

1.1.1. Anthropogenic modifications of the Earth system

The most debated human impact on the Earth system is probably the altered radiative forcing due to greenhouse gas emissions into the atmosphere. Especially, anthropogenic carbon

emissions from land use and land cover change (LULCC) and fossil fuel consumption have increased atmospheric carbon concentrations by more than 40% (Tans et al., 2015), at rates unprecedented in the last 400,000 years (Fig. 1.1). While in the past two centuries LULCC emissions played a larger role (Houghton, 1999), the acceleration of fossil fuel emissions in the past two decades reduced the current share of LULCC emissions to 12.5% (Houghton et al., 2012).

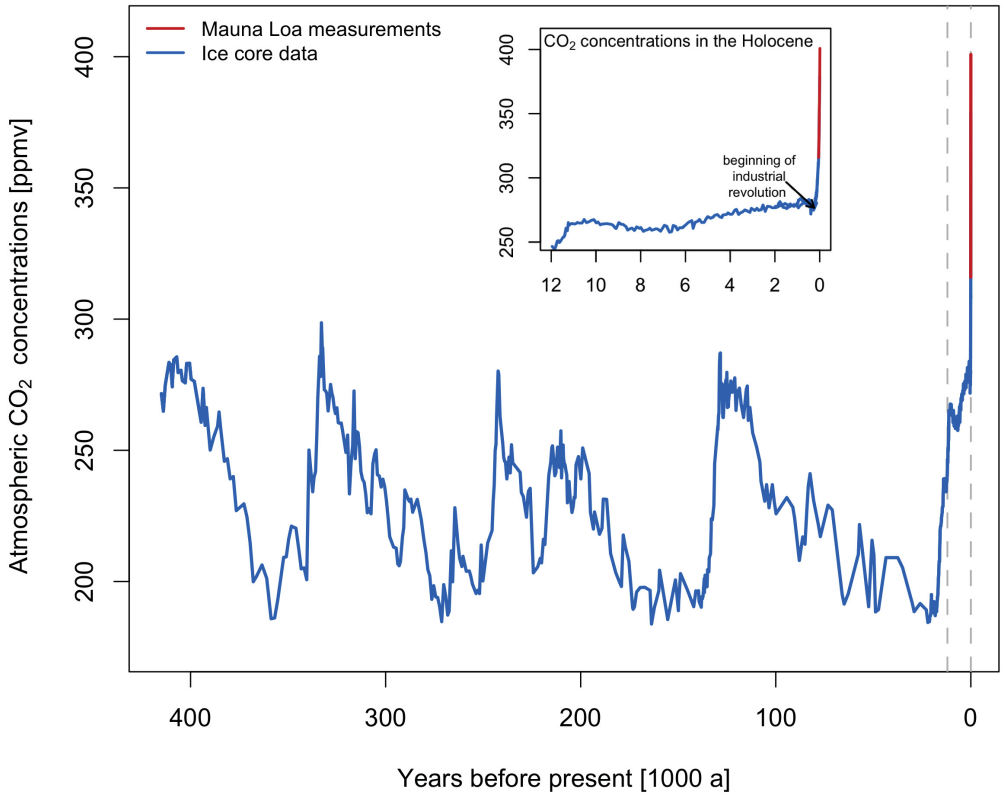

Figure 1.1.: Atmospheric CO_2 concentrations reconstructed from ice core measurements in Antarctica for the last 400,000 years (Lüthi et al., 2008; NCDC, 2012) and atmospheric measurements at Mauna Loa, Hawaii from 1959 to 2015 (Tans et al., 2015). The Holocene period is indicated by dashed grey lines in the main plot and embedded as a subplot.

In addition to the atmosphere, humanity has shaped its natural habitat – the biosphere – as well as the hydrosphere and oceans. Human engineering of natural ecosystems altered about 75% of global ice free land surface (Ellis et al., 2008) and modified the global water cycle (Gordon et al., 2005; Rost et al., 2008a). The global biogeochemical cycles of carbon and nitrogen have been significantly altered by land use intensification. About a quarter of the potential global net primary productivity is appropriated by humans for food and fibre

(Haberl et al., 2007) and agricultural practices to satisfy a growing food demand have more than doubled the global cycling of nitrogen over the last century (Fowler et al., 2013), leading to air, soil and water pollution as well as GHG emissions of nitrous oxide (N_2O) (Vries et al., 2013).

Altogether the human influence on natural ecosystems has led to an alarming biodiversity loss with current extinction rates of at least 10 (Barnosky et al., 2011) and up to 1000 (Pimm et al., 2014) times higher than the likely background rate of extinction. The current era is therefore now considered to be the beginning of the sixth mass extinction since the initial colonisation of the land approximately 540 million years ago (Barnosky et al., 2011), while being the first mass extinction driven by the actions of one single species.

Although the biosphere has proven to be relatively resilient throughout its existence, it is currently threatened in its stability (e.g. Williams et al., 2015). As an integral Earth system component, it is part of cascading feedback mechanisms and teleconnections affecting the climate system. Thus, fundamental human modifications of this system now threaten the Earth system's stability of the Holocene, the initial foundation of human development.

Most notably anthropogenic climate change induced feedbacks put humankind at risk of abrupt, irreversible and detrimental environmental change with large economic consequences (Steffen et al., 2006; Stern, 2007). Many environmental feedbacks to global warming are considered to be tipping elements (Lenton et al., 2008; Schellnhuber, 2009), whose critical point could be reached within the next century if global warming is not curbed (Schellnhuber et al., 2016). For example, abrupt monsoon changes, increasing extreme events and modified weather patterns pose a threat to global food supply and infrastructure, while sea level rise induced by the increased melting of ice shields poses a risk to coastal cities and island nations. Because the risks of such environmental feedbacks increase as global mean surface temperature deviates from pre-industrial levels (Schellnhuber et al., 2016), only reversing the accelerating trends of the Anthropocene in the near future can preserve the Earth system in its Holocene state.

1.1.2. Planetary boundaries

As a guideline to the preconditions of sustainable development of humanity, Rockström et al. (2009) proposed the concept of a safe operating space (SOS) for humanity. Within this space, humanity can evolve without the risk of triggering feedbacks that are detrimental to Earth system functioning in the Holocene-mode.

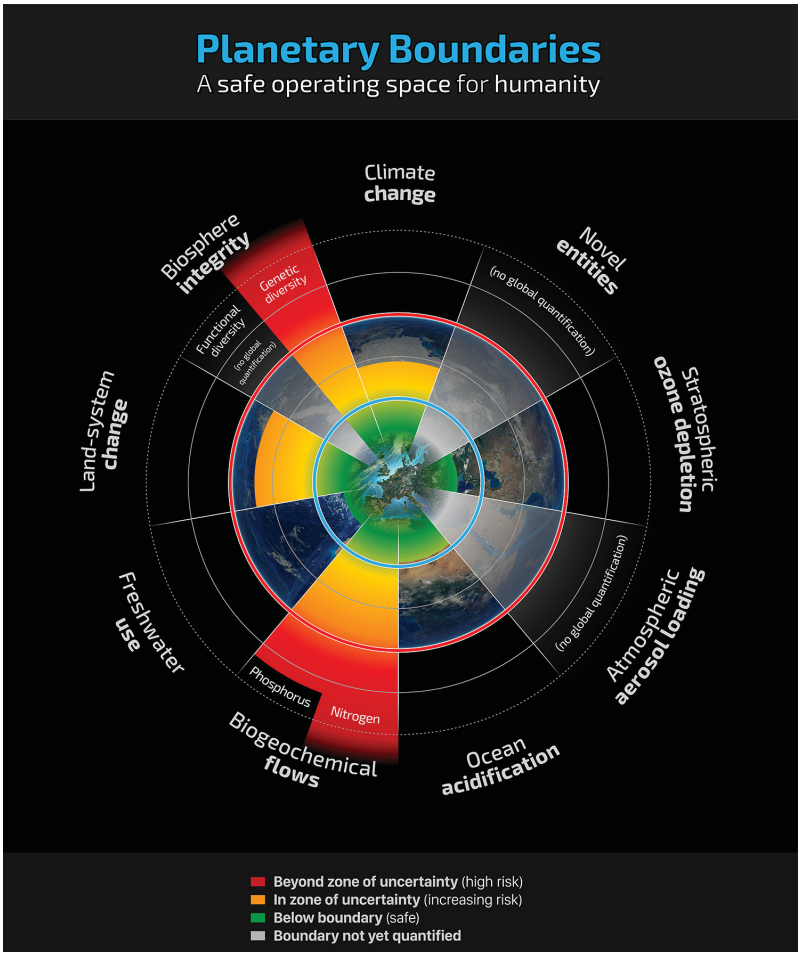

Figure 1.2.: The safe operating space, delineated by nine planetary boundaries. The current status of the Earth system with respect to the control variables of seven of the nine planetary boundaries is marked by colours (Steffen et al., 2015). Green zones are within the safe operating space, yellow marks the zones of uncertainty and red marks the transgression of the uncertainty zone. The status of the remaining planetary boundaries has not been quantified yet. (credit: F. Pharand-Deschênes /Globaïa)

The safe operating space is formed by nine planetary boundaries (PBs) of anthropogenic modification of key Earth system processes (Rockström et al., 2009; Steffen et al., 2015). These processes were identified based on their potential of triggering threshold-behaviour and gradual changes at the global or continental level (e.g. climate change) or their importance for the resilience of the Earth system, i.e. the capacity of the system to tolerate perturbations. They include the global biogeochemical cycles of carbon, water, nitrogen and phosphorous as well as biogeophysical feedbacks and purely anthropogenic influences. Each process is

identified by one or more control variables with associated PBs. The locations of the PBs are identified at normatively defined 'safe' distances from known thresholds or from identified dangerous levels and associated with an uncertainty zone (Rockström et al., 2009; Steffen et al., 2015). The uncertainty band accounts for scientific uncertainty about the exact location and allows room for manoeuvring away from impending thresholds. In a recent update (Steffen et al., 2015), regional control variables and boundaries of processes with strong sub-global operating scales were identified. In the following, the PBs (and uncertainty range in brackets) that are relevant in the context of this thesis are briefly described according to their definition in Steffen et al. (2015).

Climate change The PB for climate change is one of two identified core boundaries which provide planetary-level overarching systems for, and are regulated by, the other PBs. The boundary is proposed at an atmospheric CO_2 concentration of 350 ppmv (450 ppmv) and an increase in top-of-atmosphere radiative forcing of $+1$ Wm^{-1} ($+1.5$ Wm^{-1}). The location of the boundary is particularly motivated to safeguard the stability of polar ice sheets and regional climate patterns. In the current state, the PB for climate change is transgressed with atmospheric CO_2 concentrations of about 400 ppmv (Tans et al., 2015). Terrestrial CDR is targeted at preventing substantial transgression of this PB which would likely push the Earth system out of the Holocene-mode.

Biosphere integrity The PB for biosphere integrity forms the second core boundary, as it plays a critical role for the Earth system's resilience and its material and energy flows. Biosphere integrity has strong regional operating scales at the biome level. Its state is currently assessed via two preliminary control variables: the species extinction rate and the biodiversity intactness index (BII) (Scholes et al., 2005). Because of the large uncertainty about the role of biodiversity for ecosystem functioning, both boundaries are associated with a large uncertainty range. The boundary for extinction rate is set at 10 extinctions per million species years, (100 extinctions per million species years) and a BII of 90% (30%). The preliminary boundaries suggest that the status of biosphere integrity has already left its zone of uncertainty.

Biogeochemical flows The PB for biogeochemical flows reflects the importance of the integrity of the global nitrogen and phosphorous cycles for Earth system functioning. Control variables are the industrial and intentional biological fixation of nitrogen and phosphorous flows into the ocean, with planetary boundaries set at 62 $TgNy^{-1}$ (82 Tg Ny^{-1}) and 11 TgP y^{-1} (100 TgP y^{-1}), respectively. These aim at undermining negative side effects of artificial nitrogen and phosphorous application such as eutrophication of coastal and freshwater

systems and ocean anoxic events. The status of both boundaries is strongly influenced by regional agricultural practices. While nitrogen and phosphorous application are within safe levels in many regions, intensive agriculture, especially in the northern hemisphere, has led to a transgression of the global boundaries.

Freshwater use The global control variable of freshwater use is blue water consumption – 4000 km^3 (6000 km^3) – whereas environmental flow requirements (EFRs) are decisive for the regional control at the basin level. EFRs are derived from hydrological flow characteristics at the basin level and define the minimum flow requirements to prevent deterioration of ecosystems. The defined minimum flow requirements as share of the mean monthly discharge are 75% (45%) for low-flow months, 70% (40%) for intermediate-flow months and 45% (15%) for high-flow months. Currently, blue water consumption from industry, households and agriculture is smaller than the global boundary. Regionally, water withdrawals – mostly for irrigated agriculture – decrease river flow below the environmental flow requirements.

Land system change The PB for land system change aims at preserving essential biogeophysical feedbacks between the land surface and the atmosphere. The control variable is the amount of forest cover of the biomes that play the strongest role in regulating energy and moisture fluxes (temperate, tropical and boreal) relative to preindustrial forest cover. The biome level boundaries have been set at 85% (60%) for tropical and boreal forests and 50% (30%) for temperate forests, resulting in a globally weighted average land system change boundary of 75% (54%). The current state of the global and regional boundaries is highly sensitive to the classification of potential forest cover and to the identification of deforestation.

Ocean acidification The PB for ocean acidification is oriented towards conserving coral reefs and other marine ecosystems through maintaining carbonate chemistry. The saturation state of aragonite is proposed as the control variable with boundary value of 80% (70%) of the preindustrial annual aragonite saturation state and closely linked to atmospheric CO_2 concentrations and ocean acidification. The current ocean state (84%) is approaching the PB.

Other boundaries not focused on in this thesis are the PBs for introduction of novel entities to the environment, atmospheric aerosol loading and stratospheric ozone depletion (Steffen et al., 2015).

While the location of most boundaries is still highly uncertain and open questions remain concerning the coherence of regional and global control variables, the concept of a safe

operating space for humanity has received considerable interest from non-scientific sectors. For example, there are approaches to country scale operationalisations of the PBs concept (Cole et al., 2014; Frischknecht et al., 2014; Nykvist et al., 2013) and it was influential in the development of the sustainable development goals (SDGs) (Griggs et al., 2013).

1.1.3. Challenges for future human development

It is a major challenge for science and policy makers to identify pathways of sustainable future development within the physical boundaries of the safe operating space. On the one hand the two overarching core boundaries (climate change and biosphere integrity, refer to Sec. 1.1.2) are already within the zones of uncertainty, while the PB for biogeochemical flows is far beyond its uncertainty level (Steffen et al., 2015). On the other hand, the continuing socio-economic trends of population growth and economic growth imply even increasing demands for natural resources. For example, feeding a more prosperous global population of more than 9 billion people with higher per-capita consumption, requires substantial increase in food production (Tilman et al., 2011), whereas agricultural land use has turned out to be one of the most severe pressures on biodiversity, land system change, nitrogen and phosphorous cycling and freshwater use. Furthermore, ever-increasing fossil fuel emissions and projected increases in energy demand, are in critical contrast to the need for halting the increase in atmospheric CO_2 concentrations.

The criticality of GHG emissions has received large political and public attention and humanity now recognises its effect on the functioning of the Earth system. With this awareness, three – not necessarily independent – modes of action remain: mitigation, adaptation and climate engineering (Fig. 1.3). TCDR strategies play a role in most of these (ref. to Sec. 1.2.3).

Mitigation Mitigation aims at avoiding severe impacts of global warming. This requires a significant reduction of GHG emissions, implying a substantial decarbonisation of the energy sector and economy, together with an effective management of terrestrial carbon pools. Because the first impacts of climate change are already observed, mitigation is highly time sensitive. In order to avoid triggering substantial thresholds of the climate system such as the destabilisation of polar ice sheets, it is required to limit the global mean surface temperature increase to less than 2°C relative to preindustrial levels (Schellnhuber et al., 2016).

Adaptation Adaptation requires the modification of infrastructure and management to cope with feedbacks of the climate system to global warming. Adaptation measures include the construction of dykes and flood defence counteracting sea level rise, protecting housing and infrastructure against extreme events and modifying agricultural practices and water

resources management to be more drought resistant. Required adaptation levels and associated economic costs are highly regionally heterogeneous and depend on the committed level of global warming. Thus adapting to global warming while high emissions continue – which is likely to result in global warming between 3.2°C and 5.4°C above preindustrial (under RCP8.5, IPCC, 2013) – can pose large challenges for humanity.

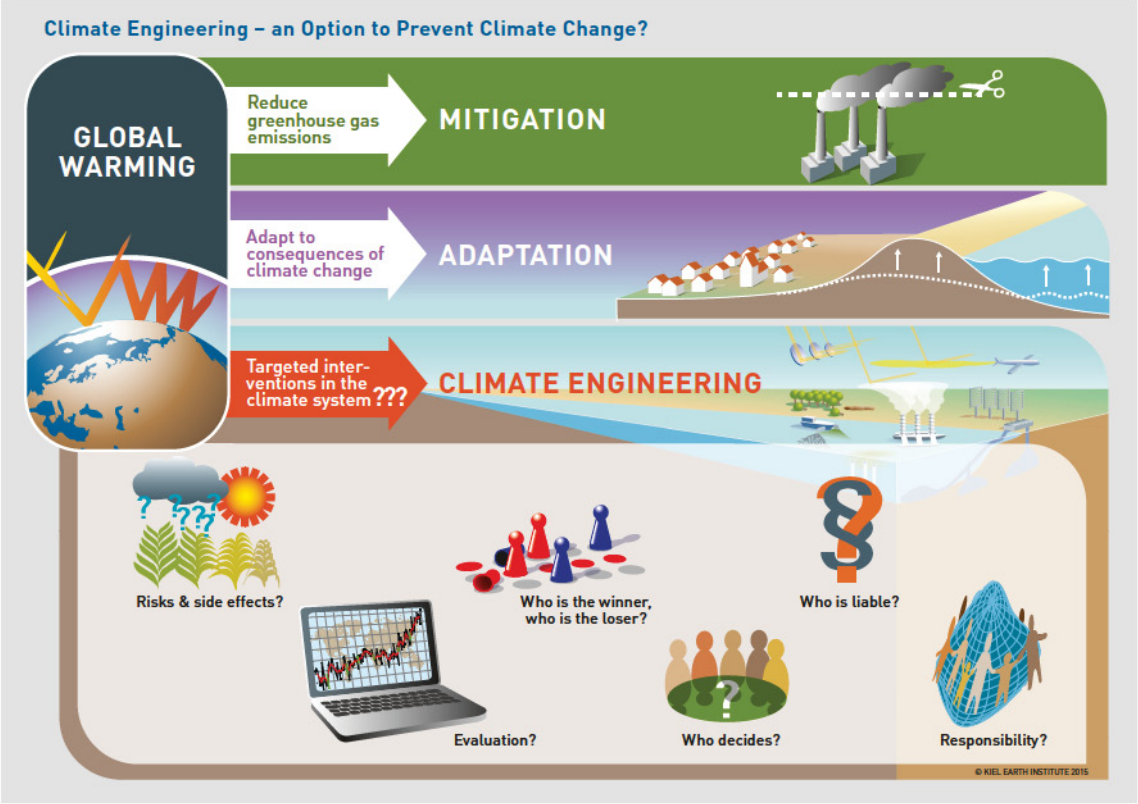

Figure 1.3.: Three possibilities of anthropogenic responses to global warming: mitigation, adaptation and climate engineering (Copyright: Kiel Earth Institute)

Climate engineering Inertia in economical, political and social mitigation commitments evoked proposals on climate engineering (CE) – also called geoengineering – the deliberate manipulation of the Earth's climate system (e.g. Keith, 2000; Shepherd et al., 2009). A wide range of potential CE methods have been proposed (e.g. Vaughan et al., 2011), which are commonly associated with high ecological, institutional and social risks and challenges (Fig. 1.3). CE methods are commonly divided into two categories: solar radiation management (SRM) and carbon dioxide removal (CDR).

SRM aims at modifying the Earth's radiation balance in order to counteract global temperature increase caused by GHG in the atmosphere. Advantages of SRM are relatively low

deployment costs and quick operation timescales. However, SRM implies an additional modification of the Earth system – associated with new risks – and would not reverse previous anthropogenic modifications. Thus, SRM could be effective in preventing temperature related threshold behaviour (instability of ice shields), but is ineffectual in reversing substantial carbon cycle modifications. Uncertainties and relevant feedbacks of SRM are assessed in the framework of GeoMIP (Kravitz et al., 2015; Kravitz et al., 2011), the first model intercomparison project on CE.
CDR encompasses various processes and technologies aiming at reducing atmospheric CO_2 concentrations, the main cause of global warming. These commonly redistribute atmospheric carbon to terrestrial, geological or maritime carbon reservoirs and are also referred to as negative emissions (NE). While CDR methods are generally associated with high economic costs and operate on longer time scales than SRM, there is still little consensus on the impacts and efficacy of CDR. This thesis advances the understanding of potentials and trade-offs of terrestrial CDR methods, which utilise the natural pathway of photosynthesis to extract carbon from the atmosphere and store it in terrestrial or geological reservoirs (refer to Section 1.2 for details). To explore the potential, risks, and challenges of different types of CDR, a model intercomparison project on CDR (CDR-MIP) was launched in the beginning of 2016 (Keller et al., 2016). In the first round of CDR-MIP experiments, large-scale afforestation is the only included tCDR method.

With the adoption of the Paris Agreement by 195 nations in the framework of the United Nations Framework Convention on Climate Change (UNFCCC) to limit global warming to well below 2°C (UNFCCC, 2015), an important step towards mitigation has been achieved in December 2015. However, it is increasingly concluded that the manifested commitment to limit global warming to well below 2°C requires temperature control with CE, typically via CDR technologies (e.g. Fuss et al., 2014; Gasser et al., 2015; Krey et al., 2013). Emission reduction efforts within the next few decades will therefore determine the course of future planetary development.

1.2. Terrestrial carbon dioxide removal

Terrestrial carbon dioxide removal comprises several proposed methods to reduce atmospheric CO_2 concentrations by increasing the carbon sink of the terrestrial biosphere. In the context of this thesis two tCDR methods – afforestation (Sec.1.2.1) and biomass plantations (Sec. 1.2.2) – are evaluated. Both methods utilise the natural pathway of photosynthesis to extract carbon from the atmosphere. Since this is a rather inefficient process, large CDR potentials are generally associated with large area and water requirements, posing trade-offs to land and water demands for agriculture and conservation purposes (Beringer et al., 2011).

As plant productivity is expected to increase with increasing atmospheric CO_2 concentrations (CO_2 fertilisation) due to higher water use efficiency (Ainsworth et al., 2004), potentials of afforestation and biomass plantations depend on underlying carbon emission scenarios. Other suggested methods of tCDR are enhancing soil carbon sequestration through land management and enhanced weathering of silicate and carbonate rocks to remove CO_2 from the atmosphere (Schuiling et al., 2006).

1.2.1. Afforestation

Afforestation of historically unforested land and reforestation of deforested land to semi-natural and managed forests aims at increasing terrestrial carbon storage via higher carbon residence times in soil and vegetation carbon pools. The carbon uptake potentials are limited and decrease over time as forests mature. Potentials of large-scale reforestation are at maximum in the order of magnitude of already committed land cover change (LCC) emissions (House et al., 2002) and could not reverse fossil fuel emissions. Afforestation and reforestation potentials considering competition with agricultural land use depend on projections of agricultural productivity increase (Arora et al., 2011). The potentials of large-scale afforestation considering land availability constraints have been estimated around 100 PgC on 345 Mha in a 100-year time frame (Nilsson et al., 1995) or up to 215 PgC on 800 Mha under high atmospheric CO_2 concentrations (Sonntag et al., 2016).

Especially afforestation of monocultures implies ecosystem shifts and associated impacts on biodiversity and would modify biogeophysical feedbacks such as moisture recycling (Vaughan et al., 2011). Furthermore, reforestation and afforestation inversely impact the Earth's radiation balance by decreasing its albedo, which can regionally outweigh the radiative forcing effect of atmospheric carbon reduction (Betts, 2000; Pongratz et al., 2010). Afforestation has also been shown to have positive impacts, e.g. carbon accumulation in severely eroded soils (Xie et al., 2013).

1.2.2. Biomass plantations

Large-scale biomass plantations are suggested to extract atmospheric CO_2 while increasing biomass supply (Shepherd et al., 2009). In contrast to afforestation, biomass is frequently harvested and subsequently concentrated and potentially stored by artificial processes (Chum et al., 2011). Especially second-generation lignocellulosic biomass plantations (e.g. *Miscanthus* and switchgrass plantations) or short rotation woody biomass plantations (e.g. willow, poplar or *Eucalyptus* plantations) are considered for tCDR. Once harvested, biomass can undergo various utilisation pathways to such as the conversion to bioenergy (with or without

subsequent carbon capture and storage (CCS) (Klein et al., 2014a), conversion to biochar via pyrolysis (Lehmann et al., 2006), long-term biomass burial in deep anoxic soil layers with low decomposition rates (Zeng et al., 2013) or it can be utilised conventionally, e.g. for construction (Sathre et al., 2010).

Energy generation from biomass is directed at substituting carbon emissions from fossil fuels but does not effectively reverse historical emissions. Only bioenergy coupled with carbon capture and storage (BECCS) in geologic reservoirs offers the potential to actually remove emitted carbon from the atmosphere (Read et al., 2005). Energy yields and carbon reduction potential from biomass harvest depend on available energy conversion and carbon capture efficiencies, the available capacity of geological storage pools and their associated leakage rates, as well as transient terrestrial carbon pool feedbacks after land conversion (Creutzig et al., 2014).

The range of reported biomass harvest potentials is very high due to differences in methodologies and assumptions about land availability and agricultural efficiencies (Dornburg et al., 2010). Some assessments consider biodiversity, land and water conservation while accounting for sustained food production (e.g. Beringer et al. (2011) with conservative harvest rates of 1.4 PgC/a or Boysen et al. (2016) with harvest rates of 5.5 PgC/a on 5% of current agricultural land). Other assessments assume high land availability for biomass plantations due to agricultural productivity increase combined with high biomass yield potentials (e.g. Smeets et al., 2007, with harvest rates of 34.4 PgC/a based on a 70% reduction of agricultural land).

Second-generation biomass plantations resemble intensively managed agricultural systems and are associated with similar negative impacts (Vaughan et al., 2011). They entail a large-scale intervention into the global carbon cycle, are associated with biodiversity loss if implemented on previously uncultivated land (Immerzeel et al., 2014), require substantial irrigation water (Berndes, 2002; Hejazi et al., 2015) and fertilisation, which could in turn increase N_2O emissions (Crutzen et al., 2008). As in the case of afforestation, biogeophysical effects could offset or overcompensate biogeochemical cooling through carbon removal, particularly in high-latitudes (Bathiany et al., 2010; Betts, 2000; Boysen et al., 2016; Creutzig et al., 2014).

1.2.3. TCDR in the context of mitigation, adaptation and climate engineering

TCDR plays an important role in the mitigation scenarios of the recent Intergovernmental Panel on Climate Change's (IPCC) representative concentration pathway scenarios (RCPs). Bioenergy without CCS provides a significant share of primary energy in a socio-economic pathway associated with high emissions from fossil fuels (RCP8.5, Riahi et al., 2011). Albeit

not classifying as tCDR, bioenergy production is associated with trade-offs that are similar to those of BECCS which are assessed in this thesis.

Reforestation is largely deployed in the intermediate emission scenario RCP4.5 (Thomson et al., 2011), which assumes considerable yield increase and dietary change resulting in a significant decrease of grasslands and croplands. BECCS is an important component of the IPCCs low-emissions scenario (RCP2.6), which shows a rapid reduction of GHG emissions through drastic policy intervention Vuuren et al., 2011. Even net negative emissions, i.e. a net removal of GHGs from the atmosphere, are required in most of the RCP2.6 simulations of the coupled model intercomparison project (CMIP5) towards the end of the century (Jones et al., 2013).

In order to have a larger than 50% chance of achieving the agreed mitigation goal to limit the increase in global average temperature to 2°C or 1.5°C (UNFCCC, 2015), integrated assessment models (IAMs) increasingly rely on large-scale BECCS to simulate compatible socio-economic pathways (Fuss et al., 2014; Gasser et al., 2015; Smith et al., 2015). While IAMs optimistically assume the availability of technologies for CCS and the commercial feasibility of large-scale BECCS deployment (Kraxner et al., 2015), it is still in the development stage (Creutzig et al., 2014; Scott et al., 2013) and its practical feasibility is being questioned (Fuss et al., 2014). Especially the availability of biomass and underground storage capacities are limiting factors (Kriegler et al., 2013) along with technical and socio-institutional challenges (Fuss et al., 2014).

Besides their integral role for mitigation and adaptation pathways, biomass plantations and afforestation are also considered part of the CE method portfolio. In this context, biomass plantations and afforestation are usually evaluated for their ability to decrease global warming from a business-as-usual high emission baseline (e.g. Boysen et al., 2016; Sonntag et al., 2016). However, these measures alone are generally not considered as feasible to counteract unmitigated global warming in the case of imminent climate catastrophes (Boysen et al., 2016; Lenton et al., 2009; Sonntag et al., 2016).

1.3. Research questions

A quantitative global assessment of potential biogeochemical impacts and side effects of large-scale terrestrial CDR on the Earth system is still lacking. Furthermore, tCDR potentials and trade-offs have so far not been evaluated in the context of multiple planetary boundaries. Previous studies have mostly focused potentials of terrestrial CDR (e.g. Arora et al., 2011; Beringer et al., 2011; Lenton, 2010; Sonntag et al., 2016), assessed regional or field-scale impacts (e.g. Georgescu et al., 2011; Tölle et al., 2014; Zimmermann et al., 2013) or evaluated

individual trade-offs at the global scale (e.g. Bonsch et al., 2014; Swann et al., 2012).
As was pointed out in the previous sections (ref. to Sec. 1.1), the biosphere is part of entangled interactions with other Earth system components. Although its initial exploitation has led to considerable carbon emissions and ecosystem degradation (Foley et al., 2005), the biosphere has been proposed as instrument to reduce atmospheric CO_2 concentrations. However, potential unintended side effects of tCDR have been identified, which might outweigh the intended effects in their consequences in terms of radiative forcing (Betts, 2000; Boysen et al., 2016; Crutzen et al., 2008) or hydrological trade-offs (Bonsch et al., 2014; Hejazi et al., 2015). In this context, it is vital to investigate trade-offs of tCDR in a holistic framework of Earth system sustainability, as for example the planetary boundaries framework (Sec. 1.1.2, Rockström et al., 2009; Steffen et al., 2015). The aim of this thesis is to provide an assessment of the potentials and associated risks of tCDR from an Earth system perspective. In particular, biogeochemical and hydrological consequences, trade-offs between tCDR and the planetary boundaries, co-evolutionary feedbacks and trade-offs of tCDR and agriculture with nature conservation (Fig. 1.4). Therefore, the questions posed below are addressed with a broad range of methods.

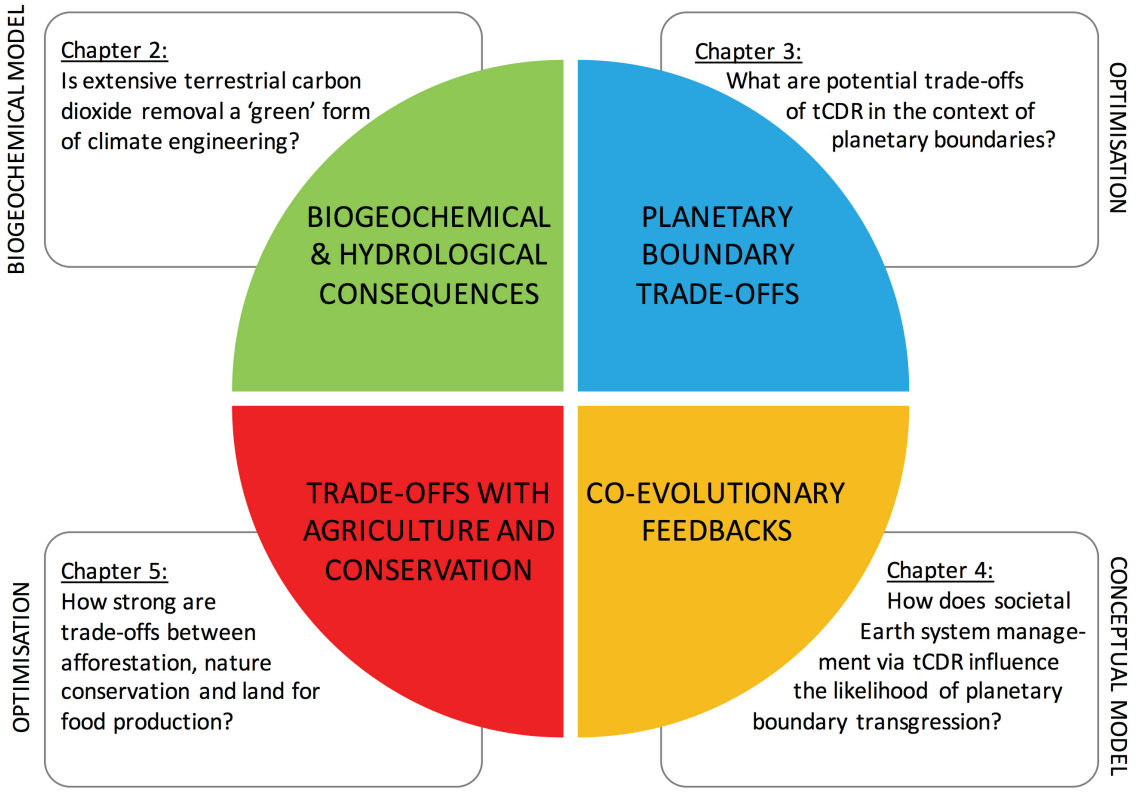

Figure 1.4.: Components of the thesis and research questions

1. Is extensive terrestrial carbon dioxide removal a 'green' form of climate engineering?

This question stems from the perception that – in comparison to other CE methods – terrestrial CDR is often considered a natural and relatively safe option as it involves the cultivation of plants (e.g. Shepherd et al., 2009). In light of the consequences of historical anthropogenic land modifications (ref. to Sec. 1.1.1), it is however, important to consider potential biogeochemical and hydrological consequences of large-scale biomass plantations. Further, it is important to assess how different types of biomass plantations (woody and herbaceous) differ in their C sequestration potential, water and nutrient requirements and associated biogeochemical and hydrological impacts. Contrasting biogeochemical impacts of biomass plantations and historical land use change with stylised scenarios informs about the potential extent of biosphere transformation under large-scale climate intervention with tCDR in comparison to historical human biosphere management. This question is approached by simulations with a state of the art dynamic vegetation model (ref. to Sec. 1.4.1).

2. What are potential trade-offs of tCDR in the context of planetary boundaries?

This question is central for addressing tCDR from an Earth system perspective. Its aim is to improve the understanding of the potential influence of tCDR deployment to the functioning of the Earth system. As indicated in Section 1.1, the Earth system is a complex system of interacting feedbacks. While the main motivation for tCDR deployment is the prevention of critical feedbacks by anthropogenic climate change, unintended side effects could trigger other critical feedbacks. Therefore it is important to incorporate multiple planetary dimensions into the assessment of tCDR. This is done by including relevant planetary boundaries into the assessment of tCDR potentials and investigating trade-offs with planetary boundaries other than climate change. A second aim is to assess if and to what extent BECCS could substitute fossil fuels and contribute to negative emissions. Multiple trade-off analyses are performed with a multi criterial optimisation model in the framework of planetary boundaries (ref. to Sec. 1.4.2).

3. How does societal Earth system management via tCDR influence the likelihood of planetary boundary transgression?

Social and political actions are important drivers of tCDR. The willingness to commit to tCDR deployment is driven by atmospheric carbon monitoring and can be expected to increase with manifesting climate impacts. However, a dynamic integration of complex interactions between the societal and environmental spheres is currently unfeasible due to fundamental

conceptual problems and high computational demands (Vuuren et al., 2016; Vuuren et al., 2012). Therefore, in the context of CE, the societal dimension is usually only included as a scenario component to model analysis and not dynamically integrated. Exceptions are first conceptual modelling approaches that simulate the interaction between human climate monitoring and societal action in the form of transitions to renewable energy (Jarvis et al., 2012) or CE (MacMartin et al., 2013). This question aims at a first analysis of the importance of dynamic co-evolutionary interactions in the tCDR context, which is approached with a conceptual model (ref. to Sec. 1.4.3).

4. How strong are trade-offs between afforestation, nature conservation and land for food production?

TCDR potentials are strongly limited because of trade-offs with land for food production and nature conservation (e.g. Beringer et al., 2011). Especially scenarios of population growth, future food demand and agricultural intensification opportunities are main drivers of the extent of future agricultural land use (Foley et al., 2011; Tilman et al., 2011). Therefore, it is important to take the drivers of agricultural land use into consideration for tCDR assessments. Widening the scope of the previous questions, this question aims at an assessment of the opportunities of land use management for both nature conservation and tCDR. In this scope, the aim is to identify terrestrial carbon sequestration potentials under optimal allocation of agricultural land use which safeguards both, food demand for different socio-agrological scenarios and sustainability constraints. This is approached with a spatially explicit land use optimisation model, maximising carbon sequestration and biodiversity conservation.

1.4. Methods of Earth system modelling

For this thesis, modelling approaches of different complexity and mathematical optimisation approaches are used to assess the above research questions (Sec. 1.3). In general, a model is a simplified representation of complex processes. Computer models usually consist of a set of algorithms and equations that are designed to adequately capture sub-processes of the modelled system. Modelling the system (i.e. running the systems model) can be used to predict the systems behaviour in the future, the present or the past, e.g. under modified external forcings. This is especially relevant if controlled experiments to determine the system's behaviour are difficult or unfeasible.

In Earth system science a wide range of methods are applied to study the co-evolutionary system of nature and anthroposphere. These range from laboratory experiments and small scale modelling to global-scale observation and monitoring and Earth system modelling (e.g.

Schellnhuber, 1999). Models of the Earth system (or components of it) generally combine and integrate a representation of our physical understanding of sub-processes or a simplification thereof. This is based on decades of careful experimentation, observation and monitoring of processes in the Earth system.

In the context of climate engineering, which aims at large-scale modification of the climate system, small scale experiments and models can only provide spatially and temporally very limited information. To conduct large-scale field experiments of CE measures to gain detectable information about their feedback to the system would already be comparable to actual deployment. Thus, global-scale simulations are essential to increase the understanding of large-scale CE potentials and the associated side effects to the Earth system. In particular, multiple model simulations can be conducted in order to examine possible system responses to varying conditions or scenarios. For this reason, models are the fundamental tools used in this thesis to assess tCDR in the Earth system.

The following sections give a brief overview on the modelling concepts that are applied in this thesis. A detailed description of the methodology relevant for the conducted research is given in independent methods sections in each chapter.

1.4.1. Dynamic global vegetation models

Dynamic global vegetation models (DGVMs) have a long history. Their development was initiated to support the identification of solutions to global change related problems (Prentice, 1989) and identify the transient effect of climate change and land use on the biosphere (Steffen et al., 1992). DGVMs are commonly comprised of different modules representing physiological, biophysical, biogeochemical and hydrological processes. These include representations of photosynthesis, transpiration, stomatal and canopy boundary-layer conductance, carbon allocation, turnover and soil and litter biogeochemistry, establishment, disturbance and mortality as well as resource competition for light, space and water (and nutrients) (Cramer et al., 2001; Sitch et al., 2003).
Driven by time series of climate data, soil characteristics and topography, DGVMs simulate ecosystem processes on an annual, monthly or daily time scale in spatially distributed grid cells which are assumed to have homogeneous conditions. Simulation outputs are spatially explicit time series of carbon (and water) fluxes and pools and vegetation distribution on daily, monthly or annual time steps. The spatial resolution, i.e. the number of gridcells, can vary significantly for different models and applications.
Vegetation dynamics are driven by net primary production (NPP), probabilities of natural disturbance and resource competition between different plant functional types (PFTs) representing various plant species. PFTs differ in their parameterisations of physiological,

morphological, phenological, bioclimatic and fire-response characteristics (Sitch et al., 2003). Due to the fundamental role of agricultural systems in the terrestrial biosphere of the Anthropocene, agricultural ecosystems have been incorporated in some state-of the-art DGVMs. Agricultural systems are usually represented by agricultural crop functional types (CFTs) which are distributed according to time-series of spatially explicit land use area input data. This allows the assessment of global-scale anthropogenic ecosystem modifications and associated land use change emissions (e.g. Bondeau et al., 2007).

Answering most of the research questions of this thesis (Sec. 1.3) requires a model of the terrestrial biosphere with a representation of agricultural land use including biomass plantations. LPJmL is currently the only DGVM that fully incorporates agricultural land use and herbaceous and woody short-rotation biomass plantations at the global scale into the terrestrial carbon and water cycle with an internally consistent modelling framework. It computes both carbon and water flows explicitly, which is crucial for the purpose of an integrated tCDR impact assessment. In this thesis, global spatially explicit simulations of the biosphere for various agricultural and tCDR land use scenarios (Chapters 2, 3 and 5) are performed with the LPJmL model.

1.4.2. Optimisation of land use scenarios

In this thesis multi-objective optimisation models are constructed in order to develop spatially explicit land use scenarios following a variety of sustainability objectives (Chapters 3 and 5). In general, optimisation aims at finding the parameters of a system that minimise or maximise an objective. For a given objective function ($f(x) : A \rightarrow F$) the element $x_0 \in A$ is desired such that $f(x_0) \leq f(x)$, $\forall x \in A$ (minimisation) or such that $f(x_0) \geq f(x)$, $\forall x \in A$ (maximisation). The point $f(x_0)$ is referred to as the global minimum, or maximum, respectively. Depending on the properties of the objective function a variety of optimisation approaches exist. If F is one-dimensional the optimisation is a single-objective optimisation. If F is multi-dimensional the optimisation problem is a multi-objective optimisation problem, regarding more than one goal simultaneously. A multi-objective optimisation function, however, can also be formulated as a single-objective optimisation by scalarising the optimisation problem, i.e. adding (weighted) single objectives into a one dimensional objective function (Hwang et al., 1979). This approach is chosen in this thesis because it increases the computational feasibility.

In global change science, integrated assessment models (IAMs) and stand-alone land use optimisation models are prominent examples of applied optimisation modelling for the development and analysis of socio-economic, policy and land use scenarios. These are generally based on economic principles and optimise economic growth or minimise costs

(e.g. Lotze-Campen et al., 2008; Luderer et al., 2011). Furthermore, optimisation models are, for example, applied to find solutions for sustainable land use (e.g. Cao et al., 2012; Seppelt et al., 2002) or water use (e.g. Grundmann et al., 2011; Jiang et al., 2016).

In Chapters 3 and 5 of this thesis, two optimisation models are developed which incorporate the states of different environmental control variables (e.g. planetary boundaries) into the objective function. To my knowledge, these are the first optimisation models that are driven solely by sustainability objectives without economic constraints. In contrast to prevalent economic optimisation, this allows for the development of spatially explicit land use scenarios (including tCDR) for a variety of sustainability constraints. Land use patterns are developed by minimising global (and regional) aggregate impacts of spatially explicit grid cells which are assumed to be independent (neglecting intercellular water flows). Thus the optimisation problems are described by linear objective functions which can be approached with linear optimisation (Sierksma, 2001).

1.4.3. Conceptual models

A conceptual model, or low-complexity model, is a relatively simple representation of a more complex system. The aim of conceptual models – in contrast to complex models such as DGVMs – is to test or to gain insight about dominating processes and interactions in the modelled system and not to quantitatively predict system behaviour. A key advantage of the simplicity of conceptual models is that they are more tractable for mathematical analysis and applicable to long time scales (Lenton, 2000). For example, conceptual models are being used to explore the co-evolutionary Earth system building on the assumption that societies and nature are interacting and should be considered as integrated socio-ecological systems (e.g. Anderies et al., 2013; Brander et al., 1998; Jarvis et al., 2012; Kellie-Smith et al., 2011; Motesharrei et al., 2014).

In this thesis (Chapter 4), a conceptual model of the co-evolutionary Earth system in the context of tCDR is developed to gain insights into the relevance of anthropogenic climate management for the response of the global carbon cycle and associated planetary boundaries. A dynamic integration of such a co-evolutionary system with complex models is currently unfeasible due to fundamental conceptual problems and high computational demands on social and environmental modelling sides (Vuuren et al., 2016; Vuuren et al., 2012).

1.5. Structure of the thesis

The dissertation consists of four first-author articles (Chapters 2 to 5) in which different aspects of tCDR are addressed with a variety of methods. The individual chapters have been published in peer-reviewed scientific journals (Chapters 2 and 4), are currently under review (Chapter 3) or to be submitted (Chapter 5). The articles have been produced in cooperation with other authors, whose contributions are listed at the end of each chapter.

Chapter 1 provides an overview on past anthropogenic interferences in the Earth system, the concept of a safe operating space for humanity and the potential role of tCDR in mitigation, adaptation and CE pathways. Moreover, the research questions of this thesis and relevant methodological approaches are outlined.

Chapter 2 develops a metric to assess the biogeochemical state of the biosphere. This is applied to compare biogeochemical and hydrological impacts of large-scale herbaceous and woody short rotation biomass plantations against the impacts associated with historical land use change simulated with LPJmL. The study highlights that biomass plantations are associated with substantial biogeochemical and hydrological impacts and should thus not be interpreted as a safe or 'green' climate engineering option.

Chapter 3 improves the understanding of the trade-offs between tCDR deployment and the status of planetary boundaries, taken as a measure for the integrity of the Holocene-state of the Earth system. With a spatially explicit optimisation, scenarios of herbaceous and woody biomass plantations are developed under consideration of multiple criteria for safeguarding the status of several planetary boundaries. This shows only limited potential for negative emissions if planetary boundaries are safeguarded.

Chapter 4 addresses the relevance of societal drivers for tCDR and the feedback of the carbon system. A conceptual earth system model is extended with a simple feedback loop mimicking societal observation of atmospheric CO_2 concentrations and response in the form of tCDR. The resilience of the co-evolutionary system is assessed with a basin stability approach, which shows that the opportunities to remain within the carbon-related planetary boundaries only exist for a small range of anticipation levels and depends critically on emission-scenarios.

Chapter 5 integrates population and food demand scenarios into tCDR assessment. It evaluates the opportunities for carbon sequestration and biodiversity conservation by improved agricultural management and reallocated land use for different population and food supply scenarios. Spatially explicit land use scenarios are developed with an optimisation approach that minimises carbon losses and the risk for biodiversity loss. They show considerable potential for terrestrial carbon sequestration if agricultural productivities increase.

Chapter 6 summarises and synthesises the findings of the individual chapters, assesses the robustness of the results and provides an outlook to promising future research questions.

2. Is extensive terrestrial carbon dioxide removal a 'green' form of climate engineering? A global modelling study [1]

Vera Heck[1,2], Dieter Gerten[1,2], Wolfgang Lucht[1,2,3], Lena R. Boysen[1,2,3]
[1] Potsdam Institute for Climate Impact Research, Research Domain 1: Earth System Analysis, Telegraphenberg A62, 14473 Potsdam, Germany
[2] Humboldt-Universität zu Berlin, Department of Geography, Berlin, Germany
[3] Integrative Research Institute on Transformations of Human-Environment Systems, Berlin, Germany

Abstract

Biological carbon sequestration through implementation of biomass plantations is currently being discussed as an option for climate engineering (CE) should mitigation efforts fail to substantially reduce greenhouse gas emissions. As it is a plant-based CE option that extracts CO_2 from the atmosphere, it might be considered a 'green' CE method that moves the biosphere closer to its natural, i.e. pre-Neolithic, state. Here, we test this hypothesis by comparing the biogeochemical (water- and carbon-related) changes induced by biomass plantations compared to those induced by historical human land cover and land use change. Results indicate that large-scale biomass plantations would produce a biogeochemical shift in the terrestrial biosphere which is, in absolute terms, even larger than that already produced by historical land use change. However, the nature of change would differ between a world dominated by biomass plantations and the current world inheriting the effects of historical land use, highlighting that large-scale tCDR would represent an additional distinct and massive human intervention into the biosphere. Contrasting the limited possibilities of tCDR to reduce the pressure on the planetary boundary for climate change with the potential negative implications on the status of other planetary boundaries highlights that tCDR via biomass plantations should not be considered a 'green' CE method but a full scale engineering intervention.

[1] An edited version of this chapter has been published as: V. Heck et al. (2016b). "Is extensive terrestrial carbon dioxide removal a 'green' form of geoengineering? A global modelling study". In: *Global and Planetary Change* 137, pp. 123–130. DOI: 10.1016/j.gloplacha.2015.12.008

2.1. Introduction

Terrestrial carbon dioxide removal (tCDR) i.e. harvesting terrestrial biomass and storing the contained carbon into inert stores or utilising it as bioenergy feedstock with subsequent carbon capture and storage is considered an effective mechanism for extracting carbon dioxide (CO_2) from the atmosphere (Caldeira et al., 2013; Lenton, 2010). Because this CE method would not require the implementation of major technologies as in the case of solar radiation management (SRM), it is frequently also considered a relatively safe option (e.g. Shepherd et al., 2009). The biomass focus of tCDR, and the fact that bioenergy produced from biomass is often regarded as green energy (e.g. Midilli et al., 2006; Wüstenhagen et al., 2006), suggest that tCDR might be seen a 'green' CE method, even with benefits for biodiversity or soil properties (e.g. Rowe et al., 2007; Schulz et al., 2009). One could thus assume that a world rich in biomass plantations would move the biogeochemical status of the biosphere partially back toward its natural, i.e. pre-Neolithic state with potential natural vegetation. The present modelling study quantifies the changes in terrestrial carbon-water biogeochemistry that a world in which the current cropland and grazing land is replaced by tCDR plantations would induce and compares them to the changes already caused by agriculture (e.g. Foley et al., 2005; Krausmann et al., 2013; Ostberg et al., 2015; Steffen et al., 2015). Because changes in carbon and water fluxes and pools on biomass plantations are important indicators of overall biogeochemical changes of biomass systems, we consider changes in the biogeochemical carbon-water state as a proxy for overall changes of the biogeochemical state of the system.

We argue that tCDR could be classified as a 'green' form of CE, if large-scale tCDR shifted the biosphere into a direction that partially reverses the effects of agriculture on terrestrial biogeochemistry. If the opposite was true, 'engineering' would truly be an appropriate term and tCDR indeed be a global-scale engineering intervention into planetary biogeochemistry, leaving the Earth even more anthropogenically altered than it presently is through global agriculture. To assess whether tCDR fits this classification of a green climate modification, we perform a set of stylised global model experiments, which enable us to assess the impacts of one century of tCDR plantations on global carbon-water biogeochemistry in comparison to the respective impacts of historical land use over the past century. The aim is not to investigate specific scenarios of potential tCDR implementation and their very consequences, but to gain basic insight into the biogeochemical differences between four contrasting 'worlds' a world of potential natural vegetation (PNV) without human interference; the present-day world with global-scale agriculture; and two hypothetical tCDR worlds where land areas currently converted to land use are instead cultivated with tCDR-oriented woody and herbaceous biomass plantations, respectively.

This analysis occurs in the wider context of discussions on possibilities to moderate climate change by CE as recently highlighted e.g. in the IPCC's summary for policy-makers (IPCC,

2013). Several CE methods have been proposed to reduce global warming should it continue unabatedly in the future and should mitigation efforts fail. They can be divided in two categories, namely SRM and carbon dioxide removal (CDR) (Caldeira et al., 2013; Vaughan et al., 2011). SRM methods meet with interest due to their relatively low deployment costs and high potential to reduce global mean temperature (Shepherd et al., 2009). However, residual (and potentially novel) climatic changes and their impacts, continued CO_2 effects, an absence of governance structure and rapid temperature increases in case of planned or unplanned termination of SRM deployment render its possible realisation highly problematic (Sillmann et al., 2015). In comparison, an implementation of tCDR could be seen as potentially less critical, albeit it would reduce global warming less effectively and more slowly (Caldeira et al., 2013; Shepherd et al., 2009).

Besides CE, biomass plantations for bioenergy production are part of mitigation portfolios projecting climate scenarios consistent with the 2° target (Fuss et al., 2014; Klein et al., 2014a). The Representative Concentration Pathways (RCPs) that peak within this century (RCP 2.6 and 4.5) both include extensive bioenergy use as well as large-scale re- and afforestation (Thomson et al., 2011; Vuuren et al., 2011), implying major restructuring of the land surface on top of existing land use change (LUC). While warming reduction potentials of large-scale biomass plantation deployment for either mitigation or CE have been discussed and reviewed (e.g. Beringer et al., 2011; Lenton, 2010; Slade et al., 2014), the overall biogeochemical impacts of such plantations have, to our knowledge, not yet been assessed at the global scale and compared to historical human biosphere management. For the sake of basic understanding we analyse the carbon-water biogeochemistry of two tCDR worlds in which either herbaceous or woody biomass plantations substitute historical land use. Simulations were performed with the LPJmL model of the terrestrial biosphere including agriculture and biomass plantations (Beringer et al., 2011; Bondeau et al., 2007; Schaphoff et al., 2013). As our prime interest is to quantify how a tCDR world would biogeochemically differ from today's agricultural world and a world with PNV, we assume that the plantations are deployed on all present land use areas. We ask the following question: Would either of the two tCDR worlds be closer to PNV than today's agriculture with respect to their global biogeochemical properties – or would the deviations of the tCDR worlds from the PNV world represent yet another major biogeochemical shift?

2.2. Methods

2.2.1. The LPJmL model

LPJmL is a process-based dynamic global vegetation model with representations of natural and managed ecosystems. It simulates key ecosystem processes such as photosynthesis, plant and soil respiration, carbon allocation, evapotranspiration, phenology and resource competition, at daily time steps with a spatial resolution of 0.5°. The carbon cycle in LPJmL is fully coupled to the hydrological cycle, which distinguishes evapotranspiration, runoff, snowmelt, soil moisture, river discharge and irrigation water use (Bloh et al., 2010; Gerten et al., 2004; Rost et al., 2008b). Simulations are driven by monthly fields of (temporally disaggregated) temperature, precipitation and cloud cover, annual atmospheric CO_2 concentrations, and data on soil texture and river flow directions. A detailed description of the processes controlling vegetation and biogeochemical dynamics can be found in (Beringer et al., 2011; Bondeau et al., 2007; Rost et al., 2008b; Sitch et al., 2003), hence only a short summary is provided here.

Natural vegetation is represented by nine plant functional types (PFTs) that dynamically evolve depending on climate (Sitch et al., 2003); agricultural vegetation is represented by 12 crop functional types (CFTs) and grazing land, with prescribed distribution and management such as irrigation (Bondeau et al., 2007). The model can further represent the growth and management of three lignocellulosic 2nd-generation biomass functional types (BFTs) on prescribed areas. These encompass fast growing, highly productive C_4 grasses, temperate deciduous trees, and tropical evergreen trees (Beringer et al., 2011). Their parameterisation is largely identical to their natural PFT equivalents and modified to represent the different growing conditions on managed plantations, such as regular plant arrangement, higher light availability and effective pest and fire control. Parameter values are selected from observations of the growth characteristics of *Miscanthus*/switchgrass cultivars for the herbaceous BFT, and willows/poplars and *Eucalyptus* plantations for the temperate and tropical woody BFTs, respectively. Overall the modifications lead to higher carbon assimilation in BFTs compared to their PFT equivalents. Growth, phenology and productivity of all plant types and the distinction between temperate and tropical woody BFTs are governed by climatic conditions and by management if applicable. In contrast to CFTs using the C_4 photosynthetic pathway, herbaceous BFTs can maintain high photosynthetic activity also at low temperatures down to 5° C (Naidu et al., 2003).

Irrigation water demand of CFTs and BFTs is determined from the soil water deficit below optimal growth of the present CFTs (Rost et al., 2008b, updated by Jägermeyr et al., 2015).

Irrigation water is withdrawn from rivers (including groundwater baseflow), lakes and reservoirs, taking into account irrigation efficiencies constrained by local renewable availability and applied via three different irrigation systems (Jägermeyr et al., 2015) after accounting for household, industry and livestock water use. Agricultural management is represented by three CFT- and country-specific parameters, calibrated to simulate the best approximation to FAOSTAT national yields from 1999-2003 as described by Fader et al. (2010). Note that in contrast to agricultural CFTs, BFTs are not calibrated due to a lack of data, but evaluated against field data in Section 2.2.2.

CFTs are harvested at maturity or when the maximum length of the growing period is reached (Bondeau et al., 2007). Harvest management of woody and herbaceous BFTs represents reported agricultural practices on second generation biomass plantations. For herbaceous BFTs 85% of the leaf mass is simulated to be harvested once or several times per year when aboveground carbon storage reaches 400 g/m^2 (e.g. Ashworth et al., 2013; Johnson et al., 2012). Management of woody BFTs reflects short rotation woody energy crops management in which young tree stems are cut down near the ground at relatively short intervals. In LPJmL the length of one rotation period, i.e. the length of the harvest cycle, is 8 years, which is rather at the upper end of reported intervals of 3-10 years (Lemus et al., 2005). However, the saplings that are cultivated on industrial plantations have usually been grown in greenhouses up to a considerable size of more than 30 cm. In LPJmL these cuttings are assumed to be grown from small saplings on the field, justifying relatively long rotation periods. Plantation lifetime is 40 years (i.e. 5 rotations), which is in line with estimates of three to seven rotations (Heller et al., 2003; Langholtz et al., 2013).

The general performance of LPJmL and its predecessor without managed land (LPJ) has been extensively validated. Simulation results of LPJmL that have successfully been compared against site specific or satellite data include: carbon flux dynamics over natural vegetation (e.g. Beer et al., 2006; Schaphoff et al., 2013; Sitch et al., 2003), agricultural carbon fluxes and yields (Bondeau et al., 2007; Fader et al., 2010), vegetation carbon and density (Beer et al., 2006; Lucht et al., 2002), water flux dynamics and river discharge (e.g. Gerten et al., 2004; Schaphoff et al., 2013), soil moisture (Wagner et al., 2003) and irrigation water demands (Jägermeyr et al., 2015; Rost et al., 2008b). Furthermore, various multi-model studies indicate that LPJmL results are well in the range between other (dynamic) global vegetation models (e.g. Friend et al., 2013; Gerten et al., 2004; Nishina et al., 2014).

2.2.2. Evaluation of biomass yields

Simulated biomass potentials strongly depend on the parameterisation of the plantation management in LPJmL, which in turn influences the simulated impacts on the terrestrial

carbon and water cycle. Therefore, a validation of biomass plantation performance against field data is essential for establishing the reliability of simulation results. Due to data scarcity concerning biogeochemical impacts of biomass plantations, we here limit our global-scale validation to reported biomass yields and refrain from a validation of specific biogeochemical processes. However, LPJmL is an internally consistent and well validated framework. Hence, the influence of parameter changes that maintain a good representation of biomass yields on simulated carbon and water impacts is limited.

A global validation is made difficult by heterogeneous properties of available field data as well as inherent differences between simulation and observation. The latter include differences in spatial scales (small-scale experimental plots vs. large-scale grid cell-based simulations) and environmental conditions (site-specific characteristics of soils, microclimate and cultivar variety vs. grid cell-scale averaged conditions). Heterogeneity of field data is mostly due to different foci of biomass yield studies and thus varying experimental setup (e.g. different soils, plant species, fertiliser and irrigation management, crop spacing and sapling size), which cause strong variations in reported yield ranges, even for similar plants and climates. Furthermore, experimental data is skewed geographically and mostly limited to North America and Europe (see Fig. 2.1). Comparisons between field data and larger-scale simulations should therefore be considered under the premise of large uncertainty on both sides.

For the evaluation of our model results despite all uncertainties, we compare the mean of the minimum and maximum reported yields from varying observation periods to 16-year (1993-2008) LPJmL-computed yield averages. To this end, irrigated and rainfed herbaceous and woody biomass plants were simulated to grow globally, wherever biophysical conditions enabled sustained growth (Fig. 2.1). The temporally averaged simulated yields were then compared to reported biomass yields of switchgrass, *Miscanthus*, poplar, willow and *Eucalyptus* plantations on experimental test-sites located in the respective grid cell. To depict the associated data uncertainties, the minimum and maximum of the reported yields are included as error bars in the scatterplots of Fig. 2.1. These are site-specific management uncertainties and reflect the diverse sources of reported yield ranges, such as variation of soil conditions, plant species, fertiliser and irrigation management, crop spacing or sapling size. Management uncertainty in LPJmL is limited to irrigation management (range of rainfed and fully irrigated), because soil conditions, plant species and plantation characteristics (e.g. crop spacing and sapling size) are parameterised and not varied here. We take this as a valid approximation of management uncertainty, because simulated yields depend strongly on irrigation water management in most regions, and the thus simulated yield range is likely to incorporate the overall management uncertainty. Experimental data included in this evaluation can be found in the supplementary material; the majority of literature is reviewed by Searle et al. (2014).

Immediate observations of our evaluation (Fig. 2.1) are large uncertainty ranges in both observed and modelled BFT yields as well as a poorly sampled spatial distribution of biomass plantations in experimental data. Furthermore, there are examples where two nearby experimental sites of the same biomass plantation type produce rather different levels of agreement with the simulation data, as in the mid-western US (Fig. 2.1a) or eastern Brazil (Fig. 2.1b). Such strong regional variations in field data are likely the result of differences in local conditions, experimental design or reporting, and unlikely to truly reveal deficiencies in our large-scale generalised modelling.

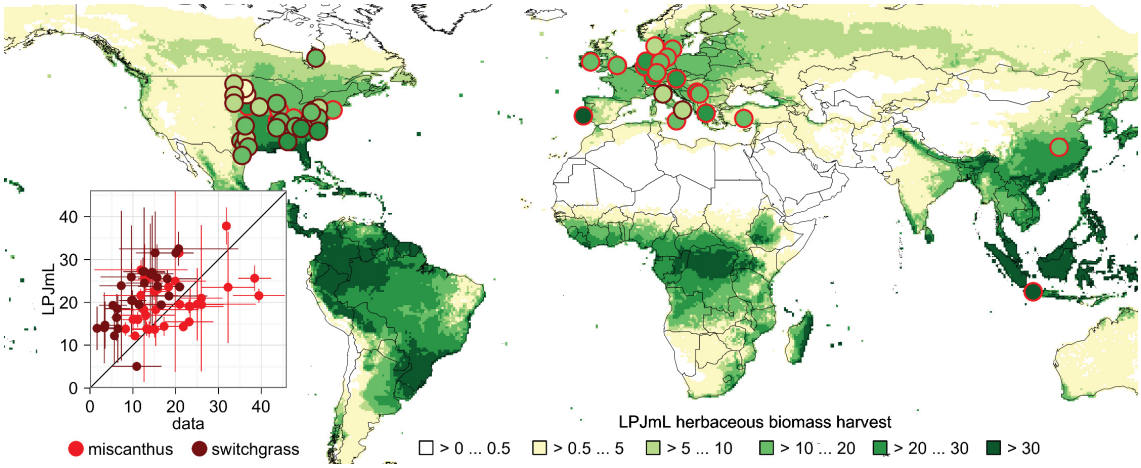

(a)Herbaceous biomass yields [t DM/ha/yr]

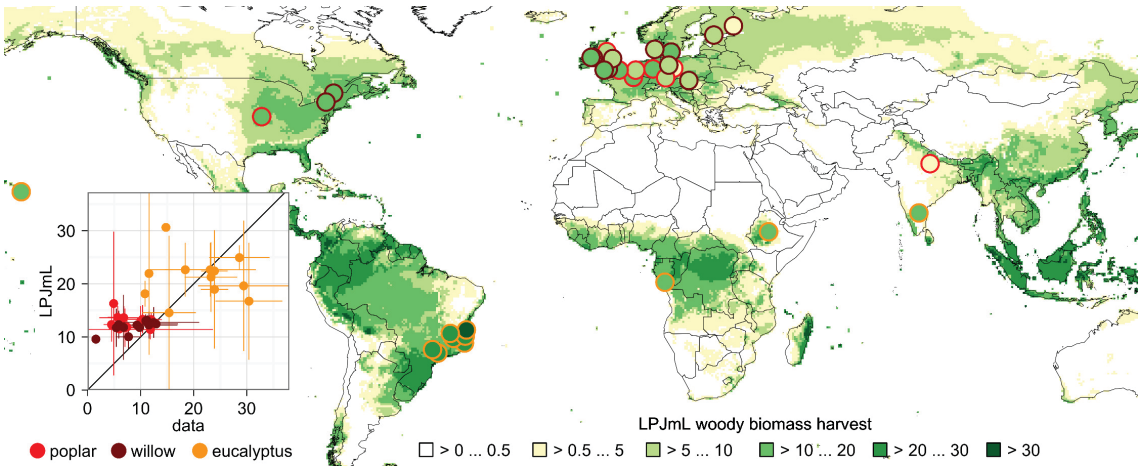

(b)Woody biomass yields [t DM/ha/yr].

Figure 2.1.: Map of simulated biomass yields from rainfed herbaceous (a) and woody (b) BFTs (averages 1993-2008). Dots indicate the location of the experimental sites and measured yield, with colours scaled to map colours. Scatterplots contrast the observed and simulated yields in the respective grid cells. Model uncertainty is derived from simulations with and without irrigation. Observation uncertainty reflects dependencies on plantation management (see text).

Considering such large uncertainties, LPJmL simulations are within the general range reported for switchgrass and *Miscanthus* yields (scatterplot in Fig. 2.1a), though with considerable scatter to both sides of the 1:1 line. A comparison of the mapped simulated yields to the observed dots in the foreground indicates that especially in the US and Europe, simulated and observed yields are similar, yet also with exceptions. A single study area in Indonesia indicates that simulated high biomass yields in the tropics should be realistic.

Despite even more degrees of freedom in the cultivation and management of woody biomass plantations (e.g. sapling size and planting density), Fig. 2.1b indicates that LPJmL simulations do not substantially deviate from the reported yields of woody biomass trees in Europe, the US and west Africa, but underestimate yields for some highly productive test sites in Brazil and southern India. However, these test sites were subject to intensive irrigation and fertilisation management, which justifies that reported yields can only be met by LPJmL with high irrigation, i.e. the upper uncertainty range. A sensitivity analysis of woody biomass plantation management parameters (results not shown) indicated that a shorter rotation period (6 years) and plantation lifetime (30 years) led to small yield reductions in *Eucalyptus* test sites and to a small yield increase in poplar and willow test sites, owing to the fact that tropical BFTs profit from longer rotation periods because of slower growth. However, the yield differences are relatively small, for example when compared to yield differences induced by CO_2 fertilisation of the 21st century. The chosen parameterisation results in the best overall match between data and observations.

2.2.3. Model setup and simulations

We assess the influence of one century of tCDR plantations (trees, tCDR-t; grass, tCDR-g) on global carbon-water biogeochemistry in comparison to the impacts of historical agricultural development during the past century (AGR simulation) and measure the differences to the potentially 'natural' vegetation state of the Earth system (PNV). For this, the LPJmL model was forced with historical climate data taken from CRU TS3.10 (Harris et al., 2014) covering the period 1901-2005. All four simulations (Table 2.1) were preceded by a 5000-year spin-up with PNV during which the climate of the years 1901-1930 was repeated, bringing soil carbon pools and natural vegetation distribution into equilibrium, and a second spin-up period of 390 years. The latter had unchanged conditions for the PNV reference simulation but introduced historical agriculture (annual cropland extent and crop type distribution per 0.5° grid cell after Portmann et al., 2010, irrigated fraction per crop type after Jägermeyr et al. (2015)) from 1700-1900 in the other simulations, allowing for a historical adjustment of carbon pools. The subsequent simulations from 1901 used the historical land use and irrigation patterns in the AGR simulation. Our tCDR scenarios assume large-scale and instantaneous implementation with the extent of current land use areas. For better comparability to AGR,

we fix tCDR-g and tCDR-t areas and irrigated cell fractions to cropland and pasture areas of 2005 (Table 2.1). For the quantification of carbon and water related impacts after ∼100 years of tCDR cultivation, we average changes in biogeochemical carbon-water states over the last 24 simulation years (1982-2005), i.e. three harvest cycles of woody plantations.

Simulation	Vegetation type	Area	2nd spin-up
PNV	potential natural vegetation	global	390 years PNV
AGR	historical land use	historical land use areas	390 years agriculture
tCDR-g	herbaceous biomass	land use areas of 2005	390 years agriculture
tCDR-t	woody biomass	land use areas of 2005	390 years agriculture

Table 2.1.: LPJmL simulations of the different worlds from 1901-2005. Land use areas (crops & pastures) and irrigation patterns as in Jägermeyr et al. (2015).

2.2.4. Biogeochemical change metrics

To determine whether tCDR worlds would imply biogeochemical alterations of similar magnitude as historical land use, we consider four variables which constitute a subset of biogeochemical variables influential for Earth system functioning, as follows:

1. Net water fluxes, here evapotranspiration (ET), important for moisture cycling and heat exchange.
2. Vegetation productivity (NPP) as a measure of biomass functionality producing the trophic basis on which all living land organisms depend.
3. The land system carbon storage pool (C), i.e. soil and litter carbon (C_{soil}) plus vegetation carbon (C_{veg}), which is essential for (climate effective) carbon storage and forms the substrate of landscapes.
4. Vegetation carbon residence time (τ), a determinant of carbon cycle intensity in vegetation that can be inferred from C_{veg} and NPP (Friend et al., 2013; Koven et al., 2015) for natural vegetation and woody biomass plantations for relatively short time steps:

$$\tau \approx \frac{C_{veg}}{NPP - \frac{\Delta C_{veg}}{\Delta t}}. \tag{2.1}$$

   Eq. 2.1 is not valid on agricultural land and herbaceous biomass plantations due to annual or multiple harvest events. Thus, the carbon residence time is determined from the crop growing period (t_{gc}): $\tau = 0.5\ t_{gc}$ on those areas.

We derive the four-dimensional biogeochemical state vector ($\vec{S}$, Eq.2.2) from the global averages of these variables and obtain local vectors at grid cell level for the period 1982 - 2005

for each of our simulations. To compensate for the different orders of magnitudes of vector components, each component is normalised to PNV on both global and local levels:

$$\vec{S_n} = \begin{pmatrix} ET/ET_{PNV} \\ NPP/NPP_{PNV} \\ C/C_{PNV} \\ \tau/\tau_{PNV} \end{pmatrix} \rightarrow S_{n_{PNV}} = \begin{pmatrix} 1 \\ 1 \\ 1 \\ 1 \end{pmatrix} \tag{2.2}$$

We choose the difference in the magnitude d and the angle θ between the normalised state vectors $\vec{S_n}$ of PNV and AGR, tCDR-t and tCDR-g, respectively, as measures of difference between the corresponding worlds (supplementary Fig. 2.4):

$$d = |\vec{S_n}| - |\vec{S_{n_{PNV}}}| \qquad \theta = \arccos\left(\frac{\vec{S_n} \cdot \vec{S_{n_{PNV}}}}{|\vec{S_n}||\vec{S_{n_{PNV}}}|}\right). \tag{2.3}$$

The difference in magnitude of two state vectors, d, is a measure of how the respective land use world differs from PNV in each of the fundamental variables (i.e. increase or decrease relative to PNV). It can be interpreted as an aggregate measure of volume changes in the biogeochemical biosphere state. The angle between vectors ('angular shift' in the following), θ, is a measure of how the vector components are differentially affected, i.e. how they change in relation to each other, thus indicating how internal system dynamics are shifted. If all state vector components are positive, angular shifts range between $0°$ and $90°$. A balanced increase of all vector components results in $\theta = 0$, whereas a change in just some vector components leads to a shift of vector direction (see supplementary Fig. 2.4).

To better understand the discrepancy between the different worlds, the components underlying the metric and other carbon and water fluxes are analysed in some more detail.

2.3. Results and discussion

2.3.1. Metrical shifts in biogeochemistry

Applying our aggregate metric of angular and absolute state vector shifts (Section 2.2.4), we find that global angular state vector shifts induced by tCDR (irrespective of whether woody or herbaceous) would tend to be higher than those induced by current agriculture, which has already had strong impacts on many Earth system components (e.g. Foley et al., 2005; Pongratz et al., 2009; Rost et al., 2008a). In other words, large-scale implementation of tCDR on current agricultural land would shift the biosphere's biogeochemical status even further away from PNV than historical land use did (angular shifts in Figure 2.2) due to higher

shifts in the interrelation of different biogeochemical components (refer to Section 2.2.4). The angular shifts of woody biomass plantations (tCDR-t) are similar in magnitude to those of AGR, whereas a tCDR-g world would even induce global shifts almost twice as large (Fig. 2.2).

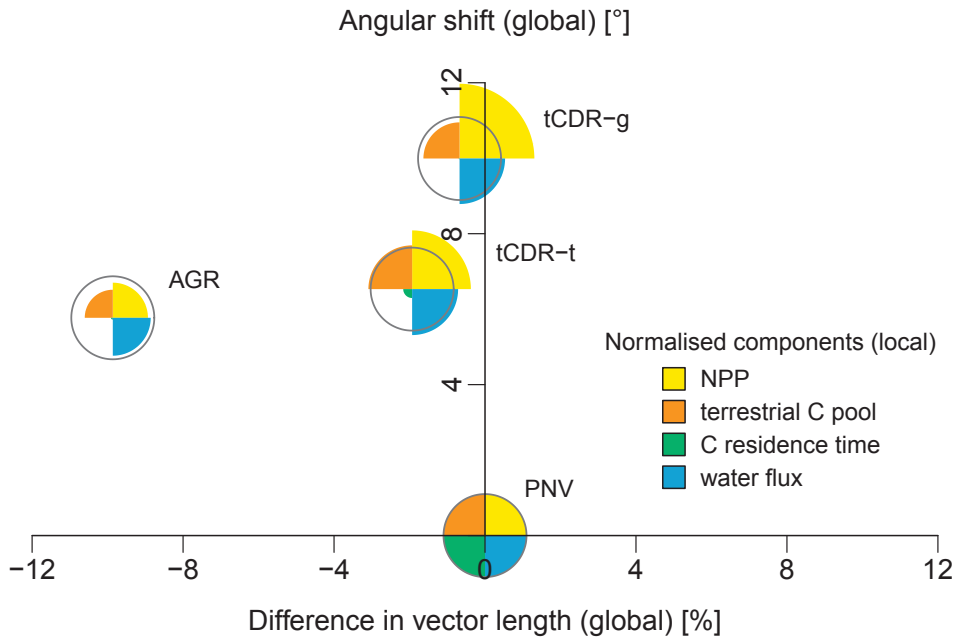

Figure 2.2.: Angular shifts (y-axis) and differences in vector length (x-axis) between the state vectors of the land use worlds and the PNV world, represented by the midpoint of the respective grey circle (indicating the components of PNV). The contributing changes (i.e. impacts on cultivated areas) are normalised to PNV and depicted as coloured components.

The biogeochemical differences underlying similar angular shifts are very different for the AGR and the tCDR worlds (position on x-axis in Fig. 2.2), pointing to dissimilarities in the nature of changes. In contrast to the effect of historical agriculture, which induces a large negative aggregate difference d to PNV, the tCDR-t and tCDR-g worlds show much smaller negative differences to PNV. However, these overall smaller differences must not be taken as evidence for tCDR worlds being closer to PNV, since d only measures the aggregate differences of the four state vector components. The actual changes of metric components (shown for the cultivated areas alone in colours in Fig. 2.2) indicate that smaller differences on tCDR areas are caused by component-specific increases and decreases, namely by increased

NPP and water fluxes, and decreased carbon pools and residence time (also see Table 2.2). In contrast, the large negative difference d between AGR and PNV is caused by decreases in all of the state vector components. Overall, we find that – besides smaller differences in C pools – both tCDR worlds show larger changes from a PNV world than historical LUC on the global scale.

The spectrum of local angular shifts on the actually cultivated areas (Fig. 2.3 c, d) is similar in the AGR and tCDR-g worlds, with the majority of shifts being in the same interval ($30° - 40°$) in both worlds. However, tCDR-g exhibits more cells with stronger angular shifts ($> 40°$) than AGR, meaning that also at the local level biogeochemical shifts are higher under tCDR-g than those brought about by historical LUC. Furthermore, we find mostly positive aggregate differences to PNV in tCDR-g in contrast to mostly negative aggregate differences in AGR (indicated by the colour scaling in Fig. 2.3), highlighting once more that the similar angular shifts refer to different causes (as found for the global sums in Fig. 2.2). This causality is reflected almost homogeneously in the spatial distribution of aggregate differences in Fig. 2.3 (see supplementary Fig. 2.5 for tCDR-t). The regional differences of tCDR-g to PNV are positive in the majority of regions, with exceptions of negative differences in the boreal region, western Africa and the western US. In contrast, historical LUC has induced negative aggregate differences to PNV in almost all parts of the world, with few exceptions of increases in dry but irrigated areas.

The retained negative and positive metric differences of tCDR and LUC across spatial scales confirm that tCDR would not establish a more natural system than historical LUC – neither on the global nor on the regional level. It implies even larger, and distinct, biogeochemical shifts away from PNV than those brought about by historical land use.

So far LUC has modified the Earth system in a way that carbon and water fluxes are smaller than under natural conditions (Pongratz et al., 2009; Rost et al., 2008a), whereas cultivation of biomass plantations would engineer the system to higher carbon (NPP, harvest) and water fluxes (ET) (Fig. 2.2, Table 2.2). Especially high carbon fluxes in and out of the biosphere and the shorter residence time of vegetation carbon point towards an intensification of the carbon cycle. Unlike the well-understood global warming-induced intensification of the hydrologic cycle (e.g. Huntington, 2006), the meaning of an intensifying carbon cycle is less obvious. However, such alterations of biogeochemical conditions are likely to have substantial effects on ecosystems on all scales, with repercussions to underlying processes (not explicitly studied here) and to the whole Earth system (Ostberg et al., 2013).

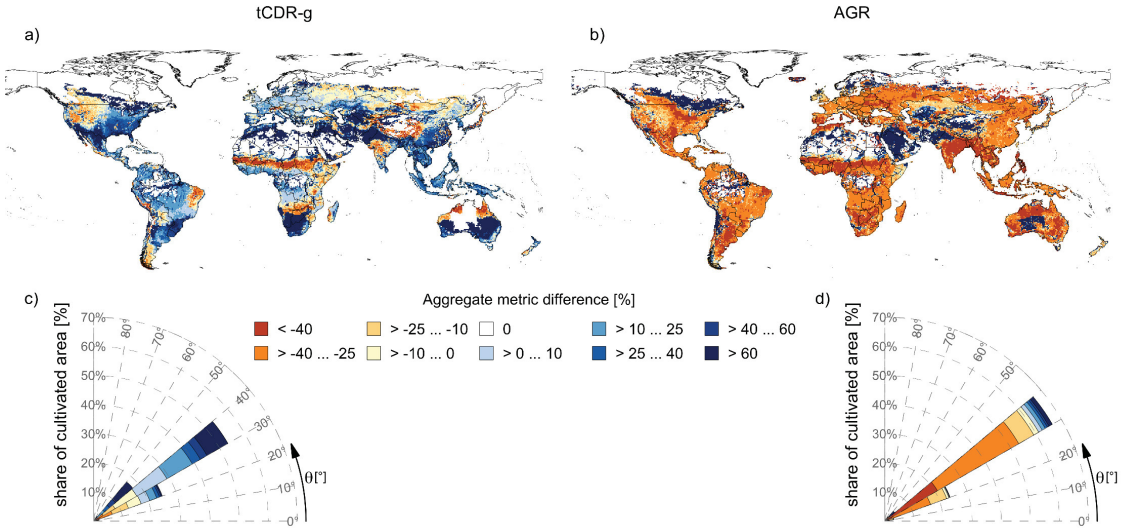

Figure 2.3.: Absolute differences on cultivated areas (top), together with their aggregation to the respective angular shifts at grid cell level (bottom) for the cultivated areas of tCDR-g (a, c) and AGR (b, d). The bottom diagrams (c, d) combine angular shifts and differences. Cells with similar angular shifts are aggregated in pie segments (radial scaling). Pie segments are coloured according to the respective metrical differences in that segment, with the same colour scaling as in the map. To avoid that results mainly reflect the cultivation pattern (i.e. that they are implicitly weighted with the cultivated fractions of cells), we calculated the metric on the actually cultivated areas only. See Fig.2.5 for tCDR-t.

2.3.2. Impacts and implications of changes in the individual metric components

We here analyse the changes in individual metric components both, quantitatively and qualitatively (supplementary Fig. 2.6, Table 2.2). For that purpose the planetary boundary concept is suited to study the severity of implications of large-scale tCDR, as the status of seven out of the nine proposed boundaries (Rockström et al., 2009; Steffen et al., 2015) is influenced by land use. The positioning of our hypothetical worlds within this framework allows us to classify the impacts of tCDR for Earth system functionality.

On the positive side, the simulated woody and herbaceous biomass yields (7.2 PgC/yr and 19.0 PgC/yr, Table 2.2) indicate that tCDR – or bioenergy production as a form of mitigation – could help to reverse the transgression of the planetary boundary for climate change, i.e. reduce global warming. Assuming combined biomass conversion and storage efficiencies of 50% (Lenton, 2010) as well as steady soil and vegetation carbon pools, we estimate a temperature reduction potential of 0.07-0.19 K after 10 years of herbaceous biomass

plantations, based on the TCRE-approach (Matthews et al., 2009), with a range of warming of 0.7 - 2.0 K per 1000 PgC (Gillett et al., 2013).

Table 2.2.: Absolute values of studied variables under conditions of PNV as well as their absolute (and percentage) differences in tCDR and AGR worlds compared to PNV, averaged over 1982-2005.

Variable	PNV	tCDR-g	tCDR-t	AGR
NPP [PgC/yr]	61	+14 (+22%)	+7 (+11%)	-3 (-5%)
Soil carbon [PgC]	2099	-62 (-3%)	+8 (+0%)	-138 (-7%)
Vegetation carbon [PgC]	776	-160 (-21%)	-122 (-16%)	-193 (-25%)
Heterotrophic respiration [PgC/yr]	54	-3 (-6%)	+1 (+2%)	-8 (-15%)
Harvest [PgC/yr]	–	19	7	9
ET [km^3/yr]	63159	+1418 (+2%)	+1474 (+2%)	-60 (-0%)
Evaporation [km^3/yr]	7666	+1225 (+16%)	+2257 (+29%)	+6952 (+91%)
Interception loss [km^3/yr]	8777	-98 (-1%)	-41 (-0%)	-1712 (-20%)
Transpiration [km^3/yr]	46717	+291 (+1%)	-741 (-2%)	-5300 (-11%)
Discharge [km^3/yr]	55134	-2149 (-4%)	-2261 (-4%)	-722 (-1%)
Irrigation water consumption [km^3/yr]	–	1344	1501	1164

According to the present findings, this potential implies significant NPP increase on biomass plantations, which was the most crucial difference between current agriculture and tCDR in our aggregate metric, as land use in the form of tCDR is up to 20% more productive than PNV around the world (supplementary Fig. 2.6). This is in strong contrast to the current situation (AGR), where NPP only increased in dry areas with irrigation and in other intensively managed agricultural areas (e.g. in parts of Europe, supplementary Fig. 2.6). While DeLucia et al. (2014) estimate high potential NPP increases for crops with low nitrogen requirements and high water use efficiency, Haberl et al. (2013) argue that global NPP is limited by biospheric constraints and unlikely to exceed current NPP. However, our evaluation of the simulated yields (Section 2.2.2) indicates that – in intensively managed systems – productivity and biomass yields are of realistic magnitude.

Nonetheless, the simulated NPP increase would imply more or less intensive nutrient and water management, with direct feedbacks to the status of other planetary boundaries such as those for biogeochemical flows and freshwater use. We estimate N fertiliser requirements of 50-150 kg N/ha/yr for herbaceous biomass plantations, in line with many respective field studies (Section 2.5, supplementary material), assuming replenishment of harvested N and a biomass N content between 0.5% (Karp et al., 2008; Kauter et al., 2001) and 1.5 % (Yu et al., 2013). The simulated herbaceous biomass harvest would thus require an N fixation significantly higher than the currently proposed planetary boundary value (62 TgN/yr)

(Steffen et al., 2015). Also, N_2O emissions resulting from fertilisation have a high global warming potential which in turn decreases the temperature reduction potential.

Overall, simulated impacts on global water dynamics are smaller than those on carbon dynamics (Table 2.2). There are however large deviations between tCDR and AGR that contribute to the contrasting metric differences. ET in both tCDR worlds is significantly higher compared to both the present and the PNV world (mostly below 40° N, supplementary Fig. 2.6) due to higher plant transpiration and interception. As a corollary, irrigation water consumption in the tCDR worlds is simulated to be 15% to 28% higher than currently (Table 2.2), which would imply a position closer to the planetary freshwater boundary (currently positioned at 4000 km^3/yr and being approached fast, Gerten et al. (2015)). The higher ET and increased irrigation water consumption in our tCDR worlds (caused by longer growing periods, higher vegetation density and higher transpiration) lead ultimately to more significant discharge reductions than under historical land use.

Further biogeophysical changes due to large-scale tCDR, such as changes in albedo or surface roughness (Bagley et al., 2014) are likely to influence local and regional climate (Georgescu et al., 2011; Tölle et al., 2014), with possible teleconnections at global scale (Swann et al., 2012). These changes strongly depend on the cultivation region, as well as the replaced vegetation (Caiazzo et al., 2014). Nevertheless, a large-scale modification of terrestrial biogeophysics with impacts on the atmospheric circulation might also be significant at the global scale and thus represent high risks of transgressing the global land-system boundary (motivated along the exchange of energy, water and momentum between the land surface and the atmosphere; Steffen et al., 2015).

Last but not least, the acquisition of large areas for biomass plantations poses risks for biodiversity, which is often the main concern of bioenergy sustainability studies (Dornburg et al., 2010). The impacts on biodiversity in a tCDR world − and thus on the status of the planetary boundary for biosphere integrity − are difficult to estimate in the context of our study since they depend vastly on plant choice, plantation management and the replaced land use system. Comparing agricultural systems to biomass plantations, especially woody biomass plantations are shown to maintain higher biodiversity than intensive agricultural systems (Lindenmayer et al., 2004; Londo et al., 2005; Schulz et al., 2009). However, there are conflicting views on biodiversity impacts when replacing pastures with biomass plantations (as in our tCDR simulations) (Felton et al., 2010; Hsu et al., 2010; Sage et al., 2010; Werling et al., 2014). Overall, tCDR might pose slightly smaller risks to biosphere integrity boundary than historical LUC.

Similar to the biogeochemical metric shifts analysed above (Section 2.3.1), the influence of tCDR on the status of the planetary boundaries demonstrates once more that biomass plantations do not represent a more natural system than today's agricultural system. While

our analysis has shown that large-scale tCDR could reduce the degree of transgression of the planetary boundary for climate change (and potentially that for ocean acidification, which is directly related to atmospheric CO_2 concentration), it would at the same time result in a similar or even higher pressure on other boundaries such as those for land-system change, biosphere integrity, biogeochemical flows, and freshwater use than today's agriculture-dominated world. This would be especially true if tCDR were implemented alongside current agriculture.

2.4. Conclusions

In conclusion, our analysis has shown that shifts in carbon-water biogeochemistry induced by tCDR with large-scale biomass plantations would be even higher than those induced by historical land use. The nature of those tCDR-induced shifts, however, differs from those historical shifts. This means that the large-scale implementation of tCDR would not be a 'green' transition back to a more natural state of the biosphere, but rather another major human engineering intervention into terrestrial biogeochemistry, moving Earth further into a historically unprecedented state of anthropogenic imprint. Eventually, the possible, yet limited, contributions of tCDR to reduce climate change would come at the price of similar or higher pressures on the planetary boundaries for land-system change, biosphere integrity, biogeochemical (nitrogen and phosphorus) flows, and freshwater use. We thus argue that tCDR must be considered a form of full-fledged engineering with massive biogeochemical shifts and unknown side-effects thereof.

Acknowledgements This work was funded by the DFG in the context of the CE-Land project of the Priority Program “Climate Engineering: Risks, Challenges, Opportunities?” (SPP 1689).

Author contributions VH and WL designed the study and developed the biogeochemical change metric. VH collected the data for the evaluation of biomass yields, modified model parameters to improve the model performance and performed the simulations and analysis. VH prepared the manuscript with contributions from all co-authors.

2.5. Supplementary material

Experimental data included in the evaluation of biomass yield simulations by LPJmL (Sec. 2.2.2) and a description of model parameter adjustments are attached in Appendix A.

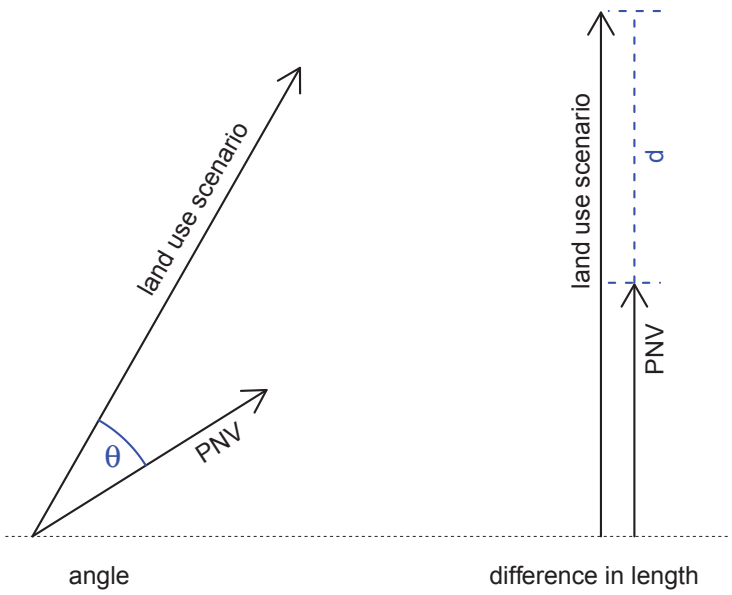

Figure 2.4.: Schematic angular shifts Θ and difference in vector length d, between a land use scenario and PNV state vector in two dimensions.

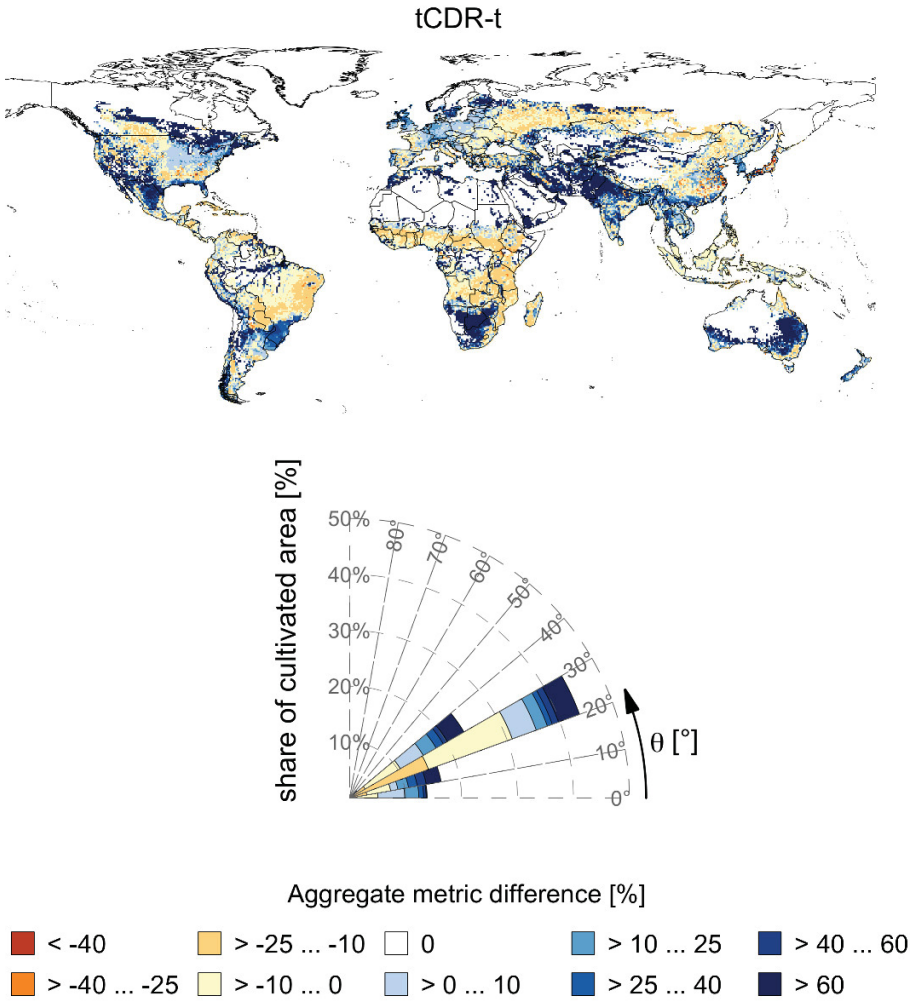

Figure 2.5.: Absolute differences on cultivated areas (top), together with their aggregation to the respective angular shifts at grid cell level (bottom) for the cultivated areas of tCDR-t. The bottom diagram combines angular shifts and differences. Cells with similar angular shifts are aggregated in pie segments (radial scaling). Pie segments are coloured according to the respective metrical differences in that segment, with the same colour scaling as in the map. To avoid that results mainly reflect the cultivation pattern (i.e. that they are implicitly weighted with the cultivated fractions of cells), we calculated the metric on the actually cultivated areas only.

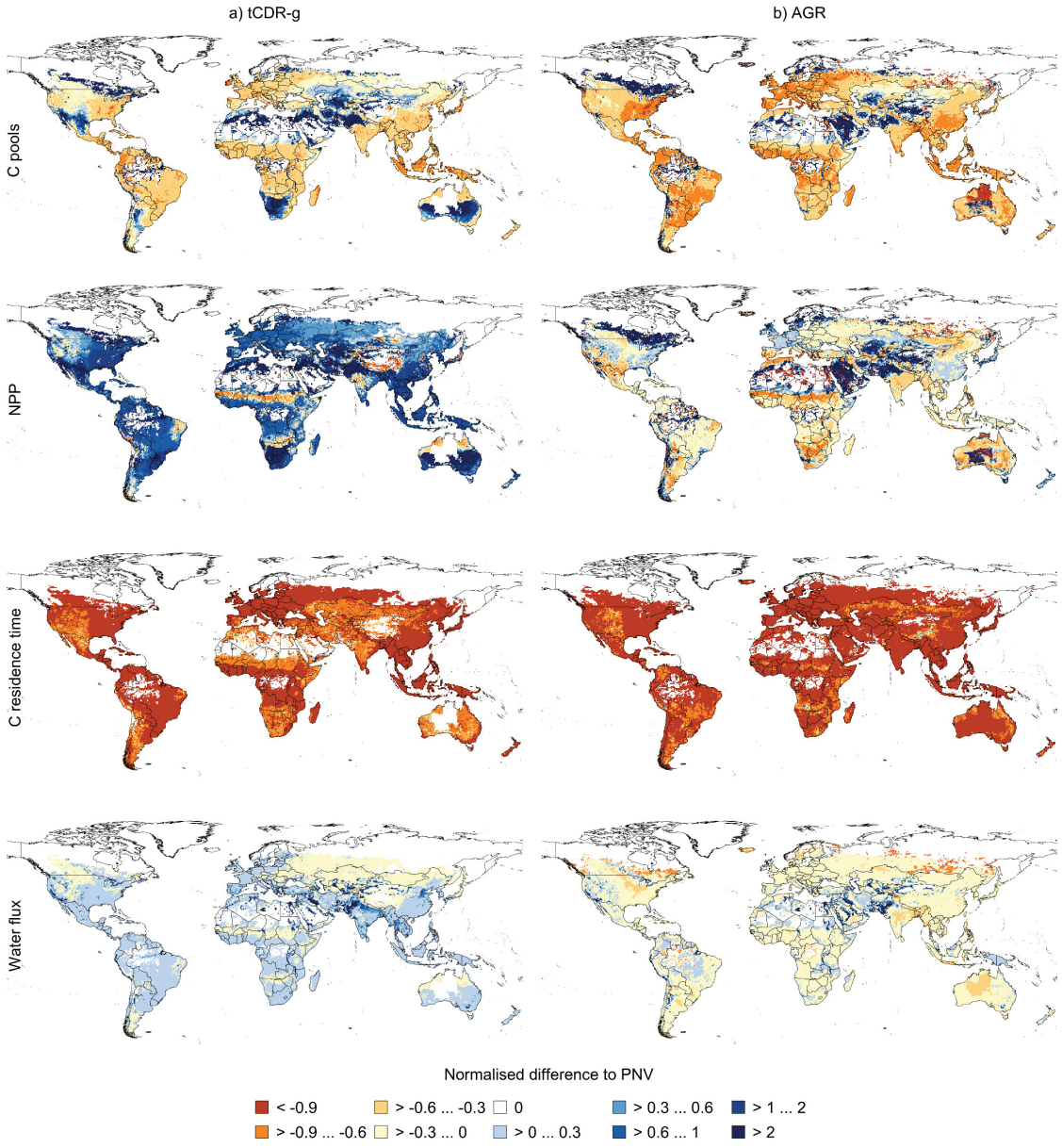

Figure 2.6.: Normalised differences of the metric components on the cultivated areas (C pools, NPP, C residence time and water flux)

3. Are biomass-based negative emissions compatible with safeguarding planetary boundaries? [1]

Vera Heck[1,2], Dieter Gerten[1,2], Wolfgang Lucht[1,2,3]

[1] Potsdam Institute for Climate Impact Research, Research Domain 1: Earth System Analysis, Telegraphenberg A62, 14473 Potsdam, Germany

[2] Humboldt-Universität zu Berlin, Department of Geography, Unter den Linden 6, 10099 Berlin, Germany

[3] Integrative Research Institute on Transformations of Human-Environment Systems, Unter den Linden 6, 10099 Berlin, Germany

3.1. Main manuscript

With the Paris Agreement 195 nations committed to 'holding the increase in the global average temperature to well below 2°C above pre-industrial levels and pursue efforts to limit the temperature increase to 1.5°C' (UNFCCC, 2015). It is noted that this requires 'a balance between anthropogenic emissions by sources and removals by sinks of greenhouse gases in the second half of the century' (UNFCCC, 2015), implying net zero greenhouse gas (GHG) emissions. This either calls for a complete decarbonisation of the energy sector or a balance between positive and negative emissions (NE) (Rogelj et al., 2015; Sanderson et al., 2016). In fact, modelled socio-economic pathways compatible with a 2°C or 1.5°C goal depend upon NE via bioenergy with carbon capture and storage (BECCS) (Fuss et al., 2014; Gasser et al., 2015). However, large-scale deployment of BECCS would have consequences for global land use (Vuuren et al., 2011) implying significant impacts on other Earth system components besides atmospheric CO_2 concentrations (Heck et al., 2016b; Vaughan et al., 2011). Here we explore the option space of NE via BECCS and potential trade-offs with planetary boundaries (PBs) in the context of a 'safe operating space' for global societal development (Rockström et al., 2009; Steffen et al., 2015). We

[1] This manuscript is currently under review at Nature Climate Change for publication as a letter.

show that while BECCS is intended to lower the pressure on the planetary boundary (PB) for climate change, large-scale bioenergy production would most likely steer the Earth system closer to the PB for freshwater use and lead to further transgression of the PBs for land system change, biosphere integrity and biogeochemical flows.

Negative emissions can fulfil several purposes. In a prospective, 2°C or 1.5°C warmer world with balanced sinks and sources of GHG emissions, they can allow for limited remaining fossil fuel use and/or compensate remaining agricultural or natural emissions (e.g. forest fires) or carbon leakages. If a complete decarbonisation of the fossil fuel and agricultural sectors is achieved, NEs could sequester CO_2 to reduce atmospheric CO_2 concentrations. Currently, BECCS is discussed as a promising NE technology (Schleussner et al., 2016). It is therefore of considerable interest to examine the implications of achieving NE via BECCS in a holistic framework, such as the framework of a 'safe operating space' (Rockström et al., 2009; Steffen et al., 2015) – delineated by nine PBs for human perturbations of the Earth system.

Here, we quantitatively assess trade-offs between BECCS and the status of five out of nine PBs for a scenario of 2° global warming above preindustrial and an underlying agricultural land use pattern to be maintained for food production. We consider the two PBs identified as core PBs, climate change and biosphere integrity, as well as the PBs for land-system change, biogeochemical flows and freshwater use, which are already transgressed except for the PB for freshwater use (Steffen et al., 2015). The latter four PBs have sub-global operating scales which are recognised in the definition of regional boundaries underpinning the global-level boundaries (Table 3.1, Steffen et al., 2015). To capture the importance of regional change for the functioning of the Earth System we adopt these regional boundaries as environmental limits. Each (global and regional) boundary is set at the safe end of a zone of uncertainty. At the other end of the uncertainty zone a dangerous zone of high risk to change in Earth System functioning begins (Steffen et al., 2015).

Within this framework we distribute herbaceous or woody biomass plantations (irrigated or rainfed) around a fixed agricultural land use pattern using a spatially explicit multiobjective optimisation approach (see Methods). Two alternative optimisation objectives are examined in this study: i) maximising biomass yields for NE under the constraints of regional boundaries and their uncertainty zones and ii) achieving prescribed biomass yields for NE while minimising the impacts on global PBs. We measure the state of the Earth system with respect to each of the five PBs via global and regional control variables and their uncertainty range (Table 3.1, see Methods for details). The optimised biomass plantation patterns are combined with the agricultural baseline and assessed for biogeochemical and PB impacts with the well-established global biogeochemical and hydrological model LPJmL, driven by an ensemble of 19 climate scenarios scaled to reach a global warming of 2° in in the second

half of the century (Heinke et al., 2013) and capturing differences in the spatial patterns produced by 19 GCMs (see Methods). To obtain NE and energy potentials we consider two alternative biomass conversion pathways. One with a high capture rate (90%) such as biomass to hydrogen (B2H2) which yields a decarbonised energy carrier with high energy conversion efficiency (0.55) (Klein et al., 2014b) and one with a lower capture rate (48%) and conversion efficiency (0.41) such as biomass to liquid fuels (B2L) (Klein et al., 2014b). Input of fossil fuels for biomass production and transportation is assumed to be 10% of the primary energy content (Edenhofer et al., 2011; Qin et al., 2006).

In the agricultural baseline scenario – developed as one component of a socio-economic pathway achieving the 2°C-goal (namely RCP2.6 without biomass plantations Hurtt et al. (2011) and Vuuren et al. (2011)) – the global PBs for climate change, biosphere integrity, land system change and nitrogen flows are transgressed even further than at present for today's land use pattern (Table 3.1). Thus, in a strict sense, navigation of human development within the safe operating space is not compatible with this scenario as BECCS would put additional pressure on the PBs. However, the PB for climate change has been identified as a core boundary, the substantial and persistent transgression of which would drive the Earth system out of the Holocene state (Steffen et al., 2015). To prevent an imminent transgression out of the climate change uncertainty zone might justify the transgression of one or more other boundaries. Nonetheless, the status of regional boundaries should remain within the safe zone or at least within the uncertainty zone, because a substantial transgression of regional boundaries can generate feedbacks to large-scale processes (Steffen et al., 2015).

Therefore, we evaluate biomass-based NE while ensuring adherence to regional safe limits (i.e., avoiding the uncertainty zone of increasing risk of system change) or to the regional uncertainty zone (i.e. allowing transgression into the uncertainty zone, but not into the dangerous zone of high risks). Figure 3.1 shows a large resulting range of NE potentials. Small opportunities for biomass plantations in regionally safe zones result in a marginal CCS potential of 0.13 GtC/a with the more efficient conversion to hydrogen or 0.07 GTC/a if biomass is converted to liquid fuel (Fig. 3.1). Taking into account the related LUC emissions and input of fossil fuels for production, the resulting actual NE potential is smaller than 0.1 GtC/a (Fig. 3.1), corresponding to approximately 1% of current emissions. Thus, if regional safe limits are adhered to, NEs can only marginally contribute to balancing remaining emissions or reducing atmospheric CO_2 concentrations.

Boundary	control variable		status RCP2.6 in 2050 (without BECCS)	
	global	regional	global	regional
climate change	maximal atmospheric CO_2 concentration (350ppm - 450 ppm)	not defined	not known (442ppm with BECCS)	not defined
biosphere integrity	minimum global biodiversity intactness index (BII) (90%- 30%)	minimum BII per continental biomes (90% - 30%)	75.6% (current: 76.8%)	individual continental biomes: 99 to 29%
land system change	maximum forest cover reduction (25% - 46%)	maximum forest cover reduction per continental biome (tropical:15%-40%, temperate: 50% - 70%, boreal: 15% - 40%)	27% (current: 26%)	tropical: 26% (5-35%), temperate: 44% (39-61%), boreal: 17% (13-30%)
biogeochemical flows (N)	maximal intentional biological N fixation (62 TgN/a)	maximal atmospheric NH_3 concentration ($1\mu g\ m^{-3}$ - $3\ \mu gm^{-3}$) and N concentrations in surface runoff (1.0 mg Nl^{-1} - 2.5 mg Nl^{-1})	141 TgN/a (current: 121.5 TgN/a (Bouwman et al., 2011))	approx. transgression in 22-7% (NH_3 in atmosphere) and 64-48% (N in runoff) of land use grid-cells
freshwater use	maximum blue water consumption (4000 $km^3\ yr^{-1}$)	maximum monthly withdrawal as percentage of mean monthly discharge (low-flow months: 25%-55%; intermediate-flow months: 30%-60%; high-flow months: 55%-85%)	1396km^3 (model range: 1379km^3-1422km^3) (current: 1192km^3)	maximum withdrawal is exceeded in 24%-21% of catchments (multi-model mean)

Table 3.1.: Control variables of the considered planetary boundaries with the proposed uncertainty range (in brackets) (Steffen et al., 2015) and the status calculate here, considering the agricultural land use reference (RCP2.6 without bioenergy). Model ranges and means are obtained from LPJmL simulations of the land use reference driven by an ensemble of 19 climate scenarios with a global warming of 2°C (see Methods).

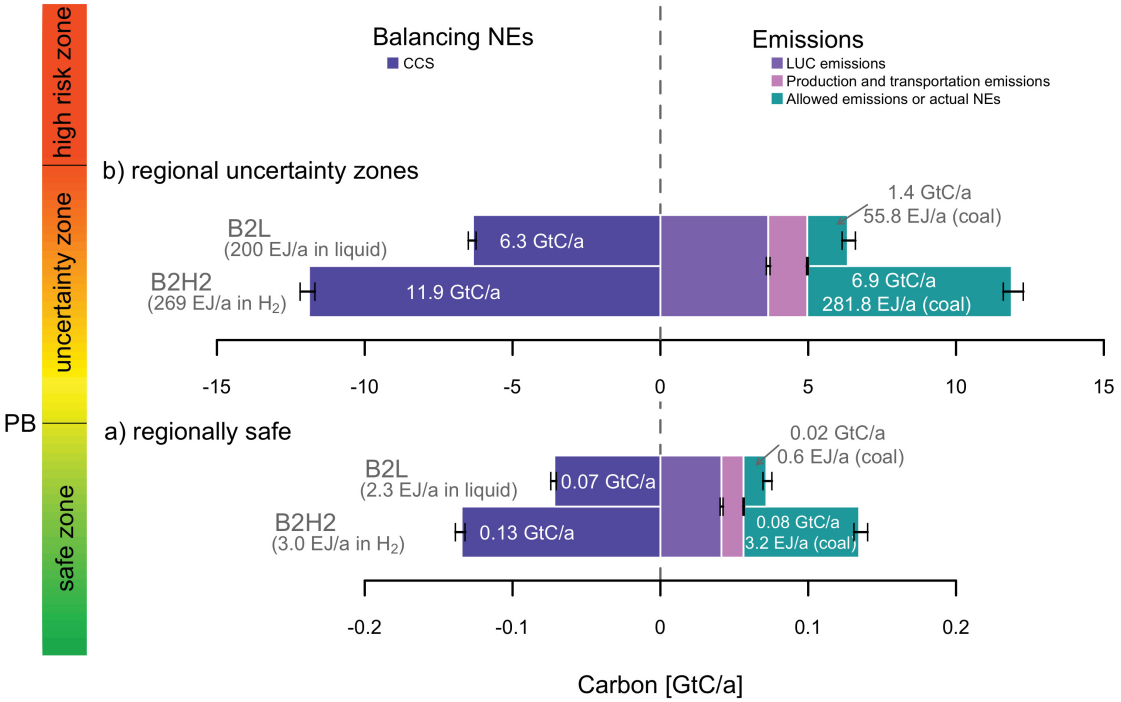

Figure 3.1.: Emission balance for two biomass conversion pathways with low (B2L) and high (B2H2) efficiency. Biomass yields are optimised under the constraints of staying within a) regionally safe or b) regional uncertainty zones. Allowed emissions or actual emissions are derived from CCS potentials, subtracting emissions associated with LUC, production and transportation of biomass. Error bars reflect the range of LPJmL simulations driven by an ensemble of 19 climate scenarios with a global warming of 2°C (see Methods).

Relaxing the optimisation constraint to allow a transgression of regional safe limits but staying within the uncertainty zone increases the potential for BECCS significantly. With the more efficient B2H2 pathway, the CCS potential is 11.9 GtC/a (Fig. 3.1) while producing 269 EJ/a in form of hydrogen. The conversion to liquid fuels halves the CCS potential and energy yields are reduced by 20% compared to the hydrogen pathway. The actual potential of NE, however, is smaller than the CCS potential because of substantial LUC emissions of 3.6 GtC/a (averaged over a 32-year timespan) and emissions associated with biomass production and transportation (Fig. 3.1). Thus, NEs of 1.4 GtC/a (B2L) up to 6.9 GtC/a (B2H2) could be achieved when discarding the precautionary principle and exploiting the full regional uncertainty zone.

If these NEs are completely used for balancing fossil fuel emissions, primary energy of 56 EJ/a to 280 EJ/a from coal could be offset. The wide range of NE potentials reflects major uncertainties related to the mix of BECCS technologies. Nonetheless, these NE potentials are rather optimistic because logistic challenges related to possible carbon storage rates or

the availability of geological storage sites near biomass plantations are not accounted for. Furthermore, at this point in time only a few BECCS demonstration power plants exist and even obtaining the lower range NE potential (1.4 GtC/a) would require substantial upscaling and further development of CCS technologies (Herzog, 2011).

Due to the considerable reduction of CCS potentials by LUC emissions (Fig. 3.1) we further performed the optimisation with a modified objective of maximising the net flux of biomass yields minus LUC emissions. Overall, this increases NE potentials slightly (+1% for B2H2 and +35% for B2L) because of avoided LUC emissions (Supplementary Fig. 3.4). Optimised biomass potentials, however, are smaller than those of biomass yield optimisation neglecting LUC effects. This reduces CCS rates and energy generation by 9%. These findings highlight a trade-off between NE and bioenergy production: while NE potentials are higher if LUC emissions are considered, energy production potentials decrease.

Because of these optimisation constraints (i.e. to stay within regionally safe limits or the riskier uncertainty zone), biomass plantations are only allocated to regions with little or no impact by agriculture in the baseline. Even though regional limits are being considered, allocation of additional biomass plantations adds to the transgression of PBs at the global scale. Figure 3.2 shows the state of the Earth system with respect to the global PBs for the two optimisation constraints. It illustrates that in the process of decreasing the pressure on the PB for climate change with BECCS, additional pressure is exerted onto other globally defined PBs. With the regional safe constraint, almost no biomass plantations can be implemented. Thus, the values of the PB control variables are almost the same as in the agricultural baseline (dashed grey line). Under the constraint allowing for exploitation of regional uncertainty zones many global PB control variables are severely impacted while the potential for NEs increases, especially under conversion to hydrogen (B2H2) (Fig. 3.2).

In the scenario considering regional uncertainty rather than safe limits, allocation of biomass plantation on 709 Mha) increase land use area by 14% compared to the agricultural baseline, implying deforestation of 568 Mha (+ 9% forest loss). This adds significant pressure on biodiversity (+ 6% loss of biodiversity intactness, see Methods). The biomass potential largely stems from herbaceous biomass with relatively low nitrogen requirements (Roncucci et al., 2015). Nonetheless, fertiliser requirements further alter global biogeochemical flows (+ 65 TgN/a fertilisation). Most of the optimised biomass plantations are irrigated because water availability in productive regions without large agricultural water appropriation is generally high. Consequently, water consumption by biomass plantations more than doubles irrigation water consumption (+ 1167 km^3). Such massive irrigation of biomass plantations benefits plant productivity (on average 26 tDM/ha) and thus reduces land requirements and impacts on biodiversity.

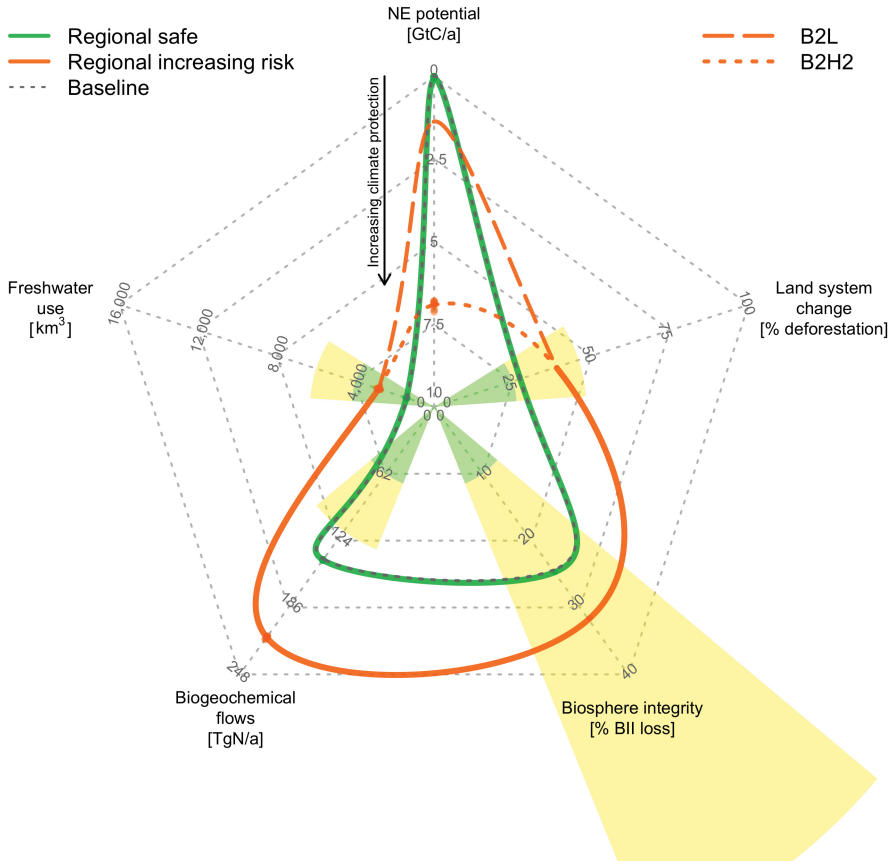

Figure 3.2.: Status of PB control variables when optimised biomass plantations are combined with the RCP2.6 agricultural baseline (without bioenergy). NE potentials are depicted for the biomass conversion to hydrogen (B2H2) and conversion to liquid (B2L). Error bars reflect the range of LPJmL simulations driven by an ensemble of 19 climate scenarios with a global warming of 2°C (see Methods). Green and yellow planes indicate the global safe and uncertainty zones (Steffen et al., 2015).

We assess the trade-off between freshwater use and biodiversity conservation in more detail (Fig. 3.3). We adopt the second optimisation objective prescribing biomass yields while minimising the impacts on different global PBs independent of regional constraints. Unsurprisingly, the higher the targeted biomass yields, the higher the transgression of global PBs. While the alteration of biogeochemical flows always increases with biomass yields because of fertilisation requirements, the added pressure on the other PBs depends on the conservation objectives that are given priority.

Under the objective of minimising the impact on biosphere integrity (Fig. 3.3a), biomass plantations are mostly allocated on grasslands or savannahs with relatively low species

richness. High biomass targets (up to 20 GtC/a) can be met without adding a lot of pressure on the global PBs for biosphere integrity and land system change when regional limits are not considered. This is, however, only possible when land use efficiency is increased by substantial irrigation of biomass plantations. Overall, global water consumption reaches levels that transgress the PB for freshwater use for biomass yields larger than 5 GtC/a and exit the global uncertainty zone for biomass yields larger than 10 GtC/a (Fig. 3.3a).

The guiding objective of freshwater saving (Fig. 3.3b) implies significant water saving potentials for the same biomass yields (2100 km^3 - 6600 km^3 for 5 GtC/a - 20 GtC/a, respectively). To achieve this, biomass plantations are allocated in productive regions with high water availability. This implies, however, high deforestation rates – especially in the tropics – causing a larger pressure on the PBs for biosphere integrity and land system change (Fig. 3.3b). Furthermore, land use change emissions from deforestation result in overall smaller NE potentials from the same biomass yields.

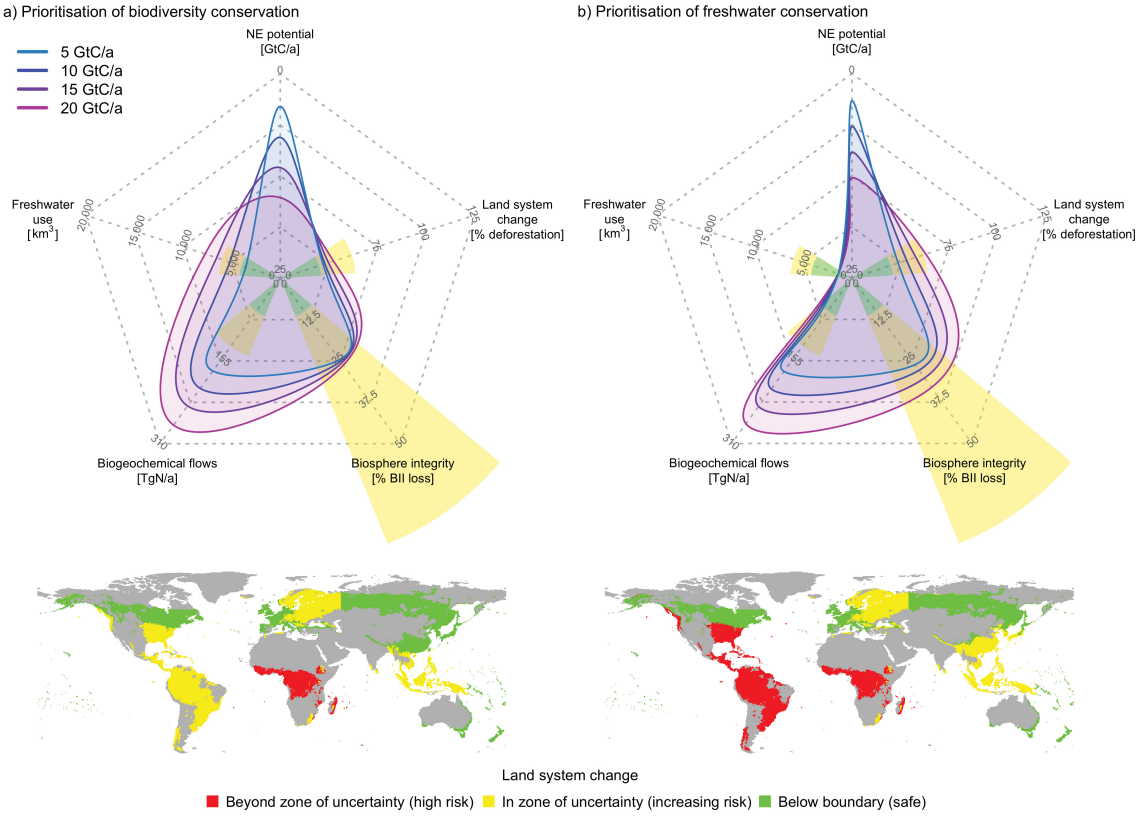

Figure 3.3.: The effect of conservation objectives for different biomass targets: a) prioritisation of biodiversity conservation and b) prioritisation of freshwater conservation. Negative emission potentials are depicted for the biomass conversion pathway to hydrogen (B2H2). Maps show the regional status of the control variable for land system change for biomass yields of 15 GtC/a.

The biogeochemical simulation results in this study provide an alternative viewpoint to economic optimisation studies identifying BECCS as an economically feasible technology for achieving negative emissions (Klein et al., 2014b; Vuuren et al., 2011). In particular, we have shown clear trade-offs between PBs and negative emissions. Respecting environmental constraints according to the PB framework yields almost zero potential for NE with BECCS. Thus, an adoption of the PBs as precautionary policy goals would have strong implications for mitigation requirements compatible with the 2° goal. Only the exploitation of the biosphere into a zone of increasing risk of triggering feedbacks at the planetary scale can provide considerable NE potentials. However, these strongly depend on the efficiency of biomass utilisation and are subject to large uncertainties regarding the potential scale, economic feasibility, as well as public and legal acceptance of CCS (Herzog, 2011; Watson et al., 2014). Overall, even the most optimistic biomass conversion and CCS efficiencies would by far not be sufficient to balance fossil emissions without substantial mitigation leading to far-reaching decarbonisation.

3.2. Methods

We use the process-based dynamic global vegetation model LPJmL, with representations of natural ecosystems and managed croplands including biomass plantations to simulate key ecosystem processes and coupled carbon and hydrological cycles (Gerten et al., 2004; Rost et al., 2008b). LPJmL has been extensively validated for carbon cycles (Sitch et al., 2003), agricultural crop and biomass production (Bondeau et al., 2007; Fader et al., 2010; Heck et al., 2016b), water flows and irrigation requirements (Gerten et al., 2004; Rost et al., 2008b). It is driven here by an ensemble of 19 temperature-stratified climate scenarios with a global warming of 2K during the 30 year mean around 2100 (Heinke et al., 2013) to simulate carbon and water fluxes and pools from 2050 to 2082 on a spatial resolution of 0.5°. For the generation of optimisation inputs one medium range climate model (MPI-ESM) is used to simulate changes in soil and vegetation carbon pools related to biomass plantations and deforestation, potential irrigated and rainfed biomass yields, potential water consumption of irrigated biomass plantations and regional water availability. In case of deforestation for biomass plantations, the natural vegetation replaced is treated as a one-time biomass harvest. Optimisation outputs are evaluated by LPJmL for all 19 climate scenarios for the same time frame.

We developed an optimisation model (based on the R-package *lpSolveAPI* for linear optimisation (Konis, 2016)) that distributes herbaceous or woody biomass plantations (irrigated or rainfed) on a 0.5° grid around a baseline agricultural land use pattern, considering two alternative optimisation objectives:

1) maximisation of global biomass yield (Y) given fixed regional boundary constraints (C_{PB}^{reg}) of biosphere integrity (B), land system change (L), nitrogen flows (N) and freshwater use (W):

$$\max_{f_j \in C_{PB}^{reg}} \left(\sum_{j=1}^{n} \sum_{p} f_j^p \; y_j^p \right), \tag{3.1}$$

with f_j^p: cell fractions and y_j^p: yield of biomass plantations $p \in$ {herbaceous irrigated, herbaceous rainfed, woody irrigated, woody rainfed } in gridcells $j = 1...n$. Biomass fractions are subject to regional constraints $\{C_B^{reg}, C_L^{reg}, C_N^{reg}, C_W^{reg}\}$.
2) minimisation of impacts I on B, L, N, W for varied weights (w_{PB}) given fixed biomass yield constraints (C^Y):

$$\min_{f_j \in C^Y} \left(\sum_{j=1}^{n} w_B I_j^B + w_L I_j^L + w_N I_j^N + w_W I_j^W \right), \tag{3.2}$$

with $C^Y = \sum_{j=1}^{n} \sum_p f_j^p \; y_j^p \in \{5, 10, 15, 20\}$ GtC/a.

The agricultural baseline consists of crop and pasture areas of the harmonised global gridded land-use change scenario of the RCP2.6 scenario framework (Hurtt et al., 2011) for the year 2050. The crop land cover (excluding bioenergy plantations) was translated to match LPJmL's crop types (Boit et al., 2016). A scenario for nitrogen fixation is based on the baseline scenario (McIntyre et al., 2009) in the nutrient budget model provided by Bouwman et al. (2011). We use the land use distribution of the RCP2.6 land use scenario and adapt crop production data from LPJmL to obtain the nitrogen budget on a 0.5° resolution. Global sums of nitrogen fertiliser and nitrogen fixation by legumes are 100.3 TgN/a and 40.7 TgN/a, respectively. Spatially explicit agricultural water consumption (981 km^3/a) is simulated by LPJmL, and non-irrigation human water consumption under the SSP2 scenario (415 km^3 in 2050) was provided by the WaterGAP model (Flörke et al., 2013).

Optimisation constraints and inputs Under the regional boundary constraints (C_{PB}^{reg}, Eq. 3.1) land use expansion for bioenergy is allowed where regional boundaries are not transgressed in the agricultural baseline and until they are reached. Global control variables are used to assess the status of PBs for each optimisation scenario.
The status of land system change is derived from the potential forest cover simulated by LPJmL for historic climate data (CRU TS version3.1, Harris et al., 2014). Regional constraints are on the scale of biomes (tropical, temperate and boreal) of each continent (Table 3.1).
The global biogeochemical flows PB is approached via intended nitrogen fixation. As regional

constraints we derive grid-cell specific thresholds for nitrogen fixation (limiting N runoff to surface waters and NH_3 air concentrations, Table 3.1) based on the approach used to assess the global PB for nitrogen flows (Vries et al., 2013) (see Supplementary for details). Nitrogen fertiliser requirements for biomass plantations are derived from biomass harvest under the assumption that extracted nitrogen (0.15% N in dry matter for herbaceous biomass (Roncucci et al., 2015) and 0.5% N in dry matter for woody biomass (Kauter et al., 2001)) is replenished with an efficiency of 50% (Lassaletta et al., 2014).
Several interim control variables have been proposed for the PB for biosphere integrity (Steffen et al., 2015). Acknowledging large associated uncertainties, we calculate a measure similar to one of the proposed control variables, the biodiversity intactness index (BII) (Scholes et al., 2005; Steffen et al., 2015):

$$BII = \frac{\sum_s \sum_l ER_s A_l I_{s,l}}{\sum_s \sum_l ER_s A_l}, \tag{3.3}$$

for species groups $s \in$ {amphibians, birds, mammals, vascular plants} and land cover $l \in$ {natural, cultivated, plantation}, with ER_s = endemism richness of species s, A_l=land area of land cover l and $I_{s,l}$ = intactness of species s with land cover l (see Supplementary for details). This BII is calculated globally and for 71 continental biomes.

The status of global freshwater use is the sum of baseline water consumption and irrigation water consumption of biomass plantations simulated by LPJmL. Regional boundary constraints limit blue water withdrawals on the scale of both, river basins and grid-cells (Table 3.1). Irrigation water availability for biomass plantations is determined at grid cell level as the mean (over the biomass irrigation period) of monthly water availability from LPJmL minus baseline withdrawals (and environmental requirements, depending on the constraints).

Ackowledgements We thank Lex Bouwman for providing the nitrogen budget model and helpful suggestions. We also thank Holger Kreft and Carsten Meyer for providing the endemism richness data set and Benjamin Bodirsky for discussions on the planetary boundary for biogeochemical flows. This research was funded by the DFG in the context of the CE-Land project of the Priority Program "Climate Engineering: Risks, Challenges, Opportunities?" (SPP 1689). We acknowledge the European Regional Development Fund (ERDF), the German Federal Ministry of Education and Research and the Land Brandenburg for supporting this project by providing resources on the high performance computer system at the Potsdam Institute for Climate Impact Research.

Author contributions VH designed the study with input from DG and WL. VH developed the methodology, performed all simulations, analysed the results and created the figures. VH led the writing process with contributions from DG and WL.

3.3. Supplementary material

3.3.1. Supplementary results

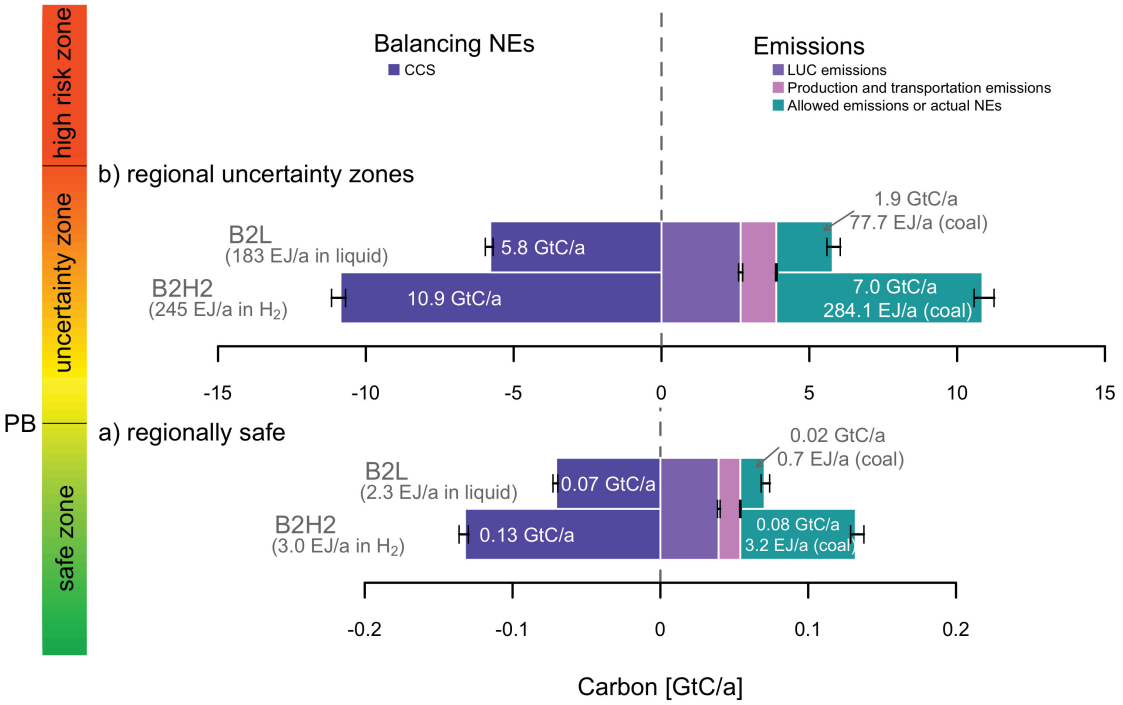

Figure 3.4.: Emission balance for two biomass conversion pathways (B2L and B2H2) under the objective of carbon balance optimisation. Net carbon fluxes are optimised under the constraints of staying within regionally safe (a) or uncertainty (b) zones. Error bars reflect the range of 19 GCMs.

Supplementary optimisation with a modified objective to maximise the net carbon flux instead of biomass yields (as shown in Fig. 3.1 Under this optimisation objective, land use change emissions are avoided, which in turn results in smaller biomass yield (and bioenergy) potentials. this leads to a net increase negative emission potentials, compared to the optimisation of biomass yields. However, bioenergy potentials are reduced.

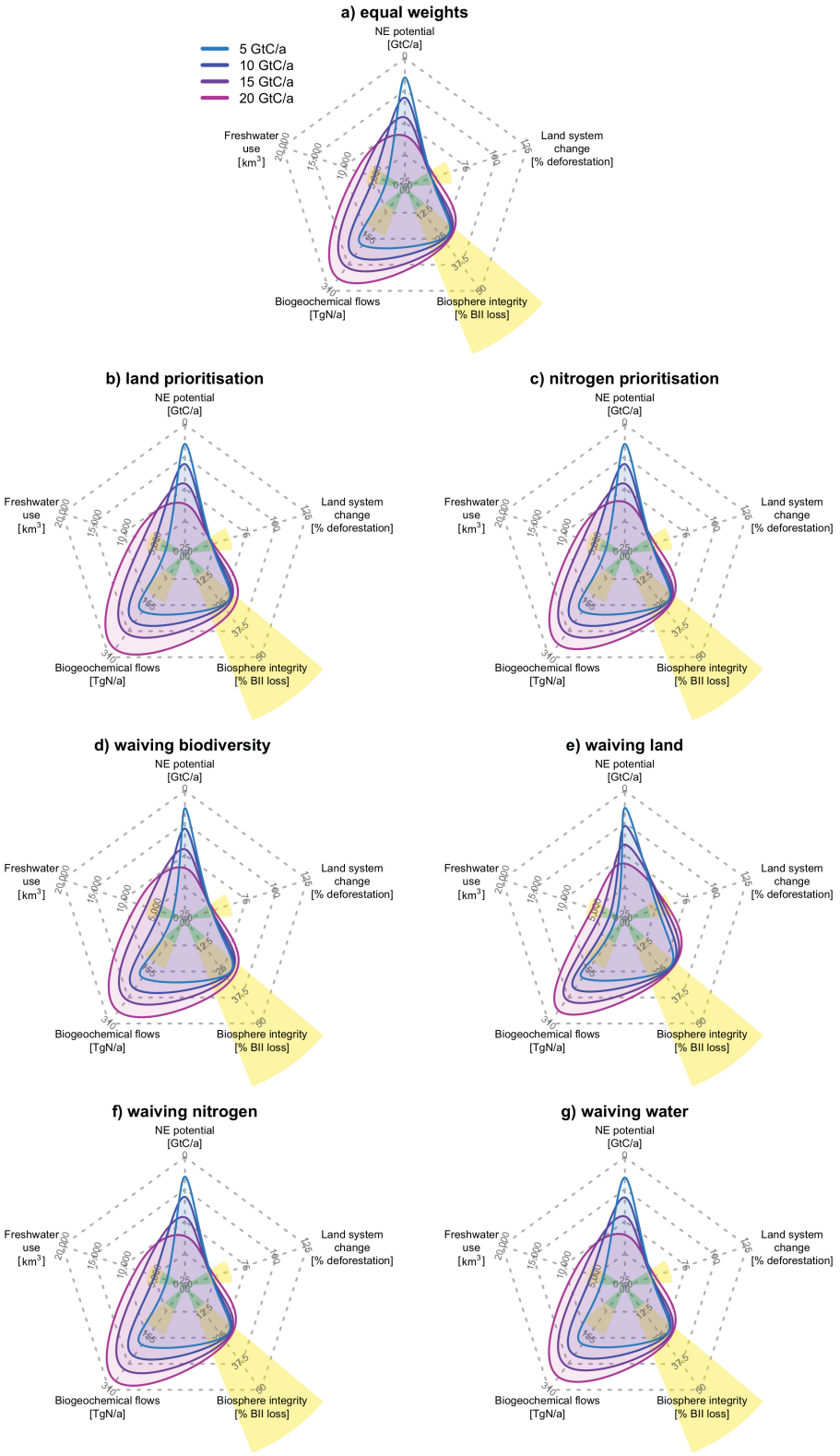

Figure 3.5.: The effect of different conservation objectives for different biomass demands. Negative emission potentials are depicted for the biomass conversion pathway to hydrogen (B2H2).

Figure 3.5 shows results of the second optimisation objective to minimise the impacts on global planetary boundaries for fixed biomass yield constraints. Results are depicted for varying the weights on each global boundary (ref. to Methods and Fig. 3.1). Equal weights on all PBs (a) result in little pressure o biodiversity and land system change, whereas freshwater and fertiliser are increasingly used. This is because, biodiversity and land conservation are complementary in most regions and thus outweigh conservation of water and biogeochemical flows. Similar results are obtained for land prioritisation (b, with weights 1 except weight 9 on land) with somewhat higher fertiliser requirement and pressure on biodiversity. Even under the prioritisation of reducing nitrogen fertiliser (c, with weights 1 except weight 9 on fertilisation), biogeochemical flows are altered substantially. This is because our optimisation assumes fertiliser requirements linear to biomass harvest, which is prescribed in this optimisation. Subplots d) to g) of Figure 3.5 show optimisation results for all weights set to 9, except the waived constraint, which is set to 1. Again, results are similar because biodiversity and land are complementary. Only waiving global land system change from the optimisation objective, reduces irrigation water. This again highlights the trade-off between water and land conservation.

3.3.2. Supplementary methods

Details on the LPJmL modelling procedure to generate optimisation inputs

LPJmL was used to determine the potential changes in carbon pools and fluxes under conversion to biomass plantations, as well as potential irrigation water requirements and availability. All simulations were preceded by a 5000-year spin-up with natural vegetation, bringing soil carbon pools and vegetation distribution into equilibrium. A subsequent second spin-up period of 390 years introduces historical agriculture with annual cropland extent and crop type distribution per 0.5° grid cell after Hurtt et al. (2011) (land cover classes were translated to match LPJmL's crop functional types, see Boit et al. (2016) for details) and irrigated fraction per crop type after Jägermeyr et al. (2015) from 1700-1900, allowing for a historical adjustment of carbon pools. During the spin-ups, the climate (historical climate data from CRU TS3.10 (Harris et al., 2014) of the years 1901-1930 was repeated. A third simulation from 1901-2050 serves as spin-up for the actual simulations. This uses the agricultural land use change scenario of the RCP2.6 (Hurtt et al., 2011) without biomass plantations and a temperature-stratified climate scenario with a global warming of 2K during the 30yr mean around 2100, reproducing the median response of the CMIP3 MPI-ESM (Heinke et al., 2013).

Table 3.2 summarises LPJmL simulations and their purpose for the optimisation. Biomass plantations are cultivated in regions where climate conditions allow biomass harvests higher than 5 tDM/ha/a (Hastings et al., 2009).

Simulation	Land use	Period	Purpose
1	PNV	1901-2100	i) potential historical biomes, ii) potential water availability without land use
2	constant agr. land use of 2050	2050-2082	i) carbon pools of natural vegetation, ii) agricultural water use, iii) water availability after anthropogenic water use (without biomass plantations)
3	rainfed herbaceous biomass around agr. land use of 2050	2050-2082	i) potential changes in carbon pools by biomass plantation, ii) potential biomass harvest
4	rainfed woody biomass around agr. land use of 2050	2050-2082	as above
5	irrigated herbaceous biomass around agr. land use of 2050	2050-2082	i) potential changes in carbon pools by biomass plantation, ii) potential biomass harvest, iii) potential irrigation water requirements and blue water consumption
6	irrigated woody biomass around agr. land use of 2050	2050-2082	as above

Table 3.2.: LPJmL simulation protocol for the generation of optimisation inputs.

Details on the calculation of selected planetary boundary constraints

Biogeochemical flows The status of the global biogeochemical flows PB is approached via the intended nitrogen fixation (chemical N fixation in fertilisers and anthropogenically induced biological N fixation by legumes (Vries et al., 2013). The scenario for nitrogen fixation in the RCP2.6 baseline is based on the International Assessment of Agricultural Knowledge, Science, and Technology for Development (IAASTD) baseline scenario (McIntyre et al., 2009).

On the regional scale we considered the control variables used to assess the global PB for nitrogen flows (Vries et al., 2013): atmospheric NH_3 concentrations with critical limits of $[N]_{crit} = 1\mu$g m^{-3} to 3 μgm^{-3} and N concentrations in surface runoff with proposed critical limits of $[N]_{crit}$ =1.0 mg Nl^{-1} to 2.5 mg Nl^{-1} (Vries et al., 2013). As proposed by Vries et al.

(2013) we calculate critical global losses of a given N compound to either air or water by

$$N_{losses;crit} = N_{losses;present}\ RI_{Ncompound}, \tag{3.4}$$

with the risk indicator $RI = [N]_{crit}/[N]_{present}$ and $[N]_{present}$ being the present concentration of the respective control variable. In contrast to Vries et al. (2013) we do not limit RI to values smaller or equal to 1, as this would strictly forbid additional or initial fertilisation in areas that are not close to the regional thresholds, thus forbidding fertilisation on all primary and unfertilised land. Based on the respective range of critical limits, we obtain a range of global RI of 1.79 - 5.36 for atmospheric NH_3 concentrations and 0.61 - 1.53 for N in surface runoff using global average values of $NH_{3-present}$= 0.56μg m^{-3} and $N_{runoff-present}$ = 1.63 mg Nl^{-1} (Vries et al., 2013). Assuming that the ratio between N fixation and polluting compounds does not change (Vries et al., 2013), we multiply the respective RI by the agricultural nitrogen fixation of 121.5 Tg N in the year 2000 (Bouwman et al., 2011). To derive grid cell specific thresholds for nitrogen fixation limiting NH_3 concentrations we divide the global critical value by the global land area. The grid cell threshold for limiting N runoff to surface waters is calculated by dividing the global critical value by surface runoff in the agricultural baseline scenario. Under the regional optimisation constraints C_N^{reg}, biomass plantations can be allocated until the the combined nitrogen fixation by agriculture and biomass plantations the reaches one of the regional thresholds.

Biosphere integrity The biosphere intactness index (BII) (Scholes et al., 2005) is one of several interim control variables that have been proposed for the PB for biosphere integrity (Steffen et al., 2015). Acknowledging large uncertainties associated with the status of this PB, we calculate a measure similar the proposed BII:

$$BII = \frac{\sum_s \sum_l ER_s A_l I_{s,l}}{\sum_s \sum_l ER_s A_l}, \tag{3.5}$$

for species groups $s \in$ {amphibians, birds, mammals, vascular plants} and land cover $l \in$ {natural, cultivated, plantation}, with ER_s = endemism richness of species s, A_l= land area of land cover l and $I_{s,l}$ = intactness of species s with land cover l. Endemic richness instead of proposed species richness is used to incorporate individual regional contribution to genetic diversity, which is the motivation for the second interim control variable (Steffen et al., 2015). Endemic richness data of terrestrial vertebrates were available on a 1° resolution and vascular plants for 90 terrestrial biogeographic regions (Kier et al., 2009). Due to the lack of global impact data, we adopted expert impact estimates of South Africa (Scholes et al., 2005) for a rough first estimate of species intactness on cultivated land or plantations. This implies that the absolute BII-values on the global or regional scale are highly uncertain. However, regional differences are respected in the spatial allocation of biomass plantations because the

intactness estimates serve only as a factor to heterogeneously distributed endemic richness. The BII is calculated for the whole globe (global PB) and for 71 continental biomes. For the regional optimisation constraint (C_B^{reg}) biomass plants can be cultivated in the respective biome if the BII is higher than 90% (safe limit) or 30% (uncertainty limit).

Freshwater use The PB for freshwater use has two different control variables for the global and regional scale (blue water consumption and environmental water flows, respectively. The basin-scale environmental water flows boundary limits blue water withdrawal along rivers to percentages of the mean monthly flow. It is calculated with the Variable Monthly Flow (VMF) method (Pastor et al., 2014) accounting for intra-annual variability in terms of high-, intermediate- and low-flow months (ref. to Table 3.1).

In the optimisation water availability for irrigation is always limited at the grid-cell level and at the level of water basins. Without the regional boundary constraints, irrigation of biomass plantations is possible to the extent of mean available water over the irrigation period after subtracting agricultural withdrawals and withdrawals for households, industry and livestock from the monthly water availability. Because upstream-downstream effects of water withdrawals are not considered in the linear optimisation program, water availability is additionally limited at the basin level with an additional constraint that water withdrawals in each basin may not exceed the basin discharge. This assumes that water can be transported within a basin, but neglects irrigation water from groundwater.

Under the regional boundary constraint on freshwater use (C_W^{reg}), the available water for irrigation of biomass plantations in each water basin is calculated as the mean available water over the irrigation period after subtracting monthly environmental water flows, agricultural withdrawals and withdrawals for households, industry and livestock from the monthly water availability. The same calculation is applied at the grid-cell level to limit water withdrawals and sustain environmental water flows at the cell-level.

4. Collateral transgression of planetary boundaries due to climate engineering by terrestrial carbon dioxide removal [1]

Vera Heck[1,3], Jonathan F. Donges[1,2], Wolfgang Lucht[1,2,4]

[1] Earth System Analysis, Potsdam Institute for Climate Impact Research, Telegraphenberg A62, 14473 Potsdam, Germany

[2] Stockholm Resilience Centre, Stockholm University, Kräftriket 2B, 114 19 Stockholm, Sweden

[3] Department of Geography, Humboldt University, Unter den Linden 6, 10099 Berlin, Germany

[4] Integrative Research Institute on Transformations of Human-Environment Systems, Humboldt University, Unter den Linden 6, 10099 Berlin, Germany

Abstract

The planetary boundaries framework provides guidelines for defining thresholds in environmental variables. Their transgression is likely to result in a shift in Earth system functioning away from the relatively stable Holocene state. As the climate system is approaching critical thresholds of atmospheric carbon, several climate engineering methods are discussed, aiming at a reduction of atmospheric carbon concentrations to control the Earth's energy balance. Terrestrial carbon dioxide removal (tCDR) via afforestation or bioenergy production with carbon capture and storage are part of most climate change mitigation scenarios that limit global warming to less than 2°C.

We analyse the co-evolutionary interaction of societal interventions via tCDR and the natural dynamics of the Earth's carbon cycle. Applying a conceptual modelling framework, we

[1] An edited version of this chapter has been accepted for publication in Earth System Dynamics (Sept. 2016) and is published as a discussion paper: V. Heck et al. (2016a). "Collateral transgression of planetary boundaries due to climate engineering by terrestrial carbon dioxide removal". In: *Earth System Dynamics Discussions*, pp. 1–24. DOI: 10.5194/esd-2016-22

analyse how the degree of anticipation of the climate problem and the intensity of tCDR efforts with the aim of staying within a 'safe' level of global warming might influence the state of the Earth system with respect to other carbon-related planetary boundaries.

Within the scope of our approach, we show that societal management of atmospheric carbon via tCDR can lead to a collateral transgression of the planetary boundary of land system change. Our analysis indicates that the opportunities to remain in a desirable region within carbon-related planetary boundaries only exist for a small range of anticipation levels and depend critically on the underlying emission pathway. While tCDR has the potential to ensure the Earth system's persistence within a carbon safe operating space under low emission pathways, it is unlikely to succeed in a business-as-usual scenario.

4.1. Introduction

Rockström et al. (2009) introduced the concept of a safe operating space (SOS) for humanity, delineated by nine global planetary boundaries, some of which take into account the existence of tipping points or nonlinear thresholds in the Earth system (Kriegler et al., 2009; Lenton et al., 2008; Schellnhuber, 2009) and may frame sustainable development. Particularly, the state of the Earth system with respect to climate change has received strong political attention, as atmospheric carbon concentrations have already entered the uncertainty zone of the planetary boundary of climate change, set at an atmospheric CO_2 concentration of 350 ppmv to 450 ppmv (Steffen et al., 2015).

The Paris climate agreement (UNFCCC, 2015) aims at limiting global temperature increase to well below 2°C above pre-industrial levels, while currently greenhouse gas emissions are still growing. Fuss et al. (2014) have highlighted that more than 85% of IPCC scenarios that are consistent with the 2° goal require net negative emissions before 2100. Particularly, terrestrial carbon dioxide removal (tCDR) via afforestation or large-scale cultivation of biomass plantations for the purpose of bioenergy production has been included in recent IPCC scenarios (Kirtman et al., 2013; Vuuren et al., 2011). Furthermore, tCDR has been proposed as a climate engineering (CE) method that could be applied in case global efforts in mitigating anthropogenic greenhouse gas emissions fail to prevent dangerous climate change (Caldeira et al., 2010).

In the context of the SOS framework, tCDR via large-scale biomass plantations could on the one hand extract carbon from the atmosphere via the natural process of photosynthesis (Shepherd et al., 2009). If the carbon accumulated in biomass is harvested and stored in deep reservoirs or used for bioenergy production in combination with carbon capture and storage (Caldeira et al., 2013), further transgression of the climate change boundary

and initial transgression of the ocean acidification boundary could be prevented. On the other hand, tCDR is likely to have unintended impacts on other Earth system components besides atmospheric carbon concentrations that is mediated by the global cycles of carbon, water and other biogeochemical compounds (Vaughan et al., 2011). For example, large-scale biomass plantations would require substantial amounts of fertiliser, irrigation water and land area, driving the Earth system closer to the planetary boundaries for biogeochemical flows, freshwater use and land system change, respectively (Heck et al., 2016b). TCDR in the form of afforestation would not be accompanied by most of these negative trade-offs. However, afforestation only has a limited potential to increase the terrestrial carbon storage while all emitted fossil carbon remains a part of the active carbon cycle. Thus, the potentials of tCDR via afforestation are small and afforestation is not included as a tCDR method in this study.

Social and political actions are important drivers of tCDR. The willingness to engage in CE or mitigation is based on monitoring of the climate system and can be expected to increase as the climate system approaches the normatively assigned climate change boundary. A holistic assessment and systemic understanding of CE therefore requires an analysis of the social and ecological co-evolutionary system.

A dynamic integration of complex interactions between the social and ecological components of the Earth system to simulate in detail the co-evolution of societies and the environment is currently unfeasible due to fundamental conceptual problems and high computational demands on both modelling sides (Vuuren et al., 2016; Vuuren et al., 2012). An emerging field of low-complexity models explores new pathways for understanding social-ecological Earth system dynamics (e.g. Anderies et al., 2013; Brander et al., 1998; Jarvis et al., 2012; Kellie-Smith et al., 2011; Motesharrei et al., 2014). For example, first simulation approaches have been reported using such conceptual models to simulate the interaction between human climate monitoring and societal action in the form of transitions to renewable energy (Jarvis et al., 2012) or climate engineering (MacMartin et al., 2013) While not aiming for realism in their quantitative evaluations, the low complexity of such conceptual models allows to understand the structure and effects of dominating feedbacks and their leading interactions, which are otherwise often hidden in the complexity of state-of-the-art full complexity Earth system models.

In this paper, we provide a conceptual but systematic analysis of the nonlinear system response to using tCDR for steering the Earth system within the SOS defined by planetary boundaries as quantified by Rockström et al. (2009) and Steffen et al. (2015). Specifically, we analyse how the trade-offs between tCDR and other planetary boundaries depend on the achievable rate and threshold of tCDR implementation; and whether particular combinations of climate and management parametrisations can safeguard a persistence within the SOS. As

a starting point, we focus on a subset of the nine proposed planetary boundaries that are most important in the context of tCDR. These are the carbon-related boundaries on climate change, ocean acidification and land-system change.

We utilise a conceptual model of the carbon cycle and expand it to explore feedbacks within and between societal and ecological spheres, while being sufficiently simple to permit an analysis of its state and parameter spaces in the form of constrained stability analysis similar to Kan et al. (2016). We do not aim to provide a quantitative assessment because in this exploratory study we choose to use a computationally efficient conceptual model to shed light onto the qualitative structure of co-evolutionary dynamics. The approach proposed here can be transferred to models of higher complexity to the extent that this is computationally feasible.

This paper is structured as follows: following the introduction (Sec. 4.1) we present a co-evolutionary model of societal monitoring and tCDR intervention in the Earth's carbon cycle and related parameter calibration procedures (Sec. 4.2). Subsequently, we present and discuss our results (Sec. 4.3) and finish with conclusions (Sec. 4.4).

4.2. Methods

In social-ecological systems modelling, societal influences and ecological responses are recognised as equally important (Berkes et al., 2000). Therefore, it can be considered essential that representations of social and ecological systems are of the same order of complexity. Increasing complexity of only one model component would not increase the accuracy of information generated by the full coupled model, but would greatly increase computational demand. In view of our objective, we require a sufficiently simple model that conceptually captures the most important processes of global carbon dynamics with respect to planetary boundaries, as well as a stylised societal management feedback loop consisting of tCDR interventions and monitoring of the climate system.

4.2.1. Co-evolutionary model of societal monitoring and tCDR intervention in the carbon cycle

The basis of our co-evolutionary model is the conceptual carbon cycle model by Anderies et al. (2013). The model covers the most basic interactions between terrestrial, atmospheric, and marine carbon pools and was developed specifically to enable a bifurcation analysis of carbon-related planetary boundaries and their interactions. We modified atmosphere-land interactions for a better representation of empirically observed Earth system carbon dynamics

and extended the model by a stylised societal management feedback loop mimicking the current focus of international policy processes on climate change. We calibrated the model in order to represent global carbon cycle dynamics consistent with observational data and simulations from detailed high-resolution Earth system models (Sec. 4.2.2). In the following, we provide an overview of the fundamental model equations. A detailed motivation of the model design and underlying assumptions is given in Anderies et al. (2013).

The adapted model consists of five interacting carbon pools: land $C_t(t)$, atmosphere $C_a(t)$, upper ocean $C_m(t)$, geologic fossil reservoirs $C_f(t)$ and a potential CE carbon sink $C_{CE}(t)$ (Fig. 4.1). All model equations are summarised in Table 4.1. Note that only the upper ocean carbon pool is included because the movement of carbon into the deep ocean occurs on longer timescales relative to those of interest, as discussed by (Anderies et al., 2013). The land carbon pool combines soil and vegetation carbon pools, implying a simple proportional partitioning of aboveground and belowground carbon pools (Anderies et al., 2013). These simplifications have been adopted because they reduce the number of state variables and we were able to qualitatively reproduce the dynamics of observed carbon pool evolution with the adapted model.

Process	Equation	
conservation of mass	$C_t(t) + C_a(t) + C_m(t) = C_0 + C_r(t) - C_{CE}(t)$	(4.1)
fossil carbon release	$\dot{C}_r(t) = r_i C_r(t)(1 - \frac{C_r(t)}{c_{max}})$	(4.2)
CE carbon storage	$\dot{C}_{CE}(t) = H_{CE}(C_t(t), C_a(t))$	(4.3)
ocean-atmosphere diffusion	$\dot{C_m}(t) = a_m(C_a(t) - \beta C_m(t))$	(4.4)
terrestrial carbon flux	$\dot{C}_t(t) = NEP(C_a(t), C_t(t)) - H(C_t(t)) - H_{CE}(C_t(t), C_a(t))$	(4.5)
net ecosystem productivity	$NEP(C_a(t), C_t(t), T(t)) = r_{tc}\left[P(T(t)) - R(T(t))\right] C_t(t)\left[1 - \frac{C_t(t)}{K(C_a(t))}\right]$	(4.6)
terrestrial carbon carrying capacity	$K(C_a(t)) = a_k e^{-b_k C_a(t)} + c_k$	(4.7)
photosynthesis	$P(T(t)) = a_p T(t)^{b_p} e^{-c_p T(t)}$	(4.8)
respiration	$R(T(t)) = a_r T(t)^{b_r} e^{-c_r T(t)}$	(4.9)
temperature	$T(C_a(t)) = a_T C_a(t) + b_T$	(4.10)
tCDR offtake flux	$H_{CE}(C_t(t), C_a(t)) = \alpha_{CE}(C_a(t))\ C_t(t)$	(4.11)
societal tCDR offtake rate	$\alpha_{CE}(C_a(t)) = \alpha_{max}\left(1 + \exp(-s_{CE}\ (C_a(t) - \tilde{C_a})\right)^{-1}$	(4.12)
other human biomass offtake flux	$H(C_t(t)) = \alpha C_t(t)$	(4.13)

Table 4.1.: Summary of equations describing the co-evolutionary model of societal monitoring and tCDR intervention in the carbon cycle building upon Anderies et al. (2013).

The co-evolutionary dynamics of the system is determined by Equations (4.1)–(4.5). Conservation of mass (Eq. 4.1) dictates that the active carbon in the system, i.e. the sum of terrestrial, atmospheric and maritime carbon, is equal to the active carbon at preindustrial times (C_0)

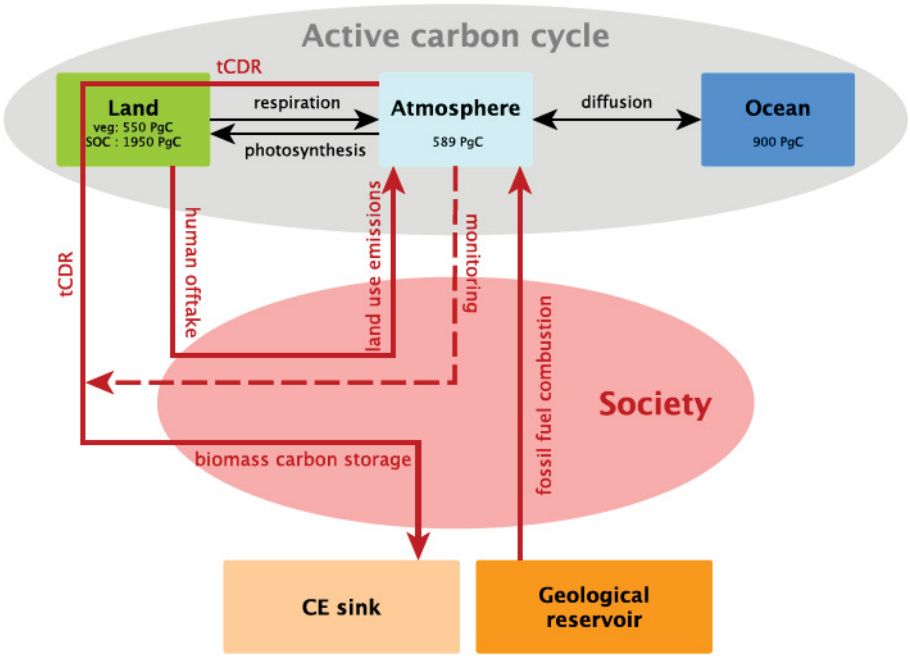

Figure 4.1.: Structure of the co-evolutionary model of societal monitoring and tCDR intervention in the carbon cycle including simulated components of the carbon cycle as well as a societal management feedback loop and their interactions. Carbon fluxes are indicated as solid lines and coloured red if influenced by society. Carbon values in the boxes indicate estimates of preindustrial carbon pools in the year 1750 AD (Batjes, 1996; Ciais et al., 2013).

plus carbon released from fossil reservoirs ($C_r(t)$) minus carbon extracted via tCDR ($C_{CE}(t)$) to permanent stores. Fossil carbon release (Eq. 4.2) is approximated by a logistic function parametrised by the maximum emitted carbon c_{max} and rate of carbon release r_i.

The social management feedback loop is motivated by proposals of CE as a management intervention in response to intolerable levels of global warming. It comprises atmospheric carbon monitoring and tCDR action conditional on the proximity to a critical threshold of atmospheric carbon content (Eq. 4.3). CE action is implemented via a tCDR carbon offtake from terrestrial carbon ($H_{CE}(t)$) and storage in a permanent (geological) sink C_{CE}. Carbon offtake for tCDR (Eq. 4.11) is defined analogous to human offtake for agriculture or land use change (Eq. 4.13), however, with a dynamic offtake rate $\alpha_{CE}(C_a(t))$ (Eq. 4.12).

TCDR characteristics are governed by three parameters: (i) implementation threshold ($\tilde{C}_a$) in terms of atmospheric carbon content, representing societal foresightedness, (ii) maximally achievable rate of tCDR (α_{max}), a measure of societies' efforts, as well as biogeochemical constraints and (iii) the slope of tCDR implementation (s_{CE}), parametrising social and

economic implementation capacities. Figure 4.2 depicts an exemplary tCDR trajectory for constant terrestrial carbon in Eq. 4.11 for two values of s_{CE}. The implementation time can be computed from the slope of tCDR-implementation by using current increase rates of atmospheric carbon as a conversion factor. With current increase rates of approximately 2 ppmv a^{-1} (Tans et al., 2015), the two depicted values of s_{CE} correspond to tCDR ramp-up times of approximately 20 years and 40 years (from 10% to 90% capacity) for s_{CE} =0.1 $ppmv^{-1}$ (solid) and s_{CE} = 0.05 $ppmv^{-1}$ (dashed), respectively.

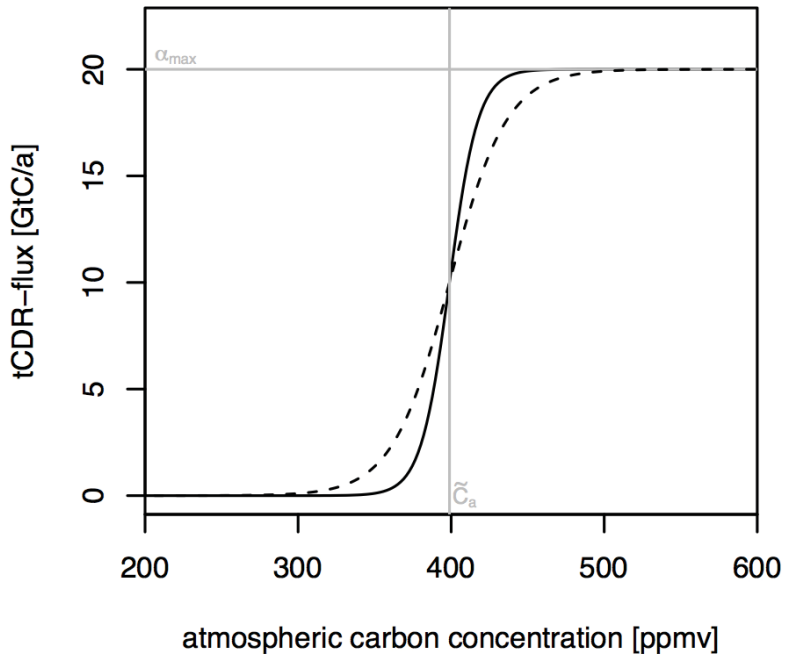

Figure 4.2.: Sigmoidal dependence of the tCDR-flux on atmospheric carbon concentrations for two values of the tCDR implementation capacity parameter (slope): s_{CE} = 0.1 $ppmv^{-1}$ (solid line) and s_{CE} = 0.05 $ppmv^{-1}$ (dashed line). The threshold parameter ($\tilde{C}_a$) is set at 400 ppmv atmospheric carbon concentration and the potentially achievable tCDR-flux is parametrised with α_{max} = 20 GtC a^{-1}.

The atmosphere and ocean carbon feedback (Eq. 4.4) is governed by diffusion, which in the model is assumed to depend on the difference between atmospheric and maritime carbon pools.

Land-atmosphere interaction is determined by both ecological and social processes: the net ecosystem productivity (Eq. 4.6), tCDR offtake (Eq. 4.11) and other human offtake for agriculture and other land use (Eq. 4.13), respectively.

Net ecosystem productivity is given by the net carbon flux of photosynthesis (Eq. 4.8) and respiration (Eq. 4.9), multiplied with the terrestrial carbon pool and a logistic dampening

function which represents competition for space, sunlight, water or nutrients. Both photosynthesis and respiration are continuous functions of global land temperature ($T(t)$, Eq. 4.10), which in turn depends linearly on atmospheric carbon content. It is important to note that in our model respiration exceeds photosynthesis for higher temperatures (Fig. 4.3). The state of equilibrium of the terrestrial carbon pool is thus determined by the land surface temperature, as well as the terrestrial carbon carrying capacity (Eq. 4.7) in the density function. In contrast to Anderies et al. (2013), we implement a dynamic terrestrial carbon carrying capacity as a function of atmospheric carbon content. This is motivated by a number of factors such as CO_2 fertilisation and a higher water use efficiency under higher atmospheric carbon concentrations, as well as higher average vegetation density in a warmer world (e.g. Drake et al., 1997; Keenan et al., 2013). For low atmospheric carbon we assume a rapid increase of terrestrial carbon storage capacity as a function of atmospheric carbon concentration and a saturation of storage capacity for high atmospheric carbon, in line with assessments of coupled carbon-cycle climate models (Heimann et al., 2008). The functional relationship in (Eq. 4.7) follows these constraints for chosen parameter values (Sec. 4.2.2).

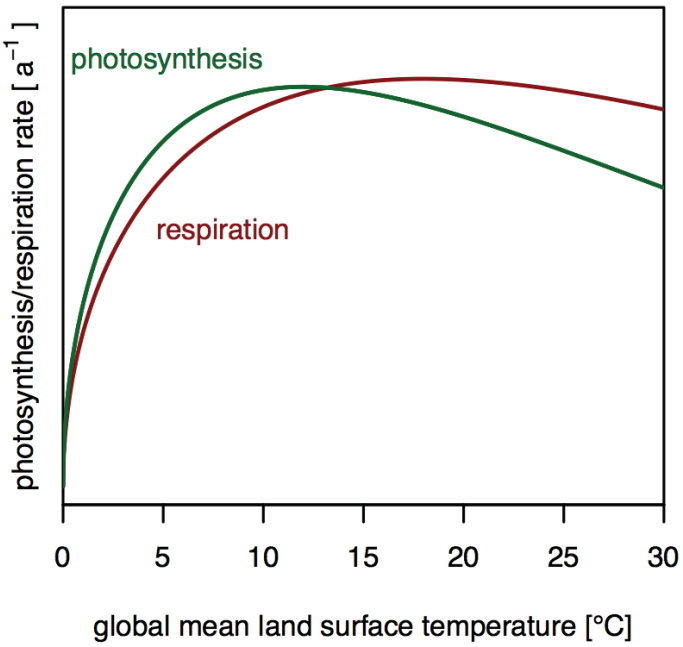

Figure 4.3.: Modelled photosynthesis and respiration rates as a function of global mean land surface temperature.

4.2.2. Calibration of model parameters

A sufficiently suitable application of a conceptual model in the context of the planetary boundaries as in Steffen et al., 2015 requires the model's ability to simulate credible transients of global carbon dynamics. In order to achieve this, we calibrated model parameters to observed carbon fluxes and pools, as well as simulation results of detailed high-resolution Earth system models.

Because we simulate relative dynamics between the different carbon compartments and do not aim at prognostics of actual time evolution of carbon pools, all carbon fluxes and pools are normalised to the the active carbon at preindustrial times, i.e. the total sum of preindustrial carbon in the year 1750 AD (3989 GtC, Fig. 4.1). All normalised parameter values are summarised in Table 4.2.

Parameter	Symbol	Value	Unit
ecosystem-dependent conversion factor	r_{tc}	2.5	a^{-1}
scaling factor for photosynthesis $P(T)$	a_p	0.48	$(20K)^{-b_p}$
scaling factor for respiration $R(T)$	a_r	0.40	$(20K)^{-b_r}$
power law exponent for increase in $P(T)$ for low T	b_p	0.5	1
power law exponent for increase in $R(T)$ for low T	b_r	0.5	1
rate of exp. decrease in $P(T)$ for high T	c_p	0.556	$(20K)^{-1}$
rate of exp. decrease in $R(T)$ for high T	c_r	0.833	$(20K)^{-1}$
scaling factor for terrestrial carbon carrying capacity	a_k	-0.6	1
rate of exp. increase for terrestrial carbon carrying capacity	b_k	13.0	1
offset for terrestrial carbon carrying capacity	c_k	0.75	1
human terrestrial carbon offtake rate	α	0.0004	a^{-1}
slope of $T - C_a$ relationship	a_T	1.06	20K
intercept of $T - C_a$ relationship	b_T	0.227	20K
carbon solubility in sea water factor	β	0.654	1
atmosphere ocean diffusion coefficient	a_m	0.0166	20K
(*) atmospheric carbon threshold of tCDR implementation	$\tilde{C_a}$	0 – 0.3	1
rapidity of tCDR ramp-up (tCDR implementation capacity)	s_{CE}	200	1
(*) maximum tCDR rate	α_{max}	0 – 0.03	a^{-1}
(*) size of geological fossil carbon stock	c_{max}	0 – 0.51	1
industrialisation rate	r_i	0.03	a^{-1}
climate change boundary	b_a	0.21	1
land system change boundary	b_l	0.59	1
ocean acidification boundary	b_m	0.31	1

Table 4.2.: Calibrated model parameters. After normalisation to preindustrial carbon pools, remaining units are years (a) and temperature (20K). Parameters marked with an asterisk (*) are varied during the analysis and the parameter range is stated.

Temperature

For the calibration of the linear relationship between temperature and atmospheric carbon content (Eq. 4.10) we used the transient response to cumulative CO_2 emissions (TCRE) with a reported global mean surface temperature increase per emitted carbon of 2K/1000GtC (Gillett et al., 2013; Joos et al., 2013). Assuming an airborne fraction of 0.5 (Gloor et al., 2010; Knorr, 2009), the global mean temperature increase rate per atmospheric carbon increase (Eq. 4.10) is approximately twice the temperature increase rate of emitted carbon (TRCE), i.e. 2K/500GtC in the atmosphere. From this global surface temperature increase rate (2/3 ocean and 1/3 land surface), the global land surface temperature increase can be inferred via the global land/sea warming ratio of approximately 1.6 (Sutton et al., 2007). Thus, we approximate a global land surface warming rate of 5.3K/1000GtC remaining in the atmosphere. The y-offset (b_T in Eq. 4.10) was inferred via global land surface temperature anomalies from 1880–2000 (Jones et al., 2012), a global average (1880–2000) land temperature of 8.5 °C (NOAA, 2015b) and observed monthly mean CO_2 concentrations (Mauna Loa, 1959–2000, Tans et al., 2015).

Ocean-atmosphere dynamics

The carbon solubility in sea water factor (β) is directly determined by the assumption of pre-industrial equilibrium between upper-ocean and atmospheric carbon ($\dot{C}_m(0) = 0$). From this and a present carbon flux from the atmosphere to the ocean of $\dot{C}_m(t_{tod}) = 2.3$ GtC a^{-1} (Ciais et al., 2013) follows the atmosphere-ocean diffusion coefficient a_m.

Terrestrial dynamics

Photosynthesis and respiration are calibrated according to temperature relationships reported in the literature. However, literature generally specifies temperature relationships at small temporal and spatial scales in controlled environments, whereas our model equations refer to a global average of day and night-time temperature. Thus, only a rough estimation of the relationship between temperature and photosynthesis/respiration for model calibration is possible. As in Anderies et al. (2013), we assume a maximum of respiration at a global land surface temperature of 18 °C (supported by Yuan et al. (2011)), determining the ratio of parameters b_r/c_r =18 °C (Fig. 4.3). We choose a maximum of photosynthesis at 12 °C, incorporating a CO_2 fertilisation feedback indirectly via the dependence of temperature on atmospheric carbon ($b_p/c_p = 12$ °C). The amplitudes of photosynthesis and respiration functions (a_r and a_p, respectively) are approximated for agreement with carbon fluxes reported in Ciais et al. (2013). Note that the functional form of carbon fluxes is not decisive for the model dynamics, however, it is important that the curves of photosynthesis and respiration intersect

at some temperature limit where ecosystem respiration exceeds photosynthesis. With our parametrisation this is the case at a global mean land surface temperature of approximately 13 °C, which is 4.5 °C warmer than the 20th century average global mean land surface temperature (NOAA, 2015b). This is in line with multi-model assessments in carbon reversal studies (e.g. Friend et al., 2013; Heimann et al., 2008).

The terrestrial carbon carrying capacity $K(C_a(t))$ in $\dot{C}_t(t)$ determines how much carbon can be accumulated in the terrestrial system at maximum, as long as photosynthesis exceeds respiration (refer to Eq. 4.6). $K(C_a(t))$ was calibrated to represent both, past long term climatic and terrestrial carbon changes (last glacial maximum to Holocene) (Crowley, 1995; François et al., 1998; Joos et al., 2004; Kaplan et al., 2002) and prognostics of climate change impacts on terrestrial carbon storage (Friend et al., 2013; Joos et al., 2001; Lucht et al., 2006), to capture terrestrial changes due to climate variability (Fig. 4.4).

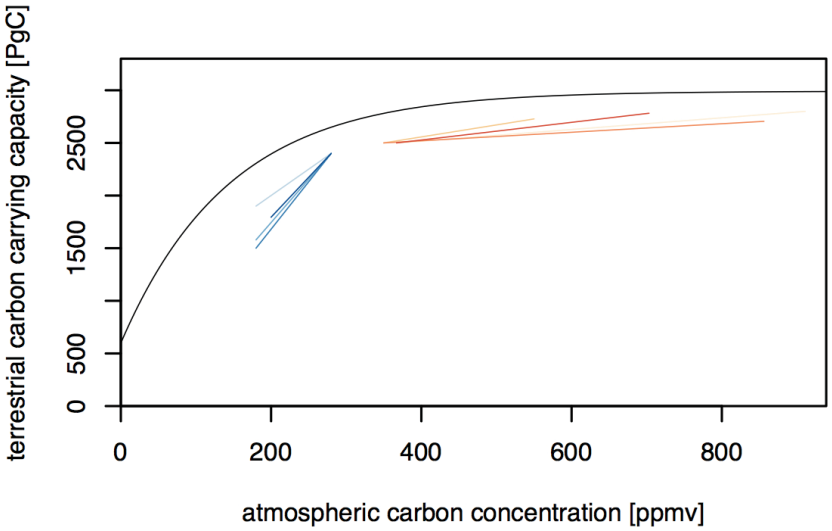

Figure 4.4.: Approximated terrestrial carbon carrying capacity (black line). Blue lines represent approximate changes in terrestrial carbon storage published in Crowley (1995), François et al. (1998), Joos et al. (2004), and Kaplan et al. (2002). Red lines represent simulated changes in terrestrial carbon storage due to climate change reported by Friend et al. (2013), Joos et al. (2001), and Lucht et al. (2006).

Human activities such as fires, deforestation and agricultural land use that affect terrestrial carbon stocks are summarised as human offtake of biomass and are presently estimated at $H(t_{tod}) = 1.1$ GtC a^{-1} (Ciais et al., 2013). With a present terrestrial carbon pool of $C_t(t_{tod}) = 2470$ GtC we calculate the human offtake rate $\alpha = H(t_{tod})/C_t(t_{tod})$.

Fossil fuel emissions

The size of the geological fossil carbon stock c_{max} determines the carbon released from fossil reservoirs (Eq. 4.2) and plays an important role for carbon dynamics (Sec. 4.3.4). In the scope of this study, c_{max} is varied to assess different baseline emissions following the cumulative emissions of the representative concentration pathways (RCPs). RCP2.6 is a low-emission scenario with cumulative emissions of approximately 880 GtC ($c_{max} = 0.2$) (Vuuren et al., 2011). The two medium emission scenarios RCP4.5 and RCP6.0 have cumulative emissions of approximately 1200 GtC ($c_{max} = 0.31$) (Thomson et al., 2011) and 1400 GtC ($c_{max} = 0.36$) (Masui et al., 2011), respectively. RCP8.5 represents a business as usual scenario with cumulative emissions of approximately 2000 GtC ($c_{max} = 0.51$) (Riahi et al., 2011).

4.2.3. Planetary boundaries

We use the carbon-related planetary boundaries (climate change, ocean acidification and land system change) to define the desirability of given trajectories of carbon pool evolution. The proposed locations of these boundaries are normalised to match the normalisation of our model.

The planetary boundary for climate change is proposed at 350 ppmv CO_2 equivalents in the atmosphere with an uncertainty range to 450 ppmv (Steffen et al., 2015). For our study we take the middle of the uncertainty range (400 ppmv) because critical atmospheric thresholds are likely to be located somewhere within the uncertainty range and obtain a normalised climate change boundary is at 0.21 atmospheric carbon. Ocean acidification is measured via the saturation state of aragonite and its boundary is set at 80% of the preindustrial average annual global saturation state of aragonite (Steffen et al., 2015). Since chemical processes are not explicitly represented in our model, this measure is not directly transferable to maritime carbon content. This measure is not directly transferable to maritime carbon content because it largely depends on chemical variables such as pH-value, ocean alkalinity and dissolved inorganic carbon that are not included in the model. At the current carbon content (1150 GtC), the saturation state of aragonite is at 84% of the preindustrial value (Guinotte et al., 2008). We therefore estimate the normalised ocean acidification boundary at 0.31, about 5% higher than the current value of the marine carbon stock (0.29). The land system change boundary is defined in terms of the amount of remaining forest cover, motivated by critical biogeophysical feedbacks of forest biomes to the physical climate system (Steffen et al., 2015). The global boundary has been specified as 75% of global forest cover remaining (Steffen et al., 2015). Due to the lack of biogeophysical feedbacks in the model, we translate deforestation into carbon content by measuring the loss of vegetation carbon with deforestation. We thereby neglect vegetation carbon of all non-forest biomes, while at the same time neglecting soil

carbon changes by deforestation (Heck et al., 2016b), thus approximating that soil carbon changes by deforestation are of the same order of magnitude as vegetation carbon pools of non-forest biomes. With vegetation carbon of 550 GtC (Ciais et al., 2013), we obtain a normalised land system change boundary at 0.59.

Note that the exact location and normalisation of the boundaries is not decisive for our results because we qualitatively analyse the influence of tCDR management on the existence of desirable trajectories. Slightly different sets of planetary boundaries would not qualitatively change the systemic effects reported in this study.

4.2.4. Model analysis and terminology

Our analysis of the co-evolutionary system aims at assessing transient dynamics of carbon pools with respect to planetary boundaries. First (Sec. 4.3.1), we run the model and exemplarily show the influence of socially controlled parameters of tCDR implementation on the transient carbon pool evolution. It is of particular relevance under what circumstances the simulated carbon pool trajectories (atmosphere, ocean and land) do not cross their respective planetary boundaries. We refer to the regions on the safe side of the planetary boundaries as *safe regions*. All carbon pool trajectories remaining in the respective safe region at all times are considered *safe trajectories*. For example, all atmospheric carbon trajectories that do not cross the planetary boundary for climate change (i.e. trajectories that are in the safe region of atmospheric carbon) are safe atmospheric carbon trajectories. System states with each carbon pool remaining in its respective safe region are referred to as carbon system states in the safe operating space, i.e. *safe states*.

In a nonlinear dynamical system, trajectories can be sensitive to initial conditions. The preindustrial distribution of carbon pools, as well as carbon dynamics in the Earth system are relatively well assessed, while still subject to high uncertainty (Ciais et al., 2013). Furthermore, considerable uncertainty remains with respect to our conceptual model structure and the exact values of planetary boundaries. Bearing in mind these inherent uncertainties, we explore how robust the existence of safe trajectories is under a variation of the initial conditions, i.e. the initial carbon pool distribution, and different tCDR characteristics (Sec. 4.3.2).

Such a variation of initial conditions is also a common approach to conceptualising and measuring resilience of social-ecological systems as the ability to return to an attracting state after a perturbation (Holling, 1973; Scheffer et al., 2001). A suitable approach to quantifying the likelihood of a complex system to return to an attracting state under finite perturbations is basin stability analysis (Menck et al., 2013).

In the context of planetary boundaries, not necessarily all trajectories that approach a *safe attractor* (i.e. an attractor within the SOS associated to all three planetary boundaries) would be considered safe, because they could temporarily leave the safe region. The concept of constrained basin stability (Kan et al., 2016) and related methods (Hellmann et al., 2016) provide generalisations of basin stability that allow taking transient phenomena into account. Similarly to the constrained basin stability approach, we classify different domains in the initial condition state space based on transient dynamics of carbon pools. The set of initial conditions resulting in safe carbon trajectories form the *safe domain*. We refer to this domain as the *manageable core of the SOS (MCSOS)*, as it depends on the tCDR management characteristics and the emission pathway. The *undesirable domain* is formed by all initial conditions resulting in a transgression of all three carbon boundaries at some point in time. Remaining state space domains are formed by initial conditions leading to a transgression of a subset of planetary boundaries. They are referred to as the respective *partially manageable domains (MD)* (e.g. the land manageable domain is the state space domain of initial conditions with trajectories without a transgression of the land boundary).

The computational efficiency of our model allows for a systematic analysis of the MCSOS and other domains under variation of societal parameters (tCDR management and fossil fuel emissions). We analyse how the size of all domains (MCSOS, partially MDs and the undesirable domain) varies with different tCDR characteristics (Sec. 4.3.3) and emission pathways (Sec. 4.3.4). In the spirit of Kan et al. (2016), the size of (partially) manageable domains can be interpreted as a resilience-like measure of the opportunities to stay within the carbon related SOS, taking into account inherent structural uncertainties of our model, the location of planetary boundaries, and the preindustrial carbon pool distribution. Note that the maximum extent of the MCSOS is constrained by the planetary boundaries, but it may differ from the SOS (i.e. the *safe* region), as the safety of the domain is determined by transient system dynamics, whereas the SOS is defined within static planetary boundaries.

4.3. Results and discussion

4.3.1. Carbon system trajectories subject to societal tCDR management loop

To illustrate how the co-evolutionary social-environmental system evolves with respect to carbon-related planetary boundaries, Figure 4.5 depicts trajectories of the major carbon pools with tCDR adhering to different management characteristics. All trajectories start at their respective normalised preindustrial state. The normalised planetary boundaries (Sec. 4.2.3) are indicated as dotted lines and the safe region of each boundary (refer to Sec. 4.2.4) is shaded in the respective colours. Variation of tCDR characteristics reflects

uncertainty about possible tCDR rates related to overall biomass harvesting potentials and societies'implementation capacities (Sec. 4.2.1).

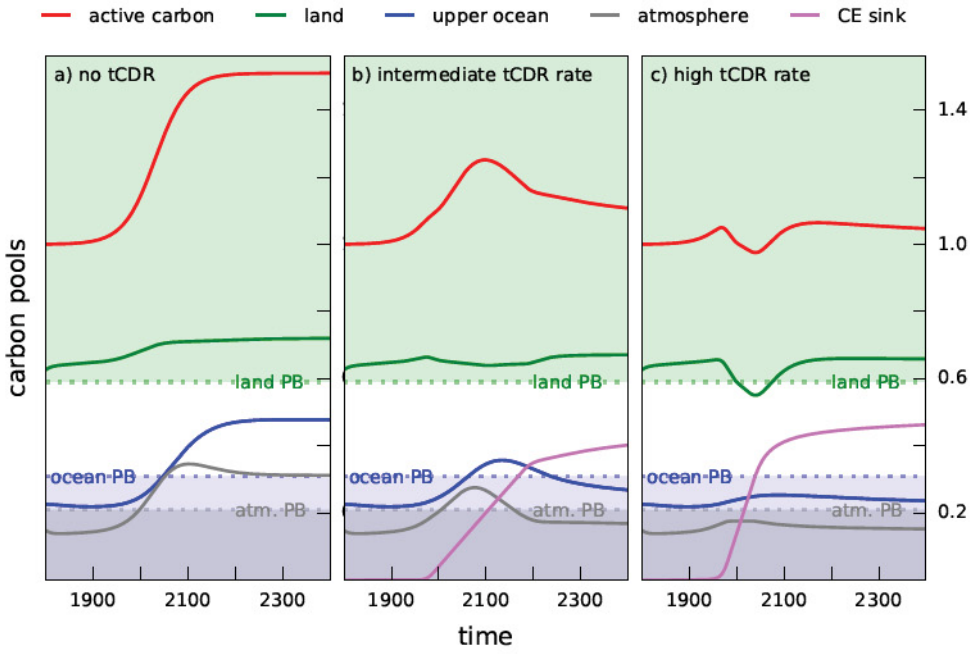

Figure 4.5.: Time evolution of the normalised carbon pools in our model of the carbon system for three tCDR configurations with a high emission baseline (cumulative emissions as in RCP8.5 (Riahi et al., 2011)): a) without tCDR ($\alpha_{max} = 0$), b) intermediate tCDR rate ($\alpha_{max} = 0.0025$) and c) high tCDR rate ($\alpha_{max} = 0.025$). Total active carbon (red) is increased by fossil fuel emissions ($c_{max} = 0.51$) with dynamic response of the terrestrial carbon pool (green), maritime carbon pool (blue) and atmospheric carbon pool (grey). The tCDR sink (purple) stores carbon extracted from the active system. Shaded areas represent the respective safe regions of land, ocean and atmosphere in green, blue and grey. Dotted lines indicate the location of the associated planetary boundaries.

The emission baseline used for all results displayed in Figure 4.5 is a business-as-usual scenario with cumulative emissions as in RCP8.5 (Riahi et al., 2011). Without tCDR (Fig. 4.5a), all fossil carbon societies emit into the atmosphere is distributed to ocean, land and atmosphere. This results in more active carbon (red), leading to carbon accumulation in all pools and a transgression of the atmosphere and ocean boundaries. In this emission scenario, the land system accumulates carbon and, thus, moves away from its planetary boundary in our model setting (note that the actual control variable of the planetary boundary of land-system change as defined by Steffen et al. (2015) is the remaining forest cover, which would not be directly modified by changing atmospheric carbon concentrations). Moreover, higher emission baselines (results not shown here) can lead to decreasing terrestrial carbon stocks when respiration dominates over photosynthesis due to strong global warming.

In Figures 4.5b) and c), the societal tCDR response via harvesting from the terrestrial carbon stock and subsequent storage starts just before the atmospheric boundary is reached ($\tilde{C}_a$=0.18∼340 ppmv). With a low tCDR rate (maximal storage flux of about 7 GtC a^{-1}, α_{max} = 0.0025), the CE sink is filled relatively slowly (Fig. 4.5b). Thus, a transient transgression of the atmosphere and ocean boundaries cannot be prevented. However, all trajectories re-enter their respective *safe* region after about 150 years. A higher tCDR rate (α_{max} = 0.025, corresponding to very high potential storage fluxes of 26 GtC a^{-1} or 5% of global biomass per year) can prevent a large increase in active carbon and thus prevents the transgression of both, atmosphere and ocean boundaries (Fig. 4.5c). However, extensive harvest from the land carbon pool then leads to a temporary transgression of the land boundary. The implementation of tCDR was thus effective in its purpose of preventing entry into a dangerous region of climate change, but at the cost of exploiting the land system to an extent that crossed the land system change boundary.

These results show that small tCDR rates (Fig. 4.5b) (or too late implementation, results not shown here) do not necessarily keep the system in the SOS. High tCDR rates (Fig. 4.5c) could seem successful when focusing on the climate change boundary, but might in fact not be feasible if other components of the carbon system are taken into account. In light of ongoing deforestation for the purpose of bioenergy production (Gao et al., 2011), this simulated collateral transgression of the land system change boundary with large-scale tCDR is an important and plausible feature of the model.

In the actual Earth system, a transgression of the land system change boundary might evoke additional trade-offs to the biogeophysical climate system (Foley et al., 2003), which are not represented in the model. For example, large tCDR rates can only be achieved by large-scale land-use change that could alter atmospheric circulations and rainfall patterns (Snyder et al., 2004) even though the carbon related climate change boundary might not be transgressed with high tCDR rates.

The carbon values stated here are primarily given as an orientation for the reader, and should not be directly interpreted with respect to tCDR feasibility assessments. However, tCDR rates of 7 GtC a^{-1} are in line with more conservative biomass harvest potentials considering biodiversity conservation and agricultural limits (Beringer et al., 2011; Dornburg et al., 2010). More idealistic assessments of tCDR rates of more than 35 GtC a^{-1} – assuming high biomass yields on more than 1/4 of global land area – have been reported as well (Smeets et al., 2007). In this context, the range of tCDR rates studied in this paper reflects both conservative and highly optimistic tCDR potentials reported in the literature.

4.3.2. State space domain structure of the Earth's carbon system subject to societal tCDR management loop

We compute the state space domain structure (refer to Sec. 4.2.4) from a sample of initial conditions around the preindustrial carbon state. We sample approximately 66,000 initial conditions from a regular grid by variation of each carbon pool by ± 0.2 around the preindustrial conditions. This range is a pragmatic choice which does not influence the following qualitative analysis. To compute the existing domains, we evolve each initial condition for 600 years in time and colour it according to the domains following from the transient properties of the trajectories of land, atmosphere and ocean carbon, as described above. The mapping of initial conditions sheds light on possible domains in the carbon system and potential transitions into other state space domains in our model of the carbon cycle. In this context, the vicinity of the preindustrial and current Earth system states to such domain boundaries in the model's initial carbon condition state space is of particular relevance.

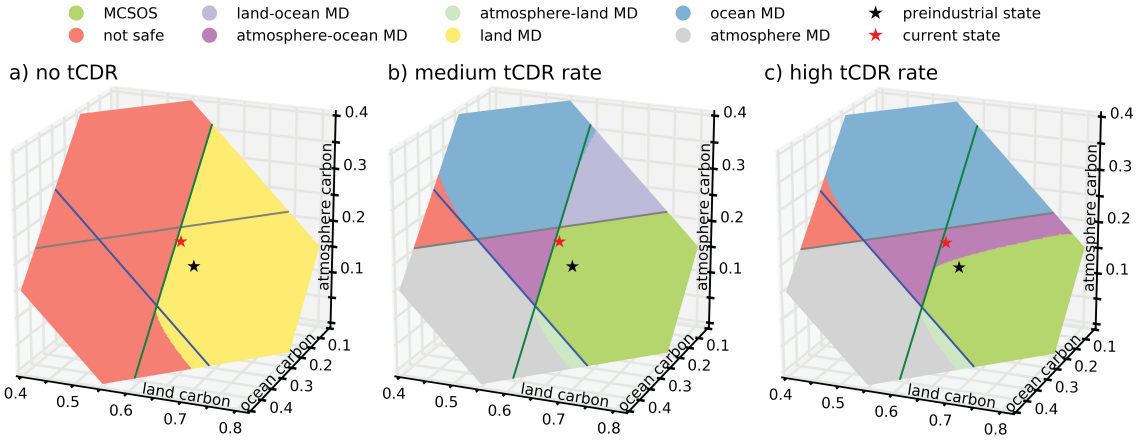

Figure 4.6.: Charting of normalised carbon system initial condition state space in our model for three tCDR management characteristics with identical, relatively low emission baseline ($c_{max} = 0.2$): a) without tCDR ($\alpha_{max} = 0$), b) intermediate tCDR rates ($\alpha_{max} = 0.004$) and c) high tCDR rates ($\alpha_{max} = 0.04$). The two-dimensional plane is formed by sampling initial conditions around the preindustrial state (variation of carbon stocks by ± 0.2 while conserving total carbon in the system). Each domain is coloured according to transient properties of trajectories starting in different state space regions. For example, the MCSOS (i.e. safe domain) is formed by the initial conditions of *safe* trajectories, whereas red indicates the initial conditions of trajectories crossing all respective planetary boundaries at some point of the simulation. Lines indicate the associated planetary boundaries of atmosphere, land and ocean in grey, green and blue, respectively.

Figure 4.6 shows the existing domains without tCDR (a), with intermediate tCDR rates (b) and with very high tCDR rates (c). The emission baseline is the same for all variations of tCDR characteristics, with cumulative emissions of approximately 880 GtC, which is

comparable to RCP2.6 cumulative emissions (Vuuren et al., 2011). The current state of the carbon cycle is located in proximity to domain borders, highlighting that it is close to a transgression of the land system and climate change boundaries. Historical emissions and land system changes have moved the state of the carbon cycle closer towards the undesirable domain, and remaining on an emission trajectory similar to RCP2.6 without tCDR results in the non-existence of the MCSOS (Fig. 4.6a). Thus, the manageable core does not exist if the implementation of tCDR management is not considered by society, even in a relatively low emission scenario.

Figures 4.6b) and c) serve as an example of how human intervention and management by tCDR can influence the size and even the existence of the MCSOS and other domains. With an implementation of tCDR, the MCSOS can be re-established, potentially to its full extent, which is directly determined by the three planetary boundaries (Fig. 4.6b). Even for a relatively low emission scenario, the tCDR threshold needs to be at sufficiently low atmospheric carbon contents ($\tilde{C}_a$ = 0.16) to prevent potential boundary transgressions. Nevertheless, because of past land use change, the current Earth system state is approaching domains with unsafe land system and climate change. If tCDR is applied under the same conditions but with a ten times higher potential tCDR rate (α_{max} = 0.04), the MCSOS shrinks due to over-exploitation of the land system for tCDR (Fig. 4.6c). The land system is over-exploited when the total human biomass offtake flux ($H_{CE} + H$) exceeds net ecosystem productivity (NEP). This decreases terrestrial carbon pools (Eq. 4.5) which in turn limits the potential for tCDR (Eq. 4.11). In Figure 4.6c) this occurs under high initial atmospheric carbon concentrations, because these result in a higher tCDR-flux for the same potential tCDR rate (α_{max}, ref. to Fig. 4.2). The current state of the carbon cycle of the Earth system is out of the MCSOS. In this case, large societal commitment to avoid a transgression of the climate change boundary leads to a collateral transgression of the land system change boundary in our model.

4.3.3. Size of manageable domains under variation of tCDR characteristics

The size and existence of the MCSOS and other state space domains depends on tCDR characteristics (refer to Sec. 4.2.4). We compute the size of the different initial condition state space domains depending on the most decisive management parameters, i.e. on the implementation threshold $\tilde{C}_a$ and on the potential maximum tCDR rate α_{max}. The size of all domains is measured in relation to the size of the considered state space section as depicted in Figure 4.6, which is given by a variation of preindustrial conditions by $\pm$ 0.2.

Figure 4.7 depicts the relative size of the MCSOS and the partially manageable domains under baseline emissions of $c_{max} = 0.4$, corresponding to cumulative emissions on the order of RCP6.0. The size of the MCSOS or partially MDs can be interpreted as a form of resilience

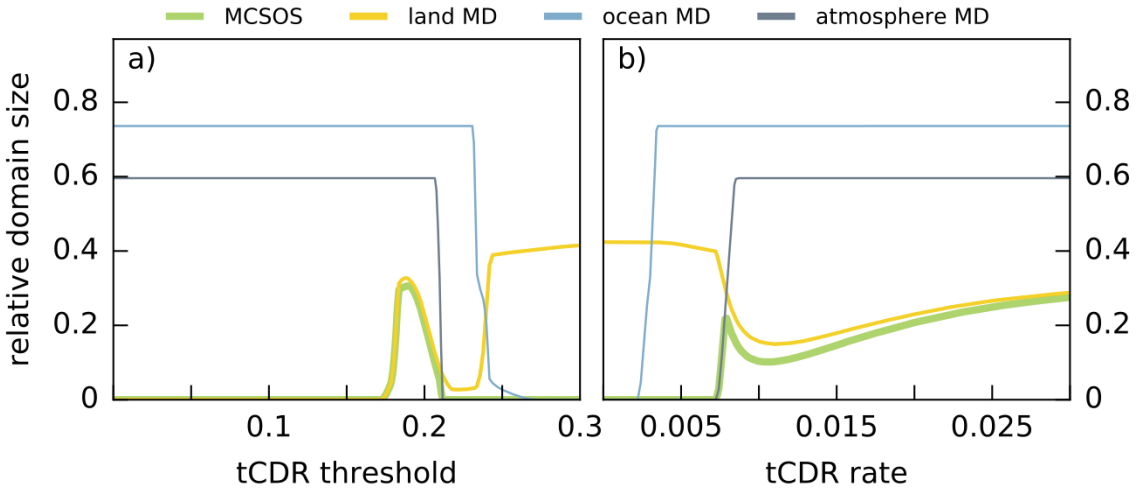

Figure 4.7.: Relative size of domains in modelled carbon system initial condition state space for normalised parameter variation of a) tCDR threshold (with $\alpha_{max} = 0.02$) and b) tCDR rate (with $\tilde{C_a} = 0.2$) for a medium emission scenario ($c_{max} = 0.4 \sim 1600$ GtC cumulative emissions). All domain sizes are given as shares of the state space region defined by a variation of the preindustrial conditions by $\pm$ 0.2.

of the system (i.e. the likelihood that the system stays within the carbon related SOS). Thus, we measure the resilience of the carbon cycle by the size of MCSOS (i.e. the opportunity of success of tCDR to maintain safe trajectories). This strongly depends on the atmospheric carbon threshold at which tCDR is implemented. Obviously, only the anticipation of an approaching planetary boundary can prevent a transgression thereof. Thresholds higher than the atmospheric carbon boundary ($b_l = 0.21$) are not sufficient in sustaining a MCSOS, because the atmosphere MD disappears by definition at $\tilde{C_a} = 0.21$ (grey line in Fig. 4.7a).

However, strong anticipation coupled with too early tCDR implementation does not necessarily maintain the system within the SOS. If tCDR is initialised at relatively low atmospheric carbon contents ($\tilde{C_a} = 0.13$ (approx. 330 ppmv) in Fig. 4.7a), the MCSOS is diminished due to a transgression of the land system change boundary at some point in time. Hence, the window of opportunity for using tCDR as a means of staying in the SOS under this exemplary fossil fuel emission scenario is limited to a relatively narrow range of tCDR implementation thresholds. The size of the land MD shows nonlinear dependence on the tCDR threshold. For thresholds between 0.2 and 0.25, the land MD is almost diminished (Fig.4.7a), because the relatively high tCDR rate ($\alpha_{max} = 0.02$) leads to an over-exploitation of the land system (ref. to Sec. 4.3.2). However, higher tCDR thresholds avoid this over-exploitation and increase the land MD, because of a later onset of tCDR and overall higher NEP due to higher atmospheric carbon contents and temperatures (Eq. 4.6).

Similar to the tCDR threshold, the parameter governing the maximal achievable rate of tCDR

plays a decisive role for the existence of the MCSOS. With a tCDR implementation threshold not far below the atmospheric carbon boundary ($\tilde{C}_a = 0.2$), high tCDR rates are required in order to maintain a MCSOS. TCDR starts being effective in maintaining a MCSOS at a rate of $\alpha_{max} > 0.007$ (corresponding to approx. 16.5 GtC a^{-1} with a fixed land carbon pool of 0.6). Rates smaller than that are not sufficient because of a lacking atmospheric MD (grey line in Fig. 4.7b).

As the tCDR threshold, also the tCDR rate influences especially the size of the land MD. For small tCDR rates, the land MD is sustained because of high atmospheric carbon concentrations small biomass extraction. Rates higher than $\alpha_{max} = 0.0075$ result in a smaller land MD due to the over-exploitation of the photosynthetic productivity of the system which is reduced by both, biomass removal and decreasing atmospheric carbon concentrations driving NEP. Higher rates, however, lead to overall smaller reductions of the land MD. This nonlinearity is evoked by the co-evolutionary feedbacks between society and the carbon cycle, which lead to a deceasing tCDR flux if the system is in the atmosphere MD. Thus, sufficiently high tCDR rates lead to fast atmospheric carbon decrease and tCDR is switched off before the land system boundary is transgressed.

This analysis of the size of initial condition state space domains suggests that the success of tCDR in sustaining the Earth system's persistence in the carbon SOS nonlinearly depends on the characteristics of tCDR implementation. On the one hand, foresightedness and anticipation of planetary boundaries are required to maintain the MCSOS, while on the other hand, too early or too intensive management could trigger co-transgressions of other planetary boundaries.

4.3.4. Opportunities and limitations of tCDR

While anticipation and appropriate management are necessary, the underlying emission scenario plays a major role in the resulting carbon dynamics. Figure 4.8 exemplarily depicts the relative MCSOS size for variations of tCDR characteristics (threshold and potential maximum rate) for emission pathways in accordance with RCP cumulative emission scenarios. The window of opportunity for successful tCDR (i.e. the size of the MCSOS) decreases with increasing emission baselines and depends on the tCDR rate and threshold. In the case of the low emission RCP2.6 scenario ($c_{max} = 0.2$), the MCSOS can be sustained for a broad range of parameter values (Fig. 4.8a). The medium emission scenarios RCP4.5 ($c_{max} = 0.31$, Thomson et al. (2011)) and RCP6.0 ($c_{max} = 0.36$, Masui et al. (2011)) show a more narrow range of tCDR characteristics that have the potential to sustain a MCSOS (Fig. 4.8b and c). In a business-as-usual RCP8.5 scenario, the room for manoeuvring to maintain a MCSOS is very small (Fig. 4.8d).

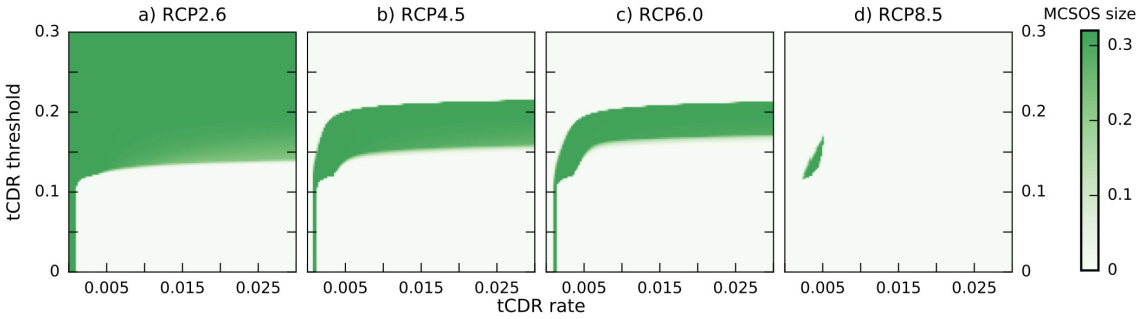

Figure 4.8.: Relative size of the MCSOS for normalised parameter variation of potential maximum tCDR rate (x-axis) and tCDR threshold (y-axis) for different underlying emission scenarios: a) RCP2.6 ($c_{max} = 0.2$), b) RCP4.5 ($c_{max} = 0.31$), c) RCP6.0 ($c_{max} = 0.36$) and d) RCP8.5 ($c_{max} = 0.51$).

Besides the dependence on the emission scenario, Fig. 4.8 highlights that for most emission scenarios the range of tCDR thresholds sustaining the MCSOS is narrow and depends on the tCDR rate. As discussed in Section 4.3.3 (for a fixed tCDR rate), tCDR thresholds higher than the atmospheric carbon boundary (0.21) are not sufficient in preventing a boundary transgression in the medium to high emission scenarios (Fig. 4.8b-d), whereas small tCDR thresholds lead to a transgression of the land system change boundary (unless tCDR rates are within a very narrow range smaller than 0.001). The variation of both, the tCDR rate and threshold, shows that smaller tCDR rates require a smaller minimal tCDR threshold as well as a smaller maximal threshold (Fig. 4.8b-d). This dependence of the success of tCDR on both, the tCDR characteristics and the underlying emission scenarios, highlights the relevance of societal intervention for global carbon dynamics. Essentially, tCDR intervention can trigger a nonlinear carbon system response through the land system when human carbon offtake exceeds NEP, which in turn causes a further reduction of NEP and tCDR potentials.

In our conceptual framework, tCDR can be effective in complementing climate change mitigation strategies as employed in low emission scenarios. However, already an RCP4.5 emission scenario narrows the range of potentially successful management options significantly in comparison to RCP2.6 emissions. Under a business-as-usual pathway, tCDR cannot be applied to maintain a MCSOS in a resilient way. In contrast to prevailing reasoning of CE as an emergency action in case of dangerous climate change (Caldeira et al., 2010), tCDR would most likely not function as an emergency option under high emission scenarios when additional sustainability dimensions reflected by other planetary boundaries are taken into account.

4.4. Conclusions

The introduced conceptual modelling approach – combining carbon cycle dynamics with a societal feedback loop of carbon monitoring and terrestrial carbon dioxide removal (tCDR) action – provides valuable insights into system-level constraints to navigating within the carbon-related safe operating space defined by several interlinked planetary boundaries. Despite the fact that the reported results cannot be taken as exact quantitative prognostics of carbon pool evolution, our analysis has shown that employing tCDR for managing the atmospheric carbon pool does not necessarily safeguard the carbon cycle in the safe operating space because of nonlinear feedbacks between tCDR management and the carbon system.

The success of maintaining a manageable core of the safe operating space depends on the degree of anticipation of climate change, the potential maximum tCDR rate, as well as the underlying emission pathway. While tCDR might be successfully deployed as part of a strong climate change mitigation scenario, it is not likely to be effective in a business-as-usual scenario. Particularly, the focus on one planetary boundary alone (e.g. climate change), may lead to navigating the Earth system out of the carbon-related safe operating space due to collateral transgression of other boundaries (e.g. land system change). In light of numerous (economically based) integrated assessment studies proposing tCDR to counteract anthropogenic emissions, our conceptual results highlight that it is vital to include integrated sustainability assessments of more advanced models to the debate on climate engineering (CE) and climate change mitigation via tCDR. In the case of tCDR, the consequences for biosphere integrity, as well as trade-offs with agricultural land use and the biogeophysical climate system must be taken into account among other sustainability dimensions reflected by planetary boundaries and beyond.

In analogy to our analysis for tCDR, the approach followed in this paper could be transferred to other CE proposals such as ocean fertilisation or solar radiation management. Additionally, it would be of interest to extend the analysis provided here and study Earth system dynamics under CE with more detailed models in line with the framework proposed by Heitzig et al. (2016), including a full topological analysis of the system with respect to the possibility of avoiding or leaving undesired domains, the reachability of desirable domains and the various management dilemmas induced by this accessibility structure.

Acknowledgements This research was performed in the context of PIK's flagship projects COPAN on Coevolutionary Pathways and OPEN on Planetary Boundaries and Opportunities. VH and WL were funded by the DFG in the context of the CE-Land project of the Priority Program "Climate Engineering: Risks, Challenges, Opportunities?" (SPP 1689). JFD thanks the Stordalen Foundation via the Planetary Boundary Research Network (PB.net) and the Earth

League's EarthDoc program for financial support. The authors gratefully acknowledge the European Regional Development Fund (ERDF), the German Federal Ministry of Education and Research and the Land Brandenburg for supporting this project by providing resources on the high performance computer system at the Potsdam Institute for Climate Impact Research. The authors are grateful to Jobst Heitzig, Dieter Gerten, Tim Kittel, Wolfram Barfuss and the two referees for helpful comments and discussions.

Author contribution VH and JFD designed the study. VH implemented and validated the model and performed the simulations and analysis. VH prepared the manuscript with contributions from all co-authors.

5. Minimising carbon and biodiversity loss – food security within the safe operating space

Vera Heck[1,2], Holger Hoff[1,3], Stefan Wirsenius[4], Carsten Meyer[5], Holger Kreft[5]

[1] Earth System Analysis, Potsdam Institute for Climate Impact Research, Telegraphenberg A62, 14473 Potsdam, Germany
[2] Department of Geography, Humboldt-Universität zu Berlin, Unter den Linden 6, 10099 Berlin, Germany
[3] Stockholm Resilience Centre, Stockholm University, Kräftriket 2B, 114 19 Stockholm, Sweden
[4] Department of Energy and Environment, Chalmers University of Technology, 412 96 Gothenburg, Sweden
[5] Biodiversity, Macroecology and Biogeography, Georg-August-University Göttingen, Büsgenweg 1, 37077 Göttingen, Germany

The following manuscript is preliminary and has not been submitted yet.

5.1. Introduction

There is increasing attention to global aspects in the sustainability debate. The 2030 Agenda for example requests 'to implement the Agenda within our own countries and at the regional and global levels'. Global environmental sustainability criteria have been defined by the Planetary Boundaries framework (Rockström et al., 2009; Steffen et al., 2015). These boundaries delimit the environmental safe operating space from a large-scale perspective, as a pre-condition for human well-being and development. With that, the Planetary Boundaries (PBs) also set guardrails within which the Sustainable Development Goals (SDGs) need to be implemented. The PBs address for example climate change (with reference to the 2°C target), phylogenetic and functional biodiversity loss, land use change (with reference to forest cover), and freshwater use (Steffen et al., 2015).

While science is exploring each of the PBs in great detail now (e.g. Gerten et al., 2013; Newbold et al., 2016; Vries et al., 2013), there has been far less attention to related planetary

opportunities, which are the flipside of the same coin. In this paper we explore such global (top-down) opportunities for sustainable development within the globally defined safe operating space, considering land use as the key issue for sustainability transitions. While land use has repercussions at the global scale, e.g. in terms of carbon sequestration (Houghton et al., 2012; Pielke et al., 2002), biodiversity loss (Cardinale et al., 2012; Newbold et al., 2016) or moisture fluxes (Boisier et al., 2014; Keys et al., 2012), it is a very local phenomenon, which responds to larger scale drivers such as national legislation or global trade.

In order to concretely support sustainability transitions and guide sustainable environmental management and resource use, smaller scales of policy- and decision-making need to be integrated with the global PB perspectives. This raises the question, what such top-down planetary opportunities imply for individual regions or countries and how consistent global approaches are with bottom-up local or national strategies or plans (e.g. national development plans). Agenda 2030 refers to this type of consistency across scales by requiring 'each government setting its own national targets guided by the global level of ambition but taking into account national circumstances'. Thus, there is a need for complementing existing systems approaches such as Integrated Water Resources Management (Agarwal et al., 2000), Ecosystem Approaches (CBD, 2000) or Landscape Approaches (DeFries et al., 2010; Sayer, 2009) (which generally address horizontal integration across sectors and disciplines) with a vertical integration component across scales and levels.

There have been numerous scenario exercises on future land use (e.g. Pereira et al., 2010; Prestele et al., 2016). Land use scenarios depend on wide range of assumptions about drivers such as population growth, technological progress and efficiency increase, lifestyle change and consumption patterns (Harfoot et al., 2014). In this paper we combine multiple sustainability criteria for land use, in particular food production, carbon sequestration and biodiversity conservation, implicitly also forest cover and water use, with a spatially explicit land use optimisation. Moreover we begin a to combine sustainability criteria at multiple spatial scales, i.e. global, regional and national. With that we explore opportunities for sustainable land use that integrates horizontally (across sectors) and vertically (across scales). We seek solutions that help to stay within the environmental safe operating space, while feeding a global population of 9.1 billion people (which is the population projection for the year 2050 in the middle-of-the-road SSP2 scenario (Yamagata et al., 2015)). We include scenarios on improvements of agricultural (crop and livestock) productivity and aim at reducing the transgression of the PBs for climate change and biosphere integrity which are integrated in our optimisation via the sustainability criteria of terrestrial carbon storage and risk to biodiversity. We further account for the PBs for land system change (control variable: forest cover fraction) and freshwater use (control variable: consumptive blue water use) (Steffen et al., 2015). Eventually we begin to apply the global solutions to individual regions and countries to assess the consequences e.g. in terms of selected SDG targets.

5.2. Methods

The optimisation of land use scenarios (Fig. 5.1) is based on simulations with the state of the art dynamic vegetation model LPJmL (ref. to Sec. 5.2.1) and data sets on biodiversity and land suitability (ref. to Sec. 5.2.4). The optimisation is driven by scenarios of agricultural productivity, global population and food demands (ref. to Sec. 5.2.5) and considers multiple constraints (ref. to Sec. 5.2.4) while maximising terrestrial carbon storage and minimising the risk to biodiversity. The optimisation model and its foundations are described in more detail in the following sections.

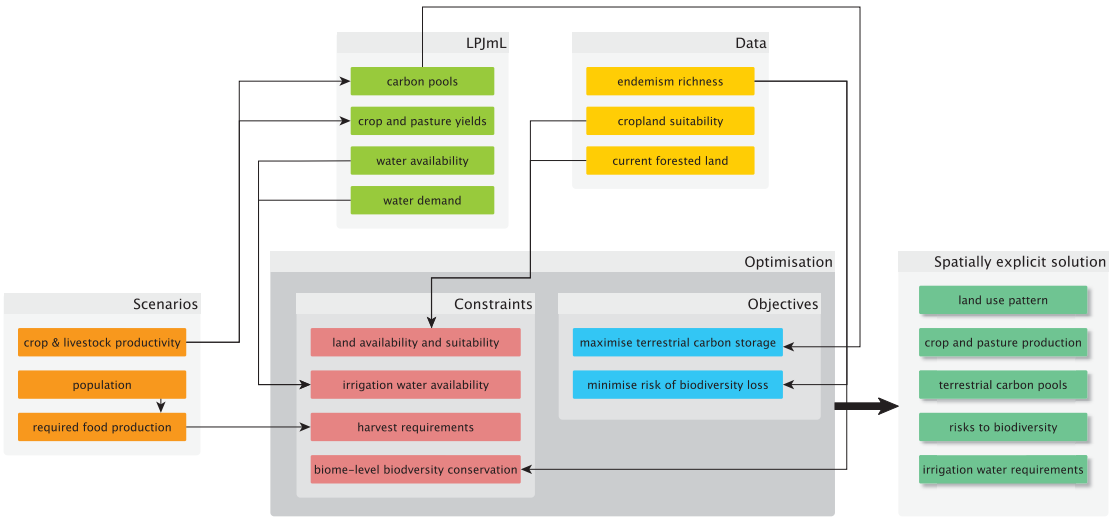

Figure 5.1.: Methodological workflow

5.2.1. LPJmL model

We use LPJmL to simulate carbon pools on natural and agricultural land, crop harvest potentials and agricultural water consumption and water availability for different agricultural efficiencies (Sec. 5.2.5). LPJmL is a process-based dynamic global vegetation model with representations of natural and managed ecosystems. It simulates key ecosystem processes of the carbon (Bondeau et al., 2007; Sitch et al., 2003) and water cycle (Gerten et al., 2004; Rost et al., 2008b; Sitch et al., 2003) at daily time steps with a spatial resolution of 0.5°. LPJmL has been extensively validated for its representation of carbon cycles (Sitch et al., 2003), agricultural crop production (Bondeau et al., 2007; Fader et al., 2010), irrigation requirements, river flows and water fluxes (Gerten et al., 2004; Rost et al., 2008b).

Natural vegetation is represented by nine plant functional types (PFTs) which are dynamically distributed depending on climate (Sitch et al., 2003); agricultural vegetation is represented by 12 crop functional types (CFTs), grazing land and biomass functional types (BFTs). The distribution and irrigation management of agricultural vegetation and biomass plantations is prescribed (Beringer et al., 2011; Bondeau et al., 2007; Jägermeyr et al., 2015)). Crop sowing and harvest dates are simulated based on CFT-specific parameters and climate characteristics (Bondeau et al., 2007; Waha et al., 2012). Agricultural management intensity is represented by three coupled CFT-specific parameters, maximum leaf area index (*LAImax*), a scaling factor for leaf-level photosynthesis (*alphaA*) and a *harvest index* describing the ratio of harvested storage organ to total above ground biomass. Agricultural production intensity is calibrated at the country level via *LAImax* which can range from 1 (lowest intensity) to 7 (highest intensity) to simulate the best approximation of national yield statistics of the Food and Agriculture Organization's FAOSTAT database from 1999-2003 (Fader et al., 2010). Crops that are not represented by the 12 CFTs are simulated as grasslands and here referred to as *others*. Grazing land and *others* are harvested to 50% as soon as the above-ground carbon pool threshold is reached.

5.2.2. LPJmL simulations

LPJmL was used to determine potential carbon pool changes and yields under the cultivation of pastures, crops (irrigated and rainfed) and *others* (irrigated and rainfed) as well as potential irrigation water requirements and water availability of irrigated crops and *others* as inputs to the optimisation model. For this purpose, LPJmL was driven by historical climate data from CRU TS3.10 (Harris et al., 2014). To bring soil carbon pools and vegetation distribution into equilibrium, all simulations were preceded by a 5000-year spin-up with potential natural vegetation (PNV) repeating climate data of the years 1901-1930. Subsequently, various potential land use configurations (see Table 5.1) are simulated from 1976-2005 with an additional spinup of 390 years allowing for the adjustment of carbon pools.

Simulation	Land use input
PNV	potential natural vegetation
CURR	current cultivated crop area according to GAEZ (Fischer et al., 2012), pasture extend from (Ramankutty et al., 2008)
PAS	pastures globally
C_r - FAO	rainfed crops globally; current crop mix in grid-cell (LPJmL crops 1-12) is maintained but scaled to 100%; grid-cells currently without crops are assigned the country mean crop mix (*LAImax* calibration to FAOSTAT)
C_r - 1/2 yield gap	spatial distribution as above, but with halved yield gaps at the country level (the gap between calibrated *LAImax* and highest *LAImax*(7) is halved)
C_i - FAO	potentially irrigated crops globally; current crop mix in grid-cell (LPJmL crops 1-12) is maintained but scaled to 100%; grid-cells currently without crops are assigned the country mean crop mix (*LAImax* calibration to FAOSTAT)
C_i - 1/2 yield gap	spatial distribution as above, but with halved yield gaps at the country level (the gap between calibrated *LAImax* and highest *LAImax* (7) is halved)
O_r	rainfed *others* globally
O_i	potentially irrigated *others* globally

Table 5.1.: LPJmL simulation protocol for the generation of optimisation inputs.

5.2.3. Optimisation model

We developed a spatially explicit land use optimisation model (based on the R-package *lpSolveAPI* for linear optimisation (Konis, 2016)) that distributes agricultural land use while minimising global terrestrial carbon pool losses (L_c) and the global risk of biodiversity loss (R_b) as well as fulfilling scenario driven food supply constraints. To this end, the grid cell fractions under cultivation of LPJmL crops (irrigated crops c_i or rainfed crops c_r), LPJmL *others* (irrigated o_i or rainfed o_r) and pastures (rainfed p) are varied on a 1.0°-grid until a global optimum is found:

$$\min_{f_{agr}} \left(w_b \; R_b(f_{agr}) + w_c L_c(f_{agr}) \right) \; | \; C_f, C_l, C_i, C_b, \tag{5.1}$$

$$\text{with } f_{agr} = f_{ci}^{j} + f_{cr} + f_{oi} + f_{or} + f_p. \tag{5.2}$$

The distribution of agricultural land use is subject to scenario driven food supply constraints on the global harvest of crops, *others* and pastures (C_f), constraints on land availability and suitability (C_l), constraints on irrigation water availability (C_i) and regional biodiversity conservation (C_b), described in Section 5.2.4. Throughout different optimisation runs, the weights on biodiversity w_b and on carbon w_c conservation are varied ($w_b + w_c = 1$).

To measure the risk of biodiversity loss, we define a global biodiversity risk indicator:

$$R_b(f^j_{agr}) = 1 - \frac{\sum_{j=1}^{n} E^j_r (1 - f^j_{agr})}{\sum_{j=1}^{n} E^j_r}, \tag{5.3}$$

based on terrestrial vertebrate endemism richness (E_r) in grid-cell j (details in SI 5.5.1) and the grid-cell fraction under agricultural land use (Eq. 5.2). In order to capture the risk of extinction from cropland expansion, we take endemism richness (Kier et al., 2009) as biodiversity indicator, which can be interpreted as the specific contribution of an area to global biodiversity. Without any agricultural land use R_b is zero whereas global full agricultural land use results in $R_b = 1$. Terrestrial carbon losses (L_c) in soil, litter and vegetation are calculated by comparing potential carbon storage under natural vegetation (C_{pnv}) to carbon storage under different agricultural land use types (C_{LU}), simulated by LPJmL (Sec. 5.2.1):

$$L_c(f^j_{LU}) = \sum_{j=1}^{n} \left(C^j_{pnv} - \sum_{LU \in c_r, c_i, o_i, o_r, p} f^j_{LU} C^j_{LU} \right). \tag{5.4}$$

In the optimisation, carbon pools are normalised to the global average of potential carbon pools per gridcell (C^j_{pnv}) and endemism richness is normalised to the global average of potential endemism richness per gridcell (E^j_r).

5.2.4. Optimisation constraints

The distribution of crop, *others* and pasture grid-cell fractions is subject to various constraints on harvest requirements, land and water availability as well as biodiversity conservation, some of which are varied throughout the study.

Harvest requirements Global sums of minimum required calories production from LPJmL crop types (in kcal/a), minimum harvest from the LPJmL-type *others* (in dry matter t/a) and minimum pasture harvest (in dry matter t/a) are prescribed in the optimisation. We use FAOSTAT's food balance sheets for 2005 (FAOSTAT, 2005) to derive vegetal calories production from the LPJmL category *others* (13.8% of the total calories production), which is not explicitly simulated by LPJmL. As yields from foddergrass (for the livestock sector) are not included in the food balance sheets but part of the *others*-category in the LPJmL land use data, we accounted for them separately, assuming 15% of the *others*-harvest to be foddergrass (Portmann et al., 2010). Further, we integrate production data for other utilities, waste and seed into the production for food (i.e. total production without production for

feed), implying a constant ratio of production for food and production for other utilities, waste and seed.
Required crop-calories production and harvest depend on population, food supply and livestock efficiency scenarios (ref. to Sec. 5.2.5). In the case of current food supply and a change in population, the required production of crops, *others* (including foddergrass) and pasture is changed linearly to population change. In the case of improved food supply and a change in population, additional calories production requirements for vegetal products are fulfilled only from the category crops, as these have an explicit representation in LPJmL and include the major energy yielding crops. In the livestock sector the shares of crops, *others*, foddergrass and pasture are kept constant in the baseline productivity scenario or changed according to livestock productivity increases.

Land availability and suitability Land availability varies for the optimised land use types. Forest areas based on intact forest landscapes (IFL) of the year 2000 (Potapov et al., 2008) and GAEZ forest land cover (Fischer et al., 2012) are restricted for all types of land use. Grazing land expansion is allowed on all other areas with net primary productivity (NNP) higher than 20 gC/m^2 (Erb et al., 2007) to exclude marginal lands. Crops and *others* expansion is allowed on potential suitable cropland derived from FAO GAEZ areas. To this end, areas with rainfed soil and terrain suitability index from 1 (very high) to 6 (marginal) for high and low input (Fischer et al., 2012) are spatially averaged to obtain potential intermediate input areas for crops and *others*.

Irrigation water availability Irrigation expansion is allowed anywhere on crop suitable areas, as long as sustainable irrigation water is available. To define water availability, we use a water stress indicator (WSI) that defines the scarcity of water for human use via the mean annual runoff (MAR) after accounting for environmental flow requirements (EFRs) (Smakhtin et al., 2004):

$$WSI = \frac{\text{withdrawal}}{MAR - EFR} \tag{5.5}$$

From Eq. 5.5 we obtain allowed withdrawals per river basin and grid-cell for different WSI levels. According to Smakhtin et al. (2004), basins are overexploited when WSI > 1, heavily exploited when $0.6 \leq$ WSI < 1, moderately exploited when $0.3 \leq$ WSI < 0.6 and sightly exploited when WSI $<$ 0.3. In this study we limit tolerable water stress to WSI ≤ 0.3 (allowing for slightly exploited basis). The effects of allowing moderately exploited basins (WSI ≤ 0.6) is shown in the supplementary material (Fig. 5.8). EFRs are set at 30% of mean annual discharge (Gerten et al., 2013).

Biodiversity conservation As an additional constraint to the objective of minimising biodiversity losses, a biome-level biodiversity conservation is introduced to prevent the risk of biome-level biodiversity extinction:

$$\sum_{j=1}^{n_b} f_{agr}^{j} E_r \geq (1 - c_b) \sum_{j=1}^{n_b} E_r, \tag{5.6}$$

with $j = 1...n_b$ grid-cells in each biome, f_{agr} fraction under agricultural land use and the parameter for biome level biodiversity conservation; $c_b \in [0, 0.9]$. The latter is varied in this study.

5.2.5. Optimisation scenarios

Overall, all optimisation scenarios are based on constant current climate patterns (ref. to Sec. 5.1) and maintain at least the primary forest cover on currently forested land. Furthermore, we maintain the current crop distribution per grid-cell (or reference to national average if currently uncultivated land is cultivated with crops) assuming that the current crop mix in itself is a historic optimisation.

We perform optimisations of land use patterns for different scenarios of food supply and crop and livestock efficiency for a global population of 2050 (9.1 billion under the SSP2 scenario (Yamagata et al., 2015)) and for a baseline population of 2005 (6.4 billion (University, 2005)). The baseline food supply is 2761kcal/cap/d with a share of 17% from animal products according to the FAO's Food Balance Sheets for 2005 (FAOSTAT, 2005). The improved food supply scenario assumes a food supply of 3000 kcal/cap/d with a share of 20% from animal products as a simplistic proxy for food security (Rockström et al., 2007).

The efficiency scenarios for the agriculture and livestock sector represent current productivity and an improved crop and livestock productivity scenario. For current crop and livestock productivity, LPJmL crop yields are calibrated to FAO statistics (Sec. 5.2.1). Current input-output ratios of produced feed calories per crops, *others*, foddergrass (15% of *others* (Portmann et al., 2010)) and pasture were derived from the Food Balance Sheets of 2005 (FAOSTAT, 2005) and are kept constant in the baseline scenario.

The improved crop and livestock productivity scenario is motivated by the fact that agricultural productivity has always increased and is expected to increase further (Bruinsma, 2009). The rate at which this will happen is, however, highly uncertain. For example, Bruinsma (2009) assumes a yield increase by about 70% by 2050 compared to 2005. For crop productivity increase, we here assume that the gap between current and obtainable yields under optimal management is reduced by 50% (as e.g. in Rockström et al., 2014) and change the calibration of LPJmL accordingly (ref. to Sec. 5.1). Thereby, the crop yields of low management systems

are increased more substantially than the yields in well managed systems. Productivity increase in the livestock sector is based on a scenario of ruminant meat substitution (RMS) (Wirsenius et al., 2010). This assumes an improved livestock productivity compared to FAO projections combined with a decrease in per-capita consumption of ruminant meat (beef and mutton) which is replaced by pork and poultry (Wirsenius et al., 2010). In the RMS scenario, feed intake per output is reduced by 5.7% for crops, by 16.9% for *others* (including foddergrass) and by 41.0% for pastures, compared to the baseline.

5.3. Results and discussion

5.3.1. Global opportunities and trade-offs of optimised land use patterns

From the land use optimisation, we obtain curves of pareto-optimal solutions, when applying different objective weights for terrestrial carbon storage (w_c), risk to biodiversity (w_b) and varying different biome level biodiversity conservation criteria (Sec. 5.2.4). Fig. 5.2 depicts the range of possible solutions for each of the considered scenarios (Sec. 5.2.5). The left ends of the pareto-optimal curves are optimisation runs with zero weight on biodiversity conservation (yielding the highest potential of carbon accumulation) while the right ends have zero weight on carbon storage (yielding the highest potential of biodiversity risk reduction). Thus, the pareto-optimal curves demonstrate trade-offs between carbon storage and biodiversity conservation.

All solutions (Fig. 5.2) ensure the prescribed food supply. As a simple proxy for food security, global food supply was prescribed at the level of 3000 kcal per capita and day with 600 kcal per capita per day from animal products to ensure sufficient protein supply. This is an increase of about 10% from the current per-capita calorie supply and 22% from the current supply of animal products. Defining food security as a certain global average per-capita calorie production assumes a free distribution (via trade) of surplus production to deficit areas (ref. to Sec. 5.3.3). Overall, most of the optimised land use patterns show significant potential to increase terrestrial carbon storage and lower the global risks to biodiversity, while providing the required food supply (Fig. 5.2).

Obviously, the potential for improving land use in terms of terrestrial carbon storage and risks to biodiversity depends on the food requirement (driven by the per-capita calorie supply and the total population size) and the agricultural productivity. The current per-capita daily supply of 2761 kcal (lighter colours) yields higher carbon sequestration potentials and lower risks to biodiversity compared to the scenario of improved per-capita calorie supply (darker colours). Improved agricultural productivity (triangles) allows for more carbon sequestration

and lower risks to biodiversity compared to current agricultural productivity (circles), ceteris paribus.

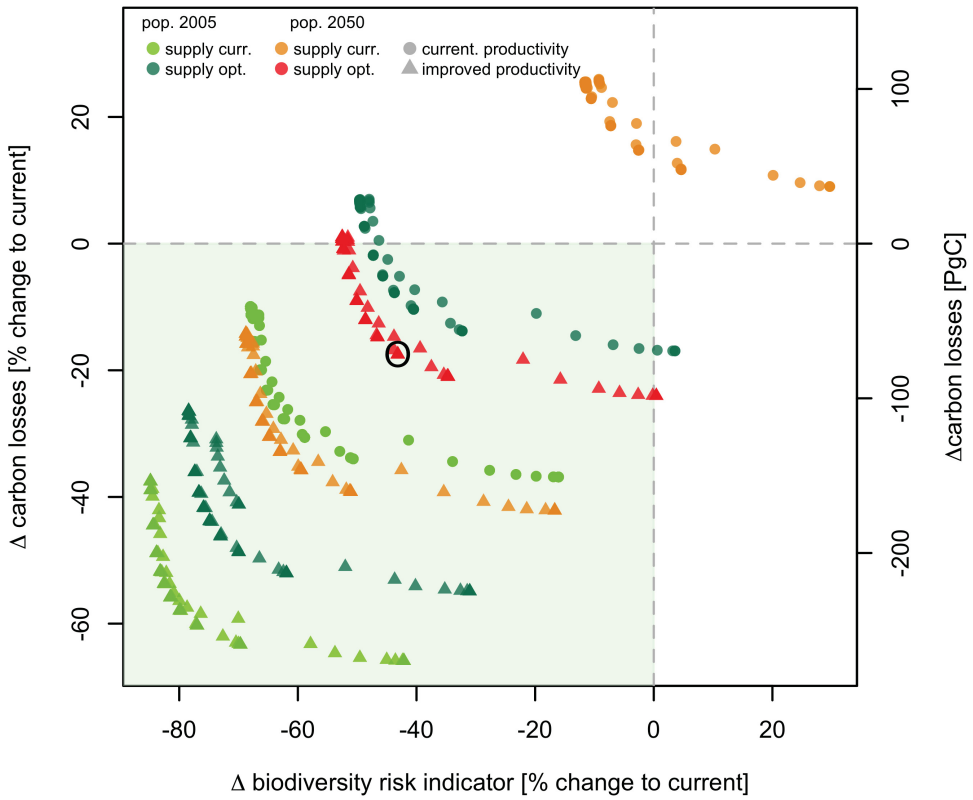

Figure 5.2.: Pareto-optimal curves for different populations, food supply levels and agricultural productivities. Each pareto-optimal curve (one colour and shape) consists of a range of solutions representing different weights on carbon and biodiversity in the objective function and different constraints on minimum biome-level biodiversity conservation. The axes depict global changes (optimised minus current land use) in the biodiversity risk indicator (x-axis) and changes (optimised minus current land use) of terrestrial carbon losses associated to land use change (vegetation and soils) (y-axis) of the optimised land use pattern, compared to current land use. The scenario marked with a circle is analysed in more detail and spatially explicit below.

Without the improvement of agricultural (crop and livestock) productivity, improved food supply (3000 kcal, 600 kcal from livestock products) cannot be achieved for a population of 9.1 billion in our optimisation (as projected in the SSP2 scenario for 2050 (Yamagata et al., 2015), no red circles in Fig. 5.2). At current agricultural productivity, per-capita daily food supply for the projected population of 2050 remains limited to current level of 2760 kcal with 17% from livestock products (orange circles). Note that in this scenario, terrestrial carbon

storage is smaller compared to current land use. Only in some of the solutions in their scenario (with $w_b > w_c$) at least achieve a reduction of the risk to biodiversity.

However, the projected population of 2050 can also be food secure at the higher per-capita daily food supply level of 3000 kcal per capita and day if agricultural productivities are increased. In that case terrestrial carbon storage can be increased by up to 98 GtC ($w_b = 0$) and risks to biodiversity can be decreased by up to 53% ($w_c = 0$), compared to the current situation (red triangles in Fig. 5.2). This, however, requires significant improvements in crop and livestock productivity in addition to the land use optimisation itself. We apply stylised improvements in agricultural productivity, i.e. a uniform reduction of all yield gaps for crops by 50% and an increase in livestock conversion efficiency and productivity, including a shift from ruminant to monogastric products (ref. to Sec. 5.2.5 and Table 5.3).

Figure 5.2 further shows that for the 2005 population the optimisation of land use patterns – when maintaining current food supply levels and current agricultural productivity – allows for terrestrial carbon sequestration of 151 GtC (long-term). This corresponds to a reduction of terrestrial carbon losses from historical land use change by up to 37% (light-green circles, Fig. 5.2). Even with improved food supply for the 2005 population, significant carbon sequestration potentials of 69 GtC exist (dark-green circles). Higher agricultural productivity could even increase this potential to 225 GtC, re-sequestering a significant share (55%) of carbon losses attributed to historical land use change.

The potential reduction of the risk to biodiversity (R_b, Eq. 5.3) is remarkable in scenarios with improved agricultural productivities (Fig. 5.2). It ranges up to -84% for the population of 2005 and current food supply (light green triangles) and -69% under current (orange triangles) or -53% under improved food supply (red triangles) for the population of 2050. Even under current agricultural productivity and when supplying 9.1 billion people with food at the current level of 2761 kcal per capita and day, biodiversity risks can be reduced by 12% (orange triangles).

Overall, the optimisation objectives to reduce the risk to biodiversity and carbon losses at the global level (Eq. 5.1) result in the re-allocation of agricultural production to regions with relatively high productivity and water availability but relatively low endemism richness and terrestrial carbon pools. The variation of the objective weights for carbon storage and biodiversity conservation, highlights trade offs between the two optimisation objectives along the pareto-optimal curves. Essentially, optimised land use patterns allowing for higher carbon sequestration potentials come at the cost of higher risks to biodiversity loss, and vice versa. This trade-off is mostly evoked by differences in relative carbon and biodiversity richness in the boreal and tropical zones. While terrestrial carbon pools in the boreal zones are high, there is relatively low endemism richness. In the tropical zone, however, endemism richness is significantly higher and potential terrestrial carbon losses are lower. Thus, high objective

weights on biodiversity conservation lead to less agricultural land use in tropical regions of high endemism richness and more land use in the northern hemisphere with pasture areas shifting to the boreal zones. The opposite occurs for high objective weight on carbon sequestration where crop and pasture areas are shifted temperate and tropical zones.

While this global top-down optimisation of land use patterns shows significant opportunities on the production and supply side, additional opportunities exist at the consumption and demand side, e.g. in terms of reducing the contribution of livestock products to food security. Thus, changing consumption patterns and in particular diet changes can significantly widen the option space.

In the following we select a middle-of-the-road solution of the scenarios of a 2050 population of 9.1 billion with improved per-capita food supply and improved agricultural productivity (pareto-optimal curve represented by red triangles in Fig. 5.2 which we analyse in more detail (Table 6.2).

Scenario characteristics	
population	2050 (9.1 billion)
food supply	optimal (3000 kcal/cap/day, 20% livestock)
agricultural productivity	yield gap closure by 50%, improved livestock efficiency combined with a 20% ruminant meat substitution
optimisation weights	$w_b = 0.2$, $w_c = 0.8$
biome-level conservation	not more than 40% of endemism richness in each biome may be affected

Scenario results	
cropland area	1997 Mha (+ 451 Mha compared to current)
grazing land	2242 Mha (- 655 Mha compared to current)
terrestrial carbon pool	2759 GtC (+ 69 GtC compared to current)
biodiversity risk indicator	0.18 (- 0.14 compared to current)
remaining forest cover	77.7% of the natural forest cover (+ 3.2% compared to current)
irrigation water consumption	1699 km^3 (+ 980 km^3 compared to current)

Table 5.2.: Characteristics and results of the selected scenario.

We make this solution (marked with a black circle in Fig. 5.2) spatially explicitly and compare it to the current land use. The resulting change in land use (optimised minus current land use) of that solution is depicted in Figure 5.3. We find that the optimisation generally shifts crop production towards mid-latitude regions of the northern hemisphere, where productivity is higher (latitudinal gradient in Fig. 5.3). While in this scenario the demand for crop calories for food and feed increases by 58% compared to 2005 population and per-capita food supply,

crop area (crops and *others*) increases only by 29% (451 Mha). Particularily in Europe, the Western US and Western Asia, cropland replaces pastures (blue colour tones), whereas crop and pasture areas increase in particular in the mid US, parts of Brazil and Sub-Saharan Africa and Russia/Kazakhstan (red colour tones).

Crop and pasture land is abandoned in some tropical and boreal zones (green colors), allowing for forest regrowth and significantly reducing the risk of biodiversity loss (Fig. 5.4). Note that this assumes a reduction in biodiversity risk if agricultural land use is turned back into forest. Because of a substantial reduction in grazing land by 655 Mha (23%) total agricultural (crop and grazing) area shrinks by 5% (204 Mha) - while still supplying 3000 kcal per capita and day for more that 9 billion people.

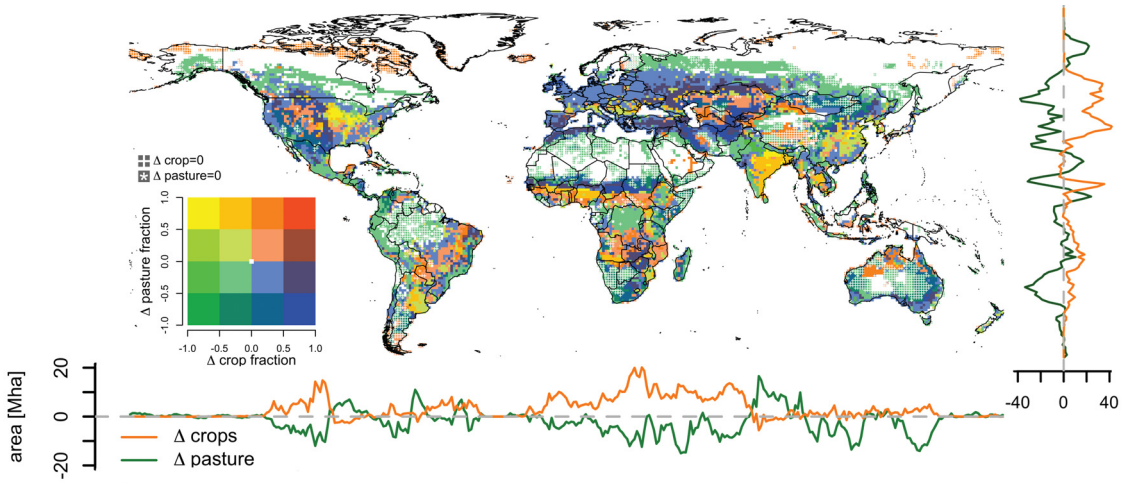

Figure 5.3.: Differences in crop and pasture fractions between the selected optimised land use scenario (Table 6.2) and current land use (optimised minus current land use). Longitudinal and latitudinal gradients depict the aggregated differences in crop and pasture areas of the respective longitudinal and latitudinal grid cells.

Agricultural land use shifts to regions with high land use efficiencies and where carbon losses and risks to biodiversity are lower per calorie produced compared to the current situation (Fig. 5.4). This reduces the total agricultural area, increasing forest land and allows for additional terrestrial carbon sequestration of 69 GtC and reducing the biodiversity risk indicator to 0.14 (from 0.33 under current land use). Terrestrial carbon storage increase almost uniformly across all latitudes, while the risk to biodiversity decreases almost uniformly across all latitudes (Fig. 5.4). This global top-down solution can be interpreted to support the 'land sparing'argument rather than the 'land sharing'argument Fischer et al., 2014 and its results need to be integrated with bottom-up sustainability criteria to eventually contribute to sustainable solutions at the local to national scale (ref. to Sec. 5.3.3).

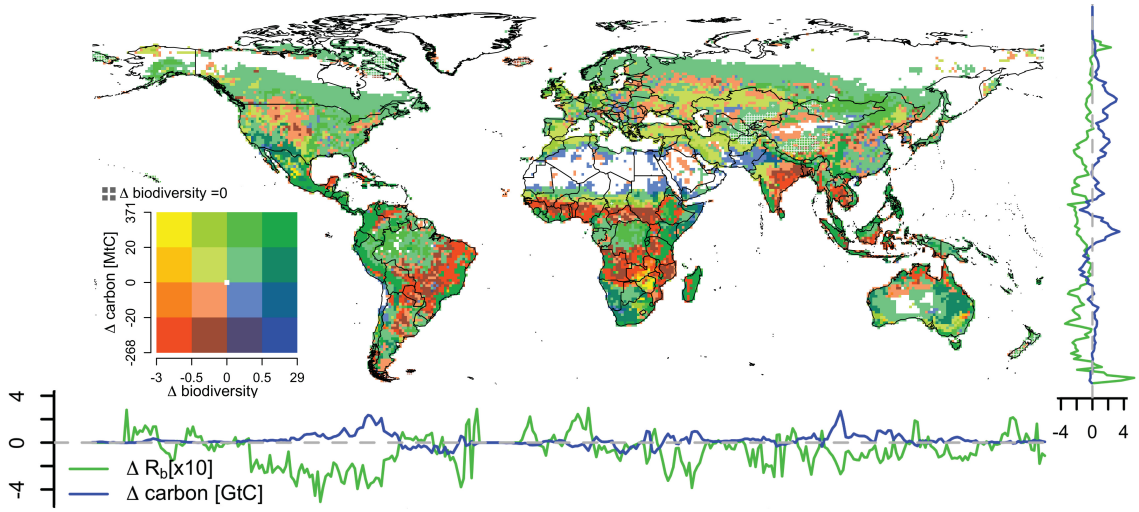

Figure 5.4.: Differences in the risk of biodiversity loss and terrestrial carbon storage between the selected optimised land use scenario (Table 6.2) and current land use (optimised minus current land use). Longitudinal and latitudinal gradients depict the differences in aggregated carbon pools and the differences biodiversity risk indicator of the respective longitudinal and latitudinal grid cells.

5.3.2. Planetary boundaries

The potential increase in global terrestrial (equilibrium) carbon storage of the selected scenario (Table 6.2) equals about 700% of current annual carbon emissions into the atmosphere (9.8 GtC/a, NOAA, 2015a) or 20% - 42% of the remaining total carbon emissions that can still be emitted into the atmosphere to likely keep global warming below 1.5 °C (i.e. 161 GtC - 338 GtC (Rogelj et al., 2016)). Thus, the optimised land use contributes to reducing the transgression of the PB for climate change which has been set at atmospheric CO_2 concentrations of 350 ppm (Steffen et al., 2015) – buying time for the transition to a low carbon economy.

Assuming that a reduction of land use pressure on endemism rich areas reduces the global species extinction rate or increases the global biodiversity intactness index (BII) (Scholes et al., 2005), the optimised land use would similarly reduce the current transgression of the PB for biosphere integrity.

Additional to carbon storage and biodiversity conservation which are explicit objectives of the optimisation, the optimised land use also helps to safeguard the PB for land use change, which is set at remaining 75% of original forest cover (85% for tropical and boreal forests and 50% for temperate forests). In total, the optimised land use allows for forest regrowth on 204 Mha compared to the current situation.

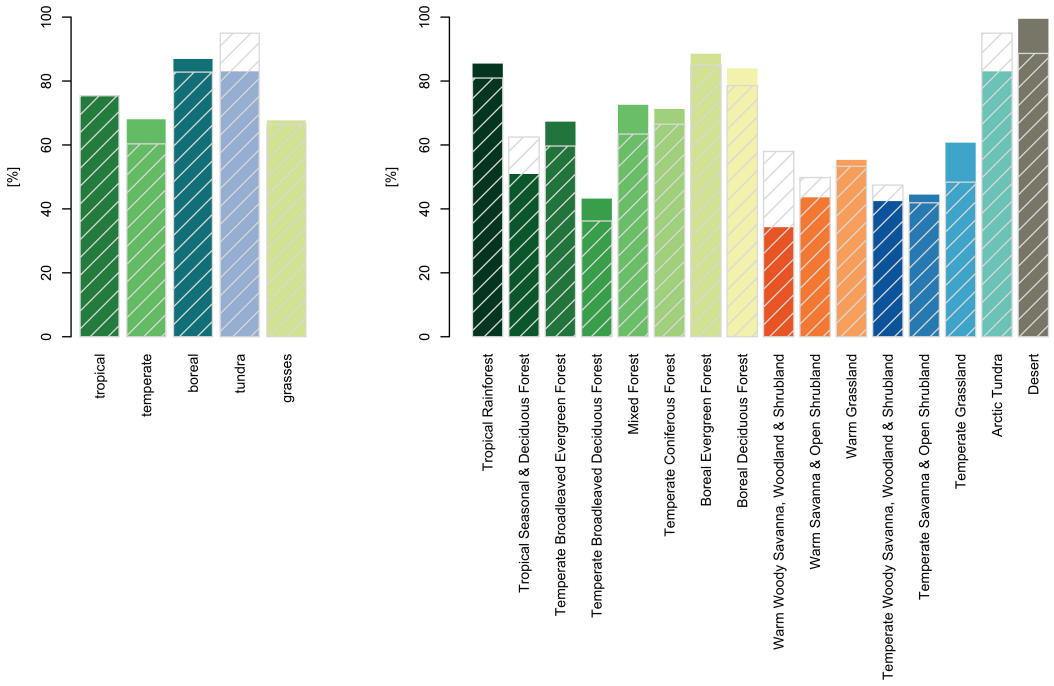

Figure 5.5.: Remaining biome as share of original biome for the optimised land use pattern (coloured bars) and the current land use patter (shaded bars). Biomes are classified into 16 biome classes based on LPJ simulations with potential natural vegetation as in Ostberg et al., 2015. Biomes on the left are aggregations of the respective biome classes.

Figure 5.5 shows the percentage of each biome that remains without any agricultural land use for the optimised (coloured bars) and current (hatched) land use. The biome classification into 16 different biome classes is based on LPJ simulations with potential natural vegetation (see Ostberg et al., 2015, for details). Globally, forests regrow slightly in the optimised land use scenario to 77.7% (from currently 74.5%) of the natural forest cover, re-entering the safe operating space of the PB land. Forest-biome level PB thresholds of remaining forest cover are almost safeguarded under the optimised land use (Fig. 5.5). However, the tropical forest cover remains almost unchanged and the land PB remains transgressed in the tropics at 75% of the original forest cover remaining. Boreal forests recover from 83% to 87% and temperate forests recover from 60% to 68% of the original forest cover. Agricultural land use is reduced in almost all biomes except warm savannas and arctic tundra (which is used for pastures, because of increased carbon pools while supplying more than the minimum gras harvest threshold set in the optimisation (ref. to Sec. 5.2.4).

Furthermore, sustainability constraints were set for irrigation water withdrawals in the optimisation (i.e. ensuring that environmental flow requirements remain at gridcell and basin scale). These constraints and the shift to more productive agricultural areas result in changes in irrigated areas and irrigation water use (Fig. 5.6). Figure 5.6 shows areas of increasing and decreasing consumptive blue water use for irrigation respectively. Especially in India, China and the MENA region, as well as in southern Europe, agricultural blue water consumption decreases (Figure 5.6), which are exactly the regions in which freshwater resources are currently over-exploited (see Steffen et al., 2015, Supplementary Material, Fig. 2D).

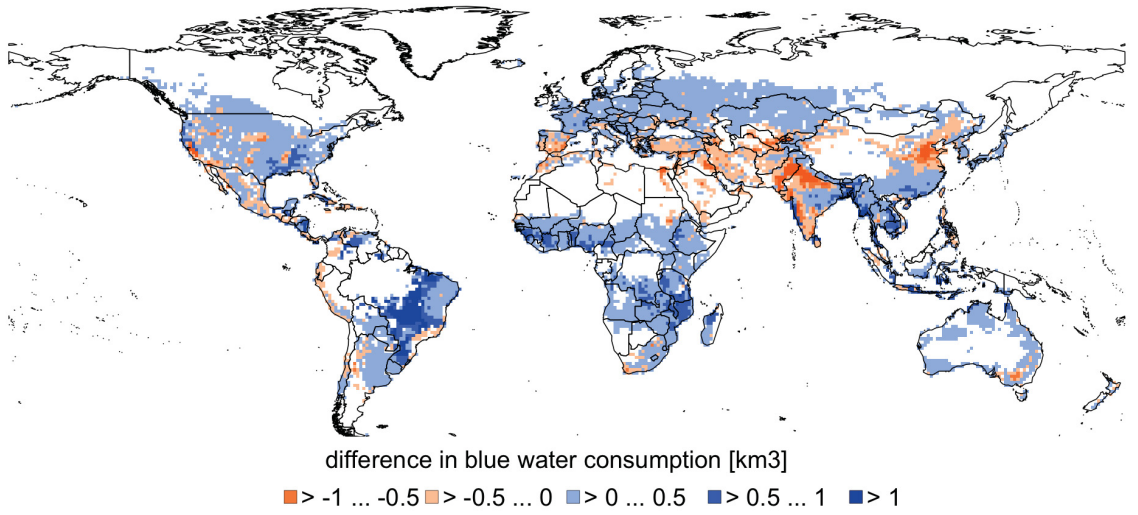

Figure 5.6.: Differences in agricultural irrigation water consumption (optimised minus current irrigation water consumption).

However, irrigation is expanded in other regions which have sufficient freshwater availability (Fig. 5.6). This additional irrigation helps to increase agricultural productivity which in turn reduces land requirements for agriculture. In total, global blue water consumption for irrigation increases from 920 km^3 to 1720 km^3. Thus, higher blue water consumption for irrigation clearly marks a trade-off to increasing overall land use efficiency. Nevertheless in this scenario, global water consumption is still within the limits of the PB for freshwater use, which is set at a global blue water consumption of 4000 km^3.

Optimisation for single factors (or even for combinations of factors) always bears the risk of negative externalities on other sectors. While we optimise for carbon sequestration (climate-), biodiversity conservation, and indirectly also for forest cover and environmental flow requirements, we did, for example, not account for energy or nitrogen use in our scenarios. Both are usually increasing with agricultural intensification, and hence pressure for example

on the PB for biogeochemical flows (which is already critically exceeded) is likely to increase further in our optimisation scenarios with improved agricultural productivity.

5.3.3. Regional and national opportunities and trade-offs

With this global land use optimisation, some global common goods, in particular climate and biodiversity, can be better protected and the main land-related (long term) sustainability criteria can be met at the global scale, so that critical processes in the Earth system such as moisture recycling can be maintained. However, this does not necessarily mean improved sustainability at the scale of individual regions or countries, implying conflicts between global and national goals.

In order to understand what the global optimisation and large-scale reconfiguration of land use mean for individual regions or countries, we first analyse which countries will not be food self-sufficient in terms of calories produced or grass produced for livestock feed, under the optimised global land use (for a future population of around 9 billion in the year 2050).

Figure 5.7a shows national self sufficiency levels under the spatial optimisation with improved agricultural efficiencies under the criteria of improved per-capita food supply for the projected national populations of 2050 (Yamagata et al., 2015). Even though global food supply is ensured, many countries do not achieve food self sufficiency. However, the optimisation allows in total more countries than at present (current land use pattern, efficiencies and population, supplementary, Fig. 5.9a) to be self sufficient. Despite this increase in the total number of food self sufficient countries, a few countries currently loose their current self sufficiency and would be required to become net importers under the optimised land use pattern (e.g. Bolivia, Ireland) .

Figure 5.7b depicts national production differences of calorie production (for food and feed) and grass attributed to the spatial optimisation of land use patterns. Therefore, calorie and grass production of the current land use pattern with improved agricultural productivities are subtracted from the production of the optimised scenario. This shows crop production increases in many countries across the globe (blue and green in Fig. 5.7b), whereas less calories are produced in South and Southeast Asia and parts of South America and subsaharan Africa (red and yellow in Fig. 5.7b).

While trade could balance production surpluses and deficits across regions, it comes at costs. Free trade may not be easily achieved due to political obstacles. Moreover trade is energy intensive and importing countries need to generate the financial resources to buy food on global markets. Furthermore, there are (perceived or real) political risks for countries giving up self sufficiency and becoming dependent on imports.

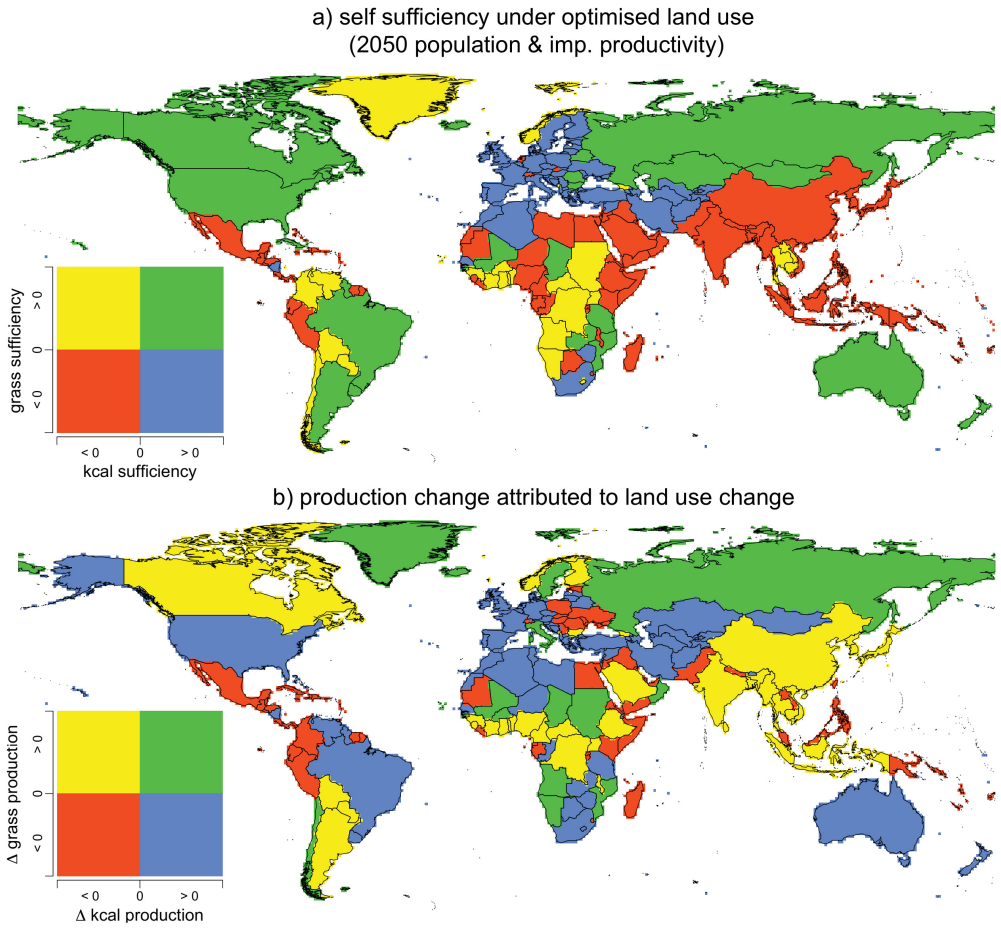

Figure 5.7.: Food self sufficiency and production change: a) country level production deficits for food self sufficiency for calorie production (for food and feed) and for grass production based on the optimal food supply criteria of 3000 kcal/cap/day with 20% from livestock under the optimised land use pattern (marked in Fig. 5.2) and b) production changes attributed to the spatial land use optimisation (optimised land use pattern minus current land use pattern with improved agricultural productivity).

Apart from food security the results of a global top-down optimisation are likely to compromise other national sustainable development goals and targets, e.g. related to land use planning, renewable energy or biofuel goals, or expansion of nature conservation areas. For example, India, China and Ethiopia explicitly state afforestation or reforestation goals in their INDCs (UNFCCC, 2016). However, land area under forest cover decreases in all of these countries under our selected global optimisation scenario. On other ends, the optimisation is in line with national goals. For example, the increase in Ethiopia's irrigated area by 970% through the optimisation is roughly in accordance with Ethiopia's target to expand irrigated area by 620% (from 127,000 ha to 785,000 ha) (GOE, 2010).

While biofuel and other renewable energy sources play an important role in national development plans, the additional land demand for biofuel production and increasing water demand for hydropower have not been considered by the optimisation. Countries aiming at increasing the share of biofuels in their energy mix, might thus be disadvantaged if agricultural land use is increased in the global optimisation. For example, Brazil becomes a net exporter in the optimisation, producing 245% of the domestically required calories to ensure per-capita food supply at 3000 kcal/day with a share of 20% from livestock. That result of the optimisation might, however, render the nations INDC to increase the share of sustainable biofuels in its energy mix to approximately 18% by 2030 infeasible due to the substantial increases in land demand for agricultural purposes.

Overall, there are potential synergies and tradeoffs between national (sustainable) development goals and the global goals as specified by the PBs. These need to be explored further and eventually reconciled across scales.

5.4. Conclusions

Large opportunities for improved land use and sustainable development exist, even for 9.1 billion people, to improve per-capita food supply levels to the level that is generally considered to provide food security (3000 kcal per capita and day), while simultaneously improving terrestrial carbon storage and biodiversity conservation. However, to achieve all of these goals simultaneously, additional improvements in agricultural productivity are required, which is in line with SDG 8.4, i.e. to improve global resource efficiency and with SDG 2.3 to double agricultural productivity. Despite globally improved land use and food security, the resulting food self-sufficiency levels and food security levels may in fact deteriorate for individual countries under such global reallocation schemes. Thus, disadvantaged countries might need to be compensated (financial or otherwise) by the beneficiaries or the international community. Such options, e.g. payments for ecosystem services (PES) or UN-REDD schemes, have already been tested in some countries to encourage ecosystem protection for local environmental sustainability, as well as for the global good.

While the land use optimisation presented here is more comprehensive than most previous attempts, there are many other optimisation criteria not yet accounted for, such as the implications for energy and nitrogen inputs of the agricultural intensification and global trade that are part of the solution. These inputs are likely to increase and lead to further transgression of the planetary boundaries for climate change and biogeochemical cycles. Furthermore, this paper focuses on environmental sustainability criteria, not attempting to assess socio-economic limitations, e.g. for the improvements in agricultural productivity, or socio-economic consequences of land use optimisation, e.g. in terms of employment or equity.

There are numerous potential synergies and tradeoffs across the different environmental dimensions, between environmental and socio-economic sustainability criteria and across scales. The latter, require alignment of local, national and global sustainable development goals, all of which need to be spelled out in more detail, quantitatively and spatially explicit.

Author contributions VH and HH designed the study, and analysed the results. VH developed the methodology, performed all simulations and created the figures. SW suggested and prepared livestock productivity scenarios, CM and HK suggested and prepared endemism richness maps. VH led the writing process with contributions from all co-authors.

5.5. Supplementary material

5.5.1. Supplementary methods

Terrestrial vertebrate endemism richness

We used 1° resolution maps of endemism richness for terrestrial vertebrates including the groups birds, mammals and amphibians. Endemism richness is calculated as the sum of the inverse global range sizes of all species present in a given spatial unit (Kier et al., 2009). Because raster cells differ in area, each species'global range size was initially estimated as the sum of areas of all raster cells that overlap their respective range map. For a given raster cell, endemism richness was then calculated as the sum of the ratios between the area of that particular cell and the areas of the cell-overlapping ranges.

Endemism richness values were calculated with a land area threshold of 50%, meaning that only raster cells with at least 50% land area were included in calculations of endemism richness. Note that the exclusion of raster cells with little land area results in the total exclusion of several species which have very restricted ranges near coasts. It thus results in a possible distortion of species richness and endemism patterns (in particular with regard to endemism-rich islands). To minimise this effect, raster cells with oceanic islands were kept in the analyses, even if their land area fell below the threshold.

Species presence/absence data for the grid cells were established by overlaying a grid onto expert opinion range maps. The range maps for mammals and amphibians are from the IUCN Red List of Threatened Species (2012). Range maps for birds are the combined BirdLife International and NatureServe datasets (2012). Only native ranges were included in the analyses, extinct, vagrant, and introduced ranges were excluded. Largely pelagic bird species were excluded, while birds that mostly inhabit land, freshwater and coastal habitats were included. To exclude marine and other fully aquatic mammal species, all cetaceans, sirenians and pinnipeds were excluded but the polar bear and two largely marine otter species were included.

Details on the ruminant meat substitution scenario

Table 5.3 lists globally aggregated numbers on feed intake per livestock output for a baseline scenario, a scenario of improved livestock productivity (ILP) and a ruminant meat substitution scenario (RMS), compiled from Wirsenius et al. (2010). The RMS scenario combines improved livestock productivity according to the ILP scenario with a substitution of pork and/or poultry for 20% of ruminant meat, which is by far the most feed and land-demanding meat

product. In this study, the percentage changes of the RMS compared to the baseline (Table 5.3) are taken as percentage changes from the current globally aggregated livestock sector (ref. to harvest requirements in Sec. 5.2.4).

Feed item	Feed intake per aggregated livestock output [Joule feed gross energy per joule human ME in products]		
	baseline	ILP	RMS
LPJmL-crops	3.5	3.3 (-5.7%)	3.3 (-5.7%)
Others (including grass crops)	2.6	2.6 (-2.6%)	2.1 (-16.9%)
Permanent pasture	12.6	9.2 (-26.8%)	7.5 (-41%)

Table 5.3.: Livestock production and feed intake (from Wirsenius et al. (2010)).

5.5.2. Supplementary results

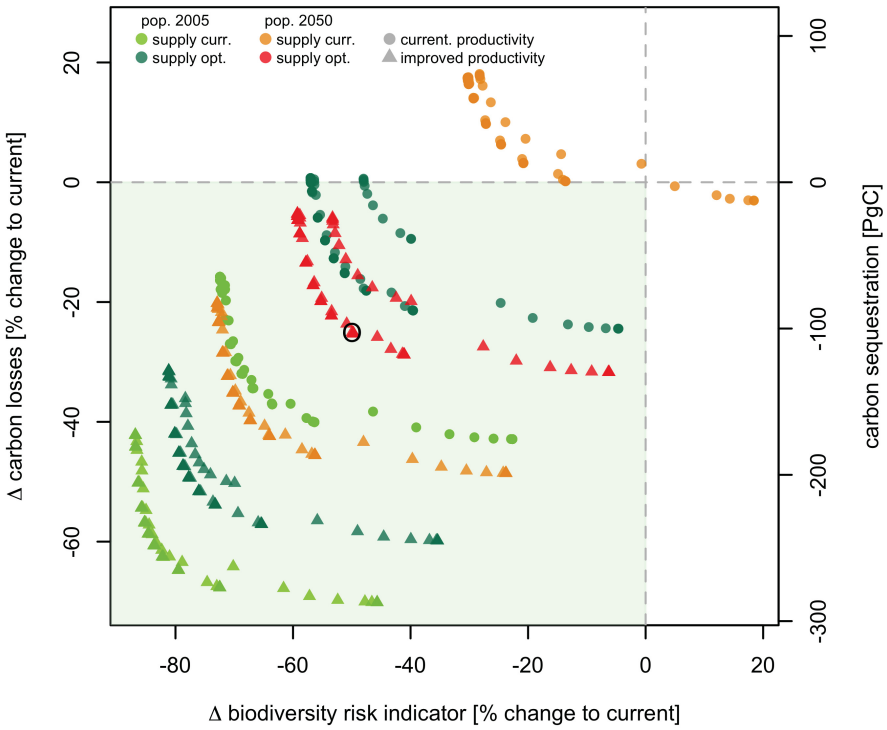

Figure 5.8.: Pareto-optimal curves for different populations, food supply levels and agricultural productivities for the optimisation allowing for a higher water stress indicator (WSI=0.6). Each pareto-optimal curve (one colour and shape) consists of a range of solutions representing different weights on carbon and biodiversity in the objective function and different constraints on minimum biome-level biodiversity conservation. The axes depict global changes (optimised minus current land use) in the biodiversity risk indicator (x-axis) and changes (optimised minus current land use) of terrestrial carbon losses associated to land use change (vegetation and soils) (y-axis) of the optimised land use pattern, compared to current land use.

Figure 5.8 shows the pareto-optimal curves from the optimisation as in Fig. 5.2 but allowing for a water stress indicator (WSI) of 0.6, i.e. allowing for moderately exploited basins. Overall, the potentials for a reduction of carbon losses and the risk to biodiversity loss are higher than for a smaller tolerable WSI (WSI=0.3 in Fig. 5.2). This is because allowance for higher irrigation water withdrawals leads to even more expansion of irrigated areas. This decreases total land requirements for agricultural production allowing for more carbon sequestration and less risks to biodiversity.

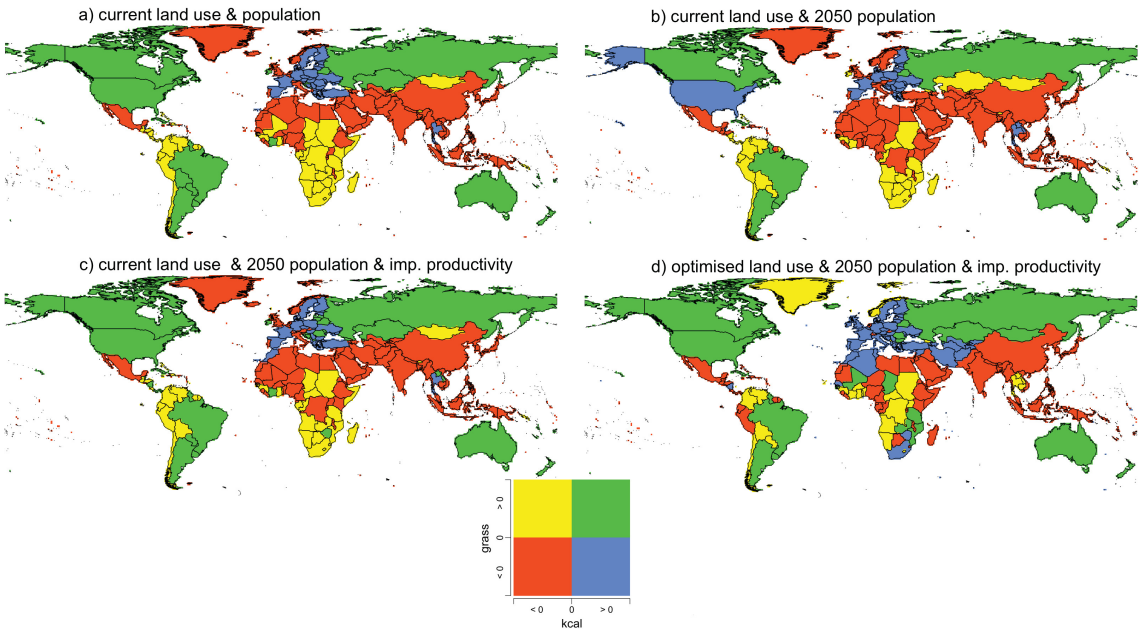

Figure 5.9.: Country level production deficits for food self sufficiency for calorie production (for food and feed) and for grass production based on the optimal food supply criteria of 3000 kcal/cap/day with 20% from livestock for a) the current population land use pattern with current agricultural productivities, b) the population of 2050 with current land use pattern and agricultural productivities, c) the population of 2050 with current land use pattern and improved agricultural productivities and d) the selected optimised land use pattern (marked in Fig. 5.2) for the population of 2050 and improved agricultural productivities.

Compared to current population growth and improved food supply (Fig. 5.7b) requires additional food production and adds pressure to terrestrial ecosystems and their carbon storage and biodiversity. Improved agricultural productivity on the same land use pattern can counteract that pressure (Fig. 5.7c). With the spatial optimisation (combining improved agricultural efficiencies and change of land use pattern, Fig. 5.7d) even more countries can be food secure under the 2050 population (and improved diets) than for the 2005 population – while terrestrial carbon storage and biodiversity conservation are improved at the same time.

6. Summary, synthesis and outlook

Terrestrial carbon dioxide removal (tCDR) technologies including bioenergy with carbon capture and storage (BECCS) (Obersteiner et al., 2001) and forestation (Dyson, 1977) are considered an option for offsetting or removing fossil fuel emissions in order to counteract or remove anthropogenic emissions. This thesis has broadened the current state of research by providing a process based trade-off analysis of tCDR, which is for the first time set in the context of planetary boundaries. Key advancements in knowledge are:

- large-scale biomass plantations manipulate global and regional biogeochemical and hydrological cycles
- climate-effective tCDR could aggravate the status of the Earth system with respect to multiple planetary boundaries
- a one-dimensional view of the climate problem bears the risk of such collateral planetary boundary transgressions
- land use management widens the option space for terrestrial carbon sequestration and biodiversity conservation under population growth but bears institutional challenges

The following sections summarise the key findings concerning the individual research questions (Sec. 6.1), discuss the robustness of the results (Sect .6.2) and conclude the findings of this thesis with perspectives for further research (Sec. 6.3).

6.1. Answers to the research questions

The different chapters of this thesis focus on individual research questions related to potentials and implications of biomass plantations and afforestation or reforestation for tCDR. As a whole, they provide a global-scale assessment of potential large-scale anthropogenic interferences in biogeochemistry (refer to Sec. 6.3).

1. Is extensive terrestrial carbon dioxide removal a 'green' form of climate engineering?

Large-scale biomass plantations are found to substantially manipulate (global and regional) biogeochemical and hydrological cycles (In Chapter 2). The dynamic global vegetation model LPJmL is used to compare the biogeochemical and hydrological implications of large-scale second-generation herbaceous and woody biomass plantations to those of historical land use change. Therefore, a biogeochemical state metric is developed to measure the differences between biomass plantations to potential natural vegetation and compare these differences to those between historical land use and potential natural vegetation.
Simulations of systemic scenarios with biomass plantations on current agricultural land use areas and under current climate show that in absolute terms biomass plantations would shift the biogeochemical status of the terrestrial biosphere even more than historical land use change. However, biogeochemical modifications through biomass plantations differ from historical modifications. For example, while historical land use change decreased net primary production (NPP) on agricultural land by 5% in comparison to natural vegetation, herbaceous or woody biomass plantations on the agricultural areas of 2005 would increase NPP by 22% or 11%, respectively. These changes in NPP constitute and drive other major alterations in regional and global carbon and moisture fluxes (summarised in Table 6.1). **This leads to the conclusion that biomass plantations at a scale that could significantly reduce atmospheric CO_2 concentrations should not be considered a 'green' climate engineering method but a full scale environmental engineering intervention.**

Table 6.1.: Summary of biogeochemical alterations through biomass plantations on current agricultural area (4.3 Gha) and historical land use. Both are compared to potential natural vegetation (PNV) and averaged over the period 1982-2005.

Variable	compared to PNV		compared to historical land use
NPP	strong increase (up to 22 %)	$\gg$	decrease (-5 %)
Soil carbon	small decrease (-3%, herbaceous) or marginal increase (+0.4%, woody)	$>$	decrease (-7 %)
Vegetation carbon	strong decrease (up to -21 %)	$>$	strong decrease (-25 %)
Evaporation	strong increase (up to 29 %)	$\ll$	strong increase (+91 %)
Interception loss	small decrease (up to -1 %)	$\gg$	strong decrease (-20 %)
Transpiration	small increase (1%, herbaceous) or small decrease (-2 %)	$\gg$	strong decrease(-11 %)
River discharge	decrease (-4 %)	$<$	decrease (-1 %)

2. What are potential trade-offs of tCDR in the context of planetary boundaries?

Trade-offs between tCDR via biomass plantations and the planetary boundaries for biosphere integrity, biogeochemical flows, land system change and freshwater use are identified in Chapters 2 to 4 (Fig. 6.1). The boundaries for land system change and biosphere integrity tend to inhibit highly productive regions such as forest regions and high biodiversity hotspots. Additionally, the boundaries for biogeochemical flows and freshwater use restrict fertilisation and irrigation of biomass plantations, which are however required to realise high biomass yields.

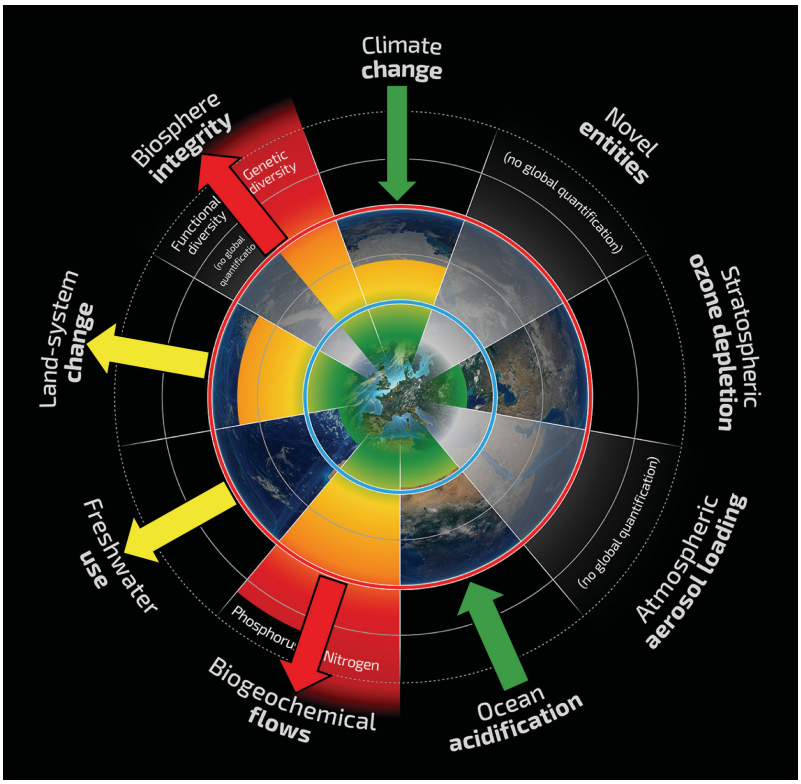

Figure 6.1.: Trade-offs between tCDR and planetary boundaries. The planetary boundaries for novel entities, stratospheric ozone depletion and atmospheric aerosol loading are not focussed on in this thesis. (credit: F. Pharand-Deschênes /Globaïa, modified)

In Chapter 3 the potentials for BECCS within the safe operating space and its trade-offs to these planetary boundaries are evaluated quantitatively. To this end, a spatially explicit optimisation model is developed which distributes biomass plantations around a fixed agricultural baseline scenario, considering the PBs for climate change, biosphere integrity, land system change, biogeochemical flows and freshwater use. Multiple land use scenarios are

developed by varying optimisation constraints reflecting global and regional representations of the planetary boundaries.
The results show that tCDR potentials are negligible if planetary boundaries were to be safe-guarded at the global and regional level. Only with a transgression of regional boundaries into a risky uncertainty zone, considerable negative emission potentials of 1.4 GtC/a to 6.9 GtC/a can be obtained for a range of biomass conversion processes. Furthermore, scenarios for minimising the risks to biodiversity loss or freshwater exploitation show clear trade-offs between biodiversity and land conservation vs. irrigation water requirements. Minimising the extend of biomass plantations in order to reduce the pressure on biodiversity and the land system requires substantial irrigation.
These trade-offs between BECCS and the further transgression of many planetary boundaries must be considered and evaluated carefully. **On the one hand tCDR via BECCS could contribute to preventing the further transgression of the PB for climate change, i.e. avoid detrimental feedbacks of the climate system, and ocean acidification. On the other hand such potentials imply the exploitation of the biosphere and increase the pressure on the planetary boundaries for biosphere integrity, biogeochemical flows, land system change and freshwater use.**

3. How does societal Earth system management via tCDR influence the likelihood of planetary boundary transgression?

Climate engineering manifests a global-scale, intended anthropogenic intervention into the climate system. However, only a few studies (e.g. Jarvis et al., 2009; MacMartin et al., 2013) feature a dynamic integration of environmental and societal components in the assessment of climate engineering or climate change mitigation.
A first step to include societal societal Earth system management via tCDR in a model of the carbon cycle is done in Chapter 4, which addresses the co-evolutionary interaction of tCDR intervention in the climate system. For this purpose, a conceptual model of the natural dynamics of the Earth's carbon cycle is modified to include a simple representation of societal tCDR intervention. This allows to evaluate the influence of societal parameters such as the degree of anticipation of the climate problem and the rate of tCDR efforts on the status of carbon-related planetary boundaries.
The results show that employing tCDR for managing the atmospheric carbon pool can lead to a collateral transgression of PBs because of nonlinear carbon cycle feedbacks. Efforts to steer the system within the carbon-related safe operating space are only effective for a small range of climate change anticipation levels and depend critically on emission-scenarios. In the conceptual modelling framework, tCDR could be successfully deployed as part of a strong climate change mitigation scenario, but would likely not be effective

in a business-as-usual scenario. **It is concluded that a societal focus solely on the PB for climate change, without an integrated sustainability assessment bears the risk of collateral boundary transgression, especially if mitigation is not included in the societal response to increasing atmospheric CO_2 concentrations.**

4. How strong are trade-offs between reforestation, nature conservation and land for food production?

Vegetation-based tCDR requires considerable area to extract substantial amounts of carbon from the atmosphere. Chapter 5 widens the scope of the previous questions by integrating population and food demand scenarios as well as sustainability constraints into tCDR assessment. Planetary opportunities for terrestrial carbon sequestration by afforestation, while feeding 9 billion people and respecting sustainability constraints such as the planetary boundaries are evaluated. To this end, global land use scenarios including crops and pastures are developed with a spatially explicit optimisation model that maximises terrestrial carbon sequestration and biodiversity conservation.
The results shed light on the magnitude of trade-offs between agricultural land use and carbon sequestration. Under current agricultural and livestock efficiencies, supplying food for 9 billion people implies further land use change emissions – rather than allowing for terrestrial carbon sequestration. **Only with substantial improvement of agricultural productivities, optimal allocation of agricultural land use and sizable expansion of irrigation, considerable but hypothetical carbon sequestration potentials up to 98 GtC can be achieved, while safeguarding global food supply and reducing the risk of biodiversity loss. Such globally optimised land use, however, implies trade-offs at regional levels in terms of sustainability goals and food supply. The required increase in trade-volumes for regional food supply, as well as in agricultural productivity imply major institutional challenges.**

population	+42% (to 9.1 billion)
per-capita food supply	+9% (livestock share +22%)
agricultural area	-214 Mha
terrestrial carbon	69 GtC sequestration
biodiversity risk	-44%
reforestation	+225 Mha (to 77.7% of the natural forest cover)
irrigation water	+980 km^3

Table 6.2.: Global changes caused by the spatial land use optimisation for a selected scenario.

6.2. Robustness of the results

The dynamic global vegetation model (DGVM) LPJmL is the methodological backbone of this dissertation and applied in Chapters 2, 3 and 5. Its performance is continuously evaluated against contemporary observation data and alternative models. For example, simulations of LPJmL or its predecessor LPJ without agricultural land use, have been compared against satellite remote sensing data and site specific carbon flux measurements to validate simulated results of vegetation distribution and carbon cycles for natural vegetation (e.g. Schaphoff et al., 2013; Sitch et al., 2003) and agricultural crops (e.g. Bondeau et al., 2007; Fader et al., 2010). Simulated hydrological processes have been compared against remote sensing data of soil moisture (e.g. Wagner et al., 2003), runoff, river discharge, water fluxes, agricultural water use and irrigation efficiencies compared well against site specific and regional observation data and state-of-the-art global hydrological models (Gerten et al., 2004; Heck et al., 2016b; Jägermeyr et al., 2015; Rost et al., 2008b).
Simulations of biomass plantations are initially evaluated against field data to establish the robustness of modelling results (Chapter 2, Sec. 2.2.2 and Appendix A). The evaluation showed relatively good agreement between observations and simulations. However, the evaluation underlined inherent uncertainties related to the heterogeneity of available field data concerning plantation setup and management, as well as environmental conditions which can not be represented perfectly with a global-scale parameterisation of DGVMs. While simulated biomass yields are within the general range of reported yields, large uncertainties remain related to the variability of actual management of large-scale biomass plantations in all regions of the globe.

Despite extensive model evaluation, a model is only a simplified representation of the current state of knowledge about individual processes. For example, the magnitude of plant productivity and carbon accumulation under increasing atmospheric CO_2 concentrations (i.e. CO_2 fertilisation, Ainsworth et al., 2004) is still uncertain. Many DGVMs (including LPJmL) lack an explicit nitrogen cycle, which increases the uncertainty in projections of (unfertilised) vegetation response to elevated CO_2. An explicit representation of the Nitrogen cycle is currently being incorporated into LPJmL but was not included in the model version used in this thesis.

Climate scenarios used in this thesis (Chapter 3), however, are limited to a global warming of 2°C, with a relatively small increase in atmospheric CO_2 concentrations compared to biomass validation levels (increase from 380 ppm in 2005 to 450 ppm in 2050). Simulations without this CO_2 increase reduce biomass yields by 1%. This suggests that the CO_2 fertilisation uncertainty is negligible in the assessed scenarios with a small increase in atmospheric CO_2 concentrations, especially in light of climatic or other model uncertainties.

Reforestation potentials (Chapter 5) are simulated under current atmospheric CO_2 concentrations. Thus, scenarios under elevated CO_2 concentrations could increase the reported carbon sequestration potentials. However, uncertainties related to food demand and agricultural efficiencies are substantially higher and have a larger influence on reforestation potentials than CO_2 fertilisation.

Additional uncertainties concerning biomass conversion processes and possibilities of carbon capture and storage are relevant in the context of negative emissions (Chapter 3). Currently, only a few BECCS demonstration power plants exist. It remains questionable to what extend CCS technologies can be scaled up because of major uncertainties relating to costs, transportation infrastructure, subsurface uncertainty, regulatory and legal issues and public acceptance (Herzog, 2011; Watson et al., 2014). Furthermore, the range of biomass conversion technologies and process efficiencies is large (ref. to Chapter 3). A plausible range of conversion and CCS efficiencies was assumed in this study, however, it remains unclear whether the calculated CCS-rates could be implemented in practice.

The dynamic integration of societal feedbacks into global carbon cycle dynamics (Chapter 4) is based on a conceptual model of the carbon cycle. As discussed in Chapter 4, conceptual modelling does not aim for quantitatively reliable results but aims for understanding of the structure and effects of dominating feedbacks and their leading interactions. Thus, the model was adapted and calibrated to conceptually capture the most important processes of global carbon dynamics and simulate plausible transients of global carbon dynamics.

6.3. Conclusions and perspectives for further research

Trade-offs between tCDR and the status of planetary boundaries (Chapters 3 and 4), as well as the implied modification of biogeochemical and hydrological cycles (Chapter 2) indicate that tCDR should be recognised as a mediator between various Earth system components and not as a one dimensional tool which can be applied to reduce atmospheric CO_2 concentrations. Considerations of bioenergy (with or without CCS) should thus take into account that aggravated environmental conditions due to large-scale biomass plantations could trigger dynamic feedbacks within the climate system.

The findings of this thesis suggest limited opportunities for sustainable tCDR because of these environmental trade-offs, land constraints and institutional challenges. Considerable land requirements for tCDR via afforestation, reforestation or biomass plantations (Chapters 2 and 3) are competing with agricultural land demands and sustainability constraints (Chapters 3, 4 and 5). Albeit, land requirements for future agricultural land use (and thus land availability for tCDR) are highly uncertain, they are likely to limit sustainable tCDR

potentials under projected population growth (Chapters 3 and 5).
Environmental and planetary sustainability constraints represent challenges for both, the agricultural sector and potentials for biomass plantations and afforestation. The current agricultural sector is far from sustainable in many aspects (e.g. Foley et al., 2005; Steffen et al., 2015) and substantial land, fertiliser and water demands for tCDR would add further challenges to a transition towards sustainable land use.
The integration of sustainability constraints and agricultural production requirements in global-scale optimisations (Chapters 3 and 5) indicates some potential for long term reforestation or negative emissions, depending on technological efficiencies. Implementing such potentials, however, would require substantial international collaboration accompanied by vast institutional challenges (e.g. the restructuring of the global agricultural and trade system or the development of carbon capturing infrastructures and carbon storage facilities distributed in all parts of the world). These might be even higher than the challenges associated with strong commitments to climate change mitigation.

A next logical step building on the results and methodology developed in this thesis would be the integration of biomass plantations into a sustainability oriented agricultural land use optimisation as presented in Chapter 5 of this thesis. The comparison between such sustainability oriented optimisation results and those of existing economically based land use optimisations could reveal synergies between economically viable and sustainable land use patterns.
Furthermore, important biogeophysical effects such as albedo modification through land cover change or altered moisture cycles through changes in evapotranspiration have not been assessed. Because they could potentially induce trade-offs to the climate system, the biogeochemical assessments of this thesis should be complimented with simulations of general circulation models (GCMs) to evaluate climatic effects of changes in moisture and energy fluxes. In practice, regional institutional and environmental conditions will be drivers of decisions for or against tCDR. In order to permit well informed decision making concerning afforestation, reforestation and bioenergy with or without CCS, bottom-up evaluations that cross-check local conditions with the provided top-down global-scale assessment would be an important step forward. Such assessments could for example inform about the likelihood of indirect land use change effects triggered by bioenergy production, i.e. triggered deforestation for agricultural purposes if agricultural land is converted to biomass plantations.
Disciplinary research in the various subsystems related to tCDR and CCS (e.g. natural science, engineering, social and policy science) as well as lifecycle assessments of bioenergy are integral components to reduce uncertainties related to tCDR. However, it is essential to combine the different disciplines to achieve a comprehensive understanding of the Earth system, technological and institutional constraints and uncertainties that is required for well informed decision making at the level of global and local governance.

Appendix

Appendix A.

Biomass yield data and model adjustments

A.1. Biomass yield data

The following data on observed biomass yields (Tables A.1 - A.5) were included in the evaluation of biomass yields in Chapter 2. Reported biomass yields of Miscanthus and Switchgrass were compared against herbaceous biomass yields simulated by LPJmL. Reported biomass yields of Willow, Poplar and Eucalyptus were compared against woody biomass yields simulated by LPJmL.

Table A.1.: Collected dry matter yield data for miscanthus

Country	Lon	Lat	min. yield [t/ha/yr]	max. yield [t/ha/yr]	Harvest time	Irrigation	Fertilisation	Plot size [m2]	Soil	Notes	Study
Turkey	32.5	38.0	12.0	1.2	November	yes	yes	10	54.6% sandy, 21.2% silt and 24.2% clay		Acaroğlu et al., 2005
US, OK	-97.1	36.1	12.4	13.1 (delayed)		no	yes	2.44 x 6.1 m	Kirkland silt loam soil	1-2 harvest/yr	Aravindhakshan et al., 2010
Indonesia (west Java)	107.7	-7.0	31.9	31.9							Blair et al., 1986
UK	-0.4	51.8	9.8	17.8	autumn/ winter	no		100	Silty clay loam; previously agricultural	Average yield over 14-year lifetime. Yields decline after 10 years. no response to N.	Christian et al., 2008
Sweden	14.0	56.0	13.1	21.5							
Denmark	9.6	56.5	9.7	16.8	autumn	only at planting	25			range: delayed / peak	Clifton-Brown et al., 2001
England	-0.4	51.8	12.4	17.8							
Germany	9.0	48.7	19.9	26.4							
Portugal	-9.2	38.7	26.0	38.5		Yes				irrigation necesssary	
Ireland	-7.3	52.7	9.0	13.4	spring/ autumn	no/yes		100	loam to sandy loam, marginal	Range: autumn / spring & irrigation / rainfed, yields declined after 10 years	Clifton-Brown et al., 2007
Italy	15.5	37.4	12.7	27.1	Feb/Oct	no/yes	no/yes	24	vertic xerochrepts soil	Range: autumn / spring harvest, fertilisation, irrigation	Cosentino et al., 2007
Greece	22.7	39.4	21.1	30.9		yes	50, 100 kgN/ha	small	clay loam, "moderate fertility"		Danalatos et al., 2007
US, IL	-88.3	40.1	3.1	20.6					Wyanet series		
US, KN	-84.5	38.1	12.6	19.0					Maury series		
US, NA	-96.5	41.2	15.6	31.2	early to late	during the	0 - 120		Tomek series	range from fertilizer and	Davis et al., 2014
US, NJ	-74.2	40.2	11.3	18.6	winter	planting year	kgN/ha		Holmdel series	annual variability	
US, VA	-79.4	36.9	9.4	16.7					Cecil series		
US, IL	-88.9	41.9	20.9	31.2	after	in 1st year				ideal conditions,	
US, IL	-88.2	40.1	33.4	45.5	senescence/peak			100		intensive preparation in pots	Heaton et al., 2008
US, IL	-88.7	37.5	34.6	42.3		no				before transplant	
Germany	6.7	51.5	17.5	28.8	spring/autumn	no	0-180 kgN/ha	132	Eutric fluvisol	Fertiliser did not affect yields	Himken et al., 1997
Denmark	9.4	56.8	7.7	8.9	spring		0, 75, 250 kgN/ha	100	Loamy sand	15.5% of giganteus plants died in first winter	Jørgensen et al., 2003
Germany	12.6	53.9	7.5	12.6							
Germany	10.8	52.6	8.8	13.5	autumn			45-300	varied		Kahle et al., 2001
Germany	9.9	49.9	6.2	19.8							
USA (mountain)	-82.6	35.4	17.7	19.0	winter	yes, until 3 months after	0-134 kgN/ha/yr planting				Palmer et al., 2014
USA (plain)	-78.1	34.7	20.3	21.3							
Austria	15.0	48.3	17.4	24.5	February	no	50-60 kgN/ha	450	good soil	>800mm precip needed for high yields, weed control necessary in first 2 yrs	Schwarz, 1993]
Serbia (Zemun)	20.3	44.8	11.4	38.7		first year only (4x 40mm)	0-100 kgN/ha	4x5m	calcerous loam light clay	yield range with standard deviation and fertiliser	Stričević et al., 2014
Serbia (Ralja)	21.0	44.4	5.3	25.4						range	
Netherlands	7.1	52.9		21.8	October	no	yes	337.5		intensive care	Werf et al., 1992
China	114.4	30.5	1.0	22.8				4x6m		various species of different origin, 2nd year harvest	Yu et al., 2013

Table A.2.: Collected dry matter yield data for switchgrass

Country	Lon	Lat	min. yield [t/ha/yr]	max. yield [t/ha/yr]	Harvest time	Irrigation	Fertilisation	Plot size [m2]	Soil	Species	Notes	Study
PA, US	-79.2	40.2	2.1	8.6	spring/ autumn	no	0-112 kgN/ha	0.014 - 1.22 ha	Silt loam	Panicum virgatum (upland varieties: Cave-in-rock, Shawnee, Trailblazer)	variation of plot size, harvest date, fertilisation	Adler et al., 2006
US, OK	-97.1	36.1	15.4	15.9		no	yes	2.44x 6.1m	Kirkland silt loam soil	Alamo	1-2 harvest/yr	Aravindhakshan et al., 2010
US, IL	-88.9	41.9	10.4	12.5	after senescence or max			10m x 10m	agricultural	P. virgatum (upland: Cave-in-rock)	ideal conditions; intensive care; herbicide needed, state averages	Heaton et al., 2008
US, IA	-93.4	41.0	6.8	13.1	autumn		56-112 kgN/ha	3m x 4.6m	grundy silty clay loam	P. virgatum (various upland and lowland cultivars)	2-4 yr old plants. Lowland ecotype advantage not as great as in TX	Lemus et al., 2002
US, KY US, NC US, TN1 US, TN2 US, VA1/2 US, VA3 US, WV	-87.8 -78.7 -88.9 -84.0 -80.4 -78.1 -79.9	37.1 35.7 35.6 35.9 37.2 38.2 39.6	8.4 5.1 7.8 11.2 9.5 11.2 12.8	17.0 16.7 16.9 24.9 27.4 20.4 20.5	summer &Nov		50-100 kgN/ha	6.1mx2.4m	Tilsit Cecil Deanburg Etowah Shottower/Chatter Davidson Dormont	Alamo/Kanlow/ Shelter/ Cave-in-Rock	range: species & cut once/cut twice	Lemus, 2004
US, SD US, SD US, SD	-96.7 -97.3 -99.8	44.2 45.8 43.7	1.0 0.8 0.8	6.0 2.5 5.9	autumn	no	0-224 kgN/ha	1.9mx6.1m	fine-silty, mixed, mesic Udic Haplus- tolls, with slope	P. virgatum	herbicide used	Mulkey et al., 2006
US, mountain US, plain	-82.6 -78.1	35.4 34.7	19.8 15.9	22.1 24.2	winter	until 3 months after planting	0-134 kgN/ha			Alamo		Palmer et al., 2014
US, Texas (stephenville) US, Texas (Temple) US, Texas (Dallas) US, Texas (College Station) US, Texas (Beeville)	-98.2 -97.4 -96.8 -96.3 -97.9	32.2 31.1 32.8 30.6 28.4	8.7 11.4 2.5 10.7 7.8	19.5 17.6 16.8 19.7 17.5		only at planting	67-134 kgN/ha	18		Alamo (most productive of 7)		Sanderson et al., 1999
PA, US	-78.0	40.7	3.3	9.4	autumn	no	25-112 kgN/ha	9mx15m	silt loam, agricultural	P. virgatum (upland: Cave-in-rock, Shawnee, Trailblazer)		Sanderson, 2008
US, ND US, SD US, NE	-100 -100 -100	47.0 44.0 42.0	5.6 4.2 5.0	5.8 8.8 7.4	autumn		varied	3-9.5 ha	good land	P. virgatum, various upland cultivars	5-yr means shown	Schmer et al., 2010
Italy	16.6	40.2	2.19	12.36		yes	yes	25mx2.7m		average of 12 genotypes		Sharma et al., 2003
US, AL	-86.0	32.0	6.8	34.6	autumn		84 kgN/ha	1.5mx6.1m	Wickham soil	P. virgatum, various upland and lowland cultivars	Higher yields at 2yrs old vs 1 yr old	Sladden et al., 1991
Italy	11.5	44.4	7.9	11.5	spring		100 kgN/ha	small to field	typical Calcaric Cambisols, previously agricultural	P. virgatum (lowland: Alamo)	Large spatial variation. 2-3 yr old plants	Di Virgilio et al., 2007

Table A.3.: Collected dry matter yield data for poplar

Country	Lon	Lat	min. yield [t/ha/yr]	max. yield [t/ha/yr]	Irrigation	Fertilisation	Plot size [m2]	Soil	Species	Notes	Study
France	3.8	49.2		10.0		50-100 kgN/ha					Berthelot et al., 2007
Germany	14.3	51.6	3.0	6.0		100-170 kgN/ha	300	former mining area (poor soil)	various	all clones were planted as 25-cm-long dormant, unrooted hardwood cuttings	Bungart et al., 2004
UK, England UK, Scotland	-2.1 -3.1	51.8 55.9	4.8 4.0	10.0 8.0			22mx22m	agricultural land	P. trichocarpa		Cannell, 1980
US, MO	-92.8	39.0	7.4	13.3	periodic in first season	no	7mx10m	fertile former fescue pasture	P. deltoids and P. deltoids x nigra	high fertility soil	Dowell et al., 2009
Germany Germany	8.9 12.2	51.4 49.1	9.9 3.8	14.0 7.5		50-100 kgN/ha		previously agricultural	various		Hofmann-Schielle et al., 1999
Belgium	4.4	51.1	2.2	11.4	irrigated at establishment		9mx11.5m	heavy clay loam with high nutrients, former landfill	various		Laureysens et al., 2004
UK	0.1	51.1	0.0	23.6	yes		300		P. & P. deltoides	high variation between genotypes	Rae et al., 2004
Germany	13.0	52.4	9.3	9.5		75 kgN/ha	0.25 ha	previously agricultural	P. maximowiczii x. P. nigra		Scholz et al., 2002
India	80.9	26.8		4.9	no	no	0.12 ha	degraded land	P. deltoides		Singh, 1998

Table A.4.: Collected dry matter yield data for willow

Country	Lon	Lat	min. yield [t/ha/yr]	max. yield [t/ha/yr]	Irrigation	Fertilisation	Plot size	Soil	Species	Notes	Study
NY, US	-76.1	42.8	10.3	11.6		100-300 kgN/ha	65			stem biomass: average over 3 years	Adegbidi et al., 2003
Ireland	7.6	54.4	8.8	17.0				"Marginal agricultural"	S. x Aquatica Gigantea	yields averaged over 9 years	McElroy et al., 1986
Slovakia	18.2	48.4	8.34	24.1		100 kgN/ha, 75 kgK/ha 35kgP/ha		loam	various	2nd & 3rd growing period, higher yields in 3rd growing period	Demo et al., 2013
Quebec	-74.1	45.1	6.2	16.9	no	no	125	previously agricultural	various	herbivory present	Labrecque et al., 2005
UK UK UK UK	-2.7 -1.6 -6.6 -3.8	51.4 54.1 54.4 51.1	9.5 9.2 6.5 11.0	13.2 10.4 12.06 11.3			4mx6m	varying quality	Tora (most productive)		Lindegaard et al., 2001
Sweden	13.6	55.8	3.9	21.0	no	rainfed	small		various		Linderson et al., 2007
Denmark	9.4	56.5	5.4	6.4		240 kgN/ha once	24 x 18 m	on a sandy loam soil	Salix triandra x Salix viminalis	young, 3 year harvest, 17.777 plants/ha	Pugesgaard et al., 2014
Germany	13.0	52.4	4.3	6.5		0-150 kg N/ha	624	Previously agricultural	S. viminalis	with underseed (grass), range from fertilisation	Scholz et al., 2002
Finland (north) Finland (south)	29.8 24.7	62.6 60.2	0.0 5.29	2.3 10.1		400 kgN/ha	Field scale	low SOM	S. viminalis	site conditions had much bigger impact than clone, commercial production, herbicide used	Tahvanainen et al., 1999

Table A.5.: Collected dry matter yield data for eucalyptus

Country	Lon	Lat	min. yield [t/ha/yr]	max. yield [t/ha/yr]	Irrigation	Fertilisation	Plot size	Soil	Species	Notes	Study
US, HI	-155.3	19.5	14.0	15.5	no	33-40 kgN/ha	30m x 30m	volcanish ash, gentle slope, formerly agricultural	E. saligna	mixed 50:50 with legume (Facaltaria moluccana) vs. monoculture	Binkley et al., 2003
India (south)	78.0	14.0	10.3	20.4	yes	0-106 kgN/ha	10x30m	Yield response to irrigation	Deep lateritic soil	E. camaldulensis, E. grandis	Hunter, 2001
Congo	12.0	-4.0		10.8		no		ferrallitic and highly desaturated, sandy to sandy-clear material	E. PF1		Laclau et al., 2000
Brazil, ARA	-40.1	-19.8	18.3	28.2				ultisol			
Brazil, CEN	-43.0	-18.6	21.3	26.5				oxisol			
Brazil, IPB	-47.0	-22.4	22.9	34.3				oxisol			
Brazil, SUZ	-39.9	-18.0	21.4	26.4	no/yes	N, P, K, Ca, Mg, B	30mx30m	ultisol		range from trad. to high fertilisation & irrigation	Stape et al., 2010
Brazil, VCP	-48.4	-21.5	11.4	25.4				entisol			
Brazil, VER	-39.6	-16.4	24.1	36.7				ultisol			
Brazil, VIP	-48.4	-21.5	14.5	31.7				entisol			
Brazil, VLM	-43.8	-17.3	20.8	38.0				oxisol			
Ethiopia	39.0	9.1	10.9	12.2			10x10 or 20x20m	average of region	Nitosols	E. globulus	Zewdie et al., 2009

A.2. Biomass parameterisation, associated uncertainty and model adjustments

The implementation of biomass functional types (BFTs) is a relatively new development of the LPJmL model (Beringer et al., 2011). Therefore, BFTs were not yet included in most model validation and uncertainty studies. However, the parameterisation of BFTs is largely identical to their natural PFT equivalents; "C4 perennial gras", "temperate broadleaved summergreen tree" and "tropical broadleaved raingreen tree". BFT parameter modifications represent the different growing conditions on managed plantations, such as regular plant arrangement, effective pest and fire control. Overall the modifications lead to higher carbon assimilation in BFTs compared to their PFT equivalents. Especially higher light availability, establishment rates and sapling size, a broader temperature range for optimal photosynthesis, as well as reduced mortality and fire occurrence lead to improved growing conditions of BFTs. Furthermore, maximum tree crown area was reduced to represent actual growing conditions and a lower limit for photosynthesis of the herbaceous BFT was implemented because some C4 biomass crops can maintain high rates of photosynthesis at low ambient temperatures.

Global plantation management parameters (for both, woody and herbaceous plantations) were chosen to reflect yields reported in literature, while at the same time also reflecting reported management practices. Parameters for woody biomass plantation management are chosen to reflect short rotation woody coppice (SRWC) management in which young tree stems are cut down near the ground at relatively short intervals. Most SRWCs are harvested in intervals of 3-10 years (Lemus et al., 2005). In LPJmL the length of the harvest cycle is at the upper end (8 years). However, the saplings that are cultivated on industrial plantations have usually been grown in greenhouses up to a considerable size of more than 30 cm. In LPJmL these cuttings are assumed to be grown from small saplings on the field, which is why the model requires rotation periods at the upper end of reported periods.

To my knowledge there are no experimental studies on the maximum rotation length, i.e. the time frame of SWRC before new individuals are planted, however plantation lifetime is expected between three to seven rotations (Heller et al., 2003; Langholtz et al., 2013). I chose a maximum rotation length of 40 years (i.e. 5 harvest events) as a realistic approximation. A reduction of the plantation lifetime would especially lead to to a higher turnover of root biomass, due to the fact that the root system would need to be established more frequently. As a consequence, soil carbon pools would be slightly higher than under longer rotation periods.

To evaluate the effect of changed SRWCs management parameters on biomass yields, I performed the LPJmL simulations for the evaluation of biomass yields (as described in Chapter 2) with a rotation length of 6 years and a plantation lifetime of 30 years (Fig.A.1a)

and compared it to the results in the manuscript with a rotation length of 8 years and a plantation lifetime of 40 years (Fig.A.1b). A shorter rotation period and plantation lifetime led to small yield reductions in Eucalyptus test sites and to a small yield increase in poplar and willow test sites. This can be explained by the fact that temperate biomass plantations such as willow plantations mature earlier than Eucalyptus plantations, which is also considered in the parameterisation of woody biomass types. Because of the earlier maturity of temperate BFTs shorter harvest periods lead to an increase in yields. Tropical BFTs however profit from longer rotation periods because of slower growth. Because the match between data and observations in Fig. A.1b) is better, a rotation length of 8 years with a plantation lifetime of 40 years are chosen.

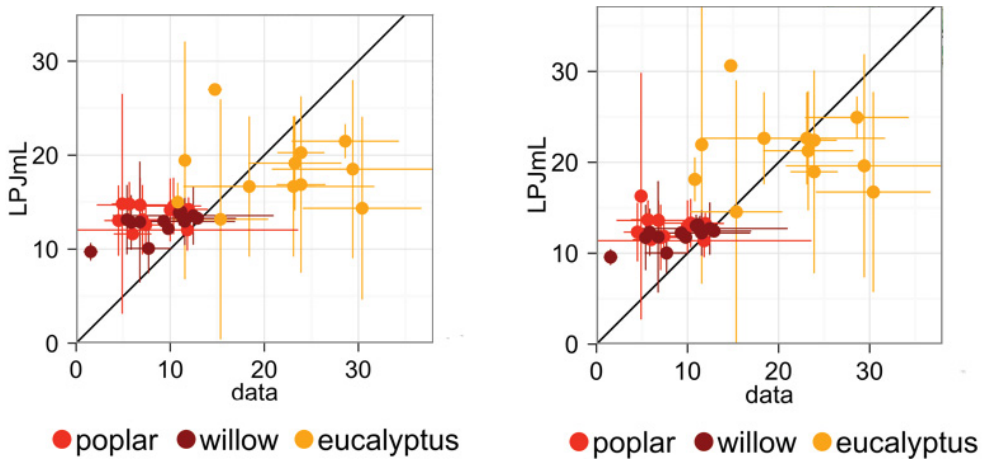

(a) rotation length: 6 years, plantation lifetime: 30 years

(b) rotation length: 8 years, plantation lifetime: 40years

Figure A.1.: The effect of changed woody rotation management on woody biomass yields simulated by LPJmL (averages 1993-2008). Yields are given in t DM/ha/yr for varied rotation lengths and plantation lifetime. Scatterplots contrast the observed and simulated yields in the respective grid cells. Model uncertainty is derived from simulations with and without irrigation. Observation uncertainty reflects dependencies on plantation management (Tables A.3 -A.5).

Furthermore, the harvest parameters of herbaceous BFTs were adapted to better match observed biomass yields from Switchgrass and Miscanthus (Tables A.1 and A.2). The most decisive parameters are the leaf mass threshold for harvest and the fraction of harvested biomass. Model simulations for various parameter sets were performed. The set of harvest threshold and harvest fraction with the best match to observations (i.e. 400 g/m_2 and 85%, respectively) was selected. In areas of low productivity, it can be the case that the harvest threshold is not reached. Then it is harvested when leaf mass has reduced to 75% of its maximum value at the end of the growing season. A harvest fraction of 85% is a realistic

value for commercial biomass plantations using agricultural machinery (e.g. Ashworth et al., 2013; Johnson et al., 2012). Increasing the harvest fraction, leads to decreasing biomass yields due to a reduction of photosynthetic capacity after the harvest event.

With this, the evaluation of simulated biomass yields shows relatively good agreement between reported and observed yields for both, herbaceous and woody biomass plantations. The harvested biomass, of course depends on plant carbon assimilation, as well as harvest parameters. Therefore the positive evaluation of simulated biomass yields provides confidence, that LPJmL – a fairly general and globally parameterised model – is able to simulate the ecosystem processes analysed in this thesis.

A different parameterisation of BFTs would of course have an influence on the simulation results. However, the influence of parameter changes that maintain a good representation of biomass yields is limited. This is mainly due to the fact that increasing NPP under biomass plantations and decreasing NPP on agricultural land is the most decisive difference out of the four metric components. While decreasing productivity on agricultural land has been validated (Bondeau et al., 2007), the high simulated productivity of biomass plantations is required in order to reproduce observed yields. Soil carbon assimilation on woody biomass plantations does to a large extent depend on the harvest management of SWRC, resulting in repeated root formation and litter generation at harvest. Experimental and model studies indicate that increasing soil carbon under SWRC is a plausible result (e.g. Grogan et al., 2002; Guo et al., 2002). Concerning herbaceous biomass plantations, several studies (e.g. Guo et al., 2002; Zimmermann et al., 2013) have found soil carbon assimilation compared to agricultural or degraded land, which is in line with simulation results for herbaceous BFTs in Chapter2. The parameter dependence of water fluxes is more complex to assess, because evapotranspiration is composed of evaporation, transpiration, and interception. These are all affected by different factors (e.g. vegetation density, plant productivity and plantation density). The simulated transpiration increases under biomass plantations, however, are plausible because of the tight coupling of water exchange and carbon assimilation. A site specific evaluation of observed water use efficiency (Jans et al., unpublished data) indicates that LPJmL values are realistic compared to literature values.

The fact that BFT parameters are largely identical to their natural PFT equivalents means that the results of the uncertainty assessment by Zaehle et al. (2005) can to a large extend be transferred to BFTs. Zaehle et al. (2005) found the largest sensitivities in parameters governing net assimilation rate and water exchange. Due to a coupling of carbon uptake and transpiration, increasing carbon fluxes are directly linked to increasing water exchange (which has also been shown in the results of Chapter 2).

Bibliography

Acaroğlu, M. and A. Şemi Aksoy (2005). "The cultivation and energy balance of Miscanthusgiganteus production in Turkey". In: *Biomass and Bioenergy* 29.1, pp. 42–48. DOI: 10.1016/j.biombioe.2005.01.002 (cit. on p. 118).

Adegbidi, H. G., R. D. Briggs, T. A. Volk, E. H. White, and L. P. Abrahamson (2003). "Effect of organic amendments and slow-release nitrogen fertilizer on willow biomass production and soil chemical characteristics". In: *Biomass and Bioenergy* 25.4, pp. 389–398. DOI: 10.1016/S0961-9534(03)00038-2 (cit. on p. 120).

Adler, P. R., M. A. Sanderson, A. A. Boateng, P. J. Weimer, and H.-J. G. Jung (2006). "Biomass Yield and Biofuel Quality of Switchgrass Harvested in Fall or Spring". In: *Agronomy Journal* 98.6, p. 1518. DOI: 10.2134/agronj2005.0351 (cit. on p. 119).

Agarwal, A., M. S. delos Angeles, R. Bhatia, I. Chéret, S. Davila-Poblete, M. Falkenmark, F. Gonzalez Villarreal, T. Jønch-Clausen, M. Aït Kadi, J. Kindler, J. Rees, P. Roberts, M. Solanes, and A. Wright (2000). *Integrated Water Resources Management, TAC background papers No. 4* (cit. on p. 84).

Ainsworth, E. A. and S. P. Long (2004). "What have we learned from 15 years of free-air CO2 enrichment (FACE)? A meta-analytic review of the responses of photosynthesis, canopy properties and plant production to rising CO2". In: *New Phytologist* 165, pp. 351–372. DOI: 10.1111/j.1469-8137.2004.01224.x (cit. on pp. 10, 112).

Anderies, J. M., S. R. Carpenter, W. Steffen, and J. Rockström (2013). "The topology of non-linear global carbon dynamics: from tipping points to planetary boundaries". In: *Environmental Research Letters* 8.4, p. 044048. DOI: 10.1088/1748-9326/8/4/044048 (cit. on pp. 18, 61–63, 66, 68).

Aravindhakshan, S. C., F. M. Epplin, and C. M. Taliaferro (2010). "Economics of switchgrass and miscanthus relative to coal as feedstock for generating electricity". In: *Biomass and Bioenergy* 34.9, pp. 1375–1383. DOI: 10.1016/j.biombioe.2010.04.017 (cit. on pp. 118, 119).

Arora, V. K. and A. Montenegro (2011). "Small temperature benefits provided by realistic afforestation efforts". In: *Nature Geoscience* 4.8, pp. 514–518. DOI: 10.1038/ngeo1182 (cit. on pp. 10, 12).

Ashworth, A. J. and P. D. Keyser (2013). "Yield and Stand Persistence of Switchgrass as Affected by Cutting Height and Variety". In: *Forage and Grazinglands* 11.1. DOI: 10.1094/FG-2013-0043-RS (cit. on pp. 25, 124).

Bagley, J. E., S. C. Davis, M. Georgescu, M. Z. Hussain, J. Miller, S. W. Nesbitt, A. VanLoocke, and C. J. Bernacchi (2014). "The biophysical link between climate, water, and vegetation in bioenergy agro-ecosystems". In: *Biomass and Bioenergy* 71, pp. 187–201. DOI: 10.1016/j.biombioe.2014.10.007 (cit. on p. 35).

Barnosky, A. D., N. Matzke, S. Tomiya, G. O. U. Wogan, B. Swartz, T. B. Quental, C. Marshall, J. L. McGuire, E. L. Lindsey, K. C. Maguire, B. Mersey, and E. A. Ferrer (2011). "Has the Earth/'s sixth mass extinction already arrived?" In: *Nature* 471.7336, pp. 51–57. DOI: 10.1038/nature09678 (cit. on p. 3).

Bathiany, S., M. Claussen, V. Brovkin, T. Raddatz, and V. Gayler (2010). "Combined biogeophysical and biogeochemical effects of large-scale forest cover changes in the MPI earth system model". In: *Biogeosciences* 7.5, pp. 1383–1399. DOI: 10.5194/bg-7-1383-2010 (cit. on p. 11).

Batjes, N. H. (1996). "Total carbon and nitrogen in the soils of the world". In: *European Journal of Soil Science* 47.2, pp. 151–163. DOI: 10.1111/j.1365-2389.1996.tb01386.x (cit. on p. 64).

Beer, C., W. Lucht, C. Schmullius, and A. Shvidenko (2006). "Small net carbon dioxide uptake by Russian forests during 1981–1999". In: *Geophysical Research Letters* 33.15, p. L15403. DOI: 10.1029/2006GL026919 (cit. on p. 25).

Beringer, T., W. Lucht, and S. Schaphoff (2011). "Bioenergy production potential of global biomass plantations under environmental and agricultural constraints". In: *GCB Bioenergy* 3.4, pp. 299–312. DOI: 10.1111/j.1757-1707.2010.01088.x (cit. on pp. 9, 11, 12, 15, 23, 24, 74, 86, 122).

Berkes, F., C. Folke, and J. Colding (2000). *Linking Social and Ecological Systems: Management Practices and Social Mechanisms for Building Resilience*. Google-Books-ID: XixuNvX2zLwC. Cambridge University Press. 480 pp. (cit. on p. 62).

Berndes, G. (2002). "Bioenergy and water—the implications of large-scale bioenergy production for water use and supply". In: *Global Environmental Change* 12.4, pp. 253–271. DOI: 10.1016/S0959-3780(02)00040-7 (cit. on p. 11).

Berthelot, A. and A. Gavaland (2007). *Produire de la Biomasse Avec les Peupliers. Fiche-Information Forêts FCBA. Fascicule #755.* (Cit. on p. 120).

Betts, R. A. (2000). "Offset of the potential carbon sink from boreal forestation by decreases in surface albedo". In: *Nature* 408.6809, pp. 187–190. DOI: 10.1038/35041545 (cit. on pp. 10, 11, 13).

Binkley, D., R. Senock, S. Bird, and T. G. Cole (2003). "Twenty years of stand development in pure and mixed stands of Eucalyptus saligna and nitrogen-fixing Facaltaria moluccana".

In: *Forest Ecology and Management* 182.1, pp. 93–102. DOI: 10.1016/S0378-1127(03)00028-8 (cit. on p. 121).

Blair, G. J., D. A. Ivory, T. R. Evans, and Australian Centre for International Agricultural Research, eds. (1986). *Forages in Southeast Asian and South Pacific agriculture: proceedings of an international workshop held at Cisarua, Indonesia; 19-23 August 1985*. ACIAR proceedings 12. Canberra: Australian Centre for International Agricultural Research. 202 pp. (cit. on p. 118).

Bloh, W. von, S. Rost, D. Gerten, and W. Lucht (2010). "Efficient parallelization of a dynamic global vegetation model with river routing". In: *Environmental Modelling & Software* 25.6, pp. 685–690. DOI: 10.1016/j.envsoft.2009.11.012 (cit. on p. 24).

Boisier, J. P., N. de Noblet-Ducoudré, and P. Ciais (2014). "Historical land-use-induced evapotranspiration changes estimated from present-day observations and reconstructed land-cover maps". In: *Hydrol. Earth Syst. Sci.* 18.9, pp. 3571–3590. DOI: 10.5194/hess-18-3571-2014 (cit. on p. 84).

Boit, A., B. Sakschewski, L. Boysen, A. Cano-Crespo, J. Clement, N. Garcia-alaniz, K. Kok, M. Kolb, F. Langerwisch, A. Rammig, R. Sachse, M. van Eupen, W. von Bloh, D. Clara Zemp, and K. Thonicke (2016). "Large-scale impact of climate change vs. land-use change on future biome shifts in Latin America". In: *Global Change Biology*, n/a–n/a. DOI: 10.1111/gcb.13355 (cit. on pp. 50, 54).

Bondeau, A., P. C. Smith, S. Zaehle, S. Schaphoff, W. Lucht, W. Cramer, D. Gerten, H. Lotze-Campen, C. Müller, M. Reichstein, and B. Smith (2007). "Modelling the role of agriculture for the 20th century global terrestrial carbon balance". In: *Global Change Biology* 13.3, pp. 679–706. DOI: 10.1111/j.1365-2486.2006.01305.x (cit. on pp. 17, 23–25, 49, 85, 86, 112, 124).

Bonsch, M., F. Humpenöder, A. Popp, B. Bodirsky, J. P. Dietrich, S. Rolinski, A. Biewald, H. Lotze-Campen, I. Weindl, D. Gerten, and M. Stevanovic (2014). "Trade-offs between land and water requirements for large-scale bioenergy production". In: *GCB Bioenergy*, n/a–n/a. DOI: 10.1111/gcbb.12226 (cit. on p. 13).

Boucher, O., G. Myhre, and A. Myhre (2004). "Direct human influence of irrigation on atmospheric water vapour and climate". In: *Climate Dynamics* 22.6, pp. 597–603. DOI: 10.1007/s00382-004-0402-4 (cit. on p. 1).

Bouwman, L., K. K. Goldewijk, K. W. Van Der Hoek, A. H. W. Beusen, D. P. Van Vuuren, J. Willems, M. C. Rufino, and E. Stehfest (2011). "Exploring global changes in nitrogen and phosphorus cycles in agriculture induced by livestock production over the 1900–2050 period". In: *Proceedings of the National Academy of Sciences of the United States of America*. DOI: 10.1073/pnas.1012878108 (cit. on pp. 44, 50, 56).

Boysen, L. R., W. Lucht, D. Gerten, and V. Heck (2016). "Impacts devalue the potential of large-scale terrestrial CO 2 removal through biomass plantations". In: *Environmental*

Research Letters 11.9, p. 095010. DOI: 10.1088/1748-9326/11/9/095010 (cit. on pp. 11–13).

Brander, J. A. and M. S. Taylor (1998). "The Simple Economics of Easter Island: A Ricardo-Malthus Model of Renewable Resource Use". In: *The American Economic Review* 88.1, pp. 119–138 (cit. on pp. 18, 61).

Bruinsma, J. (2009). *The resource outlook to 2050: By how much do land, water and crop yields need to increase by 2050?* (Cit. on p. 90).

Bungart, R. and R. F. Hüttl (2004). "Growth dynamics and biomass accumulation of 8-year-old hybrid poplar clones in a short-rotation plantation on a clayey-sandy mining substrate with respect to plant nutrition and water budget". In: *European Journal of Forest Research* 123.2, pp. 105–115. DOI: 10.1007/s10342-004-0024-8 (cit. on p. 120).

Caiazzo, F., R. Malina, M. D. Staples, P. J. Wolfe, S. H. L. Yim, and S. R. H. Barrett (2014). "Quantifying the climate impacts of albedo changes due to biofuel production: a comparison with biogeochemical effects". In: *Environmental Research Letters* 9.2, p. 024015. DOI: 10.1088/1748-9326/9/2/024015 (cit. on p. 35).

Caldeira, K., G. Bala, and L. Cao (2013). "The Science of Geoengineering". In: *Annual Review of Earth and Planetary Sciences* 41.1, pp. 231–256. DOI: 10.1146/annurev-earth-042711-105548 (cit. on pp. 22, 23, 60).

Caldeira, K. and D. W. Keith (2010). "The need for climate engineering research". In: *Issues in Science and Technology* 27.1, p. 57 (cit. on pp. 60, 79).

Cannell, M. G. R. (1980). "Productivity of Closely-spaced Young Poplar on Agricultural Soils in Britain". In: *Forestry* 53.1, pp. 1–21. DOI: 10.1093/forestry/53.1.1 (cit. on p. 120).

Cao, K., B. Huang, S. Wang, and H. Lin (2012). "Sustainable land use optimization using Boundary-based Fast Genetic Algorithm". In: *Computers, Environment and Urban Systems* 36.3, pp. 257–269. DOI: 10.1016/j.compenvurbsys.2011.08.001 (cit. on p. 18).

Cardinale, B. J., J. E. Duffy, A. Gonzalez, D. U. Hooper, C. Perrings, P. Venail, A. Narwani, G. M. Mace, D. Tilman, D. A. Wardle, A. P. Kinzig, G. C. Daily, M. Loreau, J. B. Grace, A. Larigauderie, D. S. Srivastava, and S. Naeem (2012). "Biodiversity loss and its impact on humanity". In: *Nature* 486.7401, pp. 59–67. DOI: 10.1038/nature11148 (cit. on p. 84).

CBD (2000). *COP 5 Decision V/6 (Fifth Meeting of the Conference of the Parties to the Convention on Biological Diversity)* (cit. on p. 84).

Christian, D. G., A. B. Riche, and N. E. Yates (2008). "Growth, yield and mineral content of Miscanthus × giganteus grown as a biofuel for 14 successive harvests". In: *Industrial Crops and Products* 28.3, pp. 320–327. DOI: 10.1016/j.indcrop.2008.02.009 (cit. on p. 118).

Chum, H., A. Faaij, J. Moreira, G. Berndes, P. Dhamija, H. Dong, B. Gabrielle, A. G. Eng, W. Lucht, M. Mapako, O. M. Cerutti, T. McIntyre, T. Minowa, K. Pingoud, R. Bain, R. Chiang, D. Dawe, G. Heath, M. Junginger, M. Patel, J. Yang, E. Warner, D. Par?, and S. K. Ribeiro (2011). "Renewable Energy Sources and Climate Change Mitigation: Special

Report of the Intergovernmental Panel on Climate Change". In: *Renewable Energy Sources and Climate Change Mitigation*. Cambridge University Press (cit. on p. 10).

Ciais, P., C. Sabine, G. Bala, L. Bopp, V. Brovkin, J. Canadell, A. Chhabra, R. DeFries, J. Galloway, M. Heimann, C. Jones, C. Le Quéré, R. Myneni, S. Piao, and P. Thornton (2013). "Carbon and Other Biogeochemical Cycles". In: *Climate Change 2013: The Physical Science Basis. Contribution of Working Group I to the Fifth Assessment Report of the Intergovernmental Panel on Climate Change*. Ed. by T. Stocker, D. Qin, G.-K. Plattner, M. Tignor, S. Allen, J. Boschung, A. Nauels, Y. Xia, V. Bex, and P. Midgley. Cambridge, United Kingdom and New York, NY, USA: Cambridge University Press, pp. 465–570 (cit. on pp. 64, 68, 69, 71).

Clifton-Brown, J. C., J. Breuer, and M. B. Jones (2007). "Carbon mitigation by the energy crop, Miscanthus". In: *Global Change Biology* 13.11, pp. 2296–2307. DOI: 10.1111/j.1365-2486.2007.01438.x (cit. on p. 118).

Clifton-Brown, J. C., I. Lewandowski, B. Andersson, G. Basch, D. G. Christian, J. B. Kjeldsen, U. Jørgensen, J. V. Mortensen, A. B. Riche, K.-U. Schwarz, K. Tayebi, and F. Teixeira (2001). "Performance of 15 Genotypes at Five Sites in Europe". In: *Agronomy Journal* 93.5, p. 1013. DOI: 10.2134/agronj2001.9351013x (cit. on p. 118).

Cole, M. J., R. M. Bailey, and M. G. New (2014). "Tracking sustainable development with a national barometer for South Africa using a downscaled "safe and just space" framework". In: *Proceedings of the National Academy of Sciences* 111.42, E4399–E4408. DOI: 10.1073/pnas.1400985111 (cit. on p. 7).

Cosentino, S. L., C. Patanè, E. Sanzone, V. Copani, and S. Foti (2007). "Effects of soil water content and nitrogen supply on the productivity of Miscanthus × giganteus Greef et Deu. in a Mediterranean environment". In: *Industrial Crops and Products* 25.1, pp. 75–88. DOI: 10.1016/j.indcrop.2006.07.006 (cit. on p. 118).

Cramer, W., A. Bondeau, F. I. Woodward, I. C. Prentice, R. A. Betts, V. Brovkin, P. M. Cox, V. Fisher, J. A. Foley, A. D. Friend, C. Kucharik, M. R. Lomas, N. Ramankutty, S. Sitch, B. Smith, A. White, and C. Young-Molling (2001). "Global response of terrestrial ecosystem structure and function to CO2 and climate change: results from six dynamic global vegetation models". In: *Global Change Biology* 7.4, pp. 357–373. DOI: 10.1046/j.1365-2486.2001.00383.x (cit. on p. 16).

Creutzig, F., N. H. Ravindranath, G. Berndes, S. Bolwig, R. Bright, F. Cherubini, H. Chum, E. Corbera, M. Delucchi, A. Faaij, J. Fargione, H. Haberl, G. Heath, O. Lucon, R. Plevin, A. Popp, C. Robledo-Abad, S. Rose, P. Smith, A. Stromman, S. Suh, and O. Masera (2014). "Bioenergy and climate change mitigation: an assessment". In: *GCB Bioenergy*, n/a–n/a. DOI: 10.1111/gcbb.12205 (cit. on pp. 11, 12).

Crowley, T. J. (1995). "Ice Age terrestrial carbon changes revisited". In: *Global Biogeochemical Cycles* 9.3, pp. 377–389. DOI: 10.1029/95GB01107 (cit. on p. 69).

Crutzen, P. J., A. R. Mosier, K. A. Smith, and W. Winiwarter (2008). "N2O release from agro-biofuel production negates global warming reduction by replacing fossil fuels". In: *Atmos. Chem. Phys.* 8.2, pp. 389–395. DOI: 10.5194/acp-8-389-2008 (cit. on pp. 11, 13).

Crutzen, P. J. (2002). "Geology of mankind". In: *Nature* 415.6867, pp. 23–23. DOI: 10.1038/415023a (cit. on p. 1).

Danalatos, N. G., S. V. Archontoulis, and I. Mitsios (2007). "Potential growth and biomass productivity of Miscanthus×giganteus as affected by plant density and N-fertilization in central Greece". In: *Biomass and Bioenergy* 31.2, pp. 145–152. DOI: 10.1016/j.biombioe.2006.07.004 (cit. on p. 118).

Davis, M. P., M. B. David, T. B. Voigt, and C. A. Mitchell (2014). "Effect of nitrogen addition on *Miscanthus* × ¡i¿ giganteus¡/i¿ yield, nitrogen losses, and soil organic matter across five sites". In: *GCB Bioenergy*, n/a–n/a. DOI: 10.1111/gcbb.12217 (cit. on p. 118).

DeFries, R. and C. Rosenzweig (2010). "Toward a whole-landscape approach for sustainable land use in the tropics". In: *Proceedings of the National Academy of Sciences* 107.46, pp. 19627–19632. DOI: 10.1073/pnas.1011163107 (cit. on p. 84).

DeLucia, E. H., N. Gomez-Casanovas, J. A. Greenberg, T. W. Hudiburg, I. B. Kantola, S. P. Long, A. D. Miller, D. R. Ort, and W. J. Parton (2014). "The Theoretical Limit to Plant Productivity". In: *Environmental Science & Technology* 48.16, pp. 9471–9477. DOI: 10.1021/es502348e (cit. on p. 34).

Demo, M., A. Bako, D. Húska, and M. Hauptvogl (2013). "Biomass production potential of different willow varieties (Salixspp.) grown in soilclimatic conditions of south-western Slovakia". In: *Wood Research* 58.4, pp. 651–662 (cit. on p. 120).

Di Virgilio, N., A. Monti, and G. Venturi (2007). "Spatial variability of switchgrass (Panicum virgatum L.) yield as related to soil parameters in a small field". In: *Field Crops Research* 101.2, pp. 232–239. DOI: 10.1016/j.fcr.2006.11.009 (cit. on p. 119).

Dornburg, V., D. v. Vuuren, G. v. d. Ven, H. Langeveld, M. Meeusen, M. Banse, M. v. Oorschot, J. Ros, G. J. v. d. Born, H. Aiking, M. Londo, H. Mozaffarian, P. Verweij, E. Lysen, and A. Faaij (2010). "Bioenergy revisited: Key factors in global potentials of bioenergy". In: *Energy & Environmental Science* 3.3, pp. 258–267. DOI: 10.1039/B922422J (cit. on pp. 11, 35, 74).

Dowell, R. C., D. Gibbins, J. L. Rhoads, and S. G. Pallardy (2009). "Biomass production physiology and soil carbon dynamics in short-rotation-grown Populus deltoides and P. deltoides × P. nigra hybrids". In: *Forest Ecology and Management* 257.1, pp. 134–142. DOI: 10.1016/j.foreco.2008.08.023 (cit. on p. 120).

Drake, B. G., M̃. A. Gonzàlez-Meler, and S. P. Long (1997). "MORE EFFICIENT PLANTS: A Consequence of Rising Atmospheric CO2?" In: *Annual Review of Plant Physiology and Plant Molecular Biology* 48.1, pp. 609–639. DOI: 10.1146/annurev.arplant.48.1.609 (cit. on p. 66).

Dyson, F. J. (1977). "Can we control the carbon dioxide in the atmosphere?" In: *Energy* 2.3, pp. 287–291. DOI: 10.1016/0360-5442(77)90033-0 (cit. on pp. 1, 107).

Edenhofer, O., R. Pichs-Madruga, Y. Sokona, K. Seyboth, S. Kadner, T. Zwickel, P. Eickemeier, G. Hansen, S. SchlÃ¶mer, C. v. Stechow, and P. Matschoss, eds. (2011). *Renewable Energy Sources and Climate Change Mitigation*. Cambridge Books Online. Cambridge University Press (cit. on p. 43).

Ellis, E. C. and N. Ramankutty (2008). "Putting people in the map: anthropogenic biomes of the world". In: *Frontiers in Ecology and the Environment* 6.8, pp. 439–447. DOI: 10.1890/070062 (cit. on p. 2).

Erb, K.-H., V. Gaube, F. Krausmann, C. Plutzar, A. Bondeau, and H. Haberl (2007). "A comprehensive global 5 min resolution land-use data set for the year 2000 consistent with national census data". In: *Journal of Land Use Science* 2.3, pp. 191–224. DOI: 10.1080/17474230701622981 (cit. on p. 89).

Fader, M., S. Rost, C. Müller, A. Bondeau, and D. Gerten (2010). "Virtual water content of temperate cereals and maize: Present and potential future patterns". In: *Journal of Hydrology*. Green-Blue Water Initiative (GBI) 384.3, pp. 218–231. DOI: 10.1016/j.jhydrol.2009.12.011 (cit. on pp. 25, 49, 85, 86, 112).

FAOSTAT (2005). *Food Balance Sheets 2005* (cit. on pp. 88, 90).

Felton, A., E. Knight, J. Wood, C. Zammit, and D. Lindenmayer (2010). "A meta-analysis of fauna and flora species richness and abundance in plantations and pasture lands". In: *Biological Conservation* 143.3, pp. 545–554. DOI: 10.1016/j.biocon.2009.11.030 (cit. on p. 35).

Fischer, G., F. O. Nachtergaele, S. Prieler, E. Teixeira, G. Toth, H. T. van Velthuizen, L. Verelst, and D. Wiberg (2012). *Global Agro-Ecological Zones (GAEZ v3.0)*. URL: http://webarchive.iiasa.ac.at/Research/LUC/GAEZv3.0/docs/GAEZ_Model_Documentation.pdf (visited on 08/31/2016) (cit. on pp. 87, 89).

Fischer, J., D. J. Abson, V. Butsic, M. J. Chappell, J. Ekroos, J. Hanspach, T. Kuemmerle, H. G. Smith, and H. von Wehrden (2014). "Land Sparing Versus Land Sharing: Moving Forward". In: *Conservation Letters* 7.3, pp. 149–157. DOI: 10.1111/conl.12084 (cit. on p. 95).

Flörke, M., E. Kynast, I. Bärlund, S. Eisner, F. Wimmer, and J. Alcamo (2013). "Domestic and industrial water uses of the past 60 years as a mirror of socio-economic development: A global simulation study". In: *Global Environmental Change* 23.1, pp. 144–156. DOI: 10.1016/j.gloenvcha.2012.10.018 (cit. on p. 50).

Foley, J. A., M. H. Costa, C. Delire, N. Ramankutty, and P. Snyder (2003). "Green surprise? How terrestrial ecosystems could affect earth's climate". In: *Frontiers in Ecology and the Environment* 1.1, pp. 38–44. DOI: 10.1890/1540-9295(2003)001[0038:GSHTEC]2.0.CO;2 (cit. on p. 74).

Foley, J. A., R. DeFries, G. P. Asner, C. Barford, G. Bonan, S. R. Carpenter, F. S. Chapin, M. T. Coe, G. C. Daily, H. K. Gibbs, J. H. Helkowski, T. Holloway, E. A. Howard, C. J. Kucharik, C. Monfreda, J. A. Patz, I. C. Prentice, N. Ramankutty, and P. K. Snyder (2005). "Global Consequences of Land Use". In: *Science* 309.5734, pp. 570–574. DOI: 10.1126/science.1111772 (cit. on pp. 13, 22, 30, 114).

Foley, J. A., N. Ramankutty, K. A. Brauman, E. S. Cassidy, J. S. Gerber, M. Johnston, N. D. Mueller, C. O/'Connell, D. K. Ray, P. C. West, C. Balzer, E. M. Bennett, S. R. Carpenter, J. Hill, C. Monfreda, S. Polasky, J. Rockstrom, J. Sheehan, S. Siebert, D. Tilman, and D. P. M. Zaks (2011). "Solutions for a cultivated planet". In: *Nature* 478.7369, pp. 337–342. DOI: 10.1038/nature10452 (cit. on p. 15).

Fowler, D., M. Coyle, U. Skiba, M. Sutton, J. N. Cape, S. Reis, L. Sheppard, A. Jenkins, B. Grizetti, J. N. Galloway, P. Vitousek, A. Leach, L. Bouwman, K. Butterbach-Bahl, F. Dentener, D. Stevenson, M. Amann, and M. Voss (2013). "The global nitrogen cycle in the 21th century". In: *Philisophical Transactions of the Royal Society of London, B Biological Sciences* 368, p. 20130165 (cit. on p. 3).

François, L. M., C. Delire, P. Warnant, and G. Munhoven (1998). "Modelling the glacial–interglacial changes in the continental biosphere". In: *Global and Planetary Change* 16–17, pp. 37–52. DOI: 10.1016/S0921-8181(98)00005-8 (cit. on p. 69).

Friend, A. D., W. Lucht, T. T. Rademacher, R. Keribin, R. Betts, P. Cadule, P. Ciais, D. B. Clark, R. Dankers, P. D. Falloon, A. Ito, R. Kahana, A. Kleidon, M. R. Lomas, K. Nishina, S. Ostberg, R. Pavlick, P. Peylin, S. Schaphoff, N. Vuichard, L. Warszawski, A. Wiltshire, and F. I. Woodward (2013). "Carbon residence time dominates uncertainty in terrestrial vegetation responses to future climate and atmospheric CO2". In: *Proceedings of the National Academy of Sciences*, p. 201222477. DOI: 10.1073/pnas.1222477110 (cit. on pp. 25, 29, 69).

Frischknecht, R., C. Nathani, S. Büsser Knöpfel, R. Itten, F. Wyss, and P. Hellmüller (2014). *Entwicklung der weltweiten Umweltauswirkungen der Schweiz: Umweltbelastung von Konsum und Produktion von 1996 bis 2011*. Google-Books-ID: iongoQEACAAJ. Bundesamt für Umwelt, Bern. Umwelt-Wissen Nr. 1413: 120 S. book (cit. on p. 7).

Fuss, S., J. G. Canadell, G. P. Peters, M. Tavoni, R. M. Andrew, P. Ciais, R. B. Jackson, C. D. Jones, F. Kraxner, N. Nakicenovic, C. Le Quéré, M. R. Raupach, A. Sharifi, P. Smith, and Y. Yamagata (2014). "Betting on negative emissions". In: *Nature Climate Change* 4.10, pp. 850–853. DOI: 10.1038/nclimate2392 (cit. on pp. 9, 12, 23, 41, 60).

Gao, Y., M. Skutsch, O. Masera, and P. Pacheco (2011). *A global analysis of deforestation due to biofuel development*. CIFOR. 100 pp. (cit. on p. 74).

Gasser, T., C. Guivarch, K. Tachiiri, C. D. Jones, and P. Ciais (2015). "Negative emissions physically needed to keep global warming below 2°C". In: *Nature Communications* 6, p. 7958. DOI: 10.1038/ncomms8958 (cit. on pp. 9, 12, 41).

Georgescu, M., D. B. Lobell, and C. B. Field (2011). "Direct climate effects of perennial bioenergy crops in the United States". In: *Proceedings of the National Academy of Sciences* 108.11, pp. 4307–4312. DOI: 10.1073/pnas.1008779108 (cit. on pp. 12, 35).

Gerten, D., H. Hoff, J. Rockström, J. Jägermeyr, M. Kummu, and A. V. Pastor (2013). "Towards a revised planetary boundary for consumptive freshwater use: role of environmental flow requirements". In: *Current Opinion in Environmental Sustainability*. Aquatic and marine systems 5.6, pp. 551–558. DOI: 10.1016/j.cosust.2013.11.001 (cit. on pp. 83, 89).

Gerten, D., J. Rockström, J. Heinke, W. Steffen, K. Richardson, and S. Cornell (2015). "Response to Comment on "Planetary boundaries: Guiding human development on a changing planet"". In: *Science* 348.6240, pp. 1217–1217. DOI: 10.1126/science.aab0031 (cit. on p. 35).

Gerten, D., S. Schaphoff, U. Haberlandt, W. Lucht, and S. Sitch (2004). "Terrestrial vegetation and water balance—hydrological evaluation of a dynamic global vegetation model". In: *Journal of Hydrology* 286.1, pp. 249–270. DOI: 10.1016/j.jhydrol.2003.09.029 (cit. on pp. 24, 25, 49, 85, 112).

Gillett, N. P., V. K. Arora, D. Matthews, and M. R. Allen (2013). "Constraining the Ratio of Global Warming to Cumulative CO2 Emissions Using CMIP5 Simulations*". In: *Journal of Climate* 26.18, pp. 6844–6858. DOI: 10.1175/JCLI-D-12-00476.1 (cit. on pp. 34, 68).

Gloor, M., J. L. Sarmiento, and N. Gruber (2010). "What can be learned about carbon cycle climate feedbacks from the CO2 airborne fraction?" In: *Atmospheric Chemistry and Physics* 10.16, pp. 7739–7751. DOI: 10.5194/acp-10-7739-2010 (cit. on p. 68).

GOE (2010). *Ethiopia growth and transformation plan* (cit. on p. 100).

Gordon, L. J., W. Steffen, B. F. Jönsson, C. Folke, M. Falkenmark, and Å. Johannessen (2005). "Human modification of global water vapor flows from the land surface". In: *Proceedings of the National Academy of Sciences of the United States of America* 102.21, pp. 7612–7617. DOI: 10.1073/pnas.0500208102 (cit. on p. 2).

Griggs, D., M. Stafford-Smith, O. Gaffney, J. Rockström, M. C. Öhman, P. Shyamsundar, W. Steffen, G. Glaser, N. Kanie, and I. Noble (2013). "Policy: Sustainable development goals for people and planet". In: *Nature* 495.7441, pp. 305–307. DOI: 10.1038/495305a (cit. on p. 7).

Grogan, P. and R. Matthews (2002). "A modelling analysis of the potential for soil carbon sequestration under short rotation coppice willow bioenergy plantations". In: *Soil Use and Management* 18.3, pp. 175–183. DOI: 10.1111/j.1475-2743.2002.tb00237.x (cit. on p. 124).

Grundmann, J., N. Schütze, G. H. Schmitz, and S. Al-Shaqsi (2011). "Towards an integrated arid zone water management using simulation-based optimisation". In: *Environmental Earth Sciences* 65.5, pp. 1381–1394. DOI: 10.1007/s12665-011-1253-z (cit. on p. 18).

Guinotte, J. M. and V. J. Fabry (2008). "Ocean Acidification and Its Potential Effects on Marine Ecosystems". In: *Annals of the New York Academy of Sciences* 1134.1, pp. 320–342. DOI: 10.1196/annals.1439.013 (cit. on p. 70).

Guo, L. B. and R. M. Gifford (2002). "Soil carbon stocks and land use change: a meta analysis". In: *Global Change Biology* 8.4, pp. 345–360. DOI: 10.1046/j.1354-1013.2002.00486.x (cit. on p. 124).

Haberl, H., K. H. Erb, F. Krausmann, V. Gaube, A. Bondeau, C. Plutzar, S. Gingrich, W. Lucht, and M. Fischer-Kowalski (2007). "Quantifying and mapping the human appropriation of net primary production in earth's terrestrial ecosystems". In: *Proceedings of the National Academy of Sciences* 104.31, pp. 12942–12947. DOI: 10.1073/pnas.0704243104 (cit. on p. 3).

Haberl, H., K.-H. Erb, F. Krausmann, S. Running, T. D. Searchinger, and W. K. Smith (2013). "Bioenergy: how much can we expect for 2050?" In: *Environmental Research Letters* 8.3, p. 031004. DOI: 10.1088/1748-9326/8/3/031004 (cit. on p. 34).

Harfoot, M., D. P. Tittensor, T. Newbold, G. McInerny, M. J. Smith, and J. P. W. Scharlemann (2014). "Integrated assessment models for ecologists: the present and the future". In: *Global Ecology and Biogeography* 23.2, pp. 124–143. DOI: 10.1111/geb.12100 (cit. on p. 84).

Harris, I., P. Jones, T. Osborn, and D. Lister (2014). "Updated high-resolution grids of monthly climatic observations – the CRU TS3.10 Dataset". In: *International Journal of Climatology* 34.3, pp. 623–642. DOI: 10.1002/joc.3711 (cit. on pp. 28, 50, 54, 86).

Hastings, A., J. Clifton-Brown, M. Wattenbach, C. P. Mitchell, P. Stampfl, and P. Smith (2009). "Future energy potential of Miscanthus in Europe". In: *GCB Bioenergy* 1.2, pp. 180–196. DOI: 10.1111/j.1757-1707.2009.01012.x (cit. on p. 55).

Heaton, E. A., F. G. Dohleman, and S. P. Long (2008). "Meeting US biofuel goals with less land: the potential of Miscanthus". In: *Global Change Biology* 14.9, pp. 2000–2014. DOI: 10.1111/j.1365-2486.2008.01662.x (cit. on pp. 118, 119).

Heck, V., J. F. Donges, and W. Lucht (2016a). "Collateral transgression of planetary boundaries due to climate engineering by terrestrial carbon dioxide removal". In: *Earth System Dynamics Discussions*, pp. 1–24. DOI: 10.5194/esd-2016-22 (cit. on p. 59).

Heck, V., D. Gerten, W. Lucht, and L. R. Boysen (2016b). "Is extensive terrestrial carbon dioxide removal a 'green' form of geoengineering? A global modelling study". In: *Global and Planetary Change* 137, pp. 123–130. DOI: 10.1016/j.gloplacha.2015.12.008 (cit. on pp. 21, 41, 49, 61, 71, 112).

Heimann, M. and M. Reichstein (2008). "Terrestrial ecosystem carbon dynamics and climate feedbacks". In: *Nature* 451.7176, pp. 289–292. DOI: 10.1038/nature06591 (cit. on pp. 66, 69).

Heinke, J., S. Ostberg, S. Schaphoff, K. Frieler, C. Müller, D. Gerten, M. Meinshausen, and W. Lucht (2013). "A new climate dataset for systematic assessments of climate change

impacts as a function of global warming". In: *Geosci. Model Dev.* 6.5, pp. 1689–1703. DOI: 10.5194/gmd-6-1689-2013 (cit. on pp. 43, 49, 54).

Heitzig, J., T. Kittel, J. F. Donges, and N. Molkenthin (2016). "Topology of sustainable management of dynamical systems with desirable states: from defining planetary boundaries to safe operating spaces in the Earth system". In: *Earth Syst. Dynam.* 7.1, pp. 21–50. DOI: 10.5194/esd-7-21-2016 (cit. on p. 80).

Hejazi, M. I., N. Voisin, L. Liu, L. M. Bramer, D. C. Fortin, J. E. Hathaway, M. Huang, P. Kyle, L. R. Leung, H.-Y. Li, Y. Liu, P. L. Patel, T. C. Pulsipher, J. S. Rice, T. K. Tesfa, C. R. Vernon, and Y. Zhou (2015). "21st century United States emissions mitigation could increase water stress more than the climate change it is mitigating". In: *Proceedings of the National Academy of Sciences* 112.34, pp. 10635–10640. DOI: 10.1073/pnas.1421675112 (cit. on pp. 11, 13).

Heller, M. C., G. A. Keoleian, and T. A. Volk (2003). "Life cycle assessment of a willow bioenergy cropping system". In: *Biomass and Bioenergy* 25.2, pp. 147–165. DOI: 10.1016/S0961-9534(02)00190-3 (cit. on pp. 25, 122).

Hellmann, F., P. Schultz, C. Grabow, J. Heitzig, and J. Kurths (2016). "Survivability of Deterministic Dynamical Systems". In: *Scientific Reports* 6, p. 29654. DOI: 10.1038/srep29654 (cit. on p. 72).

Herzog, H. J. (2011). "Scaling up carbon dioxide capture and storage: From megatons to gigatons". In: *Energy Economics*. Special Issue on The Economics of Technologies to Combat Global Warming 33.4, pp. 597–604. DOI: 10.1016/j.eneco.2010.11.004 (cit. on pp. 46, 49, 113).

Himken, M., J. Lammel, D. Neukirchen, U. Czypionka-Krause, and H.-W. Olfs (1997). "Cultivation of Miscanthus under West European conditions: Seasonal changes in dry matter production, nutrient uptake and remobilization". In: *Plant and Soil* 189.1, pp. 117–126. DOI: 10.1023/A:1004244614537 (cit. on p. 118).

Hofmann-Schielle, C., A. Jug, F. Makeschin, and K. E. Rehfuess (1999). "Short-rotation plantations of balsam poplars, aspen and willows on former arable land in the Federal Republic of Germany. I. Site–growth relationships". In: *Forest Ecology and Management* 121.1, pp. 41–55. DOI: 10.1016/S0378-1127(98)00555-6 (cit. on p. 120).

Holling, C. S. (1973). "Resilience and Stability of Ecological Systems". In: *Annual Review of Ecology and Systematics* 4.1, pp. 1–23. DOI: 10.1146/annurev.es.04.110173.000245 (cit. on p. 71).

Houghton, R. A. (1999). "The annual net flux of carbon to the atmosphere from changes in land use 1850–1990*". In: *Tellus B* 51.2, pp. 298–313. DOI: 10.1034/j.1600-0889.1999.00013.x (cit. on p. 2).

Houghton, R. A., J. I. House, J. Pongratz, G. R. van der Werf, R. S. DeFries, M. C. Hansen, C. Le Quéré, and N. Ramankutty (2012). "Carbon emissions from land use and land-cover

change". In: *Biogeosciences* 9.12, pp. 5125–5142. DOI: 10.5194/bg-9-5125-2012 (cit. on pp. 2, 84).

House, J. I., I. Colin Prentice, and C. Le Quéré (2002). "Maximum impacts of future reforestation or deforestation on atmospheric CO2". In: *Global Change Biology* 8.11, pp. 1047–1052. DOI: 10.1046/j.1365-2486.2002.00536.x (cit. on p. 10).

Hsu, T., K. French, and R. Major (2010). "Avian assemblages in eucalypt forests, plantations and pastures in northern NSW, Australia". In: *Forest Ecology and Management* 260.6, pp. 1036–1046. DOI: 10.1016/j.foreco.2010.06.028 (cit. on p. 35).

Hunter, I. (2001). "Above ground biomass and nutrient uptake of three tree species (Eucalyptus camaldulensis, Eucalyptus grandis and Dalbergia sissoo) as affected by irrigation and fertiliser, at 3 years of age, in southern India". In: *Forest Ecology and Management* 144.1, pp. 189–200. DOI: 10.1016/S0378-1127(00)00373-X (cit. on p. 121).

Huntington, T. G. (2006). "Evidence for intensification of the global water cycle: Review and synthesis". In: *Journal of Hydrology* 319.1, pp. 83–95. DOI: 10.1016/j.jhydrol.2005.07.003 (cit. on p. 32).

Hurtt, G. C., L. P. Chini, S. Frolking, R. A. Betts, J. Feddema, G. Fischer, J. P. Fisk, K. Hibbard, R. A. Houghton, A. Janetos, C. D. Jones, G. Kindermann, T. Kinoshita, K. Klein Goldewijk, K. Riahi, E. Shevliakova, S. Smith, E. Stehfest, A. Thomson, P. Thornton, D. P. van Vuuren, and Y. P. Wang (2011). "Harmonization of land-use scenarios for the period 1500-2100: 600 years of global gridded annual land-use transitions, wood harvest, and resulting secondary lands". In: *Climatic Change* 109.1, pp. 117–161. DOI: 10.1007/s10584-011-0153-2 (cit. on pp. 43, 50, 54).

Hwang, C.-L. and A. S. M. Masud (1979). *Multiple objective decision making, methods and applications: a state-of-the-art survey*. Springer-Verlag. 384 pp. (cit. on p. 17).

Immerzeel, D. J., P. A. Verweij, F. van der Hilst, and A. P. C. Faaij (2014). "Biodiversity impacts of bioenergy crop production: a state-of-the-art review". In: *GCB Bioenergy* 6.3, pp. 183–209. DOI: 10.1111/gcbb.12067 (cit. on p. 11).

IPCC (2013). "Summary for Policymakers". In: *Climate Change 2013: The Physical Science Basis. Contribution of Working Group I to the Fifth Assessment Report of the Intergovernmental Panel on Climate Change*. Ed. by T. Stocker, D. Qin, G.-K. Plattner, M. Tignor, S. Allen, J. Boschung, A. Nauels, Y. Xia, V. Bex, and P. Midgley. Cambridge, United Kingdom and New York, NY, USA: Cambridge University Press, pp. 1–30 (cit. on pp. 8, 22).

Jägermeyr, J., D. Gerten, J. Heinke, S. Schaphoff, M. Kummu, and W. Lucht (2015). "Water savings potentials of irrigation systems: global simulation of processes and linkages". In: *Hydrol. Earth Syst. Sci.* 19.7, pp. 3073–3091. DOI: 10.5194/hess-19-3073-2015 (cit. on pp. 24, 25, 28, 29, 54, 86, 112).

Jarvis, A. J., D. T. Leedal, and C. N. Hewitt (2012). "Climate-society feedbacks and the avoidance of dangerous climate change". In: *Nature Climate Change* 2.9, pp. 668–671. DOI: 10.1038/nclimate1586 (cit. on pp. 15, 18, 61).

Jarvis, A., D. Leedal, C. J. Taylor, and P. Young (2009). "Stabilizing global mean surface temperature: A feedback control perspective". In: *Environmental Modelling & Software* 24.5, pp. 665–674. DOI: 10.1016/j.envsoft.2008.10.016 (cit. on p. 110).

Jiang, Y., X. Xu, Q. Huang, Z. Huo, and G. Huang (2016). "Optimizing regional irrigation water use by integrating a two-level optimization model and an agro-hydrological model". In: *Agricultural Water Management* 178, pp. 76–88. DOI: 10.1016/j.agwat.2016.08.035 (cit. on p. 18).

Johnson, P. C., C. L. Clementson, S. K. Mathanker, T. E. Grift, and A. C. Hansen (2012). "Cutting energy characteristics of Miscanthus x giganteus stems with varying oblique angle and cutting speed". In: *Biosystems Engineering* 112.1, pp. 42–48. DOI: 10.1016/j.biosystemseng.2012.02.003 (cit. on pp. 25, 124).

Jones, C., E. Robertson, V. Arora, P. Friedlingstein, E. Shevliakova, L. Bopp, V. Brovkin, T. Hajima, E. Kato, M. Kawamiya, S. Liddicoat, K. Lindsay, C. H. Reick, C. Roelandt, J. Segschneider, and J. Tjiputra (2013). "21th Century compatible CO2 emissions and airborne fraction simulated by CMIP5 Earth System models under 4 Representative Concentration Pathways". In: *Journal of Climate* 26, pp. 4398–4413. DOI: 10.1175/JCLI-D-12-00554.1 (cit. on p. 12).

Jones, P. D., D. H. Lister, T. J. Osborn, C. Harpham, M. Salmon, and C. P. Morice (2012). "Hemispheric and large-scale land-surface air temperature variations: An extensive revision and an update to 2010". In: *Journal of Geophysical Research: Atmospheres* 117 (D5), p. D05127. DOI: 10.1029/2011JD017139 (cit. on p. 68).

Joos, F., S. Gerber, I. C. Prentice, B. L. Otto-Bliesner, and P. J. Valdes (2004). "Transient simulations of Holocene atmospheric carbon dioxide and terrestrial carbon since the Last Glacial Maximum". In: *Global Biogeochemical Cycles* 18, Gb2002. DOI: 10.1029/2003gb002156 (cit. on p. 69).

Joos, F., R. Roth, J. S. Fuglestvedt, G. P. Peters, I. G. Enting, W. von Bloh, V. Brovkin, E. J. Burke, M. Eby, N. R. Edwards, T. Friedrich, T. L. Frölicher, P. R. Halloran, P. B. Holden, C. Jones, T. Kleinen, F. T. Mackenzie, K. Matsumoto, M. Meinshausen, G.-K. Plattner, A. Reisinger, J. Segschneider, G. Shaffer, M. Steinacher, K. Strassmann, K. Tanaka, A. Timmermann, and A. J. Weaver (2013). "Carbon dioxide and climate impulse response functions for the computation of greenhouse gas metrics: a multi-model analysis". In: *Atmospheric Chemistry and Physics* 13, pp. 2793–2825. DOI: 10.5194/acp-13-2793-2013 (cit. on p. 68).

Joos, F., I. C. Prentice, S. Sitch, R. Meyer, G. Hooss, G.-K. Plattner, S. Gerber, and K. Hasselmann (2001). "Global warming feedbacks on terrestrial carbon uptake under the Intergovernmental Panel on Climate Change (IPCC) Emission Scenarios". In: *Global Biogeochemical Cycles* 15.4, pp. 891–907. DOI: 10.1029/2000GB001375 (cit. on p. 69).

Jørgensen, U., J. Mortensen, J. B. Kjeldsen, and K.-u. Schwarz* (2003). "Establishment, Development and Yield Quality of Fifteen Miscanthus Genotypes over Three Years

in Denmark". In: *Acta Agriculturae Scandinavica, Section B — Soil & Plant Science* 53.4, pp. 190–199. DOI: 10.1080/09064710310017605 (cit. on p. 118).

Kahle, P., S. Beuch, B. Boelcke, P. Leinweber, and H.-R. Schulten (2001). "Cropping of Miscanthus in Central Europe: biomass production and influence on nutrients and soil organic matter". In: *European Journal of Agronomy* 15.3, pp. 171–184. DOI: 10.1016/S1161-0301(01)00102-2 (cit. on p. 118).

Kan, A. van, J. Jegminat, J. F. Donges, and J. Kurths (2016). "Constrained basin stability for studying transient phenomena in dynamical systems". In: *Physical Review E* 93.4, p. 042205. DOI: 10.1103/PhysRevE.93.042205 (cit. on pp. 62, 72).

Kaplan, J. O., I. C. Prentice, W. Knorr, and P. J. Valdes (2002). "Modeling the dynamics of terrestrial carbon storage since the Last Glacial Maximum". In: *Geophysical Research Letters* 29.22, pp. 31–1–31–4. DOI: 10.1029/2002gl015230 (cit. on p. 69).

Karp, A. and I. Shield (2008). "Bioenergy from plants and the sustainable yield challenge". In: *New Phytologist* 179.1, pp. 15–32. DOI: 10.1111/j.1469-8137.2008.02432.x (cit. on p. 34).

Kauter, D., I. Lewandowski, and W. Claupein (2001). "Pappeln in Kurzumtriebswirtschaft: Eigenschaften und Qualitätsmanagement bei der Festbrennstoffbereitstellung - Ein Überblick". In: *Pflanzenbauwissenschaften* 5.2, S. 64 –74 (cit. on pp. 34, 51).

Keenan, T. F., D. Y. Hollinger, G. Bohrer, D. Dragoni, J. W. Munger, H. P. Schmid, and A. D. Richardson (2013). "Increase in forest water-use efficiency as atmospheric carbon dioxide concentrations rise". In: *Nature* 499.7458, pp. 324–327. DOI: 10.1038/nature12291 (cit. on p. 66).

Keith, D. W. (2000). "GEOENGINEERING THE CLIMATE: History and Prospect1". In: *Annual Review of Energy and the Environment* 25.1, pp. 245–284. DOI: 10.1146/annurev.energy.25.1.245 (cit. on p. 8).

Keller, D., P. Lenton, V. Scott, and N. E. Vaughan (2016). *Carbon dioxide removal-model intercomparison project (CDR-MIP)* (cit. on p. 9).

Kellie-Smith, O. and P. M. Cox (2011). "Emergent dynamics of the climate-economy system in the Anthropocene." In: *Philosophical transactions. Series A, Mathematical, physical, and engineering sciences* 369.1938, pp. 868–86. DOI: 10.1098/rsta.2010.0305 (cit. on pp. 18, 61).

Keys, P. W., R. J. van der Ent, L. J. Gordon, H. Hoff, R. Nikoli, and H. H. G. Savenije (2012). "Analyzing precipitationsheds to understand the vulnerability of rainfall dependent regions". In: *Biogeosciences* 9.2, pp. 733–746. DOI: 10.5194/bg-9-733-2012 (cit. on p. 84).

Kier, G., H. Kreft, T. M. Lee, W. Jetz, P. L. Ibisch, C. Nowicki, J. Mutke, and W. Barthlott (2009). "A global assessment of endemism and species richness across island and mainland regions". In: *Proceedings of the National Academy of Sciences* 106.23, pp. 9322–9327. DOI: 10.1073/pnas.0810306106 (cit. on pp. 56, 88, 103).

Kirtman, B., S. Power, J. Adedoyin, G. Boer, R. Bojariu, I. Camilloni, F. Doblas-Reyes, A. Fiore, M. Kimoto, G. Meehl, M. Prather, A. Sarr, C. Schär, R. Sutton, G. van Oldenborgh, G. Vecchi, and H. Wang (2013). "Near-term Climate Change: Projections and Predictability". In: *Climate Change 2013: The Physical Science Basis. Contribution of Working Group I to the Fifth Assessment Report of the Intergovernmental Panel on Climate Change*. Ed. by T. Stocker, D. Qin, G.-K. Plattner, M. Tignor, S. Allen, J. Boschung, A. Nauels, Y. Xia, V. Bex, and P. Midgley. Cambridge, United Kingdom and New York, NY, USA: Cambridge University Press, pp. 953–1028 (cit. on p. 60).

Klein, D., F. Humpenöder, N. Bauer, J. P. Dietrich, A. Popp, B. L. Bodirsky, M. Bonsch, and H. Lotze-Campen (2014a). "The global economic long-term potential of modern biomass in a climate-constrained world". In: *Environmental Research Letters* 9.7, p. 074017. DOI: 10.1088/1748-9326/9/7/074017 (cit. on pp. 11, 23).

Klein, D., G. Luderer, E. Kriegler, J. Strefler, N. Bauer, M. Leimbach, A. Popp, J. P. Dietrich, F. Humpenöder, H. Lotze-Campen, and O. Edenhofer (2014b). "The value of bioenergy in low stabilization scenarios: an assessment using REMIND-MAgPIE". In: *Climatic Change* 123.3, pp. 705–718. DOI: 10.1007/s10584-013-0940-z (cit. on pp. 43, 49).

Knorr, W. (2009). "Is the airborne fraction of anthropogenic CO2 emissions increasing?" In: *Geophysical Research Letters* 36.21, p. L21710. DOI: 10.1029/2009GL040613 (cit. on p. 68).

Konis, K. (2016). *lpSolveAPI: R Interface to 'lp_solve' Version 5.5.2.0*. Version 5.5.2.0-17 (cit. on pp. 49, 87).

Koven, C. D., J. Q. Chambers, K. Georgiou, R. Knox, R. Negron-Juarez, W. J. Riley, V. K. Arora, V. Brovkin, P. Friedlingstein, and C. D. Jones (2015). "Controls on terrestrial carbon feedbacks by productivity vs. turnover in the CMIP5 Earth System Models". In: *Biogeosciences Discuss.* 12.8, pp. 5757–5801. DOI: 10.5194/bgd-12-5757-2015 (cit. on p. 29).

Krausmann, F., K.-H. Erb, S. Gingrich, H. Haberl, A. Bondeau, V. Gaube, C. Lauk, C. Plutzar, and T. D. Searchinger (2013). "Global human appropriation of net primary production doubled in the 20th century". In: *Proceedings of the National Academy of Sciences* 110.25, pp. 10324–10329. DOI: 10.1073/pnas.1211349110 (cit. on p. 22).

Kravitz, B., A. Robock, S. Tilmes, O. Boucher, J. M. English, P. J. Irvine, A. Jones, M. G. Lawrence, M. MacCracken, H. Muri, J. C. Moore, U. Niemeier, S. J. Phipps, J. Sillmann, T. Storelvmo, H. Wang, and S. Watanabe (2015). "The Geoengineering Model Intercomparison Project Phase 6 (GeoMIP6): simulation design and preliminary results". In: *Geosci. Model Dev.* 8.10, pp. 3379–3392. DOI: 10.5194/gmd-8-3379-2015 (cit. on p. 9).

Kravitz, B., A. Robock, O. Boucher, H. Schmidt, K. E. Taylor, G. Stenchikov, and M. Schulz (2011). "The Geoengineering Model Intercomparison Project (GeoMIP)". In: *Atmospheric Science Letters* 12.2, pp. 162–167. DOI: 10.1002/asl.316 (cit. on p. 9).

Kraxner, F., S. Fuss, V. Krey, D. Best, S. Leduc, G. Kindermann, Y. Yamagata, D. Schepaschenko, A. Shvidenko, K. Aoki, and J. Yan (2015). "The Role of Bioenergy with Carbon

Capture and Storage (BECCS) for Climate Policy". In: *Handbook of Clean Energy Systems*. John Wiley & Sons, Ltd (cit. on p. 12).

Krey, V., G. Luderer, L. Clarke, and E. Kriegler (2013). "Getting from here to there – energy technology transformation pathways in the EMF27 scenarios". In: *Climatic Change* 123.3, pp. 369–382. DOI: 10.1007/s10584-013-0947-5 (cit. on p. 9).

Kriegler, E., O. Edenhofer, L. Reuster, G. Luderer, and D. Klein (2013). "Is atmospheric carbon dioxide removal a game changer for climate change mitigation?" In: *Climatic Change* 118.1, pp. 45–57. DOI: 10.1007/s10584-012-0681-4 (cit. on p. 12).

Kriegler, E., J. W. Hall, H. Held, R. Dawson, and H. J. Schellnhuber (2009). "Imprecise probability assessment of tipping points in the climate system". In: *Proceedings of the National Academy of Sciences* 106.13, pp. 5041–5046. DOI: 10.1073/pnas.0809117106 (cit. on p. 60).

Labrecque, M. and T. I. Teodorescu (2005). "Field performance and biomass production of 12 willow and poplar clones in short-rotation coppice in southern Quebec (Canada)". In: *Biomass and Bioenergy* 29.1, pp. 1–9. DOI: 10.1016/j.biombioe.2004.12.004 (cit. on p. 120).

Laclau, J.-P., J.-P. Bouillet, and J. Ranger (2000). "Dynamics of biomass and nutrient accumulation in a clonal plantation of Eucalyptus in Congo". In: *Forest Ecology and Management* 128.3, pp. 181–196. DOI: 10.1016/S0378-1127(99)00146-2 (cit. on p. 121).

Langholtz, M., D. R. Carter, and D. L. Rockwood (2013). "Assessing the Economic Feasibility of Short-Rotation Woody Crops in Florida". In: *Forest Policy and Economics* 38 (cit. on pp. 25, 122).

Lassaletta, L., G. Billen, B. Grizzetti, J. Anglade, and J. Garnier (2014). "50 year trends in nitrogen use efficiency of world cropping systems: the relationship between yield and nitrogen input to cropland". In: *Environmental Research Letters* 9.10, p. 105011. DOI: 10.1088/1748-9326/9/10/105011 (cit. on p. 51).

Laureysens, I., J. Bogaert, R. Blust, and R. Ceulemans (2004). "Biomass production of 17 poplar clones in a short-rotation coppice culture on a waste disposal site and its relation to soil characteristics". In: *Forest Ecology and Management* 187.2, pp. 295–309. DOI: 10.1016/j.foreco.2003.07.005 (cit. on p. 120).

Lehmann, J., J. Gaunt, and M. Rondon (2006). "Bio-char Sequestration in Terrestrial Ecosystems – A Review". In: *Mitigation and Adaptation Strategies for Global Change* 11.2, pp. 395–419. DOI: 10.1007/s11027-005-9006-5 (cit. on p. 11).

Lemus, R., E. C. Brummer, K. J. Moore, N. E. Molstad, C. L. Burras, and M. F. Barker (2002). "Biomass yield and quality of 20 switchgrass populations in southern Iowa, USA". In: *Biomass and Bioenergy* 23.6, pp. 433–442. DOI: 10.1016/S0961-9534(02)00073-9 (cit. on p. 119).

Lemus, R. and R. Lal (2005). "Bioenergy Crops and Carbon Sequestration". In: *Critical Reviews in Plant Sciences* 24.1, pp. 1–21. DOI: 10.1080/07352680590910393 (cit. on pp. 25, 122).

Lemus, R. W. (2004). *Switchgrass as an Energy Crop: Fertilization, Cultivar, and Cutting Management*. URL: http://scholar.lib.vt.edu/theses/available/etd-01292004-115043/ (visited on 03/28/2014) (cit. on p. 119).

Lenton, T. M. and N. E. Vaughan (2009). "The radiative forcing potential of different climate geoengineering options". In: *Atmos. Chem. Phys.* 9.15, pp. 5539–5561. DOI: 10.5194/acp-9-5539-2009 (cit. on p. 12).

Lenton, T. M. (2000). "Land and ocean carbon cycle feedback effects on global warming in a simple Earth system model". In: *Tellus B* 52.5. DOI: 10.3402/tellusb.v52i5.17097 (cit. on p. 18).

Lenton, T. M. (2010). "The potential for land-based biological CO_2 removal to lower future atmospheric CO_2 concentration". In: *Carbon Management* 1.1, pp. 145–160. DOI: 10.4155/cmt.10.12 (cit. on pp. 12, 22, 23, 33).

Lenton, T. M., H. Held, E. Kriegler, J. W. Hall, W. Lucht, S. Rahmstorf, and H. J. Schellnhuber (2008). "Tipping elements in the Earth's climate system". In: *Proceedings of the National Academy of Sciences* 105.6, pp. 1786–1793. DOI: 10.1073/pnas.0705414105 (cit. on pp. 3, 60).

Lindegaard, K. N., R. I. Parfitt, G. Donaldson, T. Hunter, W. M. Dawson, E. G. A. Forbes, M. M. Carter, C. C. Whinney, J. E. Whinney, and S. Larsson (2001). "Comparative trials of elite Swedish and UK biomass willow varieties." In: *Aspects of Applied Biology* N (No.65), pp. 183–192 (cit. on p. 120).

Lindenmayer, D. B. and R. J. Hobbs (2004). "Fauna conservation in Australian plantation forests – a review". In: *Biological Conservation* 119.2, pp. 151–168. DOI: 10.1016/j.biocon.2003.10.028 (cit. on p. 35).

Linderson, M.-L., Z. Iritz, and A. Lindroth (2007). "The effect of water availability on stand-level productivity, transpiration, water use efficiency and radiation use efficiency of field-grown willow clones". In: *Biomass and Bioenergy* 31.7, pp. 460–468. DOI: 10.1016/j.biombioe.2007.01.014 (cit. on p. 120).

Londo, M., J. Dekker, and W. ter Keurs (2005). "Willow short-rotation coppice for energy and breeding birds: an exploration of potentials in relation to management". In: *Biomass and Bioenergy* 28.3, pp. 281–293. DOI: 10.1016/j.biombioe.2004.06.007 (cit. on p. 35).

Lotze-Campen, H., C. Müller, A. Bondeau, S. Rost, A. Popp, and W. Lucht (2008). "Global food demand, productivity growth, and the scarcity of land and water resources: a spatially explicit mathematical programming approach". In: *Agricultural Economics* 39.3, pp. 325–338. DOI: 10.1111/j.1574-0862.2008.00336.x (cit. on p. 18).

Lucht, W., I. C. Prentice, R. B. Myneni, S. Sitch, P. Friedlingstein, W. Cramer, P. Bousquet, W. Buermann, and B. Smith (2002). "Climatic control of the high-latitude vegetation greening trend and Pinatubo effect". In: *Science* 296, pp. 1687–1689 (cit. on p. 25).

Lucht, W., S. Schaphoff, T. Erbrecht, U. Heyder, and W. Cramer (2006). "Terrestrial vegetation redistribution and carbon balance under climate change". In: *Carbon Balance and Management* 1.1, p. 6. DOI: 10.1186/1750-0680-1-6 (cit. on p. 69).

Luderer, G., V. Bosetti, M. Jakob, M. Leimbach, J. C. Steckel, H. Waisman, and O. Edenhofer (2011). "The economics of decarbonizing the energy system—results and insights from the RECIPE model intercomparison". In: *Climatic Change* 114.1, pp. 9–37. DOI: 10.1007/s10584-011-0105-x (cit. on p. 18).

Lüthi, D., M. Le Floch, B. Bereiter, T. Blunier, J. M. Barnola, U. Siegenthaler, D. Raynaud, J. Jouzel, H. Fischer, K. Kawamura, and T. F. Stocker (2008). "High-resolution carbon dioxide concentration record 650,000-800,000 years before present". In: *Nature* 453.7193, pp. 379–382. DOI: 10.1038/nature06949 (cit. on p. 2).

MacMartin, D. G., B. Kravitz, D. W. Keith, and A. Jarvis (2013). "Dynamics of the coupled human–climate system resulting from closed-loop control of solar geoengineering". In: *Climate Dynamics* 43.1, pp. 243–258. DOI: 10.1007/s00382-013-1822-9 (cit. on pp. 15, 61, 110).

Masui, T., K. Matsumoto, Y. Hijioka, T. Kinoshita, T. Nozawa, S. Ishiwatari, E. Kato, P. R. Shukla, Y. Yamagata, and M. Kainuma (2011). "An emission pathway for stabilization at 6 Wm radiative forcing". In: *Climatic Change* 109.1, pp. 59–76. DOI: 10.1007/s10584-011-0150-5 (cit. on pp. 70, 78).

Matthews, H. D., N. P. Gillett, P. A. Stott, and K. Zickfeld (2009). "The proportionality of global warming to cumulative carbon emissions". In: *Nature* 459.7248, pp. 829–832. DOI: 10.1038/nature08047 (cit. on p. 34).

McElroy, G. H. and W. M. Dawson (1986). "Biomass from short-rotation coppice willow on marginal land". In: *Biomass* 10.3, pp. 225–240. DOI: 10.1016/0144-4565(86)90055-7 (cit. on p. 120).

McIntyre, B. D., H. R. Herren, J. Wakhungu, and R. T. Watson (2009). *International assessment of agricultural knowledge, science and technology for development (IAASTD): Global report*. Report (cit. on pp. 50, 55).

Menck, P. J., J. Heitzig, N. Marwan, and J. Kurths (2013). "How basin stability complements the linear-stability paradigm". In: *Nature Physics* 9.2, pp. 89–92. DOI: 10.1038/nphys2516 (cit. on p. 71).

Midilli, A., I. Dincer, and M. Ay (2006). "Green energy strategies for sustainable development". In: *Energy Policy* 34.18, pp. 3623–3633. DOI: 10.1016/j.enpol.2005.08.003 (cit. on p. 22).

Motesharrei, S., J. Rivas, and E. Kalnay (2014). "Human and nature dynamics (HANDY): Modeling inequality and use of resources in the collapse or sustainability of societies".

In: *Ecological Economics* 101, pp. 90–102. DOI: 10.1016/j.ecolecon.2014.02.014 (cit. on pp. 18, 61).

Mulkey, V. R., V. N. Owens, and D. K. Lee (2006). "Management of switchgrass-dominated conservation reserve program lands for biomass production in South Dakota." In: *Crop Science* (cit. on p. 119).

Naidu, S. L., S. P. Moose, A. K. AL-Shoaibi, C. A. Raines, and S. P. Long (2003). "Cold Tolerance of C4 photosynthesis in Miscanthus × giganteus: Adaptation in Amounts and Sequence of C4 Photosynthetic Enzymes". In: *Plant Physiology* 132.3, pp. 1688–1697. DOI: 10.1104/pp.103.021790 (cit. on p. 24).

NCDC (2012). *National Climatic Data Center*. URL: https://www.ncdc.noaa.gov/paleo/study/6091 (visited on 08/22/2016) (cit. on p. 2).

Newbold, T., L. N. Hudson, A. P. Arnell, S. Contu, A. D. Palma, S. Ferrier, S. L. L. Hill, A. J. Hoskins, I. Lysenko, H. R. P. Phillips, V. J. Burton, C. W. T. Chng, S. Emerson, D. Gao, G. Pask-Hale, J. Hutton, M. Jung, K. Sanchez-Ortiz, B. I. Simmons, S. Whitmee, H. Zhang, J. P. W. Scharlemann, and A. Purvis (2016). "Has land use pushed terrestrial biodiversity beyond the planetary boundary? A global assessment". In: *Science* 353.6296, pp. 288–291. DOI: 10.1126/science.aaf2201 (cit. on pp. 83, 84).

Nilsson, S. and W. Schopfhauser (1995). "The carbon-sequestration potential of a global afforestation program". In: *Climatic Change* 30.3, pp. 267–293. DOI: 10.1007/BF01091928 (cit. on p. 10).

Nishina, K., A. Ito, D. J. Beerling, P. Cadule, P. Ciais, D. B. Clark, P. Falloon, A. D. Friend, R. Kahana, E. Kato, R. Keribin, W. Lucht, M. Lomas, T. T. Rademacher, R. Pavlick, S. Schaphoff, N. Vuichard, L. Warszawaski, and T. Yokohata (2014). "Quantifying uncertainties in soil carbon responses to changes in global mean temperature and precipitation". In: *Earth Syst. Dynam.* 5.1, pp. 197–209. DOI: 10.5194/esd-5-197-2014 (cit. on p. 25).

NOAA (2015a). *NOAA-ESRL MLO Annual CO_2 Data, accessed at:* CO2.Earth. URL: https://www.co2.earth/annual-co2? (visited on 08/04/2016) (cit. on p. 96).

NOAA, N. C. f. E. I. (2015b). *State of the Climate: Global Analysis for Annual 2014* (cit. on pp. 68, 69).

Nykvist, B., Å. Persson, F. Moberg, L. Persson, S. Cornell, and J. Rockström (2013). *National Environmental Performance on Planetary Boundaries* (cit. on p. 7).

Obersteiner, M., C. Azar, P. Kauppi, K. Möllersten, J. Moreira, S. Nilsson, P. Read, K. Riahi, B. Schlamadinger, Y. Yamagata, J. Yan, and J.-P. v. Ypersele (2001). "Managing Climate Risk". In: *Science* 294.5543, pp. 786–787. DOI: 10.1126/science.294.5543.786b (cit. on pp. 1, 107).

Ostberg, S., W. Lucht, S. Schaphoff, and D. Gerten (2013). "Critical impacts of global warming on land ecosystems". In: *Earth Syst. Dynam.* 4.2, pp. 347–357. DOI: 10.5194/esd-4-347-2013 (cit. on p. 32).

Ostberg, S., S. Schaphoff, W. Lucht, and D. Gerten (2015). "Three centuries of dual pressure from land use and climate change on the biosphere". In: *Environmental Research Letters* 10.4, p. 044011. DOI: 10.1088/1748-9326/10/4/044011 (cit. on pp. 22, 97).

Palmer, I. E., R. J. Gehl, T. G. Ranney, D. Touchell, and N. George (2014). "Biomass yield, nitrogen response, and nutrient uptake of perennial bioenergy grasses in North Carolina". In: *Biomass and Bioenergy* 63, pp. 218–228. DOI: 10.1016/j.biombioe.2014.02.016 (cit. on pp. 118, 119).

Pastor, A. V., F. Ludwig, H. Biemans, H. Hoff, and P. Kabat (2014). "Accounting for environmental flow requirements in global water assessments". In: *Hydrol. Earth Syst. Sci.* 18.12, pp. 5041–5059. DOI: 10.5194/hess-18-5041-2014 (cit. on p. 57).

Pereira, H. M., P. W. Leadley, V. Proença, R. Alkemade, J. P. W. Scharlemann, J. F. Fernandez-Manjarrés, M. B. Araújo, P. Balvanera, R. Biggs, W. W. L. Cheung, L. Chini, H. D. Cooper, E. L. Gilman, S. Guénette, G. C. Hurtt, H. P. Huntington, G. M. Mace, T. Oberdorff, C. Revenga, P. Rodrigues, R. J. Scholes, U. R. Sumaila, and M. Walpole (2010). "Scenarios for Global Biodiversity in the 21st Century". In: *Science* 330.6010, pp. 1496–1501. DOI: 10.1126/science.1196624 (cit. on p. 84).

Pielke, R. A., G. Marland, R. A. Betts, T. N. Chase, J. L. Eastman, J. O. Niles, D. d. S. Niyogi, and S. W. Running (2002). "The influence of land-use change and landscape dynamics on the climate system: relevance to climate-change policy beyond the radiative effect of greenhouse gases". In: *Philosophical Transactions of the Royal Society of London A: Mathematical, Physical and Engineering Sciences* 360.1797, pp. 1705–1719. DOI: 10.1098/rsta.2002.1027 (cit. on p. 84).

Pimm, S. L., C. N. Jenkins, R. Abell, T. M. Brooks, J. L. Gittleman, L. N. Joppa, P. H. Raven, C. M. Roberts, and J. O. Sexton (2014). "The biodiversity of species and their rates of extinction, distribution, and protection". In: *Science* 344.6187, p. 1246752. DOI: 10.1126/science.1246752 (cit. on p. 3).

Pongratz, J., C. H. Reick, T. Raddatz, and M. Claussen (2009). "Effects of anthropogenic land cover change on the carbon cycle of the last millennium". In: *Global Biogeochemical Cycles* 23.4, n/a–n/a. DOI: 10.1029/2009GB003488 (cit. on pp. 30, 32).

Pongratz, J., C. H. Reick, T. Raddatz, and M. Claussen (2010). "Biogeophysical versus biogeochemical climate response to historical anthropogenic land cover change". In: *Geophysical Research Letters* 37.8, n/a–n/a. DOI: 10.1029/2010GL043010 (cit. on p. 10).

Portmann, F. T., S. Siebert, and P. Döll (2010). "MIRCA2000—Global monthly irrigated and rainfed crop areas around the year 2000: A new high-resolution data set for agricultural and hydrological modeling". In: *Global Biogeochemical Cycles* 24.1, GB1011. DOI: 10.1029/2008GB003435 (cit. on pp. 28, 88, 90).

Potapov, P., A. Yaroshenko, S. Turubanova, M. Dubinin, L. Laestadius, C. Thies, D. Aksenov, A. Egorov, Y. Yesipova, I. Glushkov, M. Karpachevskiy, A. Kostikova, A. Manisha, E.

Tsybikova, and I. Zhuravleva (2008). "Mapping the world's intact forest landscapes by remote sensing". In: *Ecology and Society* 13.51 (cit. on p. 89).

Prentice, I. C. (1989). *Developing a Global Vegetation Dynamics Model: Results of an IIASA Summer Workshop*. URL: http://pure.iiasa.ac.at/3223/ (visited on 08/10/2016) (cit. on p. 16).

Prestele, R., P. Alexander, M. D. A. Rounsevell, A. Arneth, K. Calvin, J. Doelman, D. A. Eitelberg, K. Engström, S. Fujimori, T. Hasegawa, P. Havlik, F. Humpenöder, A. K. Jain, T. Krisztin, P. Kyle, P. Meiyappan, A. Popp, R. D. Sands, R. Schaldach, J. Schüngel, E. Stehfest, A. Tabeau, H. Van Meijl, J. Van Vliet, and P. H. Verburg (2016). "Hotspots of uncertainty in land-use and land-cover change projections: a global-scale model comparison". In: *Global Change Biology*, n/a–n/a. DOI: 10.1111/gcb.13337 (cit. on p. 84).

Pugesgaard, S., K. Schelde, S. U. Larsen, P. E. Laerke, and U. Jørgensen (2014). "Comparing annual and perennial crops for bioenergy production - influence on nitrate leaching and energy balance". In: *GCB Bioenergy*, n/a–n/a. DOI: 10.1111/gcbb.12215 (cit. on p. 120).

Qin, X., T. Mohan, M. El-Halwagi, G. Cornforth, and B. A. McCarl (2006). "Switchgrass as an alternate feedstock for power generation: an integrated environmental, energy and economic life-cycle assessment". In: *Clean Technologies and Environmental Policy* 8.4, pp. 233–249. DOI: 10.1007/s10098-006-0065-4 (cit. on p. 43).

Rae, A. M., K. M. Robinson, N. R. Street, and G. Taylor (2004). "Morphological and physiological traits influencing biomass productivity in short-rotation coppice poplar". In: *Canadian Journal of Forest Research* 34.7, pp. 1488–1498. DOI: 10.1139/x04-033 (cit. on p. 120).

Ramankutty, N., A. T. Evan, C. Monfreda, and J. A. Foley (2008). "Farming the planet: 1. Geographic distribution of global agricultural lands in the year 2000". In: *Global Biogeochemical Cycles* 22.1, GB1003. DOI: 10.1029/2007GB002952 (cit. on p. 87).

Read, P. and J. Lermit (2005). "Bio-energy with carbon storage (BECS): A sequential decision approach to the threat of abrupt climate change". In: *Energy* 30.14, pp. 2654–2671 (cit. on p. 11).

Riahi, K., S. Rao, V. Krey, C. Cho, V. Chirkov, G. Fischer, G. Kindermann, N. Nakicenovic, and P. Rafaj (2011). "RCP 8.5—A scenario of comparatively high greenhouse gas emissions". In: *Climatic Change* 109.1, pp. 33–57. DOI: 10.1007/s10584-011-0149-y (cit. on pp. 11, 70, 73).

Rockström, J., M. Falkenmark, C. Folke, M. Lannerstad, J. Barron, E. Enfors, L. Gordon, J. Heinke, H. Hoff, and C. Pahl-Wostl (2014). "Food production: a mega water challenge (Ch. 5)". In: *Water Resilience for Human Prosperity*. Google-Books-ID: _q_6AgAAQBAJ. Cambridge University Press (cit. on p. 90).

Rockström, J., M. Lannerstad, and M. Falkenmark (2007). "Assessing the water challenge of a new green revolution in developing countries". In: *Proceedings of the National Academy of Sciences* 104.15, pp. 6253–6260. DOI: 10.1073/pnas.0605739104 (cit. on p. 90).

Rockström, J., W. Steffen, K. Noone, Å. Persson, F. S. Chapin, E. F. Lambin, T. M. Lenton, M. Scheffer, C. Folke, H. J. Schellnhuber, B. Nykvist, C. A. de Wit, T. Hughes, S. van der Leeuw, H. Rodhe, S. Sörlin, P. K. Snyder, R. Costanza, U. Svedin, M. Falkenmark, L. Karlberg, R. W. Corell, V. J. Fabry, J. Hansen, B. Walker, D. Liverman, K. Richardson, P. Crutzen, and J. A. Foley (2009). "A safe operating space for humanity". In: *Nature* 461.7263, pp. 472–475. DOI: 10.1038/461472a (cit. on pp. 3–5, 13, 33, 41, 42, 60, 61, 83).

Rogelj, J., M. Schaeffer, P. Friedlingstein, N. P. Gillett, D. P. van Vuuren, K. Riahi, M. Allen, and R. Knutti (2016). "Differences between carbon budget estimates unravelled". In: *Nature Climate Change* 6.3, pp. 245–252. DOI: 10.1038/nclimate2868 (cit. on p. 96).

Rogelj, J., M. Schaeffer, M. Meinshausen, R. Knutti, J. Alcamo, K. Riahi, and W. Hare (2015). "Zero emission targets as long-term global goals for climate protection". In: *Environmental Research Letters* 10.10, p. 105007. DOI: 10.1088/1748-9326/10/10/105007 (cit. on p. 41).

Roncucci, N., N. Nassi O Di Nasso, C. Tozzini, E. Bonari, and G. Ragaglini (2015). "Miscanthus x giganteus nutrient concentrations and uptakes in autumn and winter harvests as influenced by soil texture, irrigation and nitrogen fertilization in the Mediterranean". In: *GCB Bioenergy* 7.5, pp. 1009–1018. DOI: 10.1111/gcbb.12209 (cit. on pp. 46, 51).

Rost, S., D. Gerten, and U. Heyder (2008a). "Human alterations of the terrestrial water cycle through land management". In: *Adv. Geosci.* 18, pp. 43–50. DOI: 10.5194/adgeo-18-43-2008 (cit. on pp. 2, 30, 32).

Rost, S., D. Gerten, A. Bondeau, W. Lucht, J. Rohwer, and S. Schaphoff (2008b). "Agricultural green and blue water consumption and its influence on the global water system". In: *Water Resources Research* 44.9, W09405. DOI: 10.1029/2007WR006331 (cit. on pp. 24, 25, 49, 85, 112).

Rowe, R. L. and N. R. Street (2007). "Identifying potential environmental impacts of large-scale deployment of dedicated bioenergy crops in the UK". In: *Renewable and Sustainable Energy Reviews* 13.1, pp. 271–290. DOI: 10.1016/j.rser.2007.07.008 (cit. on p. 22).

Sage, R., M. Cunningham, A. J. Haughton, M. D. Mallott, D. A. Bohan, A. Riche, and A. Karp (2010). "The environmental impacts of biomass crops: use by birds of miscanthus in summer and winter in southwestern England". In: *Ibis* 152.3, pp. 487–499. DOI: 10.1111/j.1474-919X.2010.01027.x (cit. on p. 35).

Sanderson, B. M., B. C. O'Neill, and C. Tebaldi (2016). "What would it take to achieve the Paris temperature targets?" In: *Geophysical Research Letters*. DOI: 10.1002/2016GL069563 (cit. on p. 41).

Sanderson, M. A., R. L. Reed, W. R. Ocumpaugh, M. A. Hussey, G. Van Esbroeck, J. C. Read, C. R. Tischler, and F. M. Hons (1999). "Switchgrass cultivars and germplasm for

biomass feedstock production in Texas". In: *Bioresource Technology* 67.3, pp. 209–219. DOI: 10.1016/S0960-8524(98)00132-1 (cit. on p. 119).

Sanderson, M. A. (2008). "Upland Switchgrass Yield, Nutritive Value, and Soil Carbon Changes Under Grazing and Clipping". In: *Agronomy Journal* 100.3, p. 510. DOI: 10.2134/agronj2007.0183 (cit. on p. 119).

Sathre, R. and J. O'Connor (2010). "Meta-analysis of greenhouse gas displacement factors of wood product substitution". In: *Environmental Science & Policy* 13.2, pp. 104–114. DOI: 10.1016/j.envsci.2009.12.005 (cit. on p. 11).

Sayer, J. (2009). "Reconciling Conservation and Development: Are Landscapes the Answer?" In: *Biotropica* 41.6, pp. 649–652. DOI: 10.1111/j.1744-7429.2009.00575.x (cit. on p. 84).

Schaphoff, S., U. Heyder, S. Ostberg, D. Gerten, J. Heinke, and W. Lucht (2013). "Contribution of permafrost soils to the global carbon budget". In: *Environmental Research Letters* 8.1, p. 014026. DOI: 10.1088/1748-9326/8/1/014026 (cit. on pp. 23, 25, 112).

Scheffer, M., S. Carpenter, J. A. Foley, C. Folke, and B. Walker (2001). "Catastrophic shifts in ecosystems". In: *Nature* 413.6856, pp. 591–596. DOI: 10.1038/35098000 (cit. on p. 71).

Schellnhuber, H. J. (1999). "'Earth system' analysis and the second Copernican revolution". In: *Nature* 402, pp. C19–C23. DOI: 10.1038/35011515 (cit. on p. 15).

Schellnhuber, H. J. (2009). "Tipping elements in the Earth System". In: *Proceedings of the National Academy of Sciences* 106.49, pp. 20561–20563. DOI: 10.1073/pnas.0911106106 (cit. on pp. 3, 60).

Schellnhuber, H. J., S. Rahmstorf, and R. Winkelmann (2016). "Why the right climate target was agreed in Paris". In: *Nature Climate Change* 6.7, pp. 649–653. DOI: 10.1038/nclimate3013 (cit. on pp. 1, 3, 7).

Schleussner, C.-F., J. Rogelj, M. Schaeffer, T. Lissner, R. Licker, E. M. Fischer, R. Knutti, A. Levermann, K. Frieler, and W. Hare (2016). "Science and policy characteristics of the Paris Agreement temperature goal". In: *Nature Climate Change* 6.9, pp. 827–835. DOI: 10.1038/nclimate3096 (cit. on p. 42).

Schmer, M. R., R. B. Mitchell, K. P. Vogel, W. H. Schacht, and D. B. Marx (2010). "Spatial and Temporal Effects on Switchgrass Stands and Yield in the Great Plains". In: *BioEnergy Research* 3.2, pp. 159–171. DOI: 10.1007/s12155-009-9045-y (cit. on p. 119).

Scholes, R. J. and R. Biggs (2005). "A biodiversity intactness index". In: *Nature* 434.7029, pp. 45–49. DOI: 10.1038/nature03289 (cit. on pp. 5, 51, 56, 96).

Scholz, V. and R. Ellerbrock (2002). "The growth productivity, and environmental impact of the cultivation of energy crops on sandy soil in Germany". In: *Biomass and Bioenergy* 23.2, pp. 81–92. DOI: 10.1016/S0961-9534(02)00036-3 (cit. on p. 120).

Schuiling, R. D. and P. Krijgsman (2006). "Enhanced weathering: An effective and cheap tool to sequester CO2". In: *Climatic Change* 74.1, pp. 349–354. DOI: 10.1007/s10584-005-3485-y (cit. on p. 10).

Schulz, U., O. Brauner, and H. Gruß (2009). "Animal diversity on short-rotation coppices – a review". In: *http://literatur.vti.bund.de/digbib_extern/bitv/dko42571.pdf* 59.3, pp. 171–182 (cit. on pp. 22, 35).

Schwarz, H. (1993). "Miscanthus sinensis 'giganteus' production on several sites in Austria". In: *Biomass and Bioenergy* 5.6, pp. 413–419. DOI: 10.1016/0961-9534(93)90036-4 (cit. on p. 118).

Scott, V., S. Gilfillan, N. Markusson, H. Chalmers, and R. S. Haszeldine (2013). "Last chance for carbon capture and storage". In: *Nature Climate Change* 3.2, pp. 105–111. DOI: 10.1038/nclimate1695 (cit. on p. 12).

Searle, S. Y. and C. J. Malins (2014). "Will energy crop yields meet expectations?" In: *Biomass and Bioenergy*. 21st European Biomass Conference 65, pp. 3–12. DOI: 10.1016/j.biombioe.2014.01.001 (cit. on p. 26).

Seppelt, R. and A. Voinov (2002). "Optimization methodology for land use patterns using spatially explicit landscape models". In: *Ecological Modelling* 151.2, pp. 125–142. DOI: 10.1016/S0304-3800(01)00455-0 (cit. on p. 18).

Sharma, N., I. Piscioneri, and V. Pignatelli (2003). "An evaluation of biomass yield stability of switchgrass (Panicum virgatum L.) cultivars". In: *Energy Conversion and Management* 44.18, pp. 2953–2958. DOI: 10.1016/S0196-8904(03)00049-9 (cit. on p. 119).

Shepherd, J., K. Caldeira, P. Cox, J. Haigh, D. Keith, B. Launder, G. Mace, G. McKerron, J. Pyle, S. Rayner, C. Redgewell, and A. Watson (2009). *Geoengineering the climate: science, governance and uncertainty*. Report (cit. on pp. 1, 8, 10, 14, 22, 23, 60).

Sierksma, G. (2001). *Linear and Integer Programming: Theory and Practice, Second Edition*. 2 edition. New York: CRC Press. 656 pp. (cit. on p. 18).

Sillmann, J., T. M. Lenton, A. Levermann, K. Ott, M. Hulme, F. Benduhn, and J. B. Horton (2015). "Climate emergencies do not justify engineering the climate". In: *Nature Climate Change* 5.4, pp. 290–292. DOI: 10.1038/nclimate2539 (cit. on p. 23).

Singh, B. (1998). "Biomass production and nutrient dynamics in three clones of Populus deltoides planted on Indogangetic plains". In: *Plant and Soil* 203.1, pp. 15–26. DOI: 10.1023/A:1004388903402 (cit. on p. 120).

Sitch, S., B. Smith, I. C. Prentice, A. Arneth, A. Bondeau, W. Cramer, J. O. Kaplan, S. Levis, W. Lucht, M. T. Sykes, K. Thonicke, and S. Venevsky (2003). "Evaluation of ecosystem dynamics, plant geography and terrestrial carbon cycling in the LPJ dynamic global vegetation model". In: *Global Change Biology* 9.2, pp. 161–185. DOI: 10.1046/j.1365-2486.2003.00569.x (cit. on pp. 16, 17, 24, 25, 49, 85, 86, 112).

Sladden, S. E., D. I. Bransby, and G. E. Aiken (1991). "Biomass yield, composition and production costs for eight switchgrass varieties in Alabama". In: *Biomass and Bioenergy* 1.2, pp. 119–122. DOI: 10.1016/0961-9534(91)90034-A (cit. on p. 119).

Slade, R., A. Bauen, and R. Gross (2014). "Global bioenergy resources". In: *Nature Climate Change* 4.2, pp. 99–105. DOI: 10.1038/nclimate2097 (cit. on p. 23).

Smakhtin, V., C. Revenga, and P. Döll (2004). "Taking Into Account Environmental Water Requirements in Global-scale Water Resources Assessments". In: *Comprehensive Assessment Research Report 2,Colombo, Sri Lanka: Comprehensive Assessment Secretariat*. Google-Books-ID: 8yPeEgrCWDcC (cit. on p. 89).

Smeets, E. M. W., A. P. C. Faaij, I. M. Lewandowski, and W. C. Turkenburg (2007). "A bottom-up assessment and review of global bio-energy potentials to 2050". In: *Progress in Energy and Combustion Science* 33.1, pp. 56–106. DOI: 10.1016/j.pecs.2006.08.001 (cit. on pp. 11, 74).

Smith, P., S. J. Davis, F. Creutzig, S. Fuss, J. Minx, B. Gabrielle, E. Kato, R. B. Jackson, A. Cowie, E. Kriegler, D. P. van Vuuren, J. Rogelj, P. Ciais, J. Milne, J. G. Canadell, D. McCollum, G. Peters, R. Andrew, V. Krey, G. Shrestha, P. Friedlingstein, T. Gasser, A. Grübler, W. K. Heidug, M. Jonas, C. D. Jones, F. Kraxner, E. Littleton, J. Lowe, J. R. Moreira, N. Nakicenovic, M. Obersteiner, A. Patwardhan, M. Rogner, E. Rubin, A. Sharifi, A. Torvanger, Y. Yamagata, J. Edmonds, and C. Yongsung (2015). "Biophysical and economic limits to negative CO2 emissions". In: *Nature Climate Change* advance online publication. DOI: 10.1038/nclimate2870 (cit. on p. 12).

Snyder, P. K., C. Delire, and J. A. Foley (2004). "Evaluating the influence of different vegetation biomes on the global climate". In: *Climate Dynamics* 23.3, pp. 279–302. DOI: 10.1007/s00382-004-0430-0 (cit. on p. 74).

Sonntag, S., J. Pongratz, C. H. Reick, and H. Schmidt (2016). "Reforestation in a high-CO2 world—Higher mitigation potential than expected, lower adaptation potential than hoped for". In: *Geophysical Research Letters* 43.12, 2016GL068824. DOI: 10.1002/2016GL068824 (cit. on pp. 10, 12).

Stape, J. L., D. Binkley, M. G. Ryan, S. Fonseca, R. A. Loos, E. N. Takahashi, C. R. Silva, S. R. Silva, R. E. Hakamada, J. M. d. A. Ferreira, A. M. N. Lima, J. L. Gava, F. P. Leite, H. B. Andrade, J. M. Alves, G. G. C. Silva, and M. R. Azevedo (2010). "The Brazil Eucalyptus Potential Productivity Project: Influence of water, nutrients and stand uniformity on wood production". In: *Forest Ecology and Management*. Productivity in Tropical Plantations 259.9, pp. 1684–1694. DOI: 10.1016/j.foreco.2010.01.012 (cit. on p. 121).

Steffen, W. L., B. H. Walker, J. S. Ingram, and G. W. Koch (1992). "Global Change and Terrestrial Ecosystems. The operational plan". In: International Geosphere-Biosphere Programme, Stockholm; Report, 21 (cit. on p. 16).

Steffen, W., K. Richardson, J. Rockström, S. E. Cornell, I. Fetzer, E. M. Bennett, R. Biggs, S. R. Carpenter, W. d. Vries, C. A. d. Wit, C. Folke, D. Gerten, J. Heinke, G. M. Mace, L. M. Persson, V. Ramanathan, B. Reyers, and S. Sörlin (2015). "Planetary boundaries: Guiding human development on a changing planet". In: *Science* 347.6223, p. 1259855. DOI: 10.1126/science.1259855 (cit. on pp. 4–7, 13, 22, 33, 35, 41–44, 47, 51, 56, 60, 61, 67, 70, 73, 83, 84, 96, 98, 114).

Steffen, W., R. A. Sanderson, P. D. Tyson, J. Jäger, P. A. Matson, B. M. III, F. Oldfield, K. Richardson, H. J. Schellnhuber, B. L. Turner, and R. J. Wasson (2006). *Global Change and the Earth System: A Planet Under Pressure*. Springer Science & Business Media. 346 pp. (cit. on p. 3).

Stern, N. (2007). *The Economics of Climate Change: the Stern review*. Cambridge University Press. URL: http://www.cambridge.org/de/academic/subjects/earth-and-environmental-science/climatology-and-climate-change/economics-climate-change-stern-review (visited on 08/22/2016) (cit. on p. 3).

Stričević, R., Z. Dželetović, N. Djurović, and M. Cosić (2014). "Application of the AquaCrop model to simulate the biomass of Miscanthus x giganteus under different nutrient supply conditions". In: *GCB Bioenergy*, n/a–n/a. DOI: 10.1111/gcbb.12206 (cit. on p. 118).

Sutton, R. T., B. Dong, and J. M. Gregory (2007). "Land/sea warming ratio in response to climate change: IPCC AR4 model results and comparison with observations". In: *Geophysical Research Letters* 34.2, p. L02701. DOI: 10.1029/2006GL028164 (cit. on p. 68).

Swann, A. L. S., I. Y. Fung, and J. C. H. Chiang (2012). "Mid-latitude afforestation shifts general circulation and tropical precipitation". In: *Proceedings of the National Academy of Sciences of the United States of America* 109.3, pp. 712–716. DOI: 10.1073/pnas.1116706108 (cit. on pp. 13, 35).

Tahvanainen, L. and V.-M. Rytkönen (1999). "Biomass production of Salix viminalis in southern Finland and the effect of soil properties and climate conditions on its production and survival". In: *Biomass and Bioenergy* 16.2, pp. 103–117. DOI: 10.1016/S0961-9534(98)00074-9 (cit. on p. 120).

Tans, P. and R. Keeling (2015). *Mauna Loa CO_2 annual mean data*. URL: ftp://aftp.cmdl.noaa.gov/products/trends/co2/co2_annmean_mlo.txt (cit. on pp. 2, 5, 65, 68).

Thomson, A. M., K. V. Calvin, S. J. Smith, G. P. Kyle, A. Volke, P. Patel, S. Delgado-Arias, B. Bond-Lamberty, M. A. Wise, L. E. Clarke, and J. A. Edmonds (2011). "RCP4.5: a pathway for stabilization of radiative forcing by 2100". In: *Climatic Change* 109.1, pp. 77–94. DOI: 10.1007/s10584-011-0151-4 (cit. on pp. 12, 23, 70, 78).

Tilman, D., C. Balzer, J. Hill, and B. L. Befort (2011). "Global food demand and the sustainable intensification of agriculture". In: *Proceedings of the National Academy of Sciences* 108.50, pp. 20260–20264. DOI: 10.1073/pnas.1116437108 (cit. on pp. 7, 15).

Tölle, M. H., O. Gutjahr, G. Busch, and J. C. Thiele (2014). "Increasing bioenergy production on arable land: Does the regional and local climate respond? Germany as a case study". In: *Journal of Geophysical Research: Atmospheres* 119.6, pp. 2711–2724. DOI: 10.1002/2013JD020877 (cit. on pp. 12, 35).

UNFCCC (2015). *Adoption of the Paris Agreement, FCCC/CP/2015/L.9/Rev1, (United Nations Framework Convention on Climate Change)* (cit. on pp. 9, 12, 41, 60).

UNFCCC (2016). *INDCs as communicated by Parties* (cit. on p. 100).

University, C. f. I. E. S. I. N.-C.-. C. (2005). "Gridded Population of the World, Version 3 (GPWv3): Population Count Grid, Future Estimates". In: in collab. with U. N. Food, A. P.-. FAO, and C. I. d. A. T.-. CIAT (cit. on p. 90).

Vaughan, N. E. and T. M. Lenton (2011). "A review of climate geoengineering proposals". In: *Climatic Change* 109.3, pp. 745–790. DOI: 10.1007/s10584-011-0027-7 (cit. on pp. 8, 10, 11, 23, 41, 61).

Vitousek, P. M., H. A. Mooney, J. Lubchenco, and J. M. Melillo (1997). "Human Domination of Earth's Ecosystems". In: *Science* 277.5325, pp. 494–499. DOI: 10.1126/science.277.5325.494 (cit. on p. 1).

Vries, W. de, J. Kros, C. Kroeze, and S. P. Seitzinger (2013). "Assessing planetary and regional nitrogen boundaries related to food security and adverse environmental impacts". In: *Current Opinion in Environmental Sustainability*. Open issue 5.3, pp. 392–402. DOI: 10.1016/j.cosust.2013.07.004 (cit. on pp. 3, 51, 55, 56, 83).

Vuuren, D. P. van, P. L. Lucas, T. Häyhä, S. E. Cornell, and M. Stafford-Smith (2016). "Horses for courses: analytical tools to explore planetary boundaries". In: *Earth Syst. Dynam.* 7.1, pp. 267–279. DOI: 10.5194/esd-7-267-2016 (cit. on pp. 15, 18, 61).

Vuuren, D. P. van, L. B. Bayer, C. Chuwah, L. Ganzeveld, W. Hazeleger, B. v. d. Hurk, T. v. Noije, B. O'Neill, and B. J. Strengers (2012). "A comprehensive view on climate change: coupling of earth system and integrated assessment models". In: *Environmental Research Letters* 7.2, p. 024012. DOI: 10.1088/1748-9326/7/2/024012 (cit. on pp. 15, 18, 61).

Vuuren, D. P. van, E. Stehfest, M. G. J. d. Elzen, T. Kram, J. v. Vliet, S. Deetman, M. Isaac, K. K. Goldewijk, A. Hof, A. M. Beltran, R. Oostenrijk, and B. v. Ruijven (2011). "RCP2.6: exploring the possibility to keep global mean temperature increase below 2°C". In: *Climatic Change* 109.1, pp. 95–116. DOI: 10.1007/s10584-011-0152-3 (cit. on pp. 12, 23, 41, 43, 49, 60, 70, 76).

Wagner, W., K. Scipal, C. Pathe, D. Gerten, W. Lucht, and B. Rudolf (2003). "Evaluation of the agreement between the first global remotely sensed soil moisture data with model and precipitation data". In: *Journal of Geophysical Research: Atmospheres* 108 (D19), p. 4611. DOI: 10.1029/2003JD003663 (cit. on pp. 25, 112).

Waha, K., L. G. J. van Bussel, C. Müller, and A. Bondeau (2012). "Climate-driven simulation of global crop sowing dates". In: *Global Ecology and Biogeography* 21.2, pp. 247–259. DOI: 10.1111/j.1466-8238.2011.00678.x (cit. on p. 86).

Watson, J., F. Kern, and N. Markusson (2014). "Resolving or managing uncertainties for carbon capture and storage: Lessons from historical analogues". In: *Technological Forecasting and Social Change* 81, pp. 192–204. DOI: 10.1016/j.techfore.2013.04.016 (cit. on pp. 49, 113).

Werf, H. M. G. van der, W. J. M. Meijer, E. W. J. M. Mathijssen, and A. Darwinkel (1992). "Potential dry matter production of Miscanthus sinensis in The Netherlands". In: *Industrial Crops and Products*. Proceedings of the European Symposium on Industrial

Crops and Products 1.2, pp. 203–210. DOI: 10.1016/0926-6690(92)90020-V (cit. on p. 118).

Werling, B. P., T. L. Dickson, R. Isaacs, H. Gaines, C. Gratton, K. L. Gross, H. Liere, C. M. Malmstrom, T. D. Meehan, L. Ruan, B. A. Robertson, G. P. Robertson, T. M. Schmidt, A. C. Schrotenboer, T. K. Teal, J. K. Wilson, and D. A. Landis (2014). "Perennial grasslands enhance biodiversity and multiple ecosystem services in bioenergy landscapes". In: *Proceedings of the National Academy of Sciences* 111.4, pp. 1652–1657. DOI: 10.1073/pnas.1309492111 (cit. on p. 35).

Williams, M., J. Zalasiewicz, P. K. Haff, C. Schwägerl, A. D. Barnosky, and E. C. Ellis (2015). "The Anthropocene biosphere". In: *The Anthropocene Review*, p. 2053019615591020. DOI: 10.1177/2053019615591020 (cit. on p. 3).

Wirsenius, S., C. Azar, and G. Berndes (2010). "How much land is needed for global food production under scenarios of dietary changes and livestock productivity increases in 2030?" In: *Agricultural Systems* 103.9, pp. 621–638. DOI: 10.1016/j.agsy.2010.07.005 (cit. on pp. 91, 103, 104).

Wüstenhagen, R. and M. Bilharz (2006). "Green energy market development in Germany: effective public policy and emerging customer demand". In: *Energy Policy* 34.13, pp. 1681–1696. DOI: 10.1016/j.enpol.2004.07.013 (cit. on p. 22).

Xie, J., J. Guo, Z. Yang, Z. Huang, G. Chen, and Y. Yang (2013). "Rapid accumulation of carbon on severely eroded red soils through afforestation in subtropical China". In: *Forest Ecology and Management*. Shaping Forest Management to Climate Change 300, pp. 53–59. DOI: 10.1016/j.foreco.2012.06.038 (cit. on p. 10).

Yamagata, Y. and D. Murakami (2015). *Global dataset of gridded population and GDP scenarios*. URL: http://www.cger.nies.go.jp/gcp/population-and-gdp.html (visited on 04/21/2016) (cit. on pp. 84, 90, 92, 99).

Yu, L., G. Ding, Z. Huai, and H. Zhao (2013). "Natural variation of biomass yield and nutrient dynamics in Miscanthus". In: *Field Crops Research* 151, pp. 1–8. DOI: 10.1016/j.fcr.2013.07.001 (cit. on pp. 34, 118).

Yuan, W., Y. Luo, X. Li, S. Liu, G. Yu, T. Zhou, M. Bahn, A. Black, A. R. Desai, A. Cescatti, B. Marcolla, C. Jacobs, J. Chen, M. Aurela, C. Bernhofer, B. Gielen, G. Bohrer, D. R. Cook, D. Dragoni, A. L. Dunn, D. Gianelle, T. Grünwald, A. Ibrom, M. Y. Leclerc, A. Lindroth, H. Liu, L. B. Marchesini, L. Montagnani, G. Pita, M. Rodeghiero, A. Rodrigues, G. Starr, and P. C. Stoy (2011). "Redefinition and global estimation of basal ecosystem respiration rate". In: *Global Biogeochemical Cycles* 25.4, GB4002. DOI: 10.1029/2011GB004150 (cit. on p. 68).

Zaehle, S., S. Sitch, B. Smith, and F. Hatterman (2005). "Effects of parameter uncertainties on the modeling of terrestrial biosphere dynamics". In: *Global Biogeochemical Cycles* 19.3, GB3020. DOI: 10.1029/2004GB002395 (cit. on p. 124).

Zeng, N., A. W. King, B. Zaitchik, S. D. Wullschleger, J. Gregg, S. Wang, and D. Kirk-Davidoff (2013). "Carbon sequestration via wood harvest and storage: An assessment of its harvest potential". In: *Climatic Change* 118.2, pp. 245–257. DOI: 10.1007/s10584-012-0624-0 (cit. on p. 11).

Zewdie, M., M. Olsson, and T. Verwijst (2009). "Above-ground biomass production and allometric relations of Eucalyptus globulus Labill. coppice plantations along a chronosequence in the central highlands of Ethiopia". In: *Biomass and Bioenergy* 33.3, pp. 421–428. DOI: 10.1016/j.biombioe.2008.08.007 (cit. on p. 121).

Zimmermann, J., M. Dondini, and M. B. Jones (2013). "Assessing the impacts of the establishment of Miscanthus on soil organic carbon on two contrasting land-use types in Ireland". In: *European Journal of Soil Science* 64.6, pp. 747–756. DOI: 10.1111/ejss.12087 (cit. on pp. 12, 124).

Selbständigkeitserklärung

Ich erkläre, dass ich die Dissertation selbständig und nur unter Verwendung der von mir gemäß § 7 Abs. 3 der Promotionsordnung der Mathematisch-Naturwissenschaftlichen Fakultät, veröffentlicht im Amtlichen Mitteilungsblatt der Humboldt-Universität zu Berlin Nr. 126/2014 am 18.11.2014, angegebenen Hilfsmittel angefertigt habe.

Berlin, den _____ _____

Datum Unterschrift